

COGNITIVE ROBOTICS FOR INSECT FARMING AND VERSATILE MATERIAL HANDLING

Kamil Bujnarowski

Propositions accompanying the PhD-thesis

Cognitive Robotics for Insect Farming and Versatile Material Handling

Kamil Bujnarowski

1. Industrial collaborative robots require extensions of their reachability and degrees of freedom to become truly operable and useful in complex environments. [Chapter 3]
2. Combining high-precision electrical grippers with soft pneumatic elements enables us to create versatile manipulators capable of handling diverse materials, thereby eliminating the need for changing tools. [Chapter 4]
3. With the addition of robot arm extensions, hybrid end effectors, 3D sensors, and dynamic motion planning systems, versatile collaborative robotic manipulation frameworks can outperform classical industrial frameworks in adaptability across tasks and domains, at the cost of significantly more computational resources. [Chapter 5]
4. Robot vision is essential in enabling cognitive decision-making and adaptive motion planning of robotic manipulation systems. [Chapter 6]
5. When developing robots for insect farming, we face the task of handling tiny, highly mobile insects that burrow in substrate, hide occluded inside complex structures, and prefer living in highly humid, dark and even partially toxic environments. Therefore, insect farming provides complex test cases, challenging us to create more sophisticated robotic solutions.
6. The future of industrial collaborative robotics lies in fitting robots to problems, rather than fitting problems to robots.
7. Robots that are not properly constrained do not always behave as expected.
8. To bring robots into SMEs at scale, we cannot afford to build one robot per task.
9. In robotics, not every bug is a bad bug.

Doctoral thesis

COGNITIVE ROBOTICS FOR INSECT FARMING AND VERSATILE MATERIAL HANDLING

Kamil Bujnarowski

2026

© Kamil Bujnarowski, Maastricht 2026.
All rights reserved. No part of this publication may be reproduced, stored in a retrieval system or transmitted in any form or by any means, electronic, mechanical, photocopying, recording or otherwise, without prior written permission of the author.

Cover	Kamil Bujnarowski
Production	ProefschriftMaken
ISBN	978-94-6534-368-6

COGNITIVE ROBOTICS FOR INSECT FARMING AND VERSATILE MATERIAL HANDLING

Dissertation

To obtain the degree of Doctor at Maastricht University,
on the authority of the Rector Magnificus, Prof. Dr. Jan Smits
in accordance with the decision of the Board of Deans,
to be defended in public
on Friday the 29^{th} of May 2026, at 13:00 hours

by

Kamil Konrad Bujnarowski

Promotors

Dr. Rico Möckel (Maastricht University)
Prof. Dr. Ir. Ralf Peeters (Maastricht University)
Prof. Dr. Gerhard Weiss (Maastricht University)

Assessment Committee

Chair:
Prof. Dr. Anna Wilbik (Maastricht University)
Members:
Prof. Dr. Rainer Goebel (Maastricht University)
Prof. Dr. rer. nat. Felix Hüning (Aachen University of Applied Sciences)
Prof. Dr. René van de Molengraft (Eindhoven University of Technology)
Dr. Mirela Popa (Maastricht University)



CoRoSect This research was supported by the European Union's Horizon2020 project: 'Cognitive Robotics for automated and digitised Insect Farming' (CoRoSect), under Grant Agreement No.101016953.

To my beloved family, friends, and Ares 🐾

Contents

1 Introduction 1
- 1.1 Robotisation and Digitisation in Industry 4.0 and 5.0 3
  - 1.1.1 Reference Architectural Model Industry 4.0 . . . 3
  - 1.1.2 Collaborative Robotics and Industry 5.0 6
- 1.2 Insect Farming: a Use Case for Cognitive Robotics . . 9
  - 1.2.1 Motivation 10
  - 1.2.2 State-of-the-Art in Insect Farming Automation . 12
  - 1.2.3 Cognitive Robotics for automated and digitised Insect Farming (CoRoSect) 13
  - 1.2.4 Challenges 15
- 1.3 Research Questions and Objectives 16
- 1.4 Contributions and Significance 22
- 1.5 Thesis Structure 24

2 CoRoSect Ecosystem 29
- 2.1 Background: Insect Species Life Cycles 30
  - 2.1.1 *Acheta Domesticus* (House Cricket) 30
  - 2.1.2 *Tenebrio Molitor* (Yellow Mealworm Beetle) . . . 31
  - 2.1.3 *Hermetia Illucens* (Black Soldier Fly) 33
  - 2.1.4 Obstacles to Automation 35
- 2.2 CoRoSect Use Cases and General Requirements . . . 37
  - 2.2.1 Use Case Selection 37
  - 2.2.2 High Level Process Overview: Crickets 40
  - 2.2.3 High Level Process Overview: Mealworms 45
  - 2.2.4 High Level Process Overview: BSF 49
  - 2.2.5 Summary 53
- 2.3 CoRoSect Ecosystem 54
  - 2.3.1 Overview 54
  - 2.3.2 Robotic, Digital, and Intelligent Components . . 58
- 2.4 Relevance and Conclusion 70

3 Extension of Industrial and Collaborative Robots for Increased Work Space and Operation in Confined Spaces 73
3.1 Introduction . . . 74
3.2 Related Work . . . 76
3.3 Reachability Simulation . . . 77
3.3.1 Reachability and Manipulability Simulation . . . 77
3.3.2 Evaluation of Operation in Confined Spaces . . . 82
3.4 Experiments and Results . . . 83
3.4.1 Baseline Results . . . 83
3.4.2 Reachability . . . 84
3.4.3 Manipulability . . . 84
3.4.4 Evaluation of Operation in Confined Spaces . . . 86
3.5 Prototype Hardware Design and Discussion . . . 92
3.5.1 Structural Design . . . 92
3.5.2 Actuator Selection . . . 95
3.5.3 Control and ROS Integration . . . 96
3.5.4 Final Simulation Insights . . . 98
3.5.5 Discussion . . . 99
3.6 Conclusion . . . 101

4 Hybrid End Effector with Soft Fingers and Modular Elements for Versatile Material Handling 103
4.1 Introduction . . . 104
4.2 Related Work . . . 106
4.3 End Effector for Versatile Material Handling . . . 109
4.3.1 Hybrid End Effector Design . . . 109
4.3.2 Theoretical Modelling . . . 115
4.4 Experiments and Results . . . 127
4.4.1 Experiment Setup . . . 127
4.4.2 Results . . . 131
4.5 Discussion . . . 143
4.5.1 Future Work . . . 146
4.5.2 Grasping in Insect Farming Use Cases . . . 146
4.6 Conclusion . . . 152

5 CoRoSect Robot Cell: Hardware Design, Motion Planning, and Software Architecture 153
5.1 Introduction . . . 154
5.2 Robot Cell Design and Hardware . . . 157
5.2.1 Structural Components . . . 157
5.2.2 Sensors . . . 165
5.2.3 Electrical Components . . . 171
5.2.4 Hardware Safety Features . . . 174
5.3 Robot Control and Motion Planning . . . 177
5.3.1 Robot XML Specification . . . 177
5.3.2 Motion Planning in MoveIt! . . . 180
5.4 Experiments and Results . . . 186
5.4.1 Experiment Setup . . . 186
5.4.2 Robot Motion Planning Results . . . 192
5.4.3 Discussion . . . 192
5.5 Resulting Software Architecture . . . 196
5.5.1 Sunrise Workbench . . . 199
5.5.2 ROS Interfaces and Task Descriptions . . . 200
5.5.3 Asset Administration Shell . . . 202
5.5.4 Discussion . . . 203
5.6 Conclusion . . . 208

6 CoRoSect Robot Cell: Use Cases, Visual Inspection, and Material Handling in Insect Farming 209
6.1 Introduction . . . 210
6.2 CoRoSect Use Case Requirements and Processes . . . 213
6.2.1 Cricket Quality Management . . . 213
6.2.2 Cricket Management . . . 215
6.2.3 Mealworm Quality Management . . . 217
6.2.4 Tenebrio Molitor Oviposition Management . . . 218
6.2.5 Black Soldier Fly Larvae Quality Management . 219
6.2.6 Black Soldier Fly Oviposition Management . . . 220
6.3 Robot Vision and Virtual Workspace Representation . 223
6.3.1 Occupancy Map for Workspace Registration . . . 225
6.3.2 Surface Matching for Object Localisation . . . 228

6.4 Strategies for Flexible Manipulation 234
6.4.1 Strategies for Versatile Material Handling 234
6.4.2 Error Correction 244
6.4.3 Operating in Enclosures and with Constraints . . 246
6.4.4 Sampling Strategies for Quality Management . . 248
6.5 Use Case Results 255
6.5.1 Material Handling and Cricket Harvesting 256
6.5.2 Mealworm Oviposition Management 260
6.5.3 BSF Oviposition Management 262
6.5.4 Sampling and Visual Inspection 262
6.5.5 Quality of Visual Inspection 268
6.6 Discussion 270
6.6.1 Evaluation of Quality Management 273
6.6.2 Robot Speedup Analysis 274
6.7 Conclusion 276

7 Discussion and Conclusions 277
7.1 Capabilities, Versatility, and CoRoSect Use Cases . . 277
7.2 Addressing the Research Questions 290
7.3 General Outlook 295
7.4 Future Work 299

Bibliography 303

Impact Paragraph 329

Summary 335

Streszczenie 337

Samenvatting 343

Acknowledgments 347

Published Work 351

List of Figures

1.1 Platform Industry 4.0 4
1.2 Articulated Cobots 7
1.3 Robotisation and Automation in Insect Farming 12
1.4 General CoRoSect robot cell 14
1.5 Dissertation Outline 27

2.1 Cricket Rearing Life Cycle 30
2.2 Mealworm Rearing Life Cycle 32
2.3 BSF Rearing Life Cycle 34
2.4 Use Case breakdown 39
2.5 Cricket farming materials 41
2.6 Cricket farming use case processes 42
2.7 Mealworm rearing materials 46
2.8 Mealworm farming use case processes 47
2.9 BSF materials 50
2.10 BSF farming use case processes 51
2.11 CoRoSect Cyber-Physical Components Concept 56
2.12 CoRoSect Workcell 57
2.13 Insect Farming Robot Cell Concept 58
2.14 CoRoSect Robotic Components 61
2.15 M-Robot Diagram 63
2.16 Mobile iiwa 64
2.17 CoRoSect Full System Architecture 67
2.18 Cricket farming use case processes 68

3.1 Reachability Simulation 79
3.2 Reachability and Manipulability Targets 80
3.3 Baseline Reachability and Manipulability 85
3.4 Manipulability Baseline KUKA iiwa vs KR10r1420 . . . 86
3.5 Maximum Reachability Increasing Rail Length 87
3.6 Manipulability Increasing Rail Length with no extra DOF 88

3.7 Manipulability Increasing Rail Length with extra DOF . 89
3.8 Reachability within Insect Crate 91
3.9 Reachability within Insect Crate 92
3.10 Annotated Robot Extension 93
3.11 Annotated CAD Robot Extension 94
3.12 Constraint on robot extension Planning Loop 97
3.13 Final Prototype Manipulability 99
3.14 Linear Drive in Use Cases 100

4.1 End Effector Related Work 107
4.2 End Effector RG6 110
4.3 End Effector Annotated 111
4.4 Real EE Config 113
4.5 End-Effector Configurations 114
4.6 Grasp Types 116
4.7 Coordinate Frame, Acting Forces and Angle of Soft Finger 117
4.8 Pseudo-Rigid Body Model 121
4.9 Effect of RG6 124
4.10 Distance to Object and Bending Angle 125
4.11 RG6 Mounted on KUKA iiwa 127
4.12 Materials for Handling in Experiments 128
4.13 CoRoSect End Effector Experiment Setup 129
4.14 CoRoSect End Effector Offset Setup 130
4.15 RG6-100N-Box Forcemeter Labelled Diagram 132
4.16 Experiment Results RG6 End Effector 133
4.17 Offset Results RG6 End Effector 134
4.18 RG6 End Effector Offset Case 135
4.19 Experiment Results Hybrid End Effector 137
4.20 CEE Closing Case 138
4.21 Experiment Results Hybrid End Effector Offset 140
4.22 CEE Offset Case 142
4.23 Materials Handled in Experiments 143
4.24 Deformation of the Duck 144
4.25 RG6 Picking Insect Farming Material 147
4.26 Picking Cricket Farming Materials 149

4.27 Picking Oviposition Plate 150
4.28 Picking Inlay 151

5.1 Real Robot Cell Annotated Diagram 158
5.2 Overview of the Full CoRoSect Robot Cell 159
5.3 Overview of the CoRoSect M-Robot 160
5.4 Electrical Cabinet Annotated 162
5.5 Extension Rail Mounting 164
5.6 Point Cloud Comparison Zivid 2 L100 to Zed 2i 169
5.7 Workspace and Robot-Mounted Cameras 170
5.8 Electrical Component Overview 172
5.9 Safety Mechanisms 176
5.10 Unified Robot Description Format (URDF) Hierarchy . 179
5.11 ROS Trajectory Broadcasting 181
5.12 Motion Planning Scene 183
5.13 Planning Scene Starting Conditions 187
5.14 Planning Scene with Objects 189
5.15 Planning scene with Crate 190
5.16 Time Taken to Plan Conditions 1-5 191
5.17 Motion Plan Moments 195
5.18 Software Layer Hierarchy 196
5.19 Software Architecture Overview 197
5.20 Joint Trajectory Dissemination 201
5.21 Task Sequence as Block Diagram 202
5.22 Sunrise Safety Configuration 206
5.23 Experiment Planning Scene 208

6.1 Cricket Quality Management Use Case Robot Operations 214
6.2 Cricket Quality Management Setup 214
6.3 Cricket Management Use Case Robot Operations 215
6.4 Cricket Management Setup 216
6.5 Mealworm Quality Management Use Case Robot Operations 217
6.6 Mealworm and BSF Larvae VI Input Image 218
6.7 Mealworm Management Use Case Robot Operations . . 219

6.8 Inlay Management Setup 220
6.9 BSF Management Use Case Robot Operations 221
6.10 BSF Tent Setup 222
6.11 Occupancy Map in Planning Scene 227
6.12 Object Localization Pipeline 230
6.13 Surface Matching Process 231
6.14 Calibration Setup 232
6.15 Locating Materials for Handling 235
6.16 Handling Materials 237
6.17 OD Gripping Strategy 238
6.18 Automated Cricket Harvesting 240
6.19 Inlay Brackets and Gripping Strategy 241
6.20 Delicate Gripping Strategy 242
6.21 Door Strategy 243
6.22 Stacking Inlays with Force Feedback 244
6.23 Error Correction Diagram 245
6.24 Error Correction on Force and Visual Feedback 247
6.25 Mating Cage in Planning Scene 249
6.26 Sampling Tool and Inspection Camera Mounting 251
6.27 Sampling strategies process flow. 251
6.28 Sampling Operation 253
6.29 Visual Inspection of BSF Oviposition Device 254
6.30 Crate Scanning 255
6.31 Time and Success figures for Cricket Management . . . 257
6.32 Time and Success for Cricket Harvesting 259
6.33 Time taken for Tenebrio Molitor Oviposition Management 261
6.34 Time taken for Oviposition Management of BSF 263
6.35 Time and success figures for Cricket QA 264
6.36 Time and success figures for sampling 265
6.37 VI Larvae count Tenebrio Molitor 267
6.38 VI Larvae Count Week 5 Tenebrio Molitor Real Condition 268
6.39 VI Larvae count TM week 9 and BSF day 16 269
6.40 M-Robot Potential Speedup 275

List of Tables

3.1 Linear Extension Motor Specifications 96

5.1 Camera Data Comparison 167
5.2 Chapter 5 Experiment Results 191
5.3 Chapter 5 Experiment Follow-up 192

6.1 Chapter 6 Experiment Results Cricket Management . . 258
6.2 Chapter 6 Experiment Results Tenebrio Molitor Oviposition Management 260
6.3 Chapter 6 Experiment Results Tenebrio Molitor Oviposition Management 262
6.4 Chapter 6 Experiment Results Sampling Tenebrio Molitor 266
6.5 Chapter 6 Experiment Results Sampling BSF Larvae . . 266

Glossary

AAS Asset Administration Shell.

AGV Automated Guided Vehicle.

AI Artificial Intelligence.

AMR Autonomous Mobile Robot.

BSF Black Soldier Fly.

CoRoSect Cognitive Robotics for automated and digitised Insect Farming.

HRC Human-Robot Collaboration.

IC Intelligent Crate.

ICPS Industrial Cyber-Physical System.

IMS Information Management System.

IOT Internet of Things.

MES Manufacturing Execution System.

PLC Programmable Logic Controllers.

RAMI Reference architectural model for Industry.

ROS Robot Operating System.

RRT Rapidly Exploring Random Tree algorithm.

SME Small- and Medium-Sized Enterprises.

1

Introduction

Cognitive robotics is a field of research at the intersection of robotics and artificial intelligence (AI), concerned with equipping robotic systems with mechanisms of cognition, enabling them to perceive their environment, process information, and make context-sensitive decisions (Aly et al., 2017; Cangelosi & Asada, 2022; Levesque & Lakemeyer, 2008). This field of research addresses growing limitations of robotics in automation, as traditional robots are effective at executing pre-programmed tasks in structured environments, but cannot adapt to change, manage uncertainty, or generalise knowledge across contexts (Qadeer et al., 2024; Y. Wang, 2010). The increasing demand for customisation, shorter product life cycles, and rapid reconfiguration in manufacturing environments has shifted the focus of automation from rigid, high-throughput systems to flexible, human-centred approaches. Industrial automation, while highly efficient in stable environments, is inherently brittle: deviations from expected inputs can cause failures (Cangelosi & Asada, 2022; Galin & Meshcheryakov, 2019; Javaid et al., 2021). Traditional automation excels in controlled, repetitive, and highly predictable domains, such as assembly-line manufacturing. However, it struggles in contexts characterised by inconsistency,

variability, incomplete information, or the need for interaction with humans (Dmytriyev et al., 2024; Galin & Meshcheryakov, 2019).

In contrast to traditional automation, cognitive robots are provided the means to adapt their behaviour in response to dynamic and uncertain conditions (Aly et al., 2017). Cognitive robots address the challenges of modern industry by generalising across tasks, responding flexibly to unforeseen circumstances, and engaging in cooperative activities with human partners (Cangelosi & Asada, 2022). They represent a move from machines that merely follow predefined instructions to agents capable of reasoning, learning from experience, and pursuing goals in flexible ways (Javaid et al., 2021; Qadeer et al., 2024). By integrating AI methods into robotic architectures, cognitive robotics aims to create systems capable of perception, autonomous adaptation, and context-aware actions (Javaid et al., 2021; Qadeer et al., 2024). This can be decomposed into (1) systems used to gather and interpret data, such as visual (or other) sensors and their digital representations, and (2) systems that map this information to a robot action, based on defined rules or predictions, for example, learned policies (Singh et al., 2022). Through perception, a robot can construct internal models of its surroundings to dynamically operate in a changing environment or autonomously identify objects relevant to its tasks. Machine learning techniques, including reinforcement learning, deep neural networks, and probabilistic reasoning, enable robots to extract patterns from data, predict outcomes, and optimise actions over time (Cangelosi & Asada, 2022; Schoettler et al., 2020; K. Wang et al., 2023). These AI-driven capabilities are further combined with reasoning and planning algorithms, allowing robots to represent goals, generate motion plans, and dynamically revise strategies when conditions change (Cangelosi & Asada, 2022; Javaid et al., 2021; Qadeer et al., 2024). This integration of cognitive and decision-making capabilities enables robots to operate effectively in unstructured or changing environments where pre-programmed automation would fail. This adaptability is particularly important in domains heavily influenced by human factors such as agriculture, healthcare, service industries,

disaster response, and autonomous mobility, where processes develop over time and environments are difficult to predict/observe (Duckett et al., 2018; Lytridis et al., 2021; Ortiz et al., 2016; Pérez et al., 2016).

Cognitive robotic systems become increasingly desirable in modern industrial settings where cognitively and physically challenging processes develop over time (Ghobakhloo, 2020; Skender et al., 2019). High-frequency decision-making that controls production lines and product life cycles requires intelligent systems to perceive, analyse, and output decisions, but also the physical capabilities to affect those decisions in the real world. The deployment of adaptable cognitive robotic platforms becomes more common in highly dynamic settings, where there are too many variables to control (Galin & Meshcheryakov, 2019; Mohamed, 2018). Moreover, cognitive robots are able to manage incomplete or noisy data, which is common in real-world industrial environments, hence maintaining functionality despite inconsistencies. This versatility is critical in industries where tasks are not uniform or where production lines must frequently change to accommodate new products, smaller batch sizes, or customised outputs. This leads to the introduction of Industry 4.0 and the smart factory, where machines, sensors, and systems are interconnected through digital networks to enable autonomous monitoring, diagnostics, and decision-making (Galin & Meshcheryakov, 2019; Grau et al., 2020; Javaid et al., 2021).

1.1 Robotisation and Digitisation in Industry 4.0 and 5.0

1.1.1 Reference Architectural Model Industry 4.0

Industry 4.0 refers to the ongoing transformation of industrial production systems through the integration of advanced digital technologies, industrial cyber-physical systems (ICPSs), and data-driven decision-making processes (Hankel & Rexroth, 2015; Nagrath et al., 2022; Sandini et al., 2024; Tantawi et al., 2019).

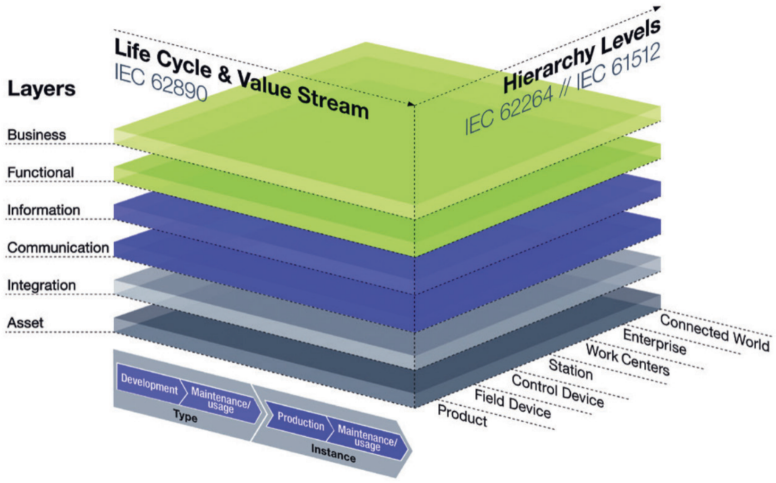


Figure 1.1: Visual representation of the Industry 4.0 as a three-dimensional coordinate system (Hankel & Rexroth, 2015). This graphic provides a mapping of required components for industrial machines to the hierarchy levels in a business, but also serves as a representation of which components are needed for a machine to fit into the Industry 4.0 paradigm, depending on their role in the factory. The 'Hierarchy' axis represents elements or functionalities common within industrial facilities. The 'Life Cycle and Value Stream' axis represents the life cycles of each of these elements. Finally, the layers represent a decomposition of complex systems like robots and machines into comprehensive individual functionalities.

Two foundational pillars of modern industry are robotisation and digitisation (Galin & Meshcheryakov, 2019; Javaid et al., 2021), both of which play roles in enhancing productivity, flexibility, robustness, and providing automation solutions to a wider range of industrial settings. At its core, Industry 4.0 represents a paradigm shift in industrialisation toward intelligent, interconnected, and highly adaptive production environments where machines, systems, and humans collaborate through seamless digital integration (Galin & Meshcheryakov, 2019; Javaid et al., 2021; Rahman et al., 2024; Sandini et al., 2024). This creates a network of communication between intelligent components

inside industrial facilities, which is made comprehensive by the Reference Architectural Model Industry 4.0 (RAMI 4.0) (Hankel & Rexroth, 2015), depicted in Figure 1.1. Following RAMI 4.0, Industry 4.0 combines information and communication technologies with manufacturing. The term encapsulates a broad set of innovations, including the Internet of Things (IOT), Artificial Intelligence (AI), machine learning, cloud computing, big data analytics, and advanced robotics (Bauer & Mäkiö, 2023; Hankel & Rexroth, 2015; Tantawi et al., 2019). The integration of advanced sensors, actuators, and real-time control algorithms has enabled robots to operate with greater autonomy, precision, and adaptability, making them essential components in the realisation of smart factories.

Robotisation refers to the widespread deployment of robotic systems to support tasks traditionally performed by human operators. These systems, ranging from articulated robotic arms to automated guided vehicles (AGVs), autonomous mobile robots (AMRs) and collaborative platforms, are currently being introduced beyond conventional assembly lines: to perform complex, dynamic tasks across logistics, quality inspection, material handling, and more in unstructured and non-highly-controlled workspaces (Rahman et al., 2024; Sandini et al., 2024; Tantawi et al., 2019). Such systems are characterised by adaptability, resource efficiency, and the ability to manage complexity through continuous learning and self-optimisation (Grau et al., 2020; Tantawi et al., 2019).

Parallel to the advancement of physical automation is the process of digitisation (Ghobakhloo, 2020; Kagermann, 2014). This is encapsulated as the transformation of analogue operations and data into digital formats that can be stored, processed, and analysed at an industrial scale (Skender et al., 2019). This includes the implementation of digital twins, real-time monitoring systems, cloud-based platforms, and machine learning algorithms to facilitate predictive maintenance, process optimisation, and data-informed decision-making (Ghobakhloo, 2020; Qi & Tao, 2018). Digitisation

provides the foundational infrastructure for the integration of robots into broader industrial ecosystems.

The combination of robotisation and digitisation enables the development of highly responsive manufacturing systems that are capable of self-optimisation, self-configuration, and adaptive behaviour in response to changing operational conditions (Brettel et al., 2016; Kagermann, 2014; Rauch, 2020). Through interconnected networks and intelligent control architectures, robotic systems can now act as services within an industrial IOT, exchanging information and collaborating autonomously to maximise efficiency and minimise downtime. However, the full realisation of Industry 4.0 depends on overcoming several technical and organisational challenges. These include interoperability and compatibility between heterogeneous systems, as well as cybersecurity, real-time data integration, and the scalability of robotic solutions in diverse manufacturing contexts (Foidl & Felderer, 2015; Mohamed, 2018). Moreover, there is a need for robotic designs, including versatile and intelligent end effectors, sensor fusion, and control strategies to meet the demands of increasingly versatile production systems (D'Avella et al., 2023; Dmytriyev et al., 2024; Qadeer et al., 2024).

1.1.2 Collaborative Robotics and Industry 5.0

Industry 5.0 is an emerging paradigm that extends the principles of Industry 4.0 while placing greater emphasis on human-centric values, sustainability, and resilience (Leng et al., 2022; Rahman et al., 2024; X. Xu et al., 2021). While Industry 4.0 is primarily associated with the digital transformation of manufacturing through cyber-physical systems, big data, and automation, Industry 5.0 represents a shift towards re-integrating human knowledge, skills, safety, and social goals into technologically advanced production systems (Leng et al., 2022; X. Xu et al., 2021). A defining feature is the collaborative interaction between humans and artificially intelligent machines (Akundi et al., 2022). Unlike fully automated production lines that minimise human

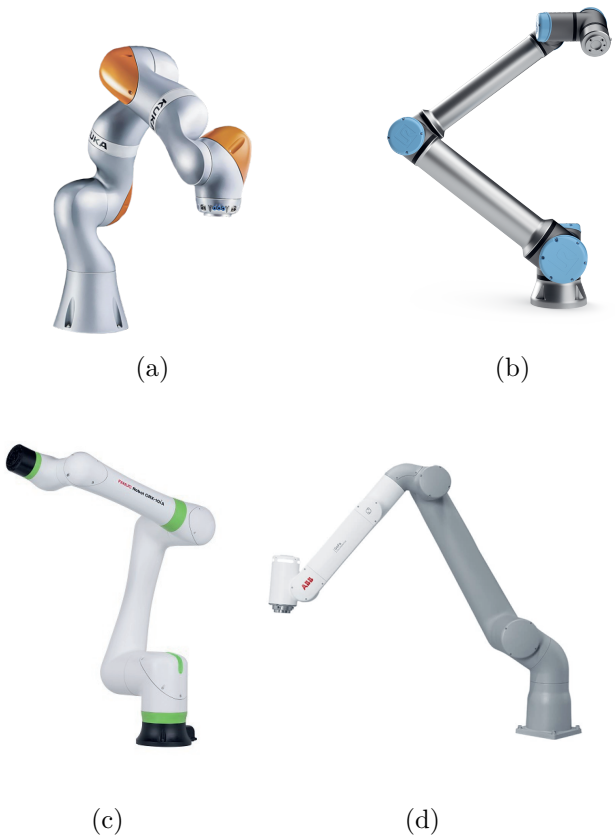


Figure 1.2: Articulated Cobots. (a) KUKA iiwa (KUKA, 2013). (b) Universal Robotics UR10e (Universal Robotics, 2018). (c) FANUC CRX-10iA (FANUC, 2024). (d) ABB GOFA (ABB, 2021).

involvement, Industry 5.0 describes an environment where cognitive robots, artificial intelligence systems, and advanced manufacturing technologies complement human expertise rather than replace it (Akundi et al., 2022; Rahman et al., 2024). Human operators provide contextual judgment, creativity, and ethical oversight, while machines contribute precision, consistency, and computational power. This

synergy is expected to enhance innovation, product personalisation, and overall system resilience.

Collaborative robots, or cobots, have emerged as a key technology (Dusadeerungsikul & Nof, 2019; Galin & Meshcheryakov, 2019; Kragic et al., 2018) within Industry 4.0 and along the trend towards Industry 5.0, offering interaction between humans and machines. As an emerging trend in automation, the use of collaborative robotics aims to introduce robots into workspaces inside factories and warehouses, where they cooperate with human co-workers to complete cognitively and physically challenging tasks. Unlike traditional industrial robots, which are typically confined within safety enclosures and programmed for controlled environments and repetitive tasks, cobots are designed to operate safely alongside human workers, enabling shared workspaces and dynamic task allocation (Fruggiero et al., 2020; Sandini et al., 2024). Although cobots are designed with inherent safety features such as force limitation and collision detection (R. Cheng, 2021; Dmytriyev et al., 2024), ensuring consistent compliance with safety standards (e.g., ISO 10218 and ISO/TS 15066) requires comprehensive risk assessment, proper system integration, and operator training. The role of a collaborative robot in an industry is as a supplement or tool to an existing workforce, facilitating an increase in productivity, capable of decision-making or decision support, and relieving the workload of unpleasant or dangerous processes (Sandini et al., 2024; Vysocky & Novak, 2016).

Among the many emerging designs and implementations of articulated collaborative robots, such as those featured in Figure 1.2, manufacturers commonly utilise internal and external sensors to provide an additional level of safety for human co-workers in their vicinity (El Zaatari et al., 2019; Vysocky & Novak, 2016). They are further enhanced through the integration of cognitive technologies and artificial intelligence (for example, machine learning models), which enable decision-making in complex situations and learning from demonstration (J. Chen et al., 2017; Grau et al., 2020; Schoettler et al., 2020; K. Wang et al., 2023). Additional sensors, cognitive

capabilities, and innate adaptability across tasks and domains give collaborative articulated robots significant advantages in complex automation tasks that require decision-making, error correction, or learning. These features not only ensure safety but also reduce the need for specialised programming or isolation. This has made cobots particularly attractive for small- and medium-sized enterprises (SMEs), where production volumes may not justify the cost and complexity of fully automated systems. When connected to manufacturing execution systems (MESs) and industrial Internet of Things (IOT) frameworks, cobots can dynamically receive instructions, report status, and coordinate with other systems in real time (Choi et al., 2014; Leitner & Mahnke, 2006; Veiga et al., 2009; X. Ye et al., 2021), integrating them into the Industry 4.0/5.0 infrastructure.

1.2 Insect Farming: a Use Case for Cognitive Robotics

The goal of this dissertation is to address the limitations of a collaborative articulated robot arm, to increase its scope and abilities within non-highly-controlled environments, and provide insight into how cognitive systems increase the versatility of robots. Specifically, the technologies presented in this dissertation are aimed at addressing challenges to the automation of unstructured, human-centred workspaces, where robots handle material, quality management, and fine manipulation tasks.

A potential environment that poses these challenges and pushes the limits of robotisation under Industry 4.0 can be found within the food production industry, specifically in the emerging field of insect farming. Insect farming presents a unique combination of variability, complexity, and sensitivity while addressing the global societal issue of food security, but is challenging to manage effectively with conventional automation (Ortiz et al., 2016). The insect farming industry offers a wide range of diverse automatable use cases, each of which provides unique conditions in material handling, fine

manipulation, quality management, or decision-making, that provide real-world test cases for cognitive robotic systems (Madau et al., 2020). Addressing these requires pushing the state-of-the-art in versatile and fine robotic manipulation to a point where a single robot can handle various workspace configurations, diverse materials, and be adaptable to process variability without the involvement of writing or training new software. This is still an unsolved problem. However, if a robot were to gain such abilities, it would allow insect farms, but also other industrial and agricultural applications, to quickly exchange materials and objects to be handled.

1.2.1 Motivation

Technological advances in agriculture, such as dedicated robotics, precision farming, automated irrigation systems, and genetically modified organisms, have the potential to increase yields and resource-use efficiency (Arora, 2018). However, the adoption of these technologies is unevenly distributed and often constrained by economic, regulatory, and infrastructural barriers (Arora, 2018; Frison, 2016; Kimbrell, 2002). The issue of food security is rapidly rising and becoming a critical challenge in the 21st century. Defined by the Food and Agriculture Organisation of the United Nations, food security exists when "all people, at all times, have physical and economic access to sufficient, safe and nutritious food that meets their dietary needs and food preferences for a healthy and active life" (Pinstrup-Andersen, 2009). This definition incorporates not only the quantity of food produced but also the distribution mechanisms, accessibility, and long-term sustainability of food systems. The growth of the world's population is forecast to reach up to 10 billion individuals by 2050 (Alexandratos & Bruinsma, 2012), all of whom need to be fed, along with the food required for livestock or companion animals. Population growth intensifies demand for agricultural outputs and exacerbates pressure on natural resources such as arable land, freshwater, and biodiversity. The global demand for meat protein alone is projected

to be 75% higher in 2050 than it was in 2005/2007 (Alexandratos & Bruinsma, 2012). Additionally, food production constitutes up to 20% of global carbon emissions, depending on which aspects of agriculture and cultivation are considered (Alexandratos & Bruinsma, 2012; Popp et al., 2010; Ritchie et al., 2024), and up to a third of all food produced ends up wasted. The over-reliance on industrial agricultural practices has raised concerns about long-term ecological sustainability, including the loss of agrobiodiversity and the overuse of chemical inputs (Frison, 2016; Kimbrell, 2002).

The environmental footprint of today's food production and concerns about self-sufficiency have created interest in producing proteins for feed and food by farming insects. The solution to meet the rising global demand for protein production may lie in the insect farming industry, especially as a food source for livestock animals. Insects offer a sustainable and efficient source of protein, fatty acids and additional minerals (Sogari et al., 2019), and allow us to close the loop on food and agricultural waste by using it as a source for rearing some species of insects. Additionally, insect farming emits considerably less greenhouse gas than most livestock (Oonincx et al., 2010) and does not require land clearing. However, the current industry of insect production cannot compete with traditional food sources on the commercial market in terms of scale. The rapidly rising demand for protein can only be met by standardisation and innovation within the mass-production process. Young and developing insect farms do not have the capital to invest in full mechanisation and automation of their insect farming processes, and coupled with high prices of edible insects, are limited in growing on the EU market (Madau et al., 2020; Ortiz et al., 2016). To meet the required industrial scale in insect production, it is necessary to enhance production efficiency, reduce labour intensity and thereby markedly decrease the production cost.



(a) (b)

Figure 1.3: Robotisation and Automation in Insect Farming (Better Insect Solutions, 2025; Viscon Group, 2025). (a) Conveyor belt for mealworm larvae processing (Better Insect Solutions, 2025). (b) Industrial robot arm for crate and storage management (Better Insect Solutions, 2025).

1.2.2 State-of-the-Art in Insect Farming Automation

Within insect farming, automation and adherence to Industry 4.0 standards have emerged as key areas of interest, with studies primarily focusing on the development of automated systems for various processes such as feeding, waste management, monitoring, and sorting of insects. These automated systems aim to streamline operations, reduce labour requirements, and enhance overall efficiency. An example is the Viscon Group (Viscon Group, 2025), who provide full automation through robotisation solutions for insect crates. However, the incorporation of collaborative and cognitive robotics into these automated processes has the potential to further boost productivity and efficiency by introducing the capability for performing tasks related to insect nursing and quality management. By working alongside human operators, collaborative robots contribute to increased productivity but also offer greater flexibility and adaptability to dynamic operational needs. This is an emerging trend in other industries as well, for example, manufacturing and agriculture (Dmytriyev et al., 2024; Dusadeerungsikul & Nof, 2019). Most

robotisation solutions for the insect farming industry remain focused on handling insect crates and maximising biomass processing, such as (Viscon Group, 2025) or (Better Insect Solutions, 2025) (Figure 1.3).

While research specifically dedicated to robotics in the insect farming industry remains limited, insights from related fields such as agricultural robotics and manufacturing automation offer inspiration for future developments (Duckett et al., 2018; Lytridis et al., 2021). Existing implemented approaches to robot vision, robot control, and task management for material handling can be used with similar processes at insect farms (Better Insect Solutions, 2025; Viscon Group, 2025). In particular, collaborative robots, more extensively used within the Industry 4.0 framework, are shown to provide added utility in terms of safety and optimisation of processes (Dusadeerungsikul & Nof, 2019; Pietrantoni et al., 2024; Vysocky & Novak, 2016). However, the emergence of a cognitive robotic system that is versatile enough to handle internal rearing and nursing processes for multiple different insect species and perform material handling has not yet been proposed.

1.2.3 Cognitive Robotics for automated and digitised Insect Farming (CoRoSect)

This dissertation presents the design and implementation of part of a cognitive robotic work cell (featured in Figure 1.4) developed with the Horizon 2020 project 'Cognitive Robotics for automated and digitised Insect Farming' (CoRoSect). CoRoSect introduces a solution based on the Reference Architecture Model for Industry 4.0 (RAMI 4.0) to support all phases of the insects' rearing cycle inside insect farms. The infrastructure is prototypically implemented, tested and validated based on end-user requirements in three of the most commonly reared insect species in the EU. A single system is used for use cases in rearing Tenebrio Molitor (Mealworms), Hermetia Illucens (Black Soldier Flies) and Acheta Domesticus (House Crickets). While part of a wider robotisation solution aimed at the automation of

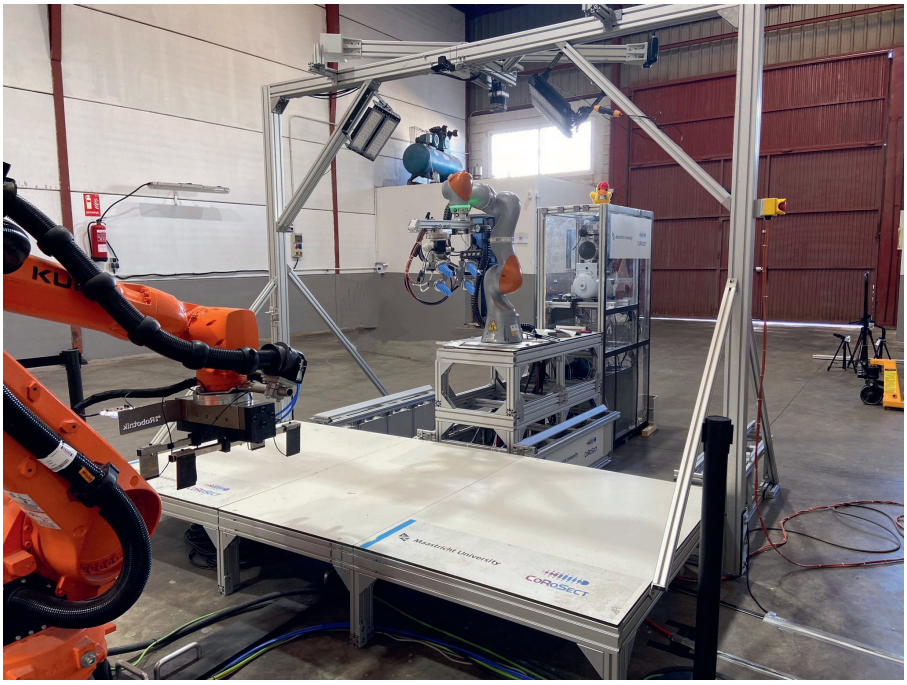


Figure 1.4: The prototype CoRoSect Robot. Image from the pilot at Entomotech (Almeria, Spain, November 2023).

insect rearing in the EU, the articulated robotic system developed in this dissertation aims specifically to handle day-to-day, repetitive operations involved in nursing insects during their life cycles, for example, providing feed and water, performing quality inspection, and delicately handling egg containers. However, large-scale automation is expensive, requiring substantial capital before a return on investment is seen. As developing enterprises, any automation solution for insect farms needs to be flexible to evolving industrial processes, changes to the warehouse configurations, and be cost-efficient. This research is focused on the development of a single robotic system that can be used within different configurations of insect farms. The dissertation describes the components involved in overcoming each

of the above-mentioned obstacles to automation and analysing the increased abilities of the system under real-world conditions.

1.2.4 Challenges

The automation of insect rearing processes poses significant difficulties due to the biological, environmental, and technical characteristics of insect production. Insect farming involves living organisms that are small, delicate, and highly variable, making standardised automation strategies difficult to apply to all use cases (Madau et al., 2020; Ortiz et al., 2016). Unlike uniform manufactured parts, insects are mobile, fragile, and prone to occlusion and unpredictable movement (Makkar et al., 2014). There is a need for frequent low-level decisions made at multiple stages of insect life cycles based on perceived parameters within the farm. Cognitive robots are needed in insect farming because they provide the flexibility, adaptability, and intelligent decision-making capabilities required to overcome obstacles that prevent conventional automation.

These challenges provide a complex environment for testing cognitive robotic systems. An inherently dynamic and uncertain environment requires robots that are at the same time precise and also capable of perception/sensing, making decisions, and adapting their behaviour in real time (Bodenhagen et al., 2014; Kuts et al., 2018). This leads to conditions that demand the development of robust and intelligent technologies, which also generally apply to wider use in industries. From a robotics perspective, the workspaces within insect farms are non-highly-controlled, subject to perturbation or misplacement of items, and many processes require expert knowledge, frequent decision-making, or direct collaboration with a human supervisor (Makkar et al., 2014; Ortiz et al., 2016). Insect farming is centred on the care, handling, and monitoring of large populations of living organisms and is rich in diverse automatable use cases. For a cognitive robot, this provides an opportunity to demonstrate (1) flexibility in handling varied materials and insect species, (2) adaptability to unique

conditions in workspaces and robustness to errors, (3) learning and decision making to distinguish between insect species/forms, infer health or growth parameters, and alter handling strategies as the population develops. Confined spaces, operation within insect crates, and the need for a delicate approach to handling insects are obstacles to the adoption of large-scale machinery. The workspaces typically use dedicated materials, not necessarily tailored to industrial automation, and are hence difficult to standardise. Robot end effectors and tools are normally specialised to perform a particular operation, optimising a highly repetitive task. However, handling diverse materials, and particularly delicate objects, requires compliant and modular grippers (Hughes et al., 2016), similar to those being implemented in agricultural robotics (Duckett et al., 2018). Obstacles to a cognitive robotic system being effective within an insect farm are identified in a limited operational space, working inside confined/enclosed spaces, handling diverse materials, adaptability to task diversity, and the need for dynamic error correction.

Deploying cognitive robots in this domain advances both the practical automation of sustainable food systems and the broader scientific objective of developing robots capable of adaptive, intelligent behaviour in real-world settings (Javaid et al., 2021; Ortiz et al., 2016; Rahman et al., 2024). The need to combine delicate robotic manipulation with AI-based strategies makes insect farming a challenging environment for testing cognitive systems in robotics.

1.3 Research Questions and Objectives

This thesis aims to contribute to the field of versatile robotics and automation, focusing on hand-in-hand hardware and software development, the incorporation of cognitive systems, and the design of mechanical elements. Each chapter highlights a significant development in hardware or software that contributes to a final versatile platform for handling day-to-day operations in insect

nursing and quality management during the insects' life cycles. The developed technologies are validated in real conditions in insect farms during the CoRoSect pilot studies (Figure 1.4). While the requirement analysis and validation of systems are performed in the context of insect farming, the research in this thesis is framed as more generally applicable across other industries. In particular, the software architectures, algorithms, mechanical tools, and cognitive systems presented in this thesis are each aimed at addressing the practical challenges of deploying an autonomous robotic system into an unstructured or potentially collaborative workspace.

The research objectives are hence framed as follows:

Research Objectives

(1) To determine addressable limitations of current commercially available collaborative articulated robots, namely in sensing, reachability, and operation in non-highly-controlled environments, such that these robots can feasibly operate within an industrial process and are adaptable across tasks, materials, and warehouse configurations.

(2) To develop a versatile robotic system for tasks such as insect nursing and quality inspection within the insect farming industry. To address the practical challenges of robotisation and develop an architecture of embedded systems and software of low-level controllers, motion planning, robot vision, flexible control strategies, and high-level task managers that help handle unstructured workspaces. The aim is for a single robotic system to perform diverse tasks and handle different materials without major reconfiguration or reprogramming.

(3) To validate the robotic system in real-world conditions at insect farms, where it performs tasks derived from insect rearing processes.

In this thesis, a prototype robotic system was developed (for the CoRoSect project), which incorporates the various systems described in each chapter. This robotic platform is used to test and validate individual innovations, and the entire finalised system is used within the premises of real insect farms, automating industrial insect rearing processes, to provide results and validation under real-world conditions.

It is guided by the following research questions, each of which is addressed within the chapters, respectively:

Research Question 1

How to quantify and measure the reach of an articulated robot over its workspace for the purpose of testing different robot configurations and extensions?

One of the strongest limiting factors encountered when implementing an articulated robot into an insect farm is the lack of reach over the required workspace. The reduced reachability and payload capacity of collaborative articulated robots compared to their industrial counterparts are known tradeoffs with their adaptability and ease of implementation in industry (Arents & Greitans, 2022; Taesi et al., 2023). This is particularly apparent in the insect farming workspace, where tight enclosures and limited manoeuvrability are common. In order to address the challenge of increasing the reach of an articulated robot arm with a mechanical solution, it is first necessary to measure the yield in operational space gained from a proposed solution.

This research question is addressed in the first half of Chapter 3, concerning the development of a simulation wherein various configurations of a KUKA iiwa with a mounted articulated robot extension are tested. The reach over the workspace is quantified using two measures: (1) reachability for one-shot reaches to target positions, and (2) manipulability for attempting motion planning to systematic orientations around a target position. The simulation is

used to validate the implementation of a robot extension, the CAD design of which is used to provide final results on reachability yield in a simulated insect farming setup.

Research Question 2

How to achieve an extension for a collaborative robot arm to increase reachability in the workspace and within enclosed spaces?

Following from research question 1, the second half of Chapter 3 addresses the mechanical and software implementation of a custom-designed robot extension. The robot extension needs to be lightweight, an affordable alternative to larger industrial robots, and improve the robot's abilities in reaching confined spaces. The requirement analysis of the robot extension stems directly from simulation results and insect farming use cases. The structural design, as well as actuator selection and hardware/software integration with a KUKA iiwa, are described. Three additional degrees of freedom are introduced to a $0.5m$ long robot extension. Operation within confined enclosures at insect farms is validated in both simulation and real conditions.

Research Question 3

How to achieve a hybrid end effector for the versatile manipulation of both rigid and delicate materials in the insect farming industry?

An articulated robot arm depends on an end effector, a hand or tool attached to the flange, to affect the world and handle materials. While rigid grippers are common in industrial developments, these are typically highly specialised tools that work with high precision and large payloads. Recent developments in soft and compliant end effectors, particularly useful in agricultural automation (Duckett et al., 2018; Lytridis et al., 2021), offer a versatile option for finer control of grasping forces, sensor feedback, and variability to material geometry. The insect farming workspace features a mix of both rigid

and deformable materials that have to be handled with care in close proximity to live insects. The diversity of material involved, featuring various shapes, sizes, surface textures, and constraints on orientations (for example, handling water-filled cylinders), requires an adaptable approach that can handle different gripping geometries without the need for reconfiguration/reprogramming, while still exerting sufficient grasping forces to secure held objects.

Research into a versatile end effector is addressed in Chapter 4, where a hybrid of soft and rigid gripping strategies is presented. A custom end effector uses soft silicone fingers and a rigid OnRobot RG6 at its core. The soft elements allow delicate material handling, compliance with object geometries, and additional tolerance to misalignment in unstructured workspaces. The rigid parts of the RG6 enable maintaining sufficient gripping strength to secure a proper grasp on materials. The gripper is modular and can house various extrusions to handle specific materials involved in insect farming. Chapter 4 presents both the hardware design, motivated by the requirements of insect farming, and the software integration through ROS. The end effector is used in repetitive gripping experiments to determine its ability to grasp common geometries and test the tolerance to misplacement offsets. These experiments, and the validation of the end effector at the CoRoSect use cases, aim to demonstrate the value of a versatile gripper and quantify the quality of the grasp in terms of resistance to outside perturbations.

Research Question 4

How can control and motion planning for a robot cell be achieved for the purpose of versatile manipulation in the insect farming industry?

An articulated robot arm requires a workspace to operate within, a platform to be mounted on, and a controller that computes collision-free motions through this environment. While a commercial robot arm will include proprietary control software to enable use of the arm, this usually encompasses only the scope of the robot arm itself, possibly with

interfaces for an additional tool and sensors. Considering an extended system, such as that of an articulated robot arm with a robot extension (Chapter 3), and the hybrid end effector (Chapter 4), control of the full robot requires a larger scope. A crucial component is a motion planning software that finds collision-free trajectories for the robot arm in a virtual environment. Furthermore, the motion planner needs to be integrated with the robot hardware and the additional articulated components in order to ensure synchronous motions. The resulting software architecture needs to span all individual components of the robotic system, enabling the use of their functionalities from a central task-management process.

This research question is addressed in Chapter 5, which describes the infrastructure of the robot cell designed for CoRoSect, consisting of a KUKA LBR iiwa 14 and the developments of Chapters 3 and 4. The practical implementation is split between (1) structural components, namely a workspace platform, mounting support structure, and various electrical components, and (2) the software architecture that connects each component to a central motion planner implemented in MoveIt! (Coleman et al., 2014). The MoveIt! framework generates trajectories synchronised for all extended joints of the robot. Robot Operating System (ROS) (Quigley et al., 2009) is used as middleware to enable communication between embedded components. The virtual motion planning environment is used in experiments to test collision-free trajectory generation within insect crates and small enclosed spaces expected at insect farms. The resulting software architecture is split between implementation on the KUKA proprietary controller (the Sunrise Workbench) and a high-level controller where external components are interfaced with the robot.

Research Question 5

How to achieve versatile manipulation in a confined environment?

To expand on the capabilities of an industrial robot arm to increase its adaptability in unstructured environments, it is necessary to

incorporate sensor data into its internal model of the workspace. It needs to be able to autonomously find objects and materials relevant to its current tasks, correct or overcome errors made by itself or other agents in the workspace, and be able to plan different trajectories depending on the state of the environment around it. This research question addresses the components necessary to enable a collaborative articulated robot arm to adapt to various configurations and use cases within insect farming, such that a single system can handle diverse materials and processes. This research question is the subject of Chapter 6. First, the use cases in insect farming are described as sequential operations that are actionable for an articulated robot. Each of these processes involves the handling of materials or tools and the identification of specific points of interest in the workspace, such as the interior of an insect crate. A robot vision system based on template matching and object localisation is integrated into the software architecture developed in Chapter 5. The core robot-vision system uses a Zivid 2 L100 3D sensor, which is precise enough to provide high-precision point clouds of the workspace from which accurate object locations are extracted. Additional flexible control strategies, error correction, and force/visual feedback are used to handle challenging workspaces in insect farming use cases. The research question is approached with an analysis of the robot cell's performance during the CoRoSect pilot studies, followed by a description of the control strategies and cognitive components required to complete a sequence of tasks in insect farming use cases.

1.4 Contributions and Significance

This dissertation aims to provide insight into overcoming the limitations of collaborative articulated robots and the obstacles to their full utilisation in unstructured, dynamic workspaces, such as those found in insect farming. While robotisation is commonplace in industry, the trend towards highly versatile systems, which can adapt between various tasks and handle diverse situations, requires the

integration of various intelligent systems and control strategies with mechanical components and sensors. This work aims to contribute insights into the development of versatile robotic systems, the necessary mechanical and virtual components in their development, and how multiple cognitive systems can be integrated together to create a single system with diverse capabilities. The proposed and developed technologies are structured into a single robot cell, which is validated in real-world conditions in use cases from the insect farming industry. These use cases offer diverse automatable tasks, involving various materials, dynamic workspaces, and challenging opportunities for delicate manipulation by a robot.

Original contributions presented in this work are twofold: (1) prototype technologies developed to address limitations of commercially available robotics, and (2) software systems used to control, interface, and synchronise multiple robotic and sensor components. Moreover, to the best of our knowledge at the time of writing this dissertation, no autonomous robotic system for performing fine manipulation and delicate tasks in insect nursing and quality management can handle use cases from all three insect species handled during CoRoSect. Furthermore, the chapters in this dissertation highlight individual, self-standing contributions that contribute to increasing the capabilities of articulated robotics, namely:

- An articulated robot extension to address the limited reachability smaller collaborative robot arms have over their workspace (Chapter 3). The robot extension is analysed in simulation and validated in real-world conditions.

- Insight into a hybrid approach to end effector design, leveraging both soft elements and rigid grasping surfaces (Chapter 4). A prototype design for a modular end effector is proposed, tested w.r.t. grasping strength and dexterity, and validated in experiments and real-world conditions. This contribution also includes a theoretical model of the end effector's behaviour.

- Another original contribution is the development of a robot cell intended for day-to-day use in insect farming and other industries (Chapter 5), developed using off-the-shelf components. The main articulated robot arm is a commercially available KUKA LBR iiwa 14, which is extended and augmented with both mechanical and intelligent systems. The significant insights are focused on the creation of a self-contained system that houses all necessary components for a versatile articulated robot arm. A software architecture centred around motion planning is a core contribution (Chapter 5), as well as the integration of vision and error correction systems and validation in real-world conditions in insect farming (Chapter 6).

Finally, the innovations presented in this dissertation are the development of both hardware and software systems hand-in-hand to achieve cognitive and adaptable robotic components. Algorithms are developed for the simulation and stabilisation of a robot extension. Both hardware and software interfaces are created to integrate 3D vision sensors, a custom end effector, and safety features into a self-sufficient robot cell mounting a KUKA iiwa. A software framework uses ROS to ensure communication between the articulated components and a central motion planning environment. Insect farming use cases are decomposed into atomic robot actions and modelled as sequences of operations, which are then executed under real-world conditions.

1.5 Thesis Structure

Following a conceptual overview of CoRoSect in Chapter 2, each chapter of this dissertation focuses on addressing a specific obstacle to robot versatility and developing a specific technology that allows handling of this challenge. The individual solutions are presented in a self-sufficient manner, but are all part of a larger system, the composition, control, and validation of which are the topics of Chapters 5 and 6. The

dissertation is structured as follows (the structure is depicted in Figure 1.5):

Chapter 2 contains the vital definition of use cases from the insect farming industry that are candidates for automation, stemming from the insect rearing processes. This chapter provides the relevant background information and the context for the CoRoSect project, which places the robotic system that is the topic of this dissertation into a larger picture. The general requirements and use cases defined in Chapter 2 are referenced throughout the other chapters to explain the design decisions and the inclusion of particular systems.

Chapter 3 covers research questions 1 and 2, concerning the limited reachability of collaborative articulated robots. A simulation is developed to determine the reach a robot has over its workspace, which is then used to evaluate a prototype robot extension that is developed to augment a KUKA LBR iiwa 14. The chapter covers both the mechanical design and the software integration of this robot extension and presents an analysis of the yield in operational space as well as a demonstration of it being used in real-world conditions.

Chapter 4 addresses research question 3 and the need for a specialised gripper for versatile material handling in industries, presenting the design and implementation of a hybrid end effector. The end effector combines both rigid and soft elements, allowing a greater scope of possible grasps. The effect of dynamically changing the distance between soft fingers is explained using mathematical models of similar soft-fingered grippers. It is evaluated for its resistance to external perturbations and its flexibility through grasping various geometries of items, and the gained tolerance to unstructured environments. The chapter contains a series of experiments conducted on gripping common items and those from the insect farming industry, using the grasping force and resistance to pulling forces to validate the quality of the grasps established on materials.

Chapter 5 combines the developments from the previous chapters into a single robotic system, consisting of a KUKA LBR iiwa 14, the

robot extension (Chapter 3), and the hybrid end effector (Chapter 4) mounted at the end, constituting an extended kinematic chain. First, the chapter covers the hardware integration of the robot into a complete work cell, including all structural elements required for mounting and workspace, and electrical components to enable communication between embedded systems. However, the focus of this chapter is on addressing research question 4 concerning the control and motion planning for the extended articulated robot. Experiments are performed in a virtual motion planning environment to validate the operation of the robot within workspaces resembling those of insect farming premises. The final goal of Chapter 5 is to develop a software architecture of communication between a virtual motion planning environment, a high-level task management system, and the low-level robot controllers, to create a system capable of synchronously executing sequences of motions that achieve insect farming tasks.

Chapter 6 addresses research question 5 and the development of the robot cell from Chapter 5 to include sensing, object localisation, force/visual feedback, error correction, and additional strategies to versatile task execution. Moreover, Chapter 6 provides an interpretation of the CoRoSect use cases as sequences of robot operations, and outlines the systems required in their automation. Finally, the chapter presents the strategies taken to perform each use case, and the results achieved in success rates, time taken to perform tasks, and additional results from specific insect farming processes.

Chapter 7 provides a discussion of the achievements and results presented throughout this dissertation, reiterating the research questions and providing answers. Final conclusions are at the end of this chapter.

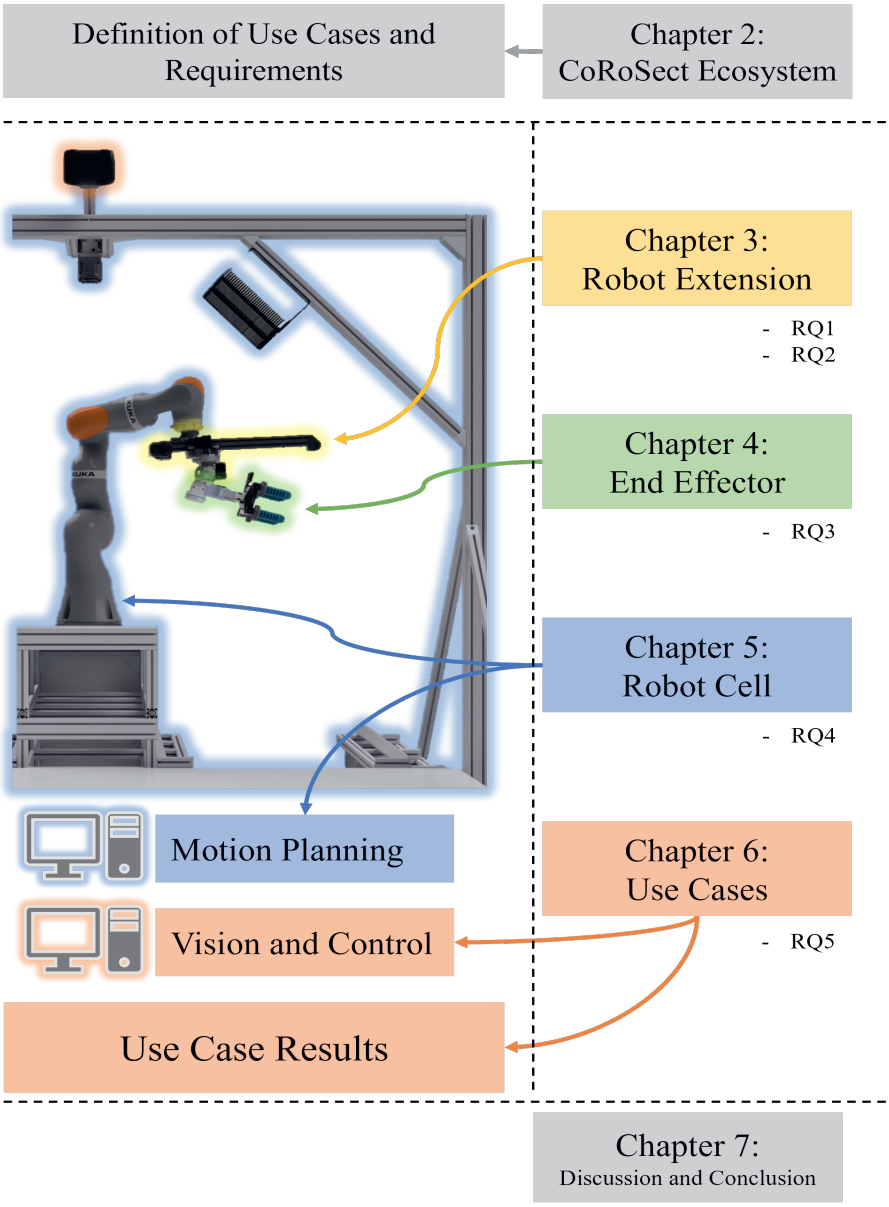


Figure 1.5: Dissertation Outline.

2

CoRoSect Ecosystem

This chapter provides background information and a requirement analysis for the Horizon 2020 project 'Cognitive Robotics for automated and digitised Insect Farming' (CoRoSect). The requirements defined in this chapter apply to each technology described in this dissertation and are referenced throughout the remaining chapters. Section 2.1 provides context on the insect species life cycles and their rearing processes, directly leading to the definition of concrete use cases in Section 2.2. Section 2.3 provides the necessary context on the CoRoSect project, of which the robotic system described in this dissertation is a part. There, the background, motivation, and connections between various robotic and intelligent CoRoSect components are described.

2

2.1 Background: Insect Species Life Cycles

The CoRoSect project conducted large-scale pilots in four insect farms across four European countries, focusing on three commonly farmed insect species: *hermetia illucens* (black soldier flies, BSFs), *tenebrio molitor* (mealworm beetles), and *acheta domesticus* (house crickets) (CoRoSect Deliverable 2.2, 2021).

2.1.1 *Acheta Domesticus* (House Cricket)

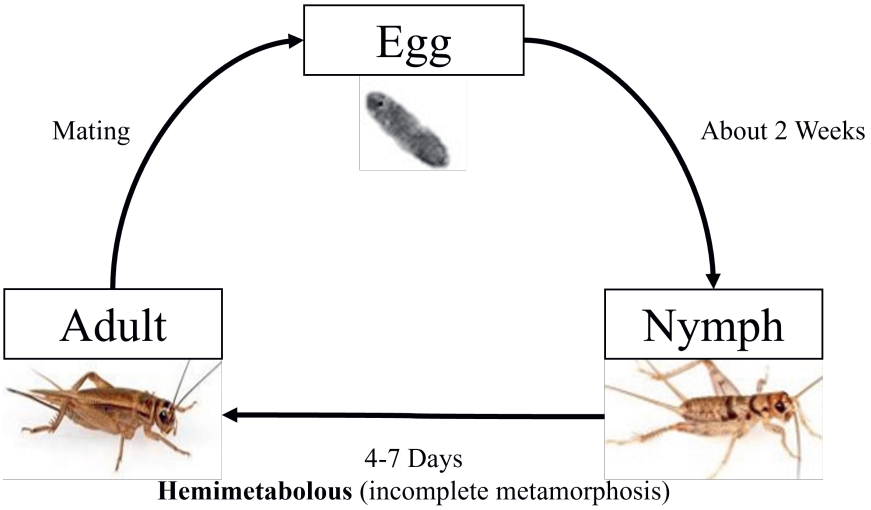


Figure 2.1: Cricket rearing life cycle. Eggs hatch after approximately 2 weeks, when a nymph is born. The cricket has no larval stage; the nymph resembles the features of the adult form, called Hemimetabolous (incomplete metamorphosis). At a favourable ambient temperature and environmental conditions, nymphs become adults after 4-7 days, after which a majority is harvested, and a portion is selected for mating.

Common house crickets are a popular species for rearing, having been reared in Europe as live feed for pets, and part of the gastronomy of various oriental countries (CoRoSect Deliverable 2.2, 2021). Their

relevant life cycle is experienced in three stages (Figure 2.1), from hatching, developing into nymphs, and finally into full adults within 49-119 days, depending on the environmental conditions (Booth & Kiddell, 2007). Their life cycle is hemimetabolous, meaning there is no larval stage for hatched nymphs, which resemble the adults and eat the same food (Lyn et al., 2011). The optimal age for harvesting for biomass yield is between 6-8 weeks, again depending on the exact rearing conditions. A cricket ready for harvesting at this stage weighs approximately $0.25g$ (Morales-Ramos et al., 2018).

The rearing process for crickets has some special requirements compared to other insect species. Tall insect crates are used to ensure jumping crickets cannot easily escape their habitat. After a breeding phase, $100g$ of freshly hatched crickets are placed within a tall crate, where each gram comprises approximately 1600 individuals (CoRoSect Deliverable 2.2, 2021). For a period of 60-85 days, the crickets develop, during which time they are provided food and water. Quality control is performed visually and by sampling a crate's population for counting, weighing, and detecting pathogens infesting the crates. Crickets are harvested once the population of a crate reaches the desired weight, yielding approximately $6kg$ live insects per crate.

2.1.2 *Tenebrio Molitor* (Yellow Mealworm Beetle)

The mealworm, which is the larval form of the yellow mealworm beetle (Figure 2.2), is an important insect species for rearing in Europe (CoRoSect Deliverable 2.2, 2021). It is one of a few insect species approved for human consumption with high nutritional value and is easily reared at an industrial scale. An adult beetle can live up to 173 days (Tatiana et al., 1999) and can produce between 250-1000 eggs after mating, 90% of which will successfully hatch (Drnevich, 2003; Ghaly & Alkoaik, 2009). The eggs are sensitive to temperature, hatching within five days at 35° to 35 days at 15° (L. Li et al., 2016; Siemianowska et al., 2013), hence requiring a climate-controlled environment for optimal industrial throughput. When hatched, the

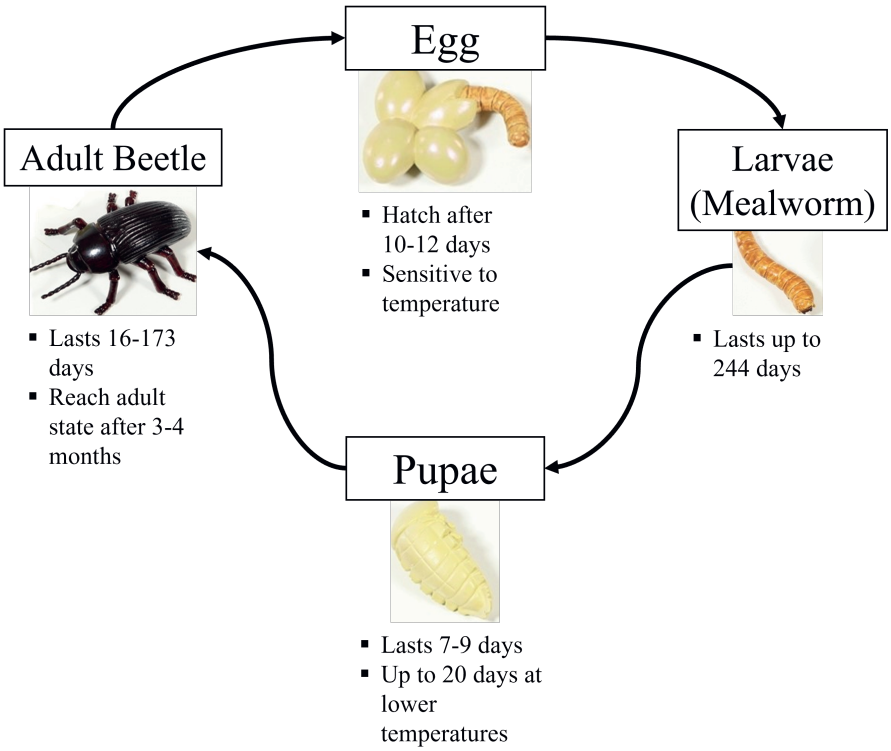


Figure 2.2: Mealworm rearing life cycle (de Lima et al., 2021). Image credit: (Alison's Montessori, 2025). Each stage lasts for a set amount of time before transitioning to the next. The larval form hatches after 10-12 days of incubation in temperature-controlled environments. As the main source of farm output, the larvae are fattened with a special diet and harvested when they reach a desired biomass yield.

larval form of the tenebrio monitor lasts up to 244 days (Figure 2.2), again depending on the ambient temperature. The average mass of the larvae ranges from $126mg$ to $220mg$ (CoRoSect Deliverable 2.2, 2021).

While each proprietary rearing process for mealworms can be unique,

it generally requires keeping a batch of adult beetles for producing eggs, so that their larval form can be reared to a desired amount of biomass. The adults are placed within crates containing oviposition devices and substrate, within which they lay their eggs. The eggs need to be separated from the substrate for maturation. After hatching, the larvae are kept within insect crates also containing substrate and their specific diet as a mixture of vegetable silage, grain mix, and water (CoRoSect Deliverable 2.2, 2021). The larvae live within the mix of substrate and food, and the crates can be easily stacked for optimised storage space. Each crate is dosed with new food on a weekly basis, and harvesting is done after the larvae reach a target size. The larvae are sorted out from within their substrate-diet mix. A portion of the maturing larvae is allowed to turn into pupae and then adults for further reproduction, while the majority is harvested for products.

2.1.3 *Hermetia Illucens* (Black Soldier Fly)

Black soldier flies (BSF) are reared for their high protein value, which is used in agriculture and pet food at the moment (CoRoSect Deliverable 2.2, 2021). Similar to mealworms, BSF larvae are harvested at the larval stage (Figure 2.3), after being fattened to a desired target biomass. A single adult female can lay 600-1000 eggs (Sheppard et al., 1998), which hatch within four days in the right environmental conditions (Sheppard et al., 1998). The larvae which hatch will be reared to weigh up to $220mg$ and are known for their voracious appetite, developing in a wide variety of organic matter and a fast metabolism. A portion of mature larvae is allowed to develop into pupae and then adults, to produce the next generation of eggs, while the majority is harvested.

As flying insects, adult BSFs are kept in cages, where they are fed and reproduce. Oviposition devices are used to store the delicate eggs, being replaced daily (CoRoSect Deliverable 2.2, 2021). After an incubation period, the eggs hatch and the larvae are placed within insect crates which contain substrate and their unique diet mix, similar to mealworms. The crates are stacked and stored in

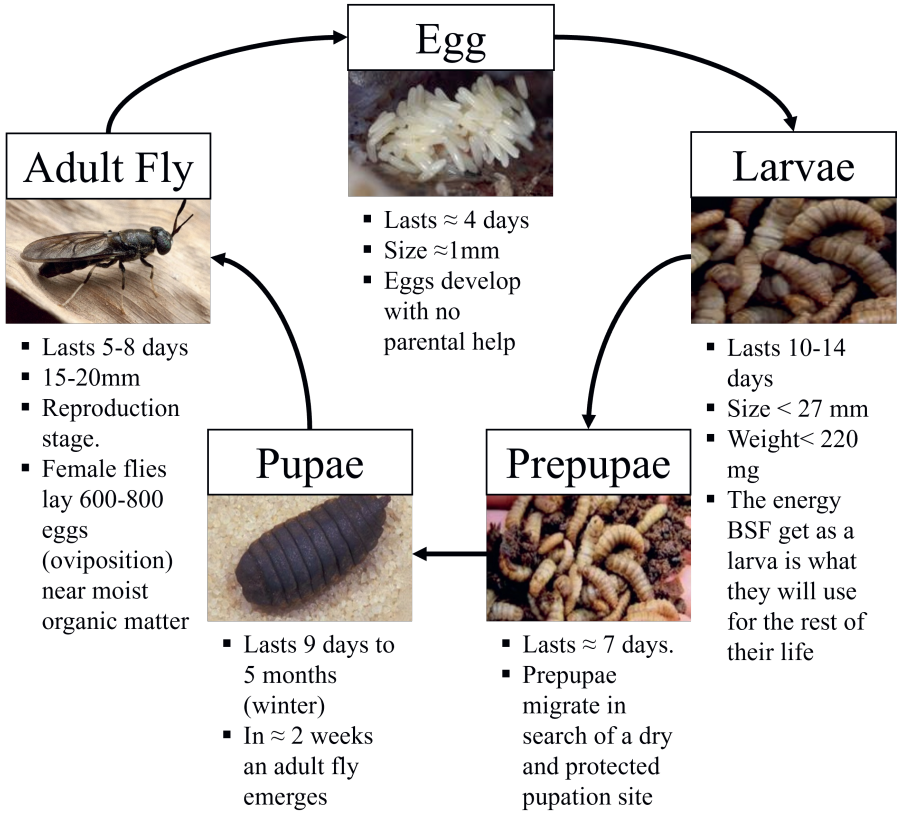


Figure 2.3: BSF rearing life cycle. Each stage lasts for a set amount of time before transitioning to the next. Clusters of eggs are incubated for up to four days before hatching into larvae. As the main source of the farming output, the larvae are harvested when they reach a desired biomass yield. BSF larvae consume a large amount of food, storing it for the rest of their life. Adult flies require little maintenance due to the large amount of energy gained during the larval stage.

environment-controlled areas to provide the optimal conditions for larval development. After up to 15 days, having reached a target size, the larvae are separated from their food and substrate mix through

sieving and processed in industrial machines to obtain final products (CoRoSect Deliverable 2.2, 2021).

2.1.4 Obstacles to Automation

Across various insect farms and species, processed insects and their larvae differ in size, developmental stages, and behaviour, while these parameters change over time during life cycles. Insect farming requires the processing of very large numbers of individuals, often in the millions (Madau et al., 2020; Ortiz et al., 2016), which demands high-throughput handling systems. However, achieving the necessary scale while maintaining care and precision in manipulation faces significant technical barriers. Many tasks require situational awareness and decision-making, internal processes develop and change over time, and knowledge of rearing processes is held by human experts. Concretely, there is a need for frequent handling of insect batches, depending on the insect development stage, in a non-uniform, corrosive, and confined environment. Low-level processes differ between insect species, but also within the development cycles of a single species. There is no general formula for insect nursing, and even subtle differences within a single batch demand the adjustment of insect management strategies.

Given the short duration of some developmental stages (for example, the egg or pupae in Figure 2.2), there is a strong interest in performing quality inspection and management of batches frequently. Such tasks are intensive in physical operations when very large populations of insects are involved, and are commonly generalised to batches of containers because constant manual inspection is infeasible. However, identifying pathogens and faults early allows action to be taken before entire batches are contaminated, which otherwise results in a direct loss of value for the insect farm. Even under optimal conditions, morphological differences between life stages or between healthy and unhealthy individuals can be subtle, requiring expert knowledge and dedicated AI-driven recognition systems. The small size and high

mobility of insects, especially larvae, make them difficult to detect and assess accurately using machine vision systems. Inspection is further complicated by the fact that insects are frequently partially embedded in their substrates. This potentially renders external imaging unreliable without disturbing the container, meaning some form of sampling or physical manipulation is typically required for each inspection process, increasing the physical involvement of the task. The required frequency and intensity of such inspection and insect management processes, especially when entangled with varied parameters within an insect species and increasing population sizes, is a core motivation driving the need for versatile automation solutions.

A clear technical obstacle derived from insect life cycles is the need for highly controlled environmental conditions of temperature, humidity, and pH, which vary over the development stages. The environment becomes highly corrosive or filled with particulate matter, which, despite preventative measures and industrial standardisation, is damaging and undesirable for robotics and machinery. Certain technologies described in the chapters of this thesis are particularly guided by this requirement to operate in a hazardous workspace, for example, the selection of actuators in Chapter 3, or the electrical components listed in Chapter 5. Furthermore, rearing facilities are typically humid, warm, and dimly lit, creating conditions that interfere with the reliability of conventional imaging equipment or dedicated machinery. Material handling is problematic in this environment because insect farming involves both the movement of the insects themselves and the substrates in which they are reared. Larvae, pupae, or adult insects are often cultivated in organic materials such as food waste or by-products (Madau et al., 2020; Ortiz et al., 2016). Rearing substrates are irregular, moist, variable in texture, ill-suited to mechanical processing, and hence challenging for a robot to handle. These properties make gripping, sorting, and transferring them with machinery or robotic systems error-prone and risk damaging the organisms, undermining the productivity and welfare of the farm.

Furthermore, during insect-rearing processes in insect farms, a variety of tasks involve both the direct handling and sampling of insects (for example, for sorting insects) as well as the handling of diverse objects specific to each insect species (such as feeding devices and support structures). Tasks that involve irregular, deformable, or cluttered objects often demand high-precision sensing, adaptive control, or learning-based approaches that go beyond stable solutions available on the market (Bodenhagen et al., 2014; D'Avella et al., 2023; Dmytriyev et al., 2024). Additionally, solutions in logistics and storage of insect containers require both optimisation of space and intelligent decision-making for the processing of specific batches depending on the insect life cycle stage. These tasks are typically operated manually, becoming bottlenecks to the farm's output without automation. As the industry develops, processes and tasks are subject to changes and optimisation, making full-scale industrialisation difficult, particularly when large amounts of capital are required. Another challenge lies in the limited manipulation and perception capabilities of many commercially available robots. This can increase the complexity and cost of implementation, particularly for SMEs lacking in-house robotics expertise. With limited reachability, degrees of freedom, and payload capacity, articulated robots may not yet be suited to all industrial environments (Makulavičius et al., 2023). However, as the range of a robot's capabilities might increase, its efficiency has to be upheld for a return on investment in industries (Andersson et al., 2021; Pietrantoni et al., 2024; Rahman et al., 2024).

2.2 CoRoSect Use Cases and General Requirements

2.2.1 Use Case Selection

In collaboration with the insect farm partners of CoRoSect (namely Nasekomo, Entomotech, Entocycle, Italian Cricket Farm, and Invertapro), specific processes were identified as high value for automation. These processes provide tangible benefits for the insect

farm in reducing labour intensity and increasing productivity, and were initially proposed based on their economic interests. While there are various expensive, hazardous, and time-consuming tasks unique to each insect species during the rearing processes, not all tasks pose technical challenges that require the development of intelligent, adaptable systems such as cognitive robots. Along with the scientific and industrial partners, the selected processes were then developed into CoRoSect **Use Cases** using lean and agile principles of system design, a series of reverse pitches, selection, and prototyping (CoRoSect Deliverable 2.1, 2021). Therefore, the use cases defined in the following section focus on the end user while accounting for technical feasibility, scientific interest, and the potential to contribute insight into more general concepts in robotisation. The final selection of use cases balances the end users' business value indicators with the technical feasibility scores and ambition of the required system. The entire process and complete specifications of each use case from the perspective of both the technology and insect farming partners of CoRoSect are found in (CoRoSect Deliverable 2.1, 2021).

The overall goal of CoRoSect was to develop a service-oriented, human-robot collaborative working environment to support and enhance the entire production pipeline in the insect farming industry, relying on the RAMI 4.0 reference architecture. The use cases relate to two main insect rearing activities in need of automation: A) Quality Management and B) Insect/Oviposition Management:

- A) Quality management is a vital step in the development of crickets, mealworm larvae, and BSF larvae, ensuring the insects have reached a target mass and size by the time they are harvested, and assuring the quality of the resulting products of proteins and oils. Quality management is typically first performed visually by an expert to estimate that the size of a population within a crate is sufficient. Sampling is performed manually by capturing some insects and measuring them in a laboratory.

	Quality Management	Insect Management
Acheta Domesticus (Cricket)	Visual Inspection	Cricket Nursing and Harvesting
Tenebio Molitor (Mealworm)	Visual Inspection and Sampling	Oviposition Management
Hermetia Illucens (Black Soldier Fly)	Visual Inspection and Sampling	Oviposition Management

Figure 2.4: Use Case breakdown by insect species and quality/insect management. Quality management requires taking a sample of insects for mealworms and BSF due to the larvae burrowing into their substrate. Insect management for crickets consists of nursing during the development of nymphs into adults. Mealworm and BSF insect management use cases focus on handling adult insects that deposit eggs into ovipositioning devices, which need to be carefully handled and replaced.

- B) Insect management is a wide description covering the individual maintenance and nursing steps undertaken by insect farm workers while the insects and larvae are developing, for example, providing food and water. Oviposition management is the handling of delicate eggs after they are laid by adult insects. Since each insect species is reared through unique processes and requires unique materials and machinery, the following sections cover the definition of the specific steps involved for each species, forming six CoRoSect use cases.

A particular challenge common to all use cases is the desire for a system that is adaptable to changing internal processes and rearing techniques. As a developing industry, insect farms are still optimising their techniques and may plan to expand their production to include multiple insect species. Investing in large-scale automation of a single production process may dramatically improve output, but it will be wasted if the species is deemed undesirable or an alternate rearing method is developed. Classical industrial machinery may sometimes be repurposed, but it is typically dedicated to a single task that it performs very well. Robotisation, particularly under the framework of Industry

4.0 and versatile automation, provides the needed versatility to changes in automatable processes. This concept is formalised as Requirement 1.

Requirement 1

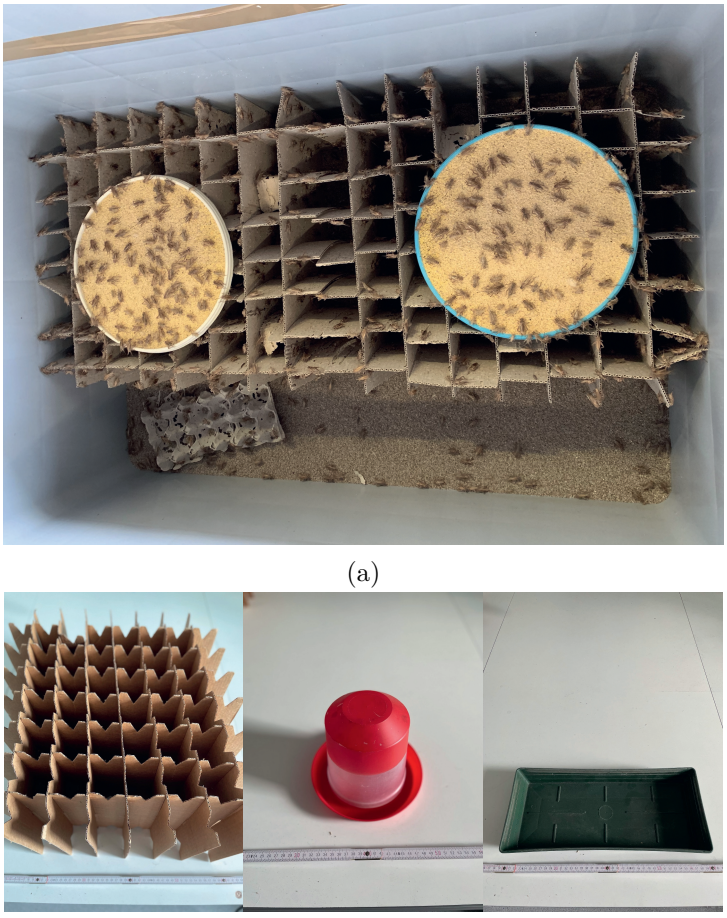
An insect farm investing in an automation solution is interested in **Minimising Costs** and **Maximising the Return on Investment** from the proposed solution.

In the context of robotics development, this means robotic components need to efficiently accomplish tasks and be utilised as much as possible with minimal downtime. Additionally, expensive components that are used only on specific occasions are not worth investing in.

2.2.2 High Level Process Overview: Crickets

Cricket crates are tall and wide (120x80x80)cm to prevent the insects from escaping (Figure 2.5a). The crates fit onto standard Europallets. Cardboard structures (Figure 2.5b) constitute their living space, allowing the crickets to climb to food and water contained in food trays (Figure 2.5d) and re-purposed drinking devices (Figure 2.5c). The insects themselves are commonly obscured except when feeding. Any sampling process is difficult due to the high agility of the crickets and their tendency to run away.

Visual inspection is used to determine whether a crate is ready to be harvested. It is performed at regular intervals, depending on the development stage of the crickets. Crates are typically inspected visually, either in a storage area where they are stacked or brought to a laboratory for thorough analysis. Automation of visual inspection, where the knowledge of experts can be leveraged to produce a labelled dataset, involves a high-resolution camera to take images of the contents of cricket crates. Analysis of rearing parameters, such as



(a)

(b) (c) (d)

Figure 2.5: Materials involved in cricket farming. (a) The interior contents of a tall cricket crate, filled with two cardboard structures and circular food trays. (b) A single cardboard structure, unfolded into a lattice. It easily folds into a flattened form for efficient storage. (c) A single drinking device, containing up to 2L of water that drips down into the bottom rim. (d) A rectangular food tray, without feed.

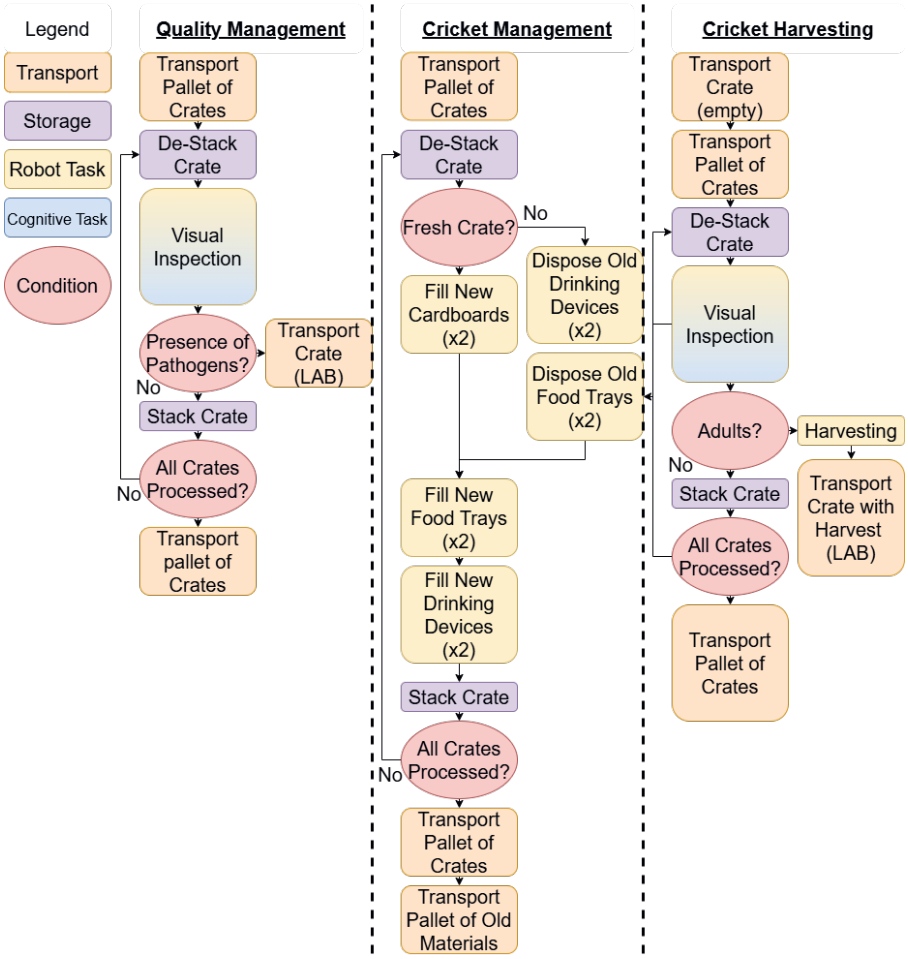


Figure 2.6: Cricket farming use case processes. Quality management is performed visually for the detection of pathogens and cricket development. Cricket management involves filling new crates with the materials in Figure 2.5. Depending on the lifecycle stage, fresh crates are filled, or old material is first disposed of from occupied crates. Harvesting requires the crickets to have reached a desired size, which is confirmed visually.

average size/weight/pathogen detection, is allocated to machine learning models, which are covered in (Papadopoulos et al., 2024) and Chapter 6. Due to their dimensions, the crates would have to be moved out of the storage area into an open workspace. A common automation approach may be to mount a camera above a conveyor belt where crates pass underneath for imaging. However, a camera mounted statically or with limited degrees of freedom cannot get close enough to obtain high-quality data of the individual crickets. While it may be possible to tailor a specific sensor configuration, an articulated robot capable of fitting into the opening of the crate, while carrying a camera, can obtain highly precise images of clusters of crickets for analysis.

Quality management and other well-established processes already existing within insect farms rely on the knowledge and expertise of workers. Augmenting existing processes with autonomous systems, for example, a dataset to train a visual inspection machine learning model, requires this expert knowledge. With the implementation of Industry 4.0, robotic components take advantage of the domain knowledge of humans through collaboration, supporting them in physically and cognitively challenging tasks. CoRoSect aims to take advantage of this, defined as Requirement 2.

Requirement 2

Human-Robot Collaboration (HRC)

Relying on the RAMI 4.0 reference framework, CoRoSect aims to leverage the already-established knowledge in insect rearing existing within insect farms instead of replacing it with automation. Through HRC, robots and workers collaborate on physically and cognitively challenging tasks to boost productivity and quality of work.

Insect management and subsequent harvesting involve nursing of the crickets as they grow to a target size. The crickets will consume their food and water over several days. Fresh food is placed in new, cleaned

trays as the old ones are taken away for sanitary reasons. The drinking devices are filled with water and lined with paper towels to prevent the insects from drowning. This cycle repeats every set number of days for each crate. The process is performed manually by workers, who place material into crates irregularly to prevent crushing insects caught underneath. It can be broken down into three sub-processes: a) filling a fresh empty crate to be ready for new insects, b) maintenance of replacing old food and water in an inhabited crate, and c) disposing of old food and water to empty the crate for harvesting. These processes are depicted in Figure 2.6. Harvesting involves vigorously shaking the cardboard residences of the crickets for them to drop into the crate, which will be emptied into a sorting machine. The crates need to be brought out of the storage area to be filled or harvested.

Obstacles to automation pertain to the size of the cricket crates, the spaces between which they need to be transported, and the non-standardisation of the materials used. Storage and transport need to be space-efficient in smaller facilities. The workspace where crates are manually filled with food trays, drinking devices, and cardboard structures is not highly controlled, meaning items are placed irregularly and may not have a steady source. Fresh material needs to be transported to this workspace while also disposing of used items. Cricket rearing utilises some unique materials compared to the other two insect species considered in CoRoSect. Their dimensions and geometry are standard, but would optimally be handled by dedicated tools that ensure proper orientations and placement. An articulated robot arm is a natural choice for reaching into the tall crates and handling materials inside, but the lack of alignment and consistency will impede performance. This highlights the need for an adaptable system, which can handle the tasks involved in cricket rearing, but can also generalise to other insect species and processes if necessary. This is formalised in Requirement 3.

Requirement 3

Versatile Automation

The robotisation solution developed by CoRoSect is required at various stages in the life cycle of various insect species. To adhere to Requirement 1 in minimising costs for the industry, a single system that is interchangeable at different points in the production line is the most desirable outcome. In the context of robotics, this indicates a need for versatile manipulation to handle various types of materials, error-correction strategies for operating in a non-highly-controlled environment, and modularity to be adaptable across farm configurations.

2.2.3 High Level Process Overview: Mealworms

Mealworms are reared in small, commercially available crates (60x40x20)cm or (60x80x20)cm (Figure 2.7), within which adult beetles and their larval form are stored in separate batches. The adults are stored within special inlays that fit tightly into these crates (Figure 2.7a), where the adult beetles lay eggs (hence the inlays are called ovipositioning inlays/devices). The inlays are also filled with substrate, which is eventually sieved through the porous bottom surface of the inlay when collecting eggs. Hatched larvae are kept in the same type of crate, albeit without the inlay. The crate is filled with substrate and feed, and larvae are dosed on top (Figure 2.7b), allowing them to live encompassed by the organic material. The crates are easily stacked and stored in climate-controlled environments, only taken out when it is time to add food, perform an inspection, or harvest. Larvae at stages of development of 5, 7, and 9 weeks old (just before harvesting) were selected by the insect farm for the CoRoSect pilot studies.

A critical challenge in quality management for mealworm larvae is that the larvae burrow into the crate of wet feed and substrate, meaning they are seldom visible from the surface. For any form of



(a) (b)

Figure 2.7: Mealworm rearing crate and ovipositioning device. (a) The ovipositioning inlay fits tightly into the insect crate and is filled with substrate (in various amounts). Adult beetles are deposited atop, where they lay their eggs. The beetles are separated later by sieving the substrate (with eggs) out through the bottom surface of the inlay. (b) The larval mealworms live in the same type of crate, encompassed by substrate and feed until they are ready for harvesting.

visual inspection to be performed, a sample is taken, where the excess material is sieved/sorted out, and the insects are inspected in a laboratory. The sample has to be large enough to be representative of the population of the crate, although samples are usually made per batch of crates. This process is performed before harvesting and at regular intervals. Strategies to sample enough larvae involve stirring the substrate or locating clusters beneath the surface. Performing this manually allows a worker to carefully take a large enough sample without harming the insects. Any approach to automating the sampling process needs compliant and delicate tools that do not kill insects during sampling, while still having industrial throughput in

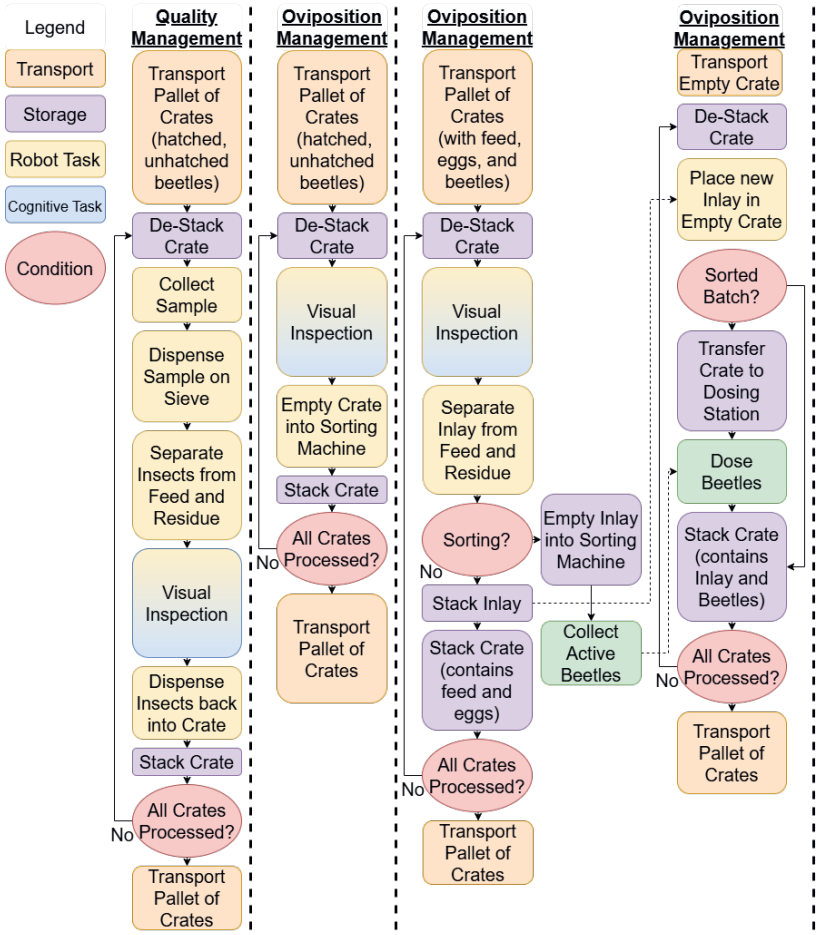


Figure 2.8: Mealworm farming use case processes. Quality management requires sampling a crate of larvae (Figure 2.7b) to be analysed by experts. Oviposition management is performed in various sequences, each resembling a stage in the life cycle. From the left column, hatched and unhatched beetles are sorted. In the next column, the crates with filled inlays need to have the eggs and substrate sieved out and the beetles collected. Inlays are stored separately. The beetles and empty inlays are transitioned to the final column, where a new batch of beetles is prepared for laying eggs.

crates inspected per day. Existing industrial solutions to sieving and sorting expedite the process, but require an autonomous system with visual and force feedback for sampling, reinforcing Requirement 3. A collaborative articulated robot can provide both of these, commonly featuring integrated force sensors for safety and can be easily outfitted with a visual sensor. Widely important among all use cases, insect well-being becomes Requirement 4.

Requirement 4

Insect Well-Being

Crushed eggs, larvae, or adult insects pose a tangible loss for an insect farm, resulting in lower end-product yield and hence a loss of profit. In particular, automation solutions with a high attrition rate, despite high throughput, are undesirable from an economic and ethical standpoint.

The oviposition management of tenebrio molitor use case focuses on the management of adult beetles within the oviposition inlays. The three columns titled 'Oviposition Management' in Figure 2.8 are an interconnected flow of three processes: collecting eggs, sorting beetles, and preparing new generations. Empty inlays are placed within freshly cleaned crates where a new batch of beetles is deposited, along with substrate and their diet of food (the crate will resemble that in Figure 2.7a). The beetles are kept until they lay eggs within the oviposition inlays. When the eggs are collected, the inlay is first shaken to sieve the substrate and eggs out into the crate, with the beetles remaining in the inlay. The crate, containing unhatched/hatched eggs, is emptied into a sorting machine to remove the excess organic material. The inlay, containing the adults, is tipped into a sorting machine, which collects the beetles, ready to be placed into another fresh crate. Both the emptied crates and inlays are then cleaned and repurposed for the next batch. This cycle repeats every incubation period for the eggs. Automation alleviates the workload involved in this repetitive process,

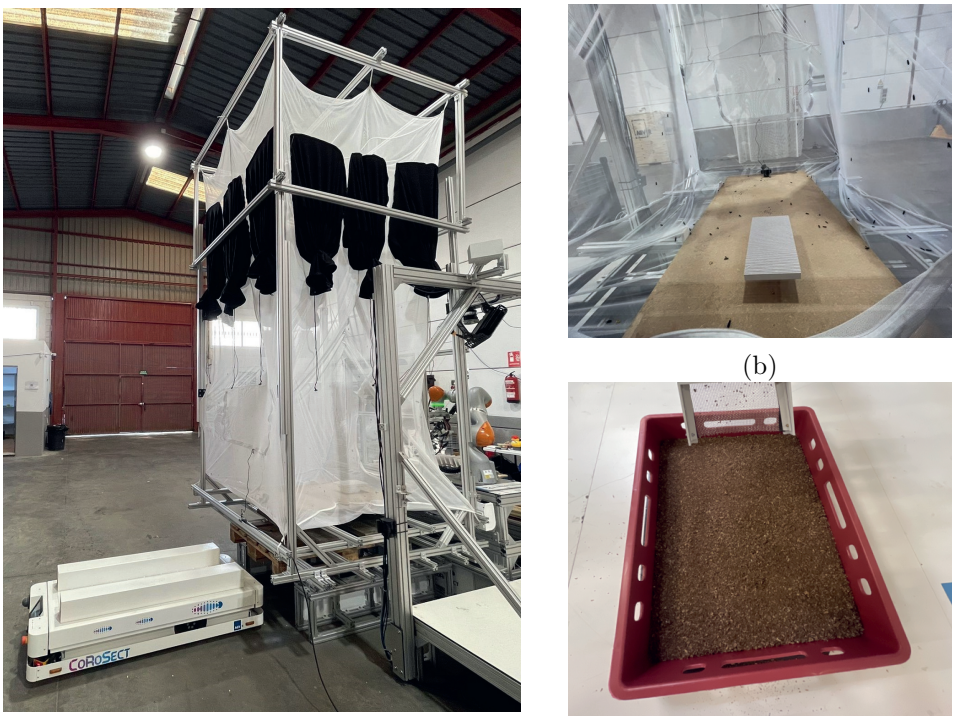
as the atomic operations of emptying crates, inlays, and sorting beetles are straightforward.

The challenges to the automation of mealworm rearing stem from the tight fit of the inlay into the insect crate (Figure 2.7a). While precision is not an issue for industrial machinery, the lack of a controlled environment in other steps of the process can compound errors before the inlay needs to be placed, causing misalignments and failed insertions. The individual steps of the ovipositioning process are highly automatable, with many potential approaches to an efficient and affordable solution. However, the potential for these sequences of tasks to be altered requires an adaptable solution, further highlighting Requirement 3. The advantage of robotisation is the potential to automate multiple stages of the rearing process with a single robotic system (or 'robot cell'), especially when the insect farming techniques are subject to change.

2.2.4 High Level Process Overview: BSF

The overview of the rearing process for BSF larvae is similar to that of mealworms. The larvae are the source of valuable products. At the start of a cycle, the BSF that are allowed to mature into adults for breeding are kept in large mating cages (Figure 2.9a), which provide them with a habitat and prevent them from escaping. The cages are equipped with small proprietary oviposition plates (Figure 2.9b) to collect eggs. When filled, the oviposition plates are removed, and the eggs are placed in incubation spaces. The hatched larvae are stored similarly to mealworms. They are stored in crates, encompassed by their feed and substrate mix (Figure 2.9c). The crates are easily stacked and stored in climate-controlled environments, only taken out when it is time to add food, perform an inspection, or harvest. Larvae at stages of development of 5 and 16 days old were selected by the insect farm for the CoRoSect pilot studies.

Quality management for BSF larvae is a comparable process to that of



(a) (b) (c)

Figure 2.9: Materials involved in BSF farming. (a) Adult BSF are kept in mating cages where they are contained and deposit eggs into special oviposition plates. The cages are tall and typically transported manually. (b) The oviposition plates are placed carefully on a pheromone tray inside the cages to attract the adult females to lay their eggs. (c) Larval BSF are stored similarly to mealworms, although the composition of the food and substrate is different. They are stored within food crates where they are encompassed by their diet mix and substrate.

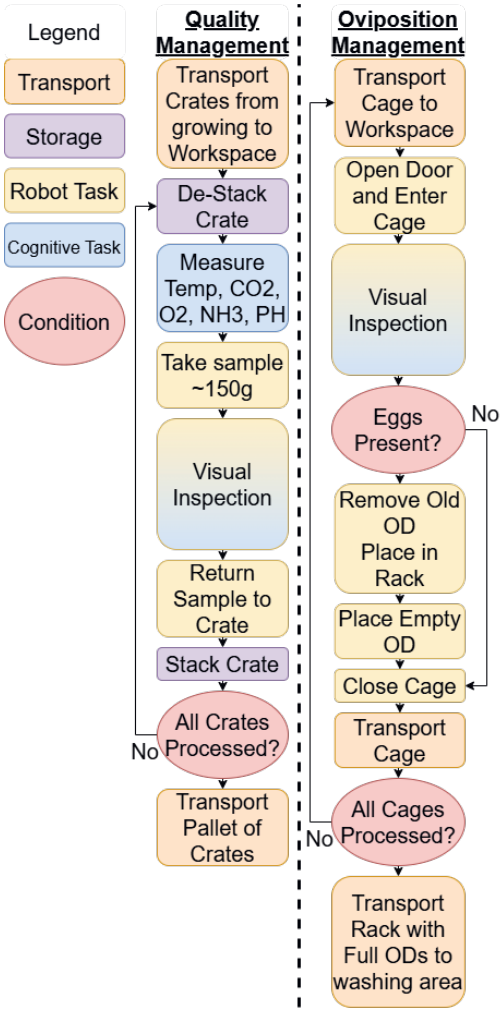


Figure 2.10: BSF farming use case processes. Quality management is performed similarly to mealworms, with a sample taken at regular intervals for inspection. Oviposition management consists of entering a mating cage and checking for eggs within the oviposition plate. Upon the presence of eggs, the plate is replaced with a new one, while preventing flies from escaping through the opening of the cage. The plates filled with eggs are stored gently in racks to be transported to an incubation area.

mealworms, where the larvae have burrowed into their substrate and must be sampled. The same challenges for sampling are present here, although with a different composition of substrate and food diet (Figure 2.9c.

Oviposition management for BSF requires operation within a heavily constrained area inside the mating cage (Figure 2.9a). Work is performed manually inside by a worker, replacing the oviposition plate carefully to prevent crushing eggs, and keeping the adult flies from escaping through the opening. Filled plates are placed into maturation racks and stored in climate-controlled environments. Empty plates are immediately refilled to continue the breeding process. Although the repetitive process is straightforward (Figure 2.10), the mating cages are not suited for classic industrial machinery and require a system capable of reaching deep into the cages through a small opening without damaging the mesh or crushing insects. Without extensive adaptation of the design of the mating cage, flies are bound to escape during the operation by a machine. Additionally, the eggs laid within the ridges of the oviposition plate are delicate enough to be crushed if pressed too hard, meaning compliant and soft elements are needed to prevent a loss. The significant lack of operational space heavily limits the potential automation solutions, and the cages are too large to be transported traditionally (e.g., with a conveyor belt or an overhead hook conveyor).

2.2.5 Summary

The identified use cases involve handling three distinct insect species: crickets, mealworm beetles, and BSF, along with their larvae. Each species is reared using unique processes and materials, as described in the section above. To develop a robotised platform to support and complete the rearing processes involved in these use cases, four high-level requirements have been identified. These general requirements for the CoRoSect robotic system are summarised as follows:

- **Requirement 1** Minimise costs. Maximise return on investment. Robotic components need to be utilised as much as possible, minimising downtime and creating value relative to their cost.
- **Requirement 2** Human-robot collaboration. Retain expert knowledge and increase productivity under the RAMI 4.0 reference framework.
- **Requirement 3** Versatile automation. Adaptability across a variety of processes and insect species.
- **Requirement 4** Insect well-being. Minimise the loss of value during repetitive tasks from an economic and ethical context.

These definitions are referenced throughout this thesis and are used to motivate design choices for a collaborative robotic platform, its add-ons, and software. Concurrently, these requirements narrow down the range of potential applicable technologies that fit into the CoRoSect ecosystem. Following Industry 4.0 standards, this ecosystem consists of digitised cognitive robotic systems that additionally need to satisfy these general requirements to be beneficial to insect farming stakeholders. Section 2.3 proceeds to define the CoRoSect ecosystem and the approaches to technology development that fit into this paradigm.



2.3 CoRoSect Ecosystem

The following sections describe the overall CoRoSect technical approach to automation within insect farming, providing context for the robotic technologies described within this thesis. The design choices of the final system architecture are motivated by the requirements and use cases described in Section 2.2.

2.3.1 Overview

CoRoSect's fundamental aim was to develop a framework for cognitive robotic systems that automate various stages of insect rearing, including tasks such as crate handling, environmental monitoring, larvae separation, and insect feeding, defined by the **use cases**. By replacing repetitive, physically and cognitively demanding manual labour with robotic procedures, the project optimises the biological, technical, and economic aspects of insect farming. The approach to automation was to create a collaborative environment where humans and robots undertake different crate processing and material handling tasks.

During insect rearing processes, repetitive tasks are performed, which involve both rigid materials, such as feeding and ovipositioning devices (Madau et al., 2020), and the direct handling of insects. Figures 2.6, 2.8, and 2.10, which show task sequences that are candidates for automation, clearly define four types of operations common between all use cases:

- **Transport**: Logistics inside the insect farm where an insect crate or material needs to be moved for a process to be accomplished (for example: moving crates to storage areas).

- **Storage**: The handling of insect crates. Stacking for storage and de-stacking for processing.

- **Robot Tasks**: Day-to-day operations that are performed during the insect rearing process, typically within insect crates. Candidates for automation.

- **Cognitive Tasks**: Processes requiring the processing of information or decision making.

The overall envisaged system is presented in Figure 2.11 as a universal approach to support rearing different insect species in different warehouse setups. It features not just a set of robotic agents, but is equipped with artificial intelligence, farm-level modelling and orchestration, a decision support system, and human-robot collaboration schemes. The final result is a system integrated with the Reference Architecture Model Industry 4.0 (RAMI 4.0) implemented as an Industrial Cyber-Physical System (ICPS).

To describe the practical implementation of CoRoSect, the standard definition of a **Work Cell** is used (Aghazadeh et al., 2011; Womack et al., 2007). A **Work Cell** is the *"Physical or logical arrangement of all resources (people, machines, material) associated with the performance of an activity, job, or task"*, and is based on the principles of lean manufacturing in (Womack et al., 2007). The notion of the CoRoSect cyber-physical dynamic-Cell (d-Cell) is introduced (Figure 2.12), which represents a dynamic and adaptive system that is responsible for a specific task at a given time. The d-Cell, as a work cell, encompasses and contains all the necessary tools, robotics, and logistics needed to accomplish specified tasks. In simplest terms, the d-Cell is a physical structure that contains all the components necessary for a robot to autonomously perform tasks. Minimally, it houses articulated robot arms that perform work, a workspace platform, sensors, intelligent systems, and accommodates input/output of relevant materials, such as insect crates or oviposition devices.

Figure 2.11: CoRoSect Cyber-Physical components as a conceptual diagram. At the core layer (orange) are intelligent systems for robot control, AI-perception, and human-robot collaboration. These layers interface directly with the physical robotic components (green), and the high-level insect farm management and decision support systems.

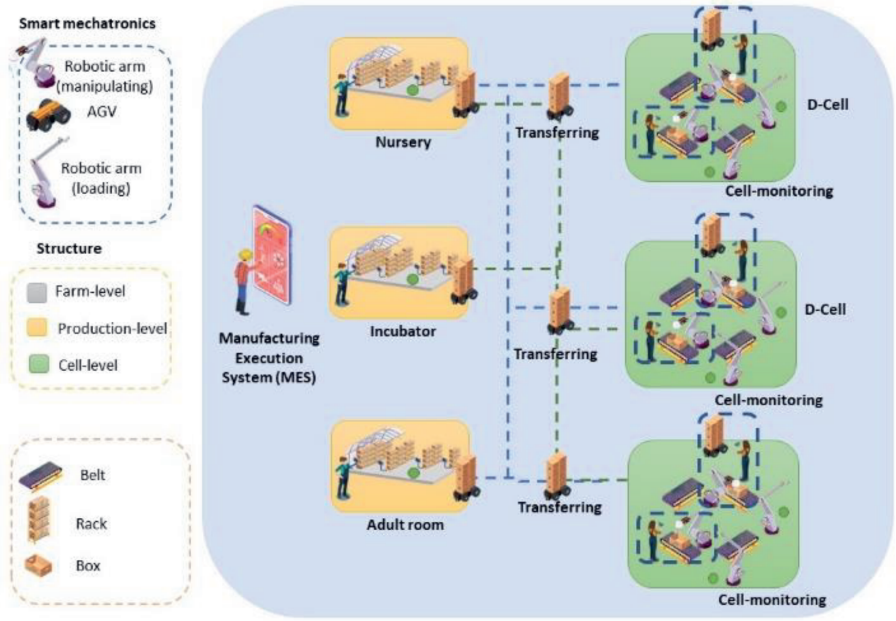


Figure 2.12: Interactions and descriptions of a CoRoSect Work Cell, denoted as the d-Cell. Each d-Cell (green) is a platform that contains all the necessary materials, programming, and robotic agents to achieve defined tasks. D-Cells can be easily parallelised by adding additional cells to increase throughput. Logistics between locations (yellow), such as storage spaces, nurseries, or laboratories, is handled by warehouse logistic robots, such as AGVs.

A concept for the physical workspace, shared by articulated robots, is shown in Figure 2.13. The use of industrial articulated robots over dedicated machinery is often justified by their flexibility, adaptability, and long-term cost-effectiveness in dynamic manufacturing environments (Almurib et al., 2012; Iqbal et al., 2016). Unlike dedicated machinery, which is optimised for a specific task or product, articulated robots can be reprogrammed and retooled for a wide range of applications, supporting mass customisation and agile production systems (per Requirement 3). This makes them particularly suitable for industries facing frequent product changeovers, variable batch sizes,

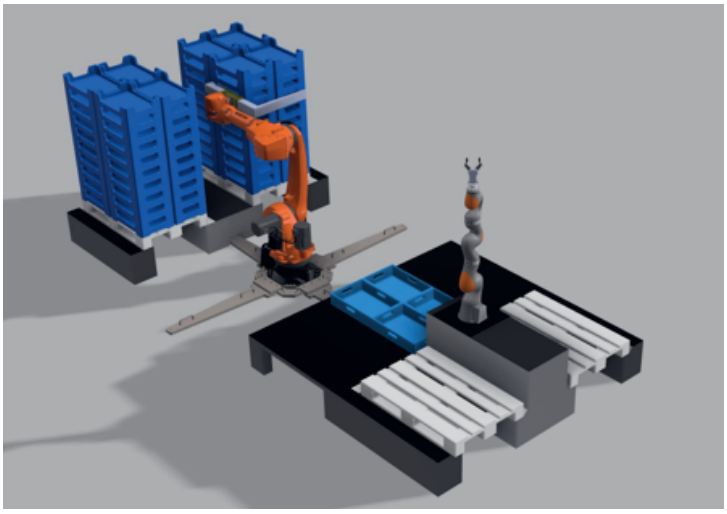


Figure 2.13: A CAD concept of a single CoRoSect d-Cell, containing two articulated robot arms. The d-Cell features the input of pallets of insect crates as material intake, and encapsulates the two robots needed to process these crates. Processing, either through insect or quality management tasks, is performed in a shared workspace to optimise the space needed for the d-Cell.

or evolving production requirements. Furthermore, articulated robots enable greater spatial reach and complex motions, allowing them to perform intricate tasks along multiple axes that would otherwise require multiple dedicated machines. From a systems engineering perspective, they also offer modular and scalable manufacturing architectures for robustness in Industry 4.0 contexts.

2.3.2 Robotic, Digital, and Intelligent Components

Following from the formulation of a CoRoSect Work Cell (d-Cell) and the definition of use cases as sequential operations (Section 2.2), the concept of the d-Cell is refined into multiple well-defined robotic components. The d-Cell encompasses the capabilities to autonomously carry out each of the following operations:

- **Transport** of insect crates between storage areas and workspaces is realised using an Automated Guided Vehicle (AGV) with an integrated sensor for navigating through the insect farm. AGVs offer consistent, 24/7 performance, improve inventory tracking, and integrate seamlessly with modern warehouse or production systems. They are especially valuable in repetitive or high-traffic transport tasks, and can handle various payloads, addressing Requirement 3.
- **Storage**, or rather the (de)stacking and moving of insect crates between the workspace and the AGV, is achieved using a fixed high-payload-capacity industrial robot, classically used in the automation industry. A specialised end effector allows gripping both large cricket crates and smaller crates used for mealworms and BSF larvae.
- **Robot Tasks**, the day-to-day insect nursing and management operations, require dedicated robotic equipment for fine manipulation. A robotic arm equipped with machine vision capabilities and appropriately designed end effectors handles repetitive work in insect nursing and quality management use cases.
- **Cognitive Tasks** are handled through various services such as AI-enabled perception, robotic action planning and control, and human-robot collaboration schemes, to handle assigned tasks. During the growing stage, larvae are checked using sensors installed in intelligent insect crates, measuring temperature, metabolic gases production, food consumption, and vibration. Based on the sensor inputs, decisions are taken regarding the type and amount of nutrition. The size of the larvae is measured by using machine vision to decide whether they are ready to be transferred to the next stage.

The system operates on the basis of a service-oriented model. The resources, responsibilities and interconnections between multiple d-Cells are managed by a high-level system, which is

capable of advanced floor state monitoring and real-time task assignment/adaptation. A light-weight Information Management System (IMS)/Manufacturing Execution System (MES) supports task allocation throughout the farm, overall task planning, as well as real-time adaptations.

Four important cyber-physical components are featured:

- **(Undercrawler) Automated Guided Vehicle (AGV)** A robotic component responsible for logistics inside the insect farm, used to transport stacks of insect crates between storage and workspace areas.
- **(De)Stacking Robot (D-Robot)** Loading and unloading the stacks transported by the AGV is performed by an articulated robot arm with a high load capacity to handle heavier insect crates.
- **Stationary Manipulation Robot (M-Robot)** Operation of dextrous and delicate tasks within crates, such as quality management and feeding, is performed by a second articulated robot arm for fine manipulation.
- **Intelligent Crates (ICs)** The adaptation of insect crates into networked components for monitoring insects and crate internal conditions such as temperature and pH.

Together, these components comprise a single system for processing insect crates. The general configuration of robotic components is depicted in Figure 2.14. The ICs monitor the crates, providing real-time insect well-being information to high-level management systems. These management systems access the robotic components to process crates at specified intervals, for example, to perform harvesting of grown larvae. During the rearing process, insect crates are stacked and stored in special environment-controlled storage areas. Due to corrosive or humid conditions and the need for efficient storage, it is impractical to place robots in the same area. Processing crates is hence performed in an external workspace, meaning the crates are taken out

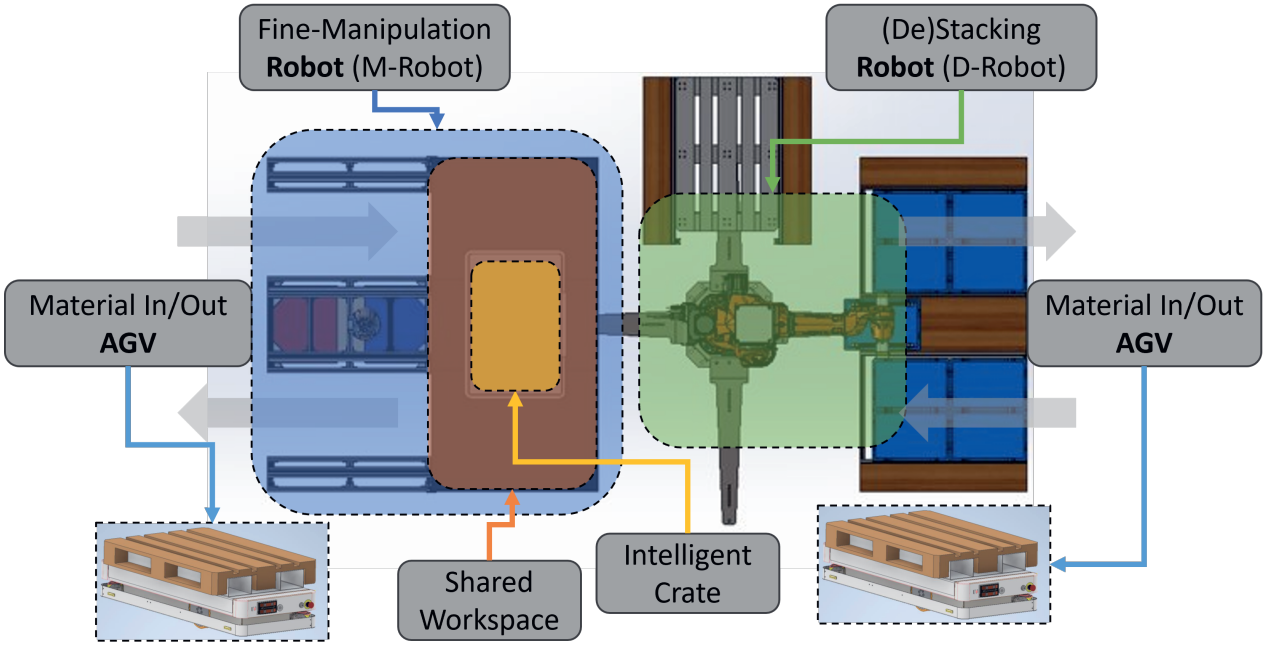


Figure 2.14: CoRoSect robotic components of the d-Cell annotated diagram. The intelligent crates (yellow box) are de-stacked into a shared workspace (orange box) by the D-Robot (green box) to be processed by the M-Robot (blue box). Image credit: (CoRoSect Deliverable 7.3, 2023; CoRoSect Deliverable 7.4, 2023)

.

of the storage area. This is handled by the AGV, which is capable of transporting pallets holding batches of crates simultaneously, to ensure the system can reach an industrial scale of throughput. The AGV lifts batched insect crates and can transport them between relevant positions designated in the insect production process. From the use case definitions in the previous section, each crate is processed individually, needing to be either filled with feed and water, an oviposition device, or inspected through direct sampling. Additionally, when stacked, the space between the crates is too small for even a small robotic manipulator to be inserted. Therefore, de-stacking of the crates from the AGV is performed by a high-payload-capacity industrial robot, nicknamed the D-Robot. The high payload capacity is required to handle the large cricket crates. The operations involved in nursing and sampling insects are too delicate for a large industrial robot, presenting the need for a smaller, gentler robot for fine manipulation, nicknamed the M-Robot. Therefore, when de-stacked by the D-Robot, the crates are placed into a workspace shared with the smaller M-Robot, which can perform the repetitive and delicate tasks involved in insect rearing. The crates are then stacked to be taken back to storage by the AGV and monitored through the ICs. The interactions between these robots in processing a pallet of crates accomplish the task sequences defined by the CoRoSect use cases. The resulting configuration of the cyber-physical components takes the form of a shared workspace between two articulated robot arms (D- and M-Robots in Figure 2.14) supplemented by the AGV in material transport and processing ICs.

The CoRoSect M-Robot

The main focus of this thesis is on the design, development, and deployment of this collaborative robot (Figure 1.4, which innovates in the area of robotic versatility and material handling. The term 'M-Robot' (also referred to in chapters as the *'robot cell'*) identifies a robotic system for fine manipulation in delicate and

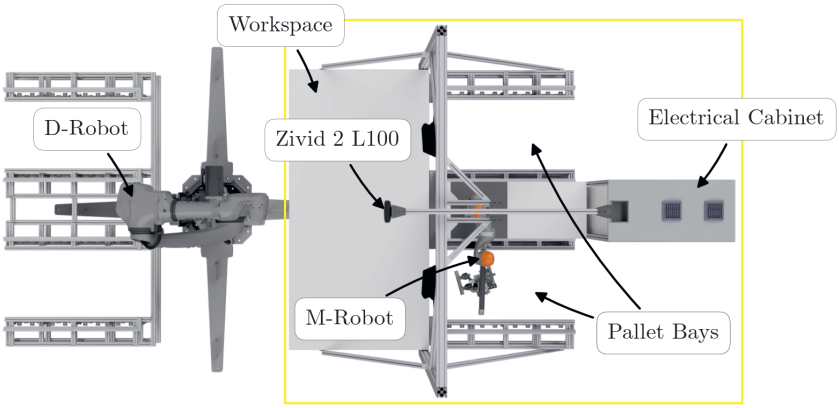


Figure 2.15: M-Robot is part of the CoRoSect d-Cell, sharing a workspace with the D-Robot. Its physical structure encompasses the workspace platform, surrounding support structure, pallet bays for material intake, and an electrical cabinet. Its construction is the topic of Chapter 5.

collaborative tasks, used specifically for day-to-day operations in insect management, nursing, and quality management (operations summarised under **Robot Tasks**). Per the dynamic conditions in insect farming (Requirement 3), robotic systems need to adapt to changing processes without the involvement of major reconfiguration or re-training. This is still an unsolved problem. However, if a robot were to gain such abilities, it would allow insect farms, but also other industrial and agricultural applications, to quickly exchange materials and develop new processes.

The M-Robot is a platform consisting of a collaborative articulated robot arm, namely a KUKA LBR iiwa 14 R820, accompanied by an infrastructure of supporting structural, mechanical, and intelligent components. The entire physical structure, referred to as the 'robot cell', is shown in Figure 2.15 in relation to the larger D-Robot. The robot cell accommodates sensors, computing infrastructure,

controllers, and mounted tools. The iiwa, as the main load-lifting component, is a 7-degree-of-freedom collaborative robot arm intended for industrial use, capable of lifting up to 14kg at the flange. Although its carrying capacity is shown to be necessary for operating at insect farms, a limitation of many collaborative robots is the limited reach within the workspace, as these robots are typically smaller than their industrial counterparts.



Figure 2.16: Mobile platform KUKA KMR iiwa. Image credit: (KUKA, 2018).

A static workspace is shared between both the D-Robot and the M-Robot, with safety protocols in place to avoid collisions. This is chosen instead of the alternate approach of a mobile manipulator, such as the iiwa mounted to a mobile platform in Figure 2.16. While mobile platforms are popular in the automation industry, they are not practical inside an insect farm. There is limited space to navigate within the storage areas, which are closed off for precise climate control. While it is possible to enter and navigate within, the movements of the mounted robot arm pose a danger to the stacked crates and cannot be easily parallelised using multiple robots. The tightly packed storage of insect crates in vertical stacks requires a stacking/de-stacking solution regardless of the mobile platform, increasing the complexity of the system. The duration of long task sequences and the need to process numerous crates sequentially leave a mobile platform largely unused while the articulated robot on top is operating. The high costs of mobile platforms, with respect to their expected utilisation, indicate they would not be worth the investment for the insect farms (per Requirement 1). Conversely, a static platform provides a stable structure that absorbs operational loads and mounts sensors to observe the robot's operating area. Within a non-highly-controlled environment, additional sensors and cameras are necessary to effectively handle dynamic object placement, error

correction, and safely collaborate with human co-workers. However, this external workspace requires materials to be brought to it instead. These services are provided by the D-Robot and AGV, which position insect crates and materials such that everything necessary for a specific task is within operational reach of the M-Robot. While the costs incurred by the AGV and D-Robot outweigh those of a mobile platform, this solution is both scalable by modularly adding additional workspaces and the utilisation of the robots is maximised, as the AGV and D-Robot are constantly performing load-lifting and logistics around the insect farm (per Requirement 1). The static area also provides a collaborative workspace for safe human-robot interactions (per Requirement 2), ensured by additional sensors and a collaborative robot arm.

The M-Robot consists of multiple components required to operate in a non-highly-controlled environment and be adaptable across insect farming configurations (per requirements 3 and 4). The KUKA iiwa collaborative robot is extended with a custom-designed robot extension (Chapter 3), giving it capabilities in reachability and versatility in tight spaces that other collaborative robots do not have. Adaptability to various processes and materials is handled by a design of versatile hardware, such as a hybrid soft-rigid end effector (Chapter 4), a software architecture centred around a digital twin and motion planning environment (Chapter 5), and the integration of cognitive systems for environment registration and handling challenging dynamic workspaces (Chapter 6). The robot is integrated according to the Reference Architecture Model Industry 4.0 (RAMI 4.0) framework. It publishes data to high-level CoRoSect management systems and receives commands from the insect farm process managers. The final prototype was developed and piloted at real insect farms, shown in Figure 1.4.

2

Digital Infrastructure

Following the RAMI 4.0 framework, every physical (robotic) component is a service provider with a respective cyber-component called a 'digital twin'. This digital representation of the physical component is used to build a service-oriented architecture of information exchange. This architecture links the insect farm's own management systems with shop-floor robotic components through a series of decision-making, process management, and data management modules (Figure 2.17) (Bauer & Mäkiö, 2023). Each cyber-physical component is managed by an Asset Administration Shell (AAS), a digital representation of an Industry 4.0 component, which collects relevant information about the physical component, making this data accessible to other factory processes.

The digital infrastructure performs three main functionalities:

- **Adaptive farm process modelling:** Each use case described in Section 2.2 is modelled as a digital process. The execution of this process relies on using the services provided by cyber-physical components, i.e. the robots in a d-Cell, to undertake the sequence of defined tasks (Figure 2.18).

- **Shop floor management and decision support:** Monitoring of crates and the state of robotic components deployed inside an insect farm is done through data collection and digital twinning. A decision support system uses this information to optimise productivity, resource management, and task scheduling.

- **Service-oriented information management:** Management of historical data, digital twins, and the current state of tasks being operated by the d-Cell is performed by the information management system (IMS). Each physical component provides its internal state and process-data through interface protocols, for example, OPC-UA (Leitner & Mahnke, 2006).

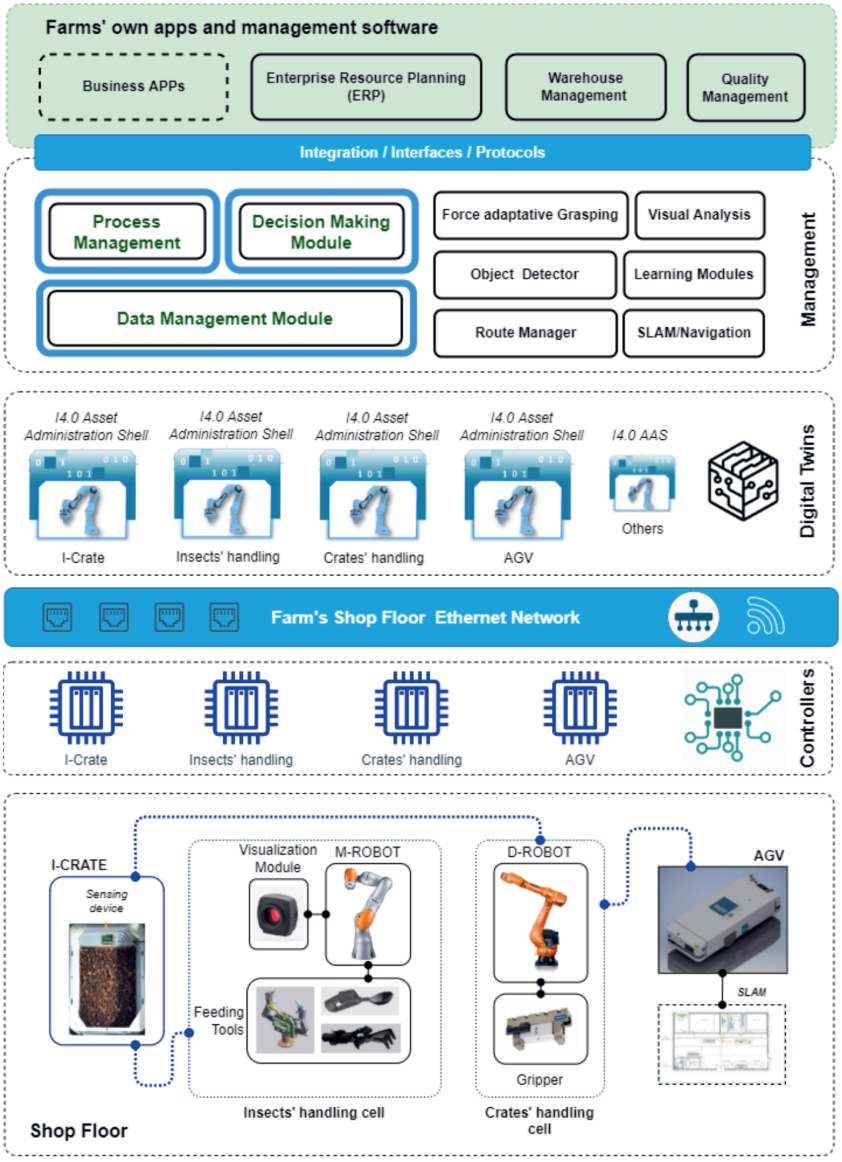


Figure 2.17: CoRoSect Full System Architecture. Credit: (Bauer & Mäkiö, 2023; CoRoSect Deliverable 2.4, 2022).

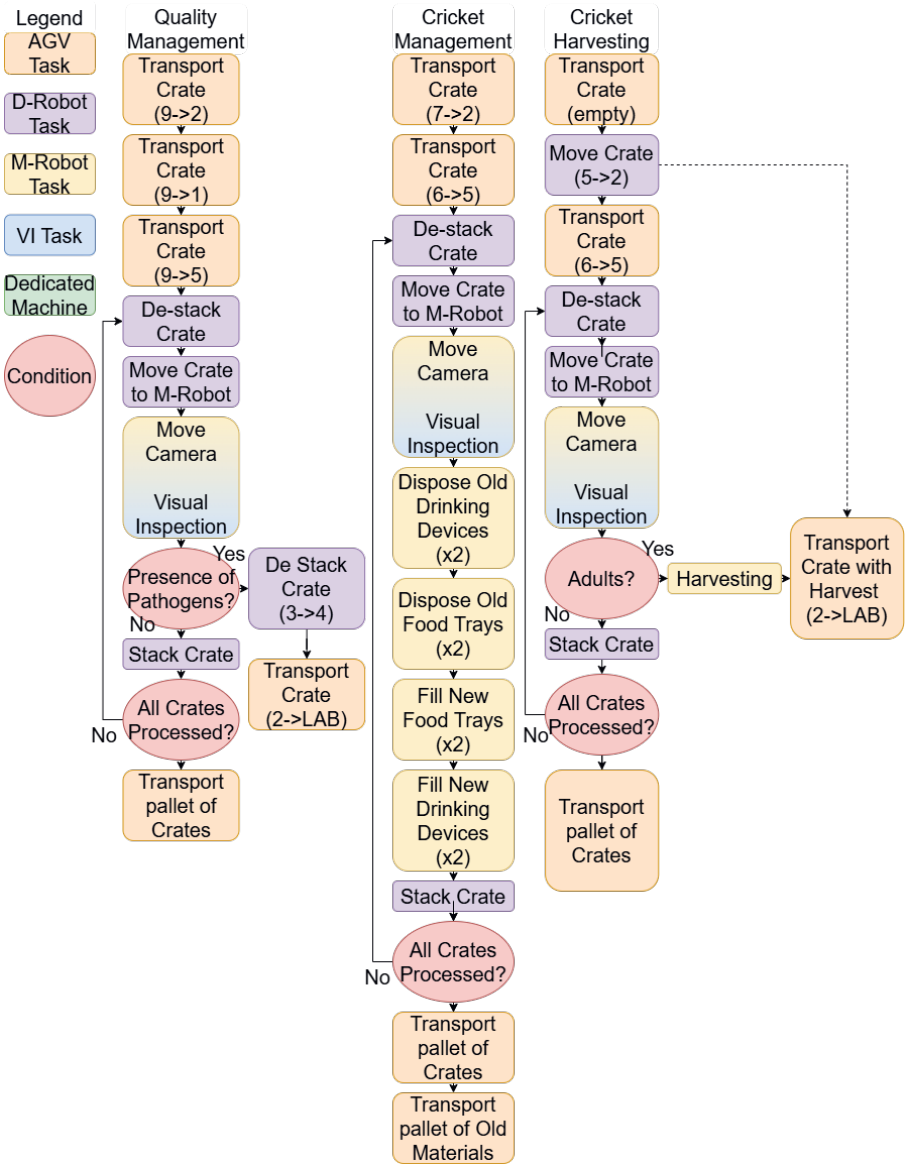


Figure 2.18: Cricket farming use case processes adapted from Figure 2.6 to fit the infrastructure and work cell developed for CoRoSect.

Half of the use cases defined in Section 2.2 are classified as quality management. Regardless of whether the insect population is sampled or not, the quality of a sample is assessed visually, by counting insects, determining their average size (and hence weight), and determining their well-being (per Requirement 4). This method is standardly already used within insect farming and leverages expert knowledge in the field of entomology. Hence, quality management automation in insect farming is also handled through visual inspection using AI models such as YOLOv8, a popular model for high-speed object detection in computer vision (Bhavana et al., 2024; Hussain, 2023; Kim et al., 2023; Varghese & Sambath, 2024). AI models, outlined in detail in (Papadopoulos et al., 2024), are used to process images taken of a sample of insects from a crate. The output is a set of variables on the ongoing rearing process within this crate. These variables include a count of insects within the image, an average size of insects, and an anomaly signal to detect pathogens. The count and weight are used to extrapolate weight and volume, giving an estimate of harvestable biomass in a crate. This information can be used by the IMS/MES to signal the harvesting of a batch.

The specific model used in CoRosSect is a custom-trained YOLOv8 (Papadopoulos et al., 2024), which is used for the detection models for each specific kind of insect.

- YOLOv8 is a member of the YOLO family (Hussain, 2023), which consists of one-stage real-time detectors. It operates at very high frames per second, which speeds up the entire CoRoSect pipeline.

- YOLOv8 showcased its performance on the COCO benchmark, where it achieved State-of-the-art accuracy and overall better mean Average Precision (mAP) compared to predecessors like YOLOv5 and YOLOv7 (Kumar & Kumar, 2023; Varghese & Sambath, 2024).

- Recent changes like the addition of new convolution schemes and the creation of an anchor-free model, which accelerates the Non-Maximum-Suppression (NMS), make it an ideal candidate for insect detection.

YOLOv8 output predictions for the instance segmentation part underwent sophisticated post-processing steps to extract critical data on each larva-insect instance. This process accurately segregates and quantifies key morphological and colourimetric attributes, such as length, width, area, and colour, of each insect, along with providing a total worm count within a frame. Such detailed analysis is instrumental for end-users in making informed decisions regarding the health status of a crate or sample.

2.4 Relevance and Conclusion

This chapter summarises the systematic definition of requirements for a digitised network of cognitive robots intended for insect farming. It provides the context for how the technical content of the following chapters fits into the overall system and advances the scientific contribution of this work. The formalisation of the general requirements is important because they encapsulate the general functions the system must address and, therefore, how the underlying technologies are shaped in the CoRoSect ecosystem.

The focus of subsequent chapters of this dissertation is the development of the cognitive robot for low-level insect handling tasks, as a digitised component in the overall CoRoSect ecosystem. Its development and associated insights into cognitive robotics are both important developments generated out of the CoRoSect project. The general requirements and use cases are referenced as motivation for design decisions and the implementation of robot capabilities throughout the upcoming chapters. In Chapter 3, the design of an extension for collaborative and industrial articulated robots is guided by Requirements 1 and 3, increasing reachability over a workspace and

providing additional degrees of freedom necessary to operate within insect crates and enclosures. Following Requirements 3 and 4, Chapter 4 describes the development and validation of an end effector for versatile material handling. It is designed to address the needs of insect farms and contributes to the field of versatile material handling. Finally, Chapters 5 and 6 present the design of a collaborative fine-manipulation robot for insect farming and the implementation of cognitive capabilities required to address the use cases and guided by Requirements 2, 3 and 4. Both the prototype technologies and their development processes are contributions to creating a framework for automation and digitisation in modern industries, particularly when adaptability, frequent decision-making, and versatile manipulation approaches are needed.

The identification of specific robotic tasks that individually contribute to the completion of insect rearing (Section 2.2) processes highlights the need for networked cognitive systems that interact and address complex use cases in a coordinated manner. The networked systems perform discrete operations but are also capable of allocating resources, adapting to changing conditions, and maintaining resilience upon disruption. Each robotic component is digitised but also makes independent decisions based on the surrounding context, contributing not only to its immediate task but also to the overall coherence of the system. The structure of the CoRoSect ecosystem illustrates that complex processes in insect farming can not be addressed through incremental improvements to existing machinery. Instead, insect farming processes require intelligent systems and robots that handle low-level decision-making, perceive workspaces, interpret observations, and adapt in real time. By demonstrating how digitised cognitive robots can be systematically linked into a networked system, the CoRoSect framework provides both a proof of concept and a reference model for other use cases and industrial applications, such as in automation for agriculture, manufacturing, or healthcare. The architecture of digitised robotic components and data management systems within CoRoSect (Bauer & Mäkiö, 2023;

CoRoSect Deliverable 2.3, 2021; CoRoSect Deliverable 2.4, 2022) is a framework that contributes to the ongoing paradigm shift of Industry 4.0 towards digitisation using data-driven, smart, networked technologies and robotics, which was presented at the FIWARE Global Summit (CoRoSect, 2023; Larrinaga, 2024).

3

Extension of Industrial and Collaborative Robots for Increased Work Space and Operation in Confined Spaces



Collaborative robots, such as the KUKA LBR iiwa, UR series from Universal Robotics, and many more, have opened new fields of applications in industries through human-robot collaboration. However, despite up to seven rotational degrees of freedom typically offered by commercial collaborative (and industrial) robots, the operational reach is often not sufficient. This prevents these robots from reaching into and operating within confined spaces autonomously or in collaboration with human co-workers. To overcome these limitations, this chapter presents a custom-made, open-source,

affordable robot arm extension to be mounted on commercial or custom-made robots. The developed solution adds three additional degrees of freedom, including a $0.5m$ *linear rail. These additional degrees of freedom of the robot extension significantly increase the reach and ability of industrial and collaborative robots to operate in narrow environments. The developed extension is demonstrated by extending a KUKA LBR iiwa 14 collaborative robot operating various insect farming use cases, including tasks such as reaching into crates for insect rearing, operating within caged enclosures, and material handling over a wider workspace. Furthermore, simulations are used to provide insights into the extended reach of the robot. Simulation results show an increase in total operational space by up to* 110%*, and a* 200% *increase in positions reachable from* $\geq 50\%$ *of tested orientations, compared to a baseline KUKA iiwa.*

3.1 Introduction

Collaborative robots (cobots) offer industries a versatile platform for automation that is adaptable across various applications (Dmytriyev et al., 2024; Dusadeerungsikul & Nof, 2019; Galin & Meshcheryakov, 2019; Taesi et al., 2023). Cobots are typically smaller than their industrial counterparts (Almurib et al., 2012; Brogårdh, 2007; Taesi et al., 2023) and feature integrated safety mechanisms, such as force sensors, allowing humans to work nearby safely (Sandini et al., 2024). Despite their versatility, cobots typically only feature six (e.g. UR series from Universal Robotics, CR series from Fanuc, and Motoman from Yaskawa) to seven (e.g. KUKA LBR iiwa robots) degrees of freedom with a maximum reach that is limited in comparison to other industrial robots, making cobots impractical in some industries where more reach or operations in confined spaces is required. Alternative solutions, such as the adaptation of the required industrial processes into a tailored workspace fitting a cobot, can be costly and are not always possible.

In this chapter, we propose an articulated, lightweight robot extension as a cost-efficient solution to increase the reach and ability of collaborative robot arms to operate in confined spaces. To demonstrate the need to extend the DOFs of collaborative robots, we analyse use cases from insect farming. Through these use cases, we demonstrate how the developed robot extension allows a KUKA LBR iiwa 14 R820 to successfully perform practical tasks that the seven axes of the standard robot would not support. We use tasks from insect farming as this industry offers a variety of challenging use cases. For example, enclosed spaces in an insect farming workspace, such as operating tall crates to rear crickets and mating cages for black soldier flies (BSF), restrict the use of a larger robot arm. The presented robot extension was designed to be compatible with various commercially available or custom-made robot arms.

We begin with a simulation of a KUKA LBR iiwa 14 (Hennersperger et al., 2017) to explore the reachability (Engemann et al., 2020) over the workspace and within confined spaces such as crates that are typically used during insect rearing processes. We use the simulation results to provide insight into the extended capabilities of the robot and to determine the length l of the robot extension necessary to cover the CoRoSect workspace. We use the simulation to study the introduction of two rotational degrees of freedom as an extension of the robot's kinematic chain. Finally, we develop a physical robot extension using Dynamixel and Teknic motors and lightweight aluminium extrusions, and provide demonstrations with robotic hardware.

The research questions posed in this chapter are:

Research Question 1

How to quantify and measure the reach of an articulated robot over its workspace for the purpose of testing different robot configurations and extensions?

Research Question 2

How to achieve an extension for a collaborative robot arm to increase reachability in the workspace and within enclosed spaces?

The first contribution in this chapter is an analysis of the reachability over an open workspace of the KUKA LBR iiwa 14 with a simulatable robot extension of variable length. The simulation tests reachability and manipulability (Engemann et al., 2020) over a grid of linearly spaced points to determine an operational envelope. The second contribution is the design and development of the physical robot extension, including the structural design and the choice of actuators. This also includes an iterative algorithm to stabilise the extension during motion planning with orientation constraints. The final prototype is mounted to a real KUKA iiwa and demonstrated in various insect farming use cases.

The chapter is structured as follows. We first cover the related work in industry and research on extending the physical capabilities of collaborative articulated robots (Section 3.2). We then present the simulation environment (Section 3.3) and the significant results (Section 3.4) that guide the design of the real robot extension (Section 3.5). Lastly, we discuss the use of our prototype robot extension and propose future work (Section 3.6).

3.2 Related Work

Cobots have gained significant attention in industrial settings due to their ability to work alongside humans in shared workspaces (Almurib et al., 2012; Brogårdh, 2007; Sandini et al., 2024; Taesi et al., 2023). However, various limitations hinder their widespread adoption (Andersson et al., 2021; Chutima, 2023; El Zaatari et al., 2019).

One key limitation of cobots is their restricted reach and payload capacity due to size and design constraints (Chutima, 2023; Taesi et al., 2023). Unlike traditional industrial robots built for reach and

heavy work, cobots are designed for safety and flexibility, limiting their range and effectiveness in large-scale tasks (Dmytriyev et al., 2024; Galin & Meshcheryakov, 2019). Research exists on improving cobot arm configurations (Taesi et al., 2023) and providing modular configurations (Romiti et al., 2021) that allow the robot to conform to the task (Javaid et al., 2021; Sandini et al., 2024). With numerous existing models of collaborative articulated robots, there is typically a selection of appropriate robots that fit specific tasks (Chutima, 2023; Rahman et al., 2024; Taesi et al., 2023). However, related work on an articulated extension of a cobot's reach remains limited.

Measuring and representing the capabilities of an articulated (or other) robot maps regions or volumes of the workspace to scores of reachability (Engemann et al., 2020; X. Gao et al., 2022; Zacharias et al., 2007, 2013). These scores are obtained in both simulation and real-condition testing. Research in collaborative robots uses this information to enhance the information available to a human co-worker (X. Gao et al., 2022), for example, in augmented reality (Newbury et al., 2022).

Economic feasibility plays a role in implementing extended reach solutions (Andersson et al., 2021). High costs associated with advanced actuators, modular extensions, or larger robots can deter small and medium-sized enterprises from adopting these innovations.

3.3 Reachability Simulation

3.3.1 Reachability and Manipulability Simulation

We define a desirable length of an extension rail as one that: (1) increases the robot's maximum reach (reachability) and (2) increases the operational envelope within which positions can be reached from various orientations (manipulability) while (3) respecting the payload constraints of the KUKA iiwa.

To systematically explore and demonstrate the increase in workspace gained through the developed robot extension, simulations have been carried out in PyBullet (Coumans & Bai, n.d.). In these simulations, we evaluate the reachability and manipulability increase by exploring different lengths of the linear extension rail of the robot extension.

The utilised metrics for reachability and manipulability are inspired by the work of (Engemann et al., 2020). We use a grid of 30 linearly spaced points in Cartesian Space to represent the operational area around the KUKA iiwa. Here, reachability is defined as the success of reaching the centre of a point $\vec{p} = [x, y, z]$ within a precision threshold $t = 0.01$m. If a point is reachable, there exists at least one solution to the inverse kinematic problem of computing joint positions for position $\vec{p}$. We allow any orientation. A target point $\vec{p}$ is reached when the Euclidean distance between the end effector tip and the target point becomes $\leq t$ for a threshold $t = 0.01$m. If a position cannot be reached within an allotted time of $0.5s$, the reach is aborted. The simulated robot arm with a robot extension is actuated to move to the computed joint positions. We plot a volume heatmap to provide a robust representation of consistently reachable regions.

Manipulability, on the other hand, is defined as the success rate of reaching a set of orientations of the end effector around a point $\vec{p}$. This simulates attempting various grasp poses at each point in the grid. A comparable measure is achieved by using sub-targets placed on the surface of a sphere around point $\vec{p_i}$ (Engemann et al., 2020). The final score for the manipulability m_i of a point is the sum of successes $s_j^i \in \{0, 1\}$ for reaching point with index i from orientation j, over k attempted orientations as calculated following equation 3.1.

$$m_i = \frac{\sum_{j=0}^{k} s_{i,j}}{k} \tag{3.1}$$

We define a position as highly manipulable when it is possible to reach $\geq 50\%$ of the total number of tested orientations ($m_i \geq 0.5$). To

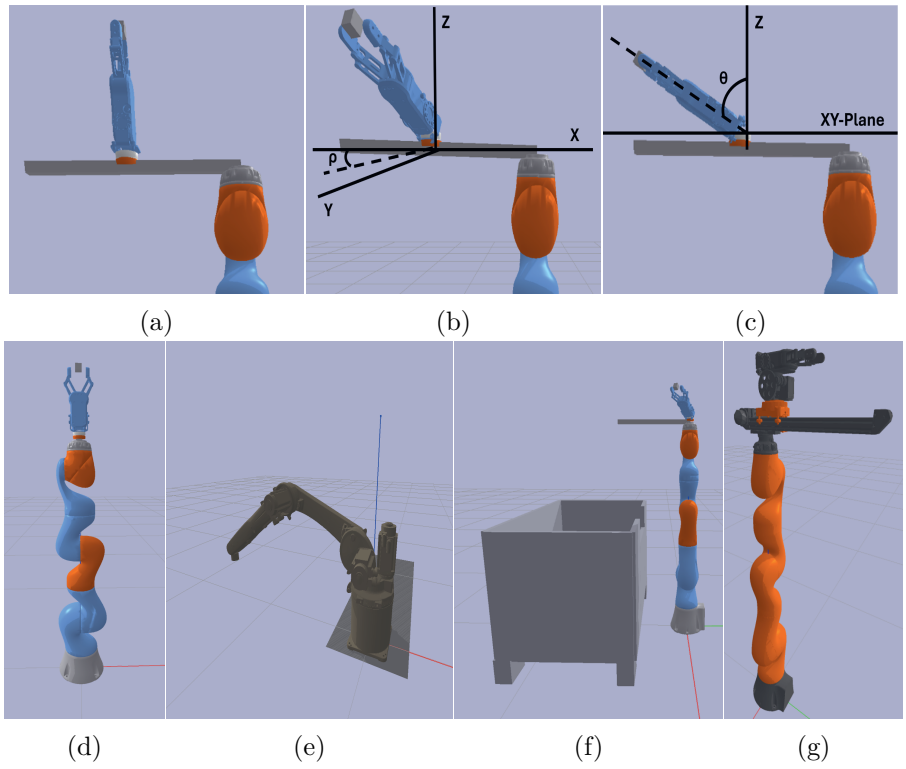


Figure 3.1: Simulation robot models: (a) Simulation model of linear rail (L1) of robot extension with a sledge to drive along the prismatic joint and RG6 gripper. (b) robot extension with first DOF for yaw around the vertical z-axis. (c) Angle for the final DOF that allows adjusting the pitch (around the xy-plane). (d) Baseline model of KUKA LBR iiwa 14 with attached RG6. (e) Baseline model of KUKA KR10r1420. (f) Configuration and relative distance between the KUKA iiwa and the crate used for rearing insects. (g) A more realistic simulation model of KUKA iiwa and robot extension based on CAD models.

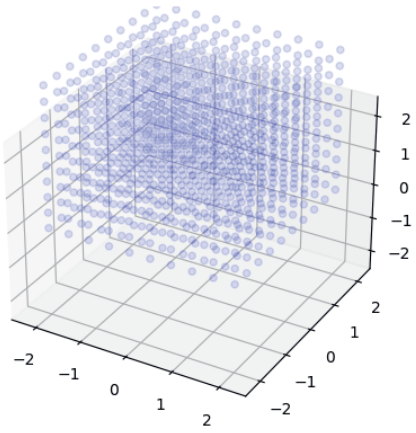


Figure 3.2: Reachability and manipulability targets in a linearly spaced grid.

demonstrate the gain in reachability and manipulability provided by the robot extension, we establish two baselines. For a lower bound, we simulate a KUKA iiwa without extension (Figure 3.1d). As a baseline upper bound, we compare to an industrial robot arm, the KUKA KR10r1420 (Figure 3.1e), that has a maximum reach of 1.420m (according to the dataset published with (Tola & Corke, 2024)), comparable to the extended KUKA iiwa at $1.320m + 0.1$m with end effector attached.

The entire simulation is outlined in Algorithm 1.

For our first experiments, we extend the URDF of the KUKA iiwa with a simplified simulation model of the robot extension to which we attach an RG6 end effector on a prismatic joint (Figure 3.1a). The upper limit of the prismatic joint is the length of the rail. The simplified model allows us to systematically generate increasing lengths l for the robot extension and create a comparison without the additional rotational

Algorithm 2 Simulation algorithm for testing reachability and manipulability. A grid of linearly spaced points is placed in ranges $[-2m, 2m]$ for the x- and y-axis and $[0, 3m]$ in the z-axis.

$h \leftarrow 0.0$ ▷ The mounting height
$t \leftarrow 0.01$ ▷ Precision threshold
$X_{range} \leftarrow [-2, 2]$
$Y_{range} \leftarrow [-2, 2]$
$Z_{range} \leftarrow [0, h + 3]$ ▷ $\geq$ 3m is out of range
$G \leftarrow [X_{range}, Y_{range}, Z_{range}]$ ▷ Linearly spaced grid
$O \leftarrow [[0, ..., \pi]; [0, ..., \pi]; [0, ..., \pi]]$ ▷ Orientations

for *point* in G **do**
  if *Reachability* **then**
    $target_{Cartesian} \leftarrow point$
    $target_{joint} \leftarrow IK(target_{Cartesian})$
    $robot.go(target_{joint})$
    if $\delta_{Euler}(robot.ee_link, target_{Cartesian}) \leq t$ **then**
      $point.score = 1$
    end if
  else if *Manipulability* **then**
    for *orientation* in O **do**
      $target_{Cartesian} \leftarrow [point, orientation]$ ▷ Full pose
      $target_{joint} \leftarrow IK(target_{Cartesian})$
      $robot.go(target_{joint})$
      if $\delta_{Euler}(robot.ee_link, target_{Cartesian}) \leq t$ **then**
        $point.reached \mathrel{+}= 1$
      end if
    end for
    $point.score = point.reached/O.size()$ ▷ Mean value
  end if
end for

degrees of freedom. We motivate that a rail extension alone (Figure 3.1a) will not effectively improve the operational envelope of the robot arm (manipulability). To compare, we implement the two additional rotational degrees of freedom (DOF) (Figures 3.1b and 3.1c) between the robot extension and the RG6 end effector to allow yaw (around the z-axis) (Figure 3.1b) and pitch (around the xy-plane) (Figure 3.1c). We test incrementally increasing lengths of the robot extension up to 1.0m in steps of 0.25m for initial reaching into insect-rearing crates (Figure 3.1f). Finally, we create a URDF of the final prototype robot extension (Figure 3.1g) to test the final design.

3.3.2 Evaluation of Operation in Confined Spaces

To evaluate the workspace gained by the robot extension when operating in confined spaces, we generate a linearly spaced grid within a virtual crate for insect rearing. A baseline test with the KUKA iiwa is performed for a robot mounted at $h = 0$ (no height offset between the robot base link and the crate). We then conduct experiments to generate reachability envelopes for incrementally increasing robot extension lengths and mounting heights (Figure 3.1f):

- **Length of the robot extension**. The attachment of a robot extension to the flange adds operational range to the robot arm. The extension presents a challenge for processing self-collisions with the additional links and affects inverse kinematics, leading to an increased number of possible solutions.
- **Height of Mounting Platform**. The optimal relative height of the robot arm with respect to the workspace varies when equipped with robot extensions of different lengths. The simulation was used to determine the height of the mounting platform, given constraints set by the CoRoSect use cases.

We place the crate at a distance of 0.15m in the x-axis from the base of the robot to minimise the distance without colliding with the base. The simulation did not include a motion planner to account for collisions

along planned motions. The tall walls of the crate pose a planning problem for the KUKA iiwa and KR10r1420 as their middle links collide with the crate before the end effector reaches inside. Hence, the volumes depicted within the crates are not optimal.

A linearly spaced grid, as shown in Figure 3.2, is generated within the virtual insect crate. A baseline test with the KUKA iiwa 14 is performed for a robot mounted at $h = 0$ (no height offset between the robot base link and the insect crate). We then conduct experiments to generate reachability envelopes for incrementally increasing robot extension lengths and mounting heights (Figure 3.1f).

3.4 Experiments and Results

3.4.1 Baseline Results

We present the simulation results as volume heatmaps. Reachability maps a binary value, i.e., either a point is reachable or not (there exists an IK solution for this point or not). Hence, the volumes show green for reachable areas in the grid and red elsewhere. Manipulability is a continuous colour scale of highly manipulable positions (green, reaching $\geq 50\%$ of the total number of possible orientations, hence a score ≥ 0.5) to unreachable positions (red).

Results from simulating a KUKA iiwa without robot extension are shown in Figure 3.3. The KUKA iiwa can most reliably reach points within 0.820m (as per its specifications), and up to 1.12m with the tip of a mounted RG6 gripper (approximately 0.3m at full closure). However, the core of highly manipulable positions is limited to the robot's base, likely due to constraints of its configuration as a cobot. The baseline KUKA iiwa reaches 1370 positions in the grid, 297 (21.7%) of which are highly manipulable (can be reached from at least ≥ 0.5 of tested orientations).

We compare to an industrial robotic arm, the KUKA KR10r1420 (from the dataset published in (Tola & Corke, 2024)) with a designed reach of

1.420m. Figure 3.4 shows that the industrial robot arm (Figure 3.4b) outmatches the KUKA iiwa (Figure 3.4a) in manipulability over a large workspace. The baseline KR10 reaches 3031 positions in the grid, 1932 (63.7%) of which are highly manipulable (can be reached from at least ≥ 0.5 of tested orientations).

3.4.2 Reachability

Figures 3.5a - 3.5d show the volume of additional reachable space when using robot extensions of length 0.25m (3.5b), 0.5m (3.5c), and 0.75m (3.5d) compared to the baseline (3.5a). The axis limits are constant in all subplots, resulting in a depicted increase in the furthest reachable point when using a longer rail. Extension lengths above 0.5m allow the robot to reach within $1.0m - 1.2$m, which is the minimum for the CoRoSect workspace (Chapter 2).

3.4.3 Manipulability

Figures 3.6a-3.6d show the manipulability score for the KUKA iiwa with robot extension. Figure 3.6 specifically shows the manipulability of points without additional rotational degrees of freedom, hence just a linear rail. The operational range increases, as expected from Figure 3.3c. However, the core volume at the centre, where points are most manipulable, does not grow with a larger rail.

Figures 3.7a-3.7d show the increase in the number of highly manipulable points (green) with the introduction of 2 additional degrees of freedom before the end effector. The volume of points that can be reached from at least half (ratio ≥ 0.5) of orientations when using a rail length of 0.5m (Figure 3.7c) reaches the original maximum reachability of the KUKA iiwa (Figure 3.5a).

We select a rail length of 0.5m as sufficient for extending the reach and manipulation abilities of a KUKA LBR iiwa 14 intended for the insect farming use cases we use as a benchmark. We used simulation to

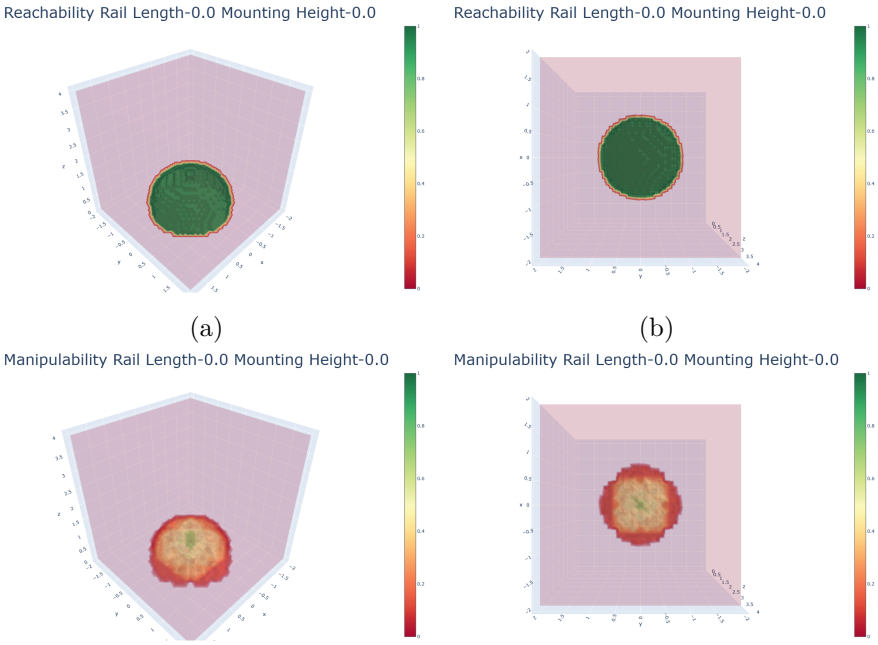
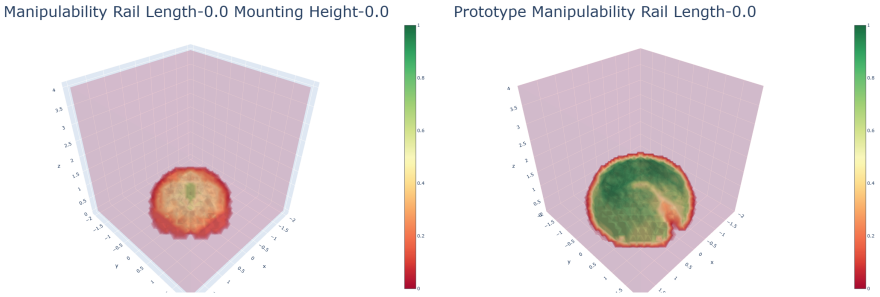


Figure 3.3: Baseline reachability and manipulability scores for a grid of 30 linearly spaced points in the ranges $[-2m, 2m]$ in x and y and $[0, 4m]$ in z. The volume maps range the manipulability score from highly manipulable (green) to non-reachable (red). (a) and (b) The baseline for maximum reachability of the KUKA iiwa from two perspectives. (a) and (b) The baseline manipulability from two perspectives.



(a) (b)

Figure 3.4: Baseline manipulability scores for a grid of 30 linearly spaced points in the ranges $[-2, 2]$ in x and y and $[0, 4]$ in z. The volume maps range the manipulability score from highly manipulable (green) to non-reachable (red). (a) The baseline manipulability for the KUKA iiwa 14 (repeated for comparison). (b) The baseline manipulability results for an industrial KUKA KR10r1420.

validate the implementation of two rotational degrees of freedom, which visibly increase the robot's ability to perform manipulation at poses in its workspace (Figures 3.6 and 3.7). The 0.5m extension, as just a linear rail, reaches 2809 positions (105% increase from baseline 1370 total number of points), where 382 (13.6%) have a score ≥ 0.5 (28.7% increase from baseline 297 highly manipulable points). Adding the rotational degrees of freedom enables reaching 3586 positions (161% increase from baseline 1370 total number of points), where 1440 (40.2%) have a score ≥ 0.5 (384.8% increase from baseline 297 highly manipulable points).

3.4.4 Evaluation of Operation in Confined Spaces

The baseline Figures 3.8a and 3.8b show the maximum reachability of the KUKA iiwa, meaning that the volumes are reachable from at least one orientation. We determined that, without a robot extension, it is impossible to operate on material that is positioned at the bottom and back wall of the crate. The reachability of points within the cricket

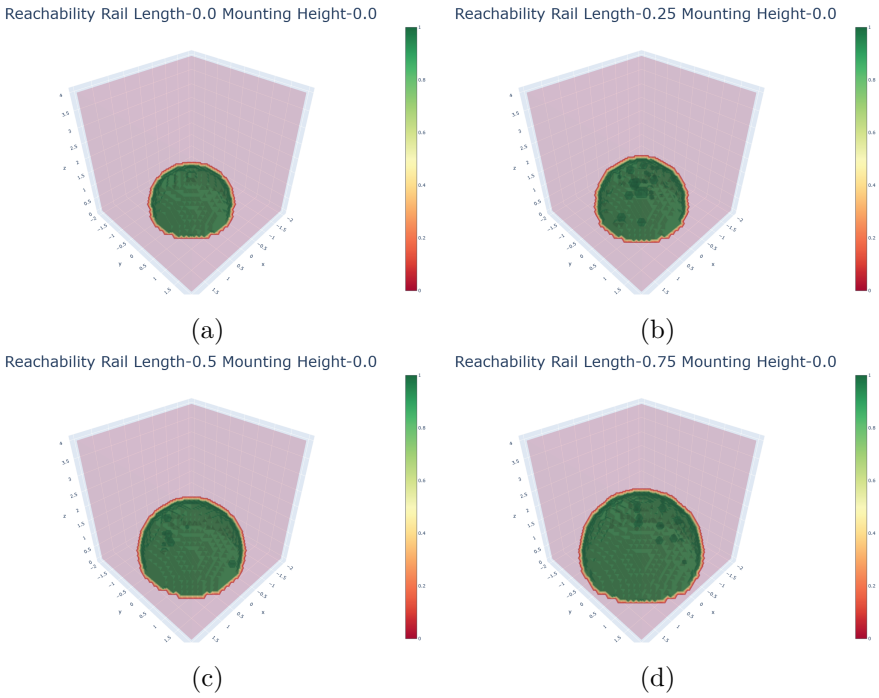


Figure 3.5: Maximum reachability scores for a grid of 30 linearly spaced points in the ranges $[-2m, 2m]$ in x and y and $[0, 4m]$ in z. (a) The baseline for direct comparison. (b) The maximum reachability using a robot extension of length 0.25m. (c) The maximum reachability using a robot extension of length 0.5m. (d) The maximum reachability using a robot extension of length 0.75m.

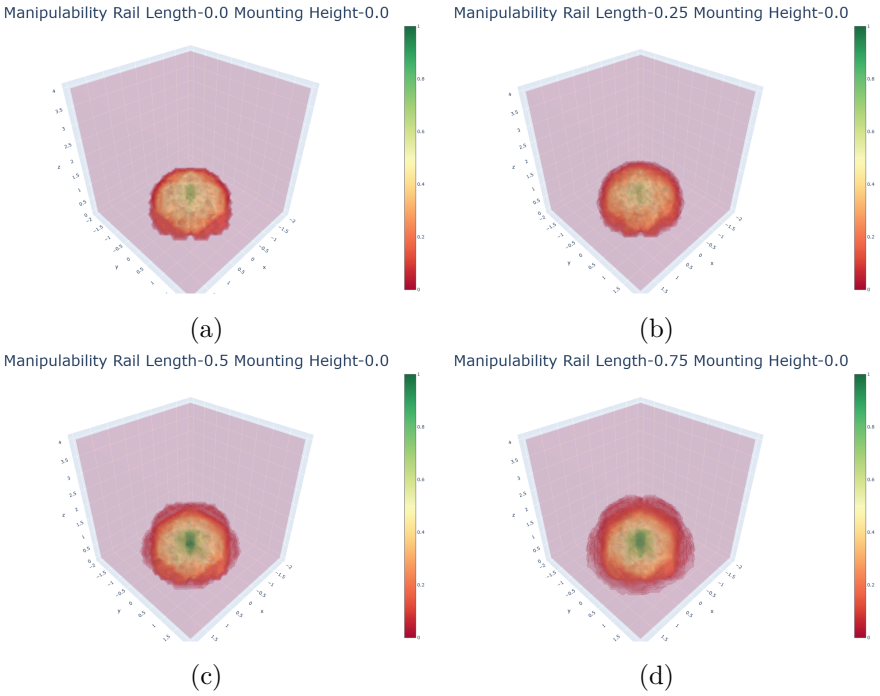


Figure 3.6: Manipulability scores a robot extension with **no** additional degrees of freedom. Results for a grid of 30 linearly spaced points in the ranges $[-2, 2]$ in x and y and $[0, 4]$ in z. The volume maps range the manipulability score from highly manipulable (green) to non-reachable (red). (a) The baseline for direct comparison. (b) The manipulability scores when using a robot extension of lengths 0.25m without additional rotational degrees of freedom. (c The manipulability scores when using a robot extension of lengths 0.5m without additional rotational degrees of freedom. (d The manipulability scores when using a robot extension of lengths 0.75m without additional rotational degrees of freedom.

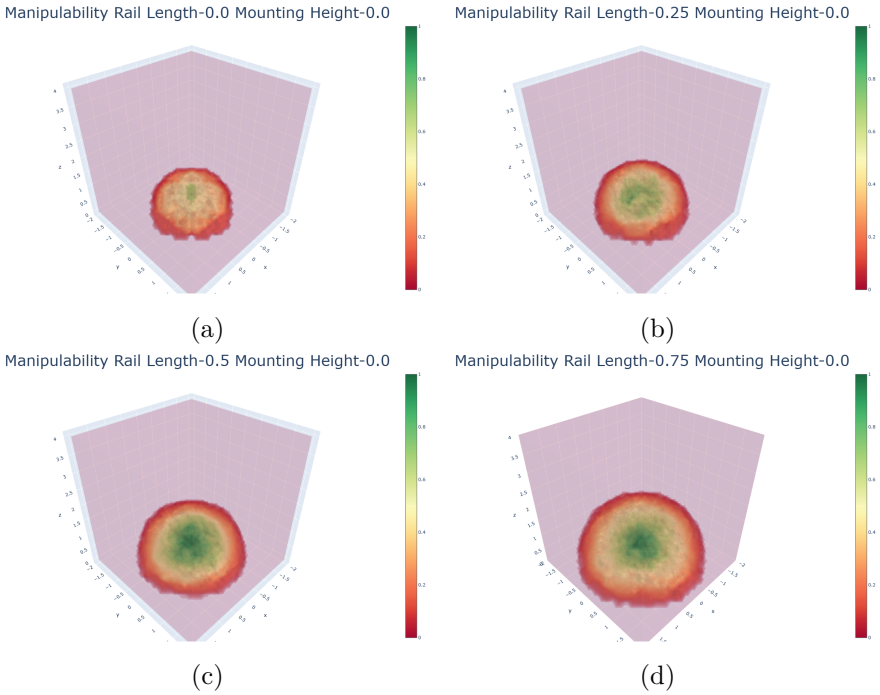


Figure 3.7: Manipulability scores a robot extension with additional degrees of freedom. Results for a grid of 30 linearly spaced points in the ranges $[-2, 2]$ in x and y and $[0, 4]$ in z. The volume maps range the manipulability score from highly manipulable (green) to non-reachable (red). (a) The baseline for direct comparison. (b) The manipulability scores when using a robot extension of lengths 0.25m with extended rotational degrees of freedom. (c The manipulability scores when using a robot extension of lengths 0.5m with extended rotational degrees of freedom. (d The manipulability scores when using a robot extension of lengths 0.75m with extended rotational degrees of freedom.

crates using a 0.25m and 0.5m robot extension is shown in Figure 3.8c and 3.8d, respectively. Figure 3.8 approximates the volume inside the crate that can be reliably accessed. With a longer robot extension, we reach deeper despite the tall walls. The inconsistencies in the volumes are explained by the lack of motion planning in the simulation, making some motions prone to collision.

We increase the mounting height of the KUKA iiwa to allow the lowest joints (particularly j2) to reach over the walls of the crate (Figure 3.1f). Figures 3.9a-3.9b show the same volume using a rail length of 0.5m at a mounting height of 0.25m and 0.5m, respectively. The approximated volumes suggest that a higher mounting point allows a more uniform distribution across a surface within the crate, but the height of this surface does not consistently reach the crate's bottom. However, we suggest that the lack of proper motion planning impedes the reach. The robot extension can theoretically reach the bottom of the crate with at least a top-down orientation.

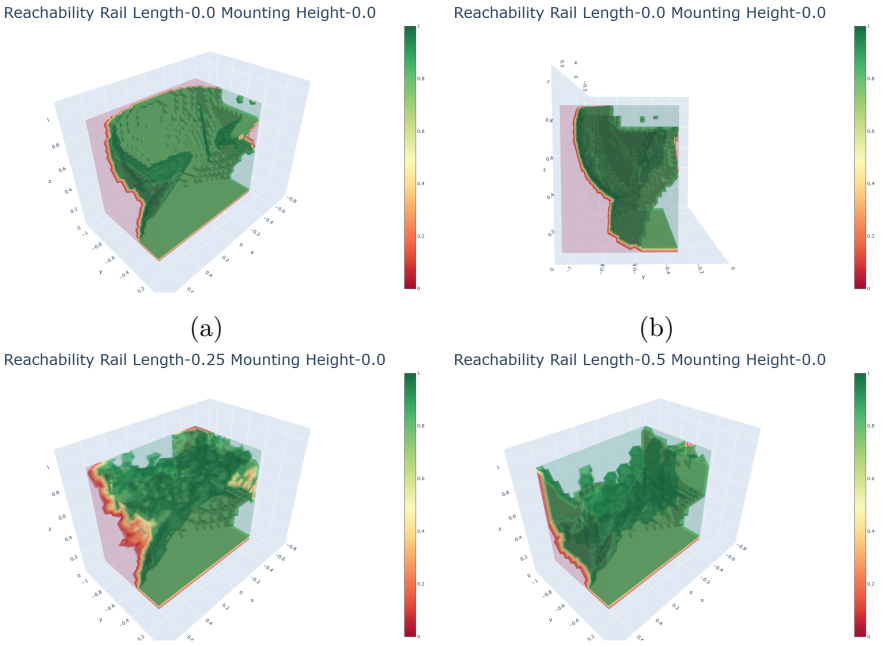
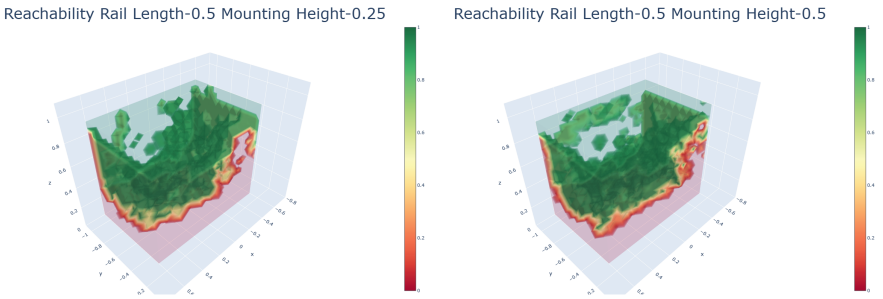


Figure 3.8: Reachability scores for linearly spaced points inside a simulated insect crate (Figure 3.1f). (a) and (b) Baseline reachability of the KUKA iiwa with the RG6 end effector inside an insect crate. (c) Volume of reachable points inside the insect crate using a robot extension of length 0.25m. (d) Volume of reachable points inside the insect crate using a robot extension of length 0.5m.



(a) (b)

Figure 3.9: The volume of accessible points when using 0.5m articulated robot extension and varying the mounting height of the robot (a) Volume of reachable points inside the insect crate using a mounting height of 0.25m. (subfigure b) Volume of reachable points inside the insect crate using a mounting height of 0.5m.

3.5 Prototype Hardware Design and Discussion

3.5.1 Structural Design

We select a rail length of 0.5m as sufficient for extending the reach of the KUKA iiwa 14 intended for CoRoSect. An additional constraint on the design of the physical prototype is the weight. A rail of length $\geq$ 0.5m with a mounted RG6 end effector (approximately 1.25kg) at full extension exceeds the permissible moments exerted on the upper KUKA iiwa joints. In the following section, the resulting robot extension, its hardware, control, and simulatable model are described.

Figure 3.10 shows the hardware of the developed robot extension, including annotations of its three main segments (L1-L4), the three featured degrees of freedom, and their corresponding actuators (A1-A3). Figure 3.11 shows the corresponding CAD design (used as a basis for the simulation model), highlighting the main segments.

The first joint is the prismatic joint, primarily responsible for increasing the work envelope of the robot. It facilitates motion between the first

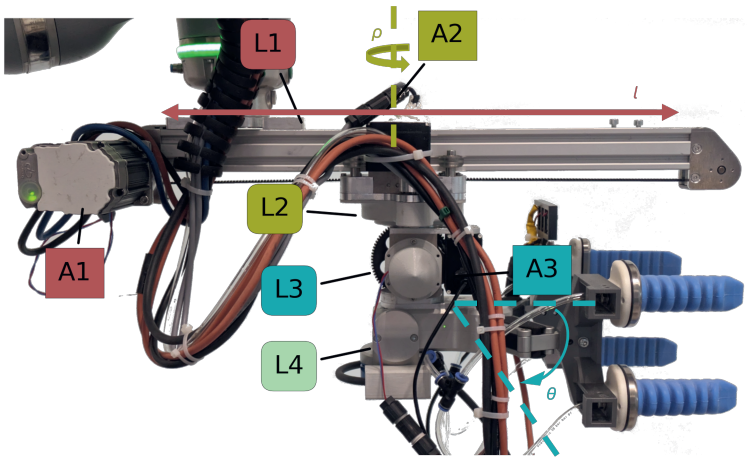


Figure 3.10: An annotated image of the robot extension hardware mounted on the flange of a robot arm. The picture includes labelled structural links and degrees of freedom. The linear rail (L1) extends by a length l and is actuated by A1 (red). The yaw ρ around the z-axis (L2) is actuated by A2 (yellow). Actuator A3 (blue) enables pitch θ (segment L3) around the xy-plane.

link of the extension L1 and the sledge L2 driving on it. The main component of L1 is a V-shaped aluminium profile, which mounts the actuator A1 driving the first joint. This motor is supported by an electromagnetic brake to increase the stiffness of the sledge while not in motion.

On L1 is the sledge (L2) that is connected to the aluminium profile of L1 with wheels and travels along its axis. This motion is realised by a timing belt connected to the pulleys of the actuator (A1) on L1. A support structure on the other side of the extension is mounted to the sledge with adjustable mountings that allow for proper tensioning of the belt.

On its side, L2 has a mounting point for the actuator A2 driving the next joint for rotation around the z-axis. To keep the connection rigid

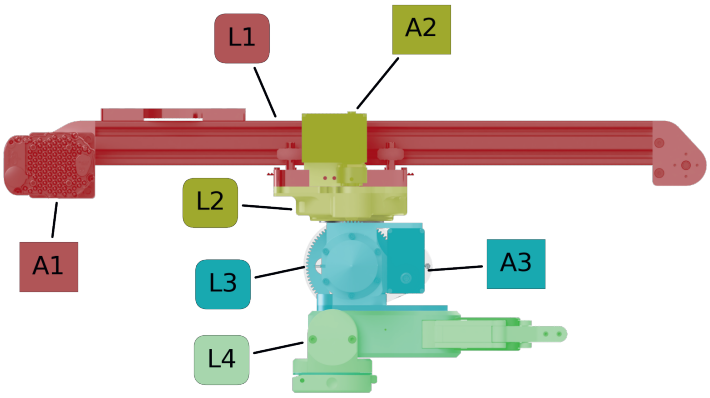


Figure 3.11: An annotated CAD design showing segments and actuators. Each colour represents the structural links of the robot extension. L1 is the linear rail. L2 is a wheeled sledge that operates along the rail. L3 connects the sledge to the end effector and houses two additional rotational degrees of freedom. L4 is an RG6 end effector. The mounting orientation of the end effector minimises the moment exerted around the robot flange when at full extension.

while allowing rotation, a slewing ring is used to connect the sledge L2 to the next link L3 of the extension. On this slewing ring is a spur gear as the base of L3. It is moved by the actuator A2 connected to L2. It also features the mounting point for the end effector (L4) as well as the motor A3 driving this last joint, responsible for tilting the end effector.

The motion is geared, and L4 is moved by a spur gear mounted on one side of the shaft, with an electromagnetic brake on the other side. Connected to L4's shaft is the end plate of the linear extension used to mount the required end-effectors for robotic manipulation. In our experiments, an RG6 industrial gripper from OnRobot has been used. The mounting plate connecting L1 to the KUKA LBR iiwa is

designed according to DIN ISO 9409-1-50-7-M6, to which iiwa's flange conforms.

Actuators and segments have been selected and designed to meet the following requirements:

- Strict weight constraints, to ensure no payload violations of the KUKA LBR iiwa. Although the iiwa 14 can carry up to 14 kilograms, this weight limit falls off rapidly at an offset from the flange. The torque limits on the iiwa joints had to allow for at least 2kg tolerance to handle materials when the robot extension is fully extended.
- Necessity of high IP ratings to guarantee performance in dusty and humid environments at insect farms and in other industrial environments.
- Use of widely available components and simple-to-manufacture custom parts, to keep the cost feasible and the extension easy to copy by researchers and SMEs.

3.5.2 Actuator Selection

Table 3.1 outlines the specifications of motors used for actuators A1, A2, and A3, respectively. For the prismatic joint, the heavier, non-geared motor A1 was chosen for its ability to deliver the higher speeds required for this axis, while maintaining sufficient torque to support the maximum payload in any orientation. The offered high speed, acceleration, and deceleration are particularly useful when fast motions are required, e.g., to shake off insects during manipulation tasks in insect farming. The motor's greater weight is positioned near the flange of the KUKA to limit the moment exerted by its weight. For the tilting and turning joints, the actuators are geared servo motors that offer a high torque-to-weight ratio of approximately 37.3. To meet the high torque requirements, both joints are equipped with spur gears, with ratios of 3.6 for A2 and 4 for A3. This configuration results in peak torques

Table 3.1: An overview of the motor specifications selected for the linear extension.

Actuator	Motor	Peak Torque [Nm]	Max Speed [RPM]	IP	Weight [kg]
A1	Teknic CPM-SCHP-2331S-ELSA	4.4	2520	IP53	1.200
A2	Dynamixel XW540-T140	6.9	72	IP68	0.185
A3	Dynamixel XW540-T140	6.9	72	IP68	0.185

of 14.25 Nm for A2 and 15.84 Nm for A3, assuming a conservative efficiency of 90%.

The extension was designed to feature similar collaborative capabilities as provided by the KUKA iiwa robot: (1) The forces of the extension are not high enough to pose a real danger to humans collaborating with the robots. Motor torques can be further limited in software to stop motions earlier if a human co-worker intervenes. (2) The robot extension also has basic robot guiding capabilities implemented. In this guiding mode, the torques of the actuators are reduced in software, so that humans can bring the joints into desired positions, which can then be recorded, a feature that is also supported by the KUKA iiwa.

The final prototype, including all structural parts and actuators, weighs approximately 6kg with a cost of up to €6250.

3.5.3 Control and ROS Integration

The Linear Extension operates under the Robot Operation System (ROS) (Quigley et al., 2009) framework and utilises two distinct controllers. Controller C1 is dedicated to the Teknic Motor A1, while the second Controller C2 manages the Dynamixel Motors A2 and A3. This division is necessary since both types of motors come with different drivers and control interfaces. Each controller offers functionalities such as position control and homing through ROS services. Additionally, both controllers monitor the safety state, published by the iiwa, and adjust or halt motion in response to this state. Both controllers implement a ROS action server compatible with

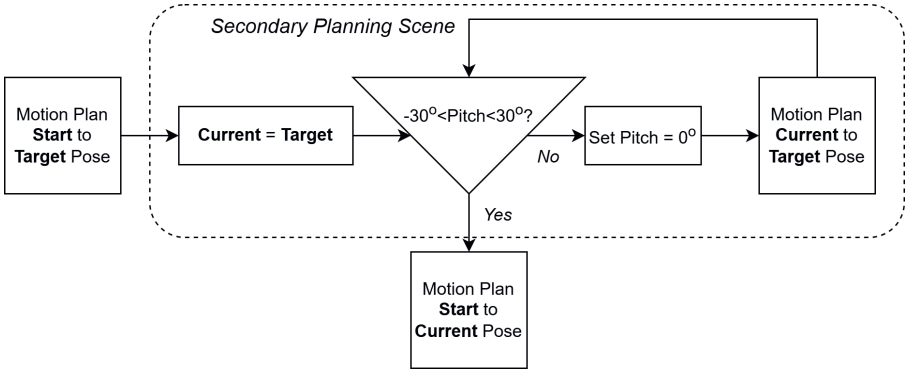


Figure 3.12: Visual diagram for iterative planning to a target pose with a constraint on a link in the middle of a kinematic chain. Two motion planning scenes are used in separate ROS namespaces. The secondary planner iteratively brings the pitch angle to the orientation limits while still reaching the target pose. The primary planner is then provided a final pose in joint space to plan from the original starting pose.

the Joint Trajectories published by MoveIt. C1 controls the Teknic Motor through the ClearPath-SC software foundation, a C++ library provided by the manufacturer. The Dynamixel motors are controlled by C2 utilising the ROBOTIS Dynamixel SDK (Software Development Kit). We use the unified robot description format (URDF) to integrate the robot extension with ROS and MoveIt! (Coleman et al., 2014; Şucan et al., 2012). Coordinated motion planning for the KUKA iiwa and robot extension is performed in MoveIt!. Synchronised motion commands to achieve the desired trajectories are distributed to the individual controllers using ROS action servers.

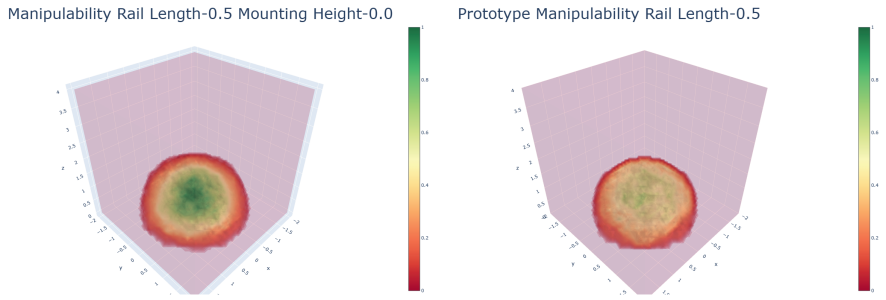
Additional software developments have been carried out to ensure reliable control when constraints on the orientation of the rail (e.g., limit pitch to $\pm 30°$) must be guaranteed during motion planning. Respecting such constraints becomes necessary, e.g., when the robot extension is used for insect harvesting or linear motion is required for entering cage doors or other confined spaces. When testing the

Open Motion Planning Library (Şucan et al., 2012), we found that constraints on the orientation of a link in the middle of the kinematic chain are sometimes ignored. Our software extension overcomes this limitation by performing iterative motion planning for the target pose within a secondary MoveIt! planning scene. Each iteration (Figure 3.12) plans a trajectory to a target pose without publishing it. If the rail link at the end of the trajectory is not within the permissible range, its pitch is reset to 0° while the other joints remain unchanged. Planning is repeated from this new starting pose, which ensures the next iteration has a rail link pitch closer to 0° (with a cutoff of 10 total iterations). The joint positions of the final iteration are then provided to the primary motion planner to perform a single spline motion from the robot's true pose to the target.

3.5.4 Final Simulation Insights

We introduce the CAD design of the prototype (Figure 3.1g) into the reachability simulation to gain final insights into the increased reach (Figure 3.13). The reachability and manipulability are increased beyond that of the baseline KUKA iiwa (Figure 3.3). The final prototype from CAD models reaches 2881 positions (210% increase in total number of points), 896 (31.1%) have a score ≥ 0.5 (302% increase in total number of highly manipulable points).

The volume of highly manipulable points for the real prototype (Figure 3.13) is lower than the theoretical (Figure 3.7) due to the practical limitations of the hardware. However, with the extension, we begin to approach the volume of highly manipulable positions (3031 reachable positions, 1932 of which are highly manipulable) of the industrial KR10r1420 (Figure 3.4b), while being able to operate in confined spaces that the KR10r1420 cannot operate within due to its lower number of degrees of freedom.



(a) (b)

Figure 3.13: Manipulability scores for a grid of 30 linearly spaced points in the ranges $[-2m, 2m]$ in x and y and $[0, 4m]$ in z. (a) The theoretical increased volume of highly manipulable points (green) when incorporating two additional rotational degrees of freedom on a simplified robot extension. (b) The manipulability scores for the final design (Figure 3.1g) when using the CAD model in simulation.

3.5.5 Discussion

We tested the developed robot extension attached to a KUKA iiwa under real conditions within the insect farming industry. We, e.g., successfully tested operation within crates used to rear crickets (Figure 3.14a). As simulated, the robot extension fits inside insect-rearing crates, and the range of the KUKA iiwa is sufficiently extended to handle the material inside the crate. We can also operate objects and material within enclosures of black-soldier-fly mating cages (Figure 3.14d) at orientations that are out of reach for the KUKA iiwa.

The tradeoff between using the KUKA iiwa with robot extension against an industrial robot lies in the payload capacity, the price, and the required versatility within a workspace. With the robot extension, we retain the flexibility and collaborative features of the KUKA iiwa within an extended workspace, taking advantage of additional rotational degrees of freedom for operation within enclosures. A limitation is the payload capacity, as carrying the robot extension and end effector leaves

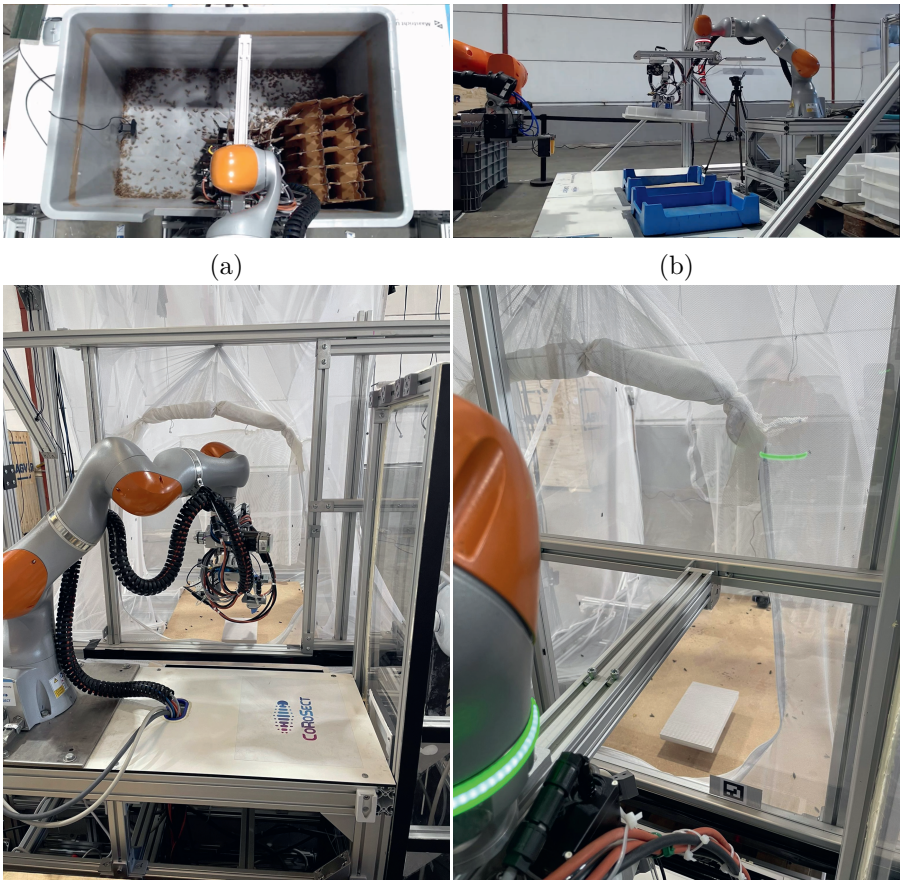


Figure 3.14: Robot extension utilised in insect farming studies. (a) Reaching into a cricket crate as performed in simulations. (b) Picking an inlay and orienting it far outside of the standard range of the KUKA iiwa. (c) Operation inside an insect mating cage, where the robot extension is fully inserted for material handling. (d) The robot extension is used to prepare for sliding open a mating cage door and operating on the material inside.

a maximum additional payload of 2kg at the maximum offset. Industrial robots offer high manipulability for large-scale automation over an open workspace and a high payload. However, particularly large industrial robots will require a highly controlled environment and may be limited by their degrees of freedom or bulk within enclosures.

3.6 Conclusion

In this chapter, we presented work in extending the operational range of a KUKA LBR iiwa 14 through a custom-made open-source articulated robot extension. We developed the robot extension for increased reachability and manipulability while maintaining a high number of degrees of freedom for operating within confined spaces. We simulate various configurations of the robot extension to motivate our final design. The prototype presented in this paper features off-the-shelf technology and integration with a KUKA iiwa and ROS. We demonstrated the robot extension on use cases from the insect farming industry, which is highly diverse in automatable tasks that commonly contain enclosures.

4

Hybrid End Effector with Soft Fingers and Modular Elements for Versatile Material Handling



In this chapter, we develop a custom end effector by extending the OnRobot RG6 with modular and soft elements to increase its flexibility for handling diverse materials of different sizes, geometries, and textures. We attach two pairs of Soft Gripping GorillaFinger SoftActuators facing each other to the fingers of the RG6, providing a soft fingertip for delicate material handling. The opening width of the RG6 allows us to dynamically adjust the distance between the soft fingers, allowing a tradeoff between a wide, dynamic gripping envelope when fully open and stability with high grasping forces when

closed. We use related work in soft gripping to establish a theoretical model of the end effector to rationalise the effect of adjusting the distance between our soft fingers. Our experimental data show that the distance between the soft fingers and the object affects the grasping force and point of contact. We demonstrate the dexterity of the hybrid design by picking common items and introducing an offset in their placement to simulate non-highly-controlled workspaces. To quantify the quality of a grasp, we test the resistance of our gripper to outside perturbation by measuring the force required to pull held objects out of a grasp. The force necessary to disrupt a grasp is higher when picking misplaced objects with the soft fingers than the base RG6 up to an offset distance of 50*mm. We record visual data for the flexible grasps established with non-rigid items to demonstrate how the soft fingers conform to the geometry of materials. We further extend the hybrid end effector by adding 3D printed slots for modular structures capable of handling items that the soft fingers cannot, such as plastic crates with abrasive or cutting sharp edges. We test our developed end effector in the insect farming industry, which is highly diverse in automatable tasks involving delicate insects, objects, and materials of various geometries and rigidity.*

4.1 Introduction

End effectors serve as the primary physical interface between an articulated robotic system and its workspace, determining the robot's ability to grasp, manipulate, and interact with objects (Feng, 2021; Reddy & Suresh, 2013; Vrochidou et al., 2022). The design and functionality of end effectors directly impact a system's applicability across different tasks, from rigid assembly operations to delicate material handling (M. Mohammed & Al-Ibadi, 2024; Reddy & Suresh, 2013; W. Ye et al., 2023). Industrial processes are moving toward greater flexibility (M. Mohammed & Al-Ibadi, 2024), customisation (Reddy & Suresh, 2013), and human-robot collaboration (Firth et al., 2022; Safeea et al., 2018). Therefore, there is a corresponding need for end effectors that can handle a wider variety of objects with

minimal reconfiguration. This shift has increased research into soft and adaptive grippers (M. Mohammed & Al-Ibadi, 2024; W. Ye et al., 2023) and modular end effector systems (Berman & Nof, 2011; Firth et al., 2022; Reddy & Suresh, 2013) capable of dealing with uncertain geometries, delicate materials, and variable payloads.

In this chapter, we develop a modular, hybrid end effector for handling both delicate, deformable, and rigid materials of various geometries and textures, matching those used in the insect farming industry in rearing multiple insect species (Requirement 3, Chapter 2). We use an OnRobot RG6 gripper as the core rigid platform for standard industrial grasping, which we extend with soft silicone elements for versatile and delicate material handling. We incorporate both rigid and soft elements to create a hybrid design capable of manipulating both rigid and delicate objects in close proximity to insects. We also present modular elements that allow us to easily change the configuration of the end effector to suit non-standard grasping that is too large or out of reach for the original RG6. The modular design addresses the need for operating on diverse materials without major reconfiguration and utilising a single robotic platform as much as possible (Requirement 1, Chapter 2). Hence, we address the following research question within the scope of this chapter:

Research Question 3

How to achieve a hybrid end effector for the versatile manipulation of both rigid and delicate materials in the insect farming industry?

The first major contribution in this chapter is the design and development of the hybrid end effector, combining an OnRobot RG6 industrial gripper with Soft Gripping GorillaFinger SoftActuators. The soft fingers conform to the geometry of a held material, establishing a secure grasp without the need for elaborate grasp synthesis. They are suited for versatile operations where various kinds of shapes and objects are involved, but offer lower grasping force than an industrial gripper (Hughes et al., 2016). Their inclusion with the RG6 allows for

dynamically changing the distance between the soft fingers to create a larger gripping envelope, making the end effector more suitable for non-highly-controlled environments. The second contribution is a theoretical model put together from related work in representing soft end effectors as pseudo-rigid bodies (H. Zhang et al., 2025) and elastic rods (Haibin et al., 2018; X. Zhou et al., 2015), to rationalise the effect on the bending angle and grasping force of changing the distance between the soft fingers using the RG6. Thirdly, the hybrid end effector is tested in grasping experiments on various common objects and those unique to insect farming. We quantify the quality of a grasp by measuring the force necessary to disrupt it and cause a held item to slip/be dropped. We perform experiments to show the effect of changing the RG6 opening width and its effect on the grasp quality. We also compare the grasp quality when picking up items at an offset, emulating misplaced materials or non-highly-controlled workspaces, to demonstrate the additional tolerance to errors and broad grasping range gained with our design.

This chapter starts with a review of related work in industrial and compliant end effectors to describe existing solutions in material handling (Section 4.2). This is followed by the description of our hybrid end effector in Section 4.3, including the hardware (Section 4.3.1) and theoretical modelling (Section 4.3.2). Section 4.4 presents the experiments and their results, which we use to quantify the capabilities of our end effector. We provide discussion and demonstrations of the end effector in material handling use cases within insect farming in Section 4.5. Section 4.6 closes the chapter with final conclusions.

4.2 Related Work

Traditionally, end effectors in industrial applications have been engineered for repetitive, high-speed operations under highly structured conditions, often prioritising rigidity, durability, and accuracy for precise handling of small parts in mass manufacturing



(a) (b) (c) (d)

Figure 4.1: Examples of common industrial end effectors (Dorna-Robotics, 2023; Universal-Robots, 2020). (a) OnRobot RG6 Two-Finger Gripper (OnRobot, 2025). (b) Schunk PHL63 Parallel Gripper (Schunk, 2025). (c) Piab PiCOBOT Vacuum Gripper (Piab, 2019). (d) Soft Gripping Modular Soft Gripper (Soft-Gripping, 2024).

applications (Birglen & Schlicht, 2018; Hughes et al., 2016; Samadikhoshkho et al., 2019; Tai et al., 2016). These end effectors commonly use pinching mechanisms such as parallel-jaw mechanisms, vacuum systems, or custom-machined tools (Tai et al., 2016; Universal-Robots, 2020) to handle specific components in high-volume manufacturing scenarios (Birglen & Schlicht, 2018; Ma et al., 2018; Reddy & Suresh, 2013; Tang et al., 2023). Depending on the intended application, a wide range of commercially available industrial gripper mechanisms are available (Dorna-Robotics, 2023; Universal-Robots, 2020), such as those in Figure 4.1. Modular and collaborative gripper platforms have been developed to support rapid tooling changes and increase robotic flexibility in settings with diverse materials (Berman & Nof, 2011; Firth et al., 2022; Saliba et al., 2010; Zhong et al., 2015).

Parallel grippers and two-fingered grippers (Figures 4.1a and 4.1b) are widely used in structured environments due to their mechanical simplicity, robustness, and repeatability (Birglen & Schlicht, 2018; Samadikhoshkho et al., 2019; Tai et al., 2016). They typically consist of two opposing jaws that open and close linearly, actuated either pneumatically or electrically (Dorna-Robotics, 2023; Universal-Robots, 2020). Their effectiveness is highest when handling rigid, regularly

shaped parts with known dimensions and consistent pose. However, parallel grippers exhibit limited adaptability to irregular or deformable objects and, in industrial settings, commonly require precise alignment to achieve reliable grasping (Tai et al., 2016).

Vacuum grippers (Figure 4.1c) operate by generating a pressure differential to create adhesion between the gripper and the object surface (Tai et al., 2016). They are particularly effective for flat, non-porous objects such as sheet metal, glass, and packaged goods, and are frequently used in pick-and-place applications. While vacuum systems require minimal mechanical complexity and can achieve high-speed operation, their effectiveness is constrained by surface texture and the presence of contaminants. Additionally, vacuum grippers provide limited holding force for heavy or irregular items and can experience reliability issues in variable environmental conditions.

Multi-fingered grippers, those with more than two opposing fingers/plates, such as in Figure 4.1d, offer greater dexterity and conformance with object geometry through multiple independently actuated fingers (Hughes et al., 2016; Tai et al., 2016). Figure 4.1d features a gripper with soft, deformable fingers, although multi-fingered configurations commonly also utilise rigid or hand-like components (Reddy & Suresh, 2013; Widhiada et al., 2015). These grippers are capable of performing a variety of grasping modes, including pinch, enveloping, and lateral grasps, and are better suited for handling complex shapes (Tai et al., 2016). Despite their versatility, fingered grippers introduce significant control challenges due to the increased degrees of freedom and the need for sophisticated planning and feedback. Their performance is highly dependent on accurate perception and model-based control strategies, which can limit their deployment in uncertain or dynamic environments (Tai et al., 2016).

Soft grippers (Figure 4.1d) address the growing demand for automation in unstructured or semi-structured environments, ranging from logistics and agriculture (Feng, 2021; M. Mohammed & Al-Ibadi, 2024; Reddy & Suresh, 2013) to healthcare (Cepolina & Razzoli,

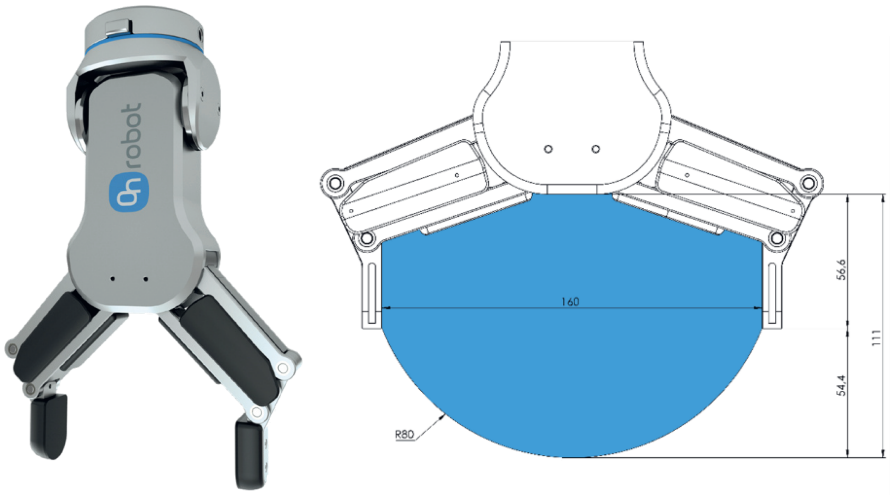
2024) and recycling (Saliba et al., 2010), has created demand for handling parts that are irregular in geometry, fragile, or variable in material properties. Research in soft robotics has introduced a new class of compliant end effectors, designed to provide passive adaptability through material deformation (Feng, 2021; Hughes et al., 2016; M. Mohammed & Al-Ibadi, 2024; Safeea et al., 2018). Soft end effectors are typically fabricated from elastomers or textiles and are actuated using pneumatic, hydraulic, or tendon-driven systems (Hughes et al., 2016). These designs enable inherently safe and gentle interactions with delicate objects, making them suitable for applications in agriculture, food handling, healthcare, and collaborative robotics (Feng, 2021; Hughes et al., 2016; M. Mohammed & Al-Ibadi, 2024; Shimoga, 1996). Despite their promise, soft end effectors present engineering tradeoffs. Their payload capacity is typically lower than rigid counterparts, and they suffer from reduced positional repeatability due to their inherent compliance (Hughes et al., 2016). Furthermore, closed-loop control of soft grippers remains a challenging problem due to the nonlinear behaviour of soft materials, limited sensor integration, and the high dimensionality of deformation (Birglen & Schlicht, 2018; Shimoga, 1996). As a result, much of the work in soft end effector design includes the development of embedded or external sensing systems, such as soft capacitive sensors, embedded strain gauges, or vision-based feedback loops, to enable responsive control strategies and improve reliability in dynamic environments.

4.3 End Effector for Versatile Material Handling

4.3.1 Hybrid End Effector Design

OnRobot RG6

The core mechanical structure of our end effector is the OnRobot RG6 (OnRobot, 2025), which has a 150mm stroke and customizable gripping force, enabling precise pressure modulation for different



(a) (b)

Figure 4.2: OnRobot RG6 end effector (OnRobot, 2025). (a) Image of the RG6 end effector with a quick-connector on top for mounting to robots. (b) Diagram of the stroke (grasping envelope) for the RG6. The maximum distance between the fingers opens to 140mm. The fingers also move along the vertical axis when closing, resulting in the blue area being within pinching range.

materials handled by the robot (Figure 4.2). While a smaller, versatile gripper, such as the RG6 (OnRobot, 2025) or a similar parallel/fingered gripper, allows for more delicate material handling, these do not have a stroke large enough to encompass some of the materials currently used in insect farming. We decided to use a rigid core structure to ensure we can carry the necessary payload for materials such as water-filled drinking devices or cricket-filled cardboard structures (Chapter 2). We selected the RG6 due to its payload capacity of up to $6 - 10$kg (depending on the grasp orientation) while maintaining a relatively low weight (1.25kg) and a range of variable gripping force ($25 - 120$N). Its compact design as a 2-finger gripper is also desirable for operating within enclosures (Chapter 2 and Chapter 3). However, the lower limit on the gripping

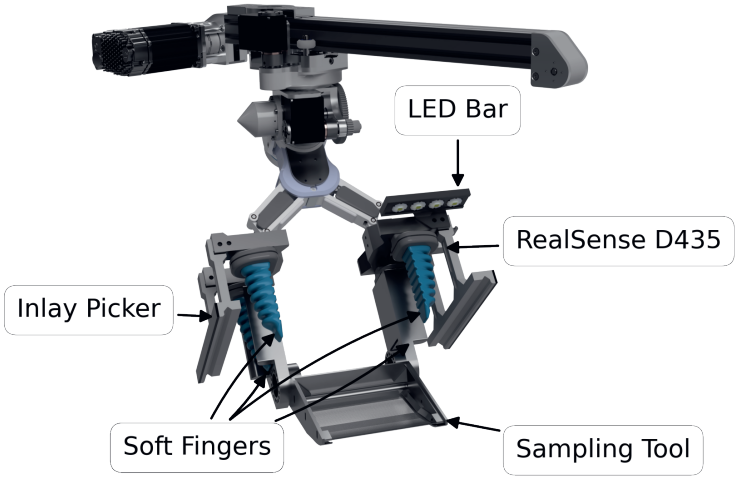


Figure 4.3: End effector annotated diagram. The core element is an OnRobot RG6 to which we attach 3D-printed interfaces. These interfaces allow us to mount the Soft Gripping Fingers SG.AG.F1.60 (Soft-Gripping, 2024), creating a hybrid between a rigid and soft end effector. The interfaces can be further extended by side brackets, denoted 'Inlay Picker', to enable outward force grasps. The RealSense D435 and LED Bar enable vision at the TCP of the gripper for applications such as visual inspection or visual serving. The 'Sampling Tool' is held securely by inflating the soft fingers against 3D-printed interfaces, enabling sampling as a mode of quality management for insect farming.

force of the RG6 (25N) is still enough to crush delicate objects, and it is unsafe for operating within insect enclosures (Requirement 4, Chapter 2). Furthermore, the RG6 grasping envelope is not wide enough for all CoRoSect materials, and its rigid structure requires precise positioning for a successful grasp. We opt to extend the RG6 with modular and soft elements to increase its flexibility for handling diverse materials of different sizes, geometries, and textures.

Soft Gripping GorillaFinger SoftActuator

We develop a custom end effector by extending the RG6 (Figure 4.3) to (1) enable delicate grasping and (2) perform grasping modalities other than pinching to handle diverse objects varying in shape, size, and material stiffness, from rigid to pliable (Hughes et al., 2016; Liu et al., 2018). The RG6 is augmented with two 3D-printed modular structures that act as interfaces for the attachment of various components. We attach four Soft Gripping Fingers SG.AG.F1.60 (Soft-Gripping, 2024), lightweight and pneumatically activated, as modular soft elements (Figure 4.5b). Each of the two pairs faces each other such that inflating the fingers enables a pinching or embracing grasp at the tool centre point (TCP). We use two pairs to provide stability when grasping larger flat-surfaced objects, such as long trays. The pneumatic system allows us to vary the pressure exerted at the fingertips to handle delicate materials with low forces. Additionally, their compliance with geometry provides additional tolerance for grasping non-uniform objects without the need for highly controlled object placement. We use the opening width of the RG6 to determine the size of the contact surface between the soft fingers and the object being grasped. Opening the RG6 completely allows the fingertips to delicately pinch a small object. Closing the RG6 increases the contact surface for the entire finger to embrace larger objects. We include interfaces for modular elements, allowing multiple configurations, such as those in Figures 4.4 and 4.5. The core RG6 also retains its rigid grasping surface for heavy materials that are not crushed when grasping at high force.

Modular Configurations

We further extend the end effector by including additional slots for attaching modular, 3D-printed structures capable of handling items that the soft fingers cannot, such as plastic crates with abrasive or cutting sharp edges. Figure 4.4 shows images of the real end effector



(a) (b) (c)

Figure 4.4: Images of the manufactured prototype end effector in three configurations. (a) The default configuration for versatile grasping features the soft fingers mounted to the RG6 and the LED bar for illumination at the TCP. (b) Addition of mounted 3D printed side brackets for inside-out grasping by opening the RG6 or de-pressurising the soft fingers. (c) The soft fingers hold a specifically designed sampling tool for visual inspection in insect farming, elaborated in the use cases described in Chapter 6.

configured for insect farming operations, namely material handling and visual inspection (through sampling). In particular, Figure 4.4c shows how the soft fingers are used to grip a sampling tool. Figure 4.5 shows CAD renders for all configurations used for insect farming use cases.

In material handling cases where a pinching or embracing grasp cannot be applied, for example, larger open objects such as the tightly fitting ovipositioning inlays, we attach additional mounted brackets (Figures 4.5d and 4.5f) to enable outwards force on the sides of the inlay by opening the RG6 from inside. These brackets are fabricated from PLA for their compliant properties and fitted with a black rubber strip. This strip is specifically added to prevent slippage of the inlays during the robot's motions, ensuring secure and stable handling. The need for some specific operations in insect farming use cases (Chapter 2) includes the handling of specialised tools, such as a sampling tool for quality control (Figure 4.5e). Upon picking the tool, the soft fingers are inflated to maintain a secure hold until the task is completed. The soft fingers absorb shock and provide impact tolerance when the tool is in use in a non-highly-controlled environment. For visual feedback at the TCP, the

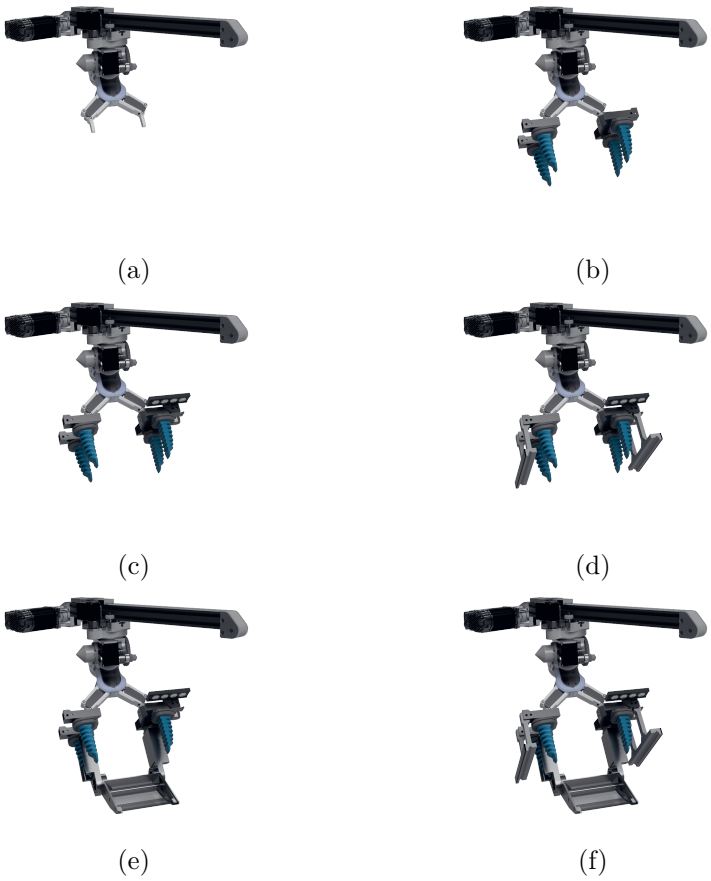


Figure 4.5: CAD visualisation of possible end effector configurations, mounted to the robot extension (Chapter 3). (a) The base RG6 without any modular elements. (b) The two pairs of soft fingers are attached to the RG6, which dynamically controls the distance between them. (c) Including the RealSense camera and an LED bar in the end effector, providing vision and an appropriate light level at the end effector. (d) Added side brackets for distributing outward force, for example, for picking from inside an item. (e) Soft fingers holding a sampling tool used in the visual inspection of insects. The tool includes a finger-hold where the soft fingers can fit perfectly to maximise surface contact. (f) All modular elements combined.

end-effector is equipped with a RealSense D435 camera and an LED bar (Figures 4.3 and 4.5c), whose brightness can be adjusted as needed.

Control and ROS Integration

The End Effector operates under the Robot Operation System (ROS) framework (Quigley et al., 2009). We use a custom Python interface based on ROS services to communicate with the OnRobot web interface and directly control the RG6. This allows us to dynamically set the opening/closing force and width without having to pre-program individually activatable programs by sending digital signals to the OnRobot control box. Additionally, we use the unified robot description format (URDF) to integrate the end effector with ROS and MoveIt! (Coleman et al., 2014; Şucan et al., 2012). The end effector URDF can be included in the robot description of an articulated robot arm for collision avoidance and motion planning. However, for simplicity, we only actuate the joints of the RG6 to provide opening and closing (for example, with MoveIt! Task Constructor (Görner et al., 2019)). The soft fingers are modelled as rigid structures for motion planning to simplify their bending behaviour.

4.3.2 Theoretical Modelling

Soft Gripper Modelling and Governing Equations

To explain the behaviour of our end effector (Bredenbeck et al., 2022; Simionescu et al., 2008) and the impact of combining an RG6 rigid gripper with soft gripping fingers, we first use the work of (X. Zhou et al., 2015) and (Haibin et al., 2018) to describe types of grasps affected by similar soft-fingered grippers (Bakhy et al., 2013; Bakhy, 2014; P. Cheng et al., 2021). (X. Zhou et al., 2015) uses Euler's theory for elastica to model a soft finger as a perfectly elastic rod, parametrised by an arc length coordinate $s \in [0, l]$ where l is the length of the soft finger, and an externally controllable intrinsic curvature profile defined $\kappa_g = \kappa_o(s)$.

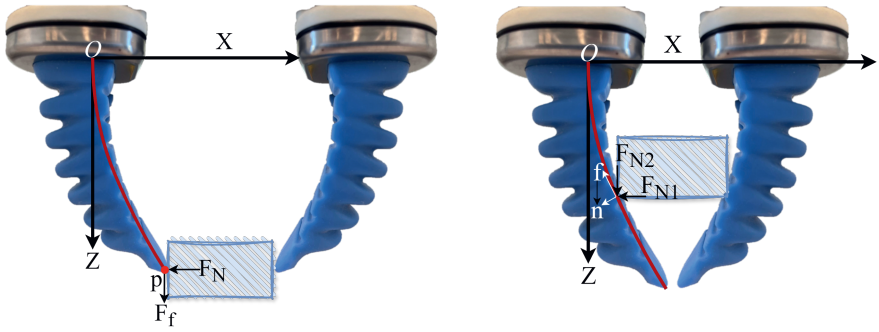
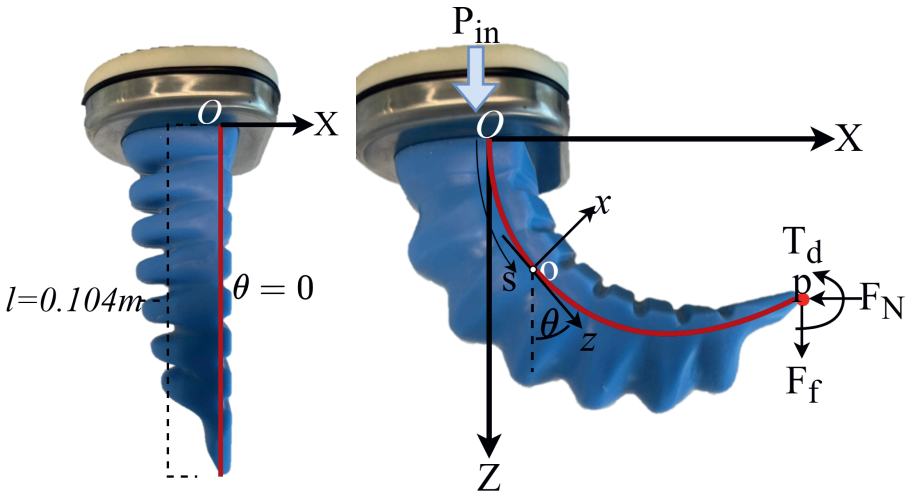


Figure 4.6: Grasp type visualisation (X. Zhou et al., 2015) with the Soft Gripping GorillaFinger SoftActuator. (a) Grasp I and II: a pinching grasp at the fingertip p of a soft actuator. Grasp II is grasped from below, mirrored around X. Items are held stable with the force of static friction F_f caused by the gripping force F_N. (b) Grasp III: an embracing/enveloping grasp where an item is held firmly within the length l of the fingers, showing two normal forces at the point of contact F_{N1} and F_{N2} resulting in the local normal n and tangential f forces.

They define three types of grasps, depicted visually in Figure 4.6. Grasp I (Figure 4.6a), and equivalently Grasp II (an upside-down Grasp I, mirrored around the X-axis), are pinching grasps where an object is held with static friction forces at the tip of the soft fingers. We define the friction force $F_f = \mu F_N$, where F_N is the normal force and μ the static friction coefficient at point p at the fingertip. Grasp type III (Figure 4.6b) is an embracing grasp, where the soft fingers envelop the object, which is now held with a friction force f tangentially to the contact surface and a normal force n, which are related to force components F_{N1} and F_{N2}. These definitions hold for grasping flat rigid surfaces, although there are cases where the contact surface is more difficult to define, for example, a triangular object where the normal force results from both the force of gravity and the gripper's orientation. We consider grasps of type I and III to be generalisations of more complicated cases, but they remain the most common when using our end effector.



(a) (b)

Figure 4.7: Elastic rod model defined by (Haibin et al., 2018) to model the behaviour of a soft finger. θ denotes the bending angle of the soft finger at an arbitrary point o characterised by arc length s away from the mounting point O. (a) A soft finger without input air pressure and no bending $\theta = 0$. The total length of the finger $l = 0.104m$. (b) A soft finger with input pressure P_{in} causes bending, moving the fingertip to point p where it is in contact with a surface, exerting grasping force F_N, static friction F_f, and bending torque T_d. At the point o, bending occurs with angle θ between the local z to global Z axis.

To arrive at a set of equations for Grasp I and III, (X. Zhou et al., 2015) parametrises $\theta(s)$ as the angle between one of the axes (X or Z) and the unit tangent vector to the curvature of the soft finger as it bends. $\theta(s)$ is a function of the arc length s. We show $\theta(s)$ in Figure 4.7b based on the coordinate diagram in (Haibin et al., 2018) (relative to the Z vertical plane). Defining $\theta(s)$ allows a formulation for the bending moment M in the rod, described by:

$$M = EI(\theta'(s) - \kappa_o(s)) \tag{4.1}$$

where EI is flexural rigidity and $\kappa_0(s)$ the intrinsic curvature as a function of s. Using equations for the total energy of the rod, (X. Zhou et al., 2015) arrives at the following sets of equations that describe a stable grasp and relate the bending angle θ with the gripping force F_N:

Grip I and II

$$\begin{aligned} &EI(\theta''(s) - \kappa_0'(s)) - \rho g(l-s)\cos\theta(s) \\ &+ F_f\cos\theta(s) - F_N\sin\theta(s) = 0, \quad s \in (0,l) \end{aligned} \tag{4.2}$$

Grip III

$$\begin{aligned} &EI(\theta''(s) - \kappa_0'(s)) - \rho g(l-s)\cos\theta(s) = 0, \quad s \in (0,\gamma) \\ &EI(\theta''(s) - \kappa_0'(s)) - \rho g(l-s)\cos\theta(s) \\ &\qquad + F_{N2}\cos\theta(s) - F_{N1}\sin\theta(s) = 0, \quad s \in (\gamma,l) \end{aligned} \tag{4.3}$$

where EI is flexural rigidity (consisting of E the modulus of elasticity and I the second moment of area in (Haibin et al., 2018)), $\kappa_0(s)$ the intrinsic curvature, ρ is mass per unit length, l is the length of the soft finger, F_N is the normal force and $F_f = \mu F_N$ the force of friction. In case of Grasp III, the contact between the held object and the elastic rod occurs at $s = \gamma$, which results in two equations for $s \in (0,\gamma)$ and $s \in (\gamma,l)$, as well as the use of two normal forces F_{N1} and F_{N2} (depicted in Figure 4.6b). These equations describe the behaviour of the soft finger at an arc-length s away from the mounting point and relate the bending angle θ to the grasping force F_N.

(Haibin et al., 2018) develops a soft gripper using shape memory alloys (SMAs) and uses a similar approach to that of an elastic rod to model the bending and gripping force while considering multiple fingers involved in a grasp. Their model begins with the Coulomb model for friction:

$$F_{mg} = \sum_{j=1}^{j_{max}} F_{fj}$$
$$F_{fj} = \mu_j F_{Nj} \tag{4.4}$$

where F_{mg} is the gravitational force of a grasped object of mass m, F_{fj} is the friction force for finger j out of j_{max} total fingers involved in the grasp, μ_j is its friction coefficient and F_{Nj} is the normal (grasping) force. (Haibin et al., 2018) provides a coordinate frame diagram of the elastic rod representation for their soft finger, which we map onto the Soft Gripping GorillaFinger in Figure 4.7. Figure 4.7b shows the bending of an elastic rod (in red) as a model for our soft finger, with forces of friction F_f, grasping force F_N, and bending torque T_d acting at the tip p where an object is held. s represents the arc length to an arbitrary point on the rod. (Haibin et al., 2018) defines $\theta(s)$ as a function of s to measure the rotational angle between the XZ coordinate frame and the local xz frame attached to the rod at s. Hence, $\theta(s)$ increases as the soft finger is actuated to bend.

(Haibin et al., 2018) uses the Cosserat Theory (Pai, 2002; Rucker & Webster III, 2011) to formulate the grasping force of their soft finger following from Figure 4.7. They derive the following set of differential equations, which relate the bending angle θ with the grasping force F_N and the displacement along the X and Z axes:

$$\begin{aligned} X'(s) &= \sin\theta(s) \\ Z'(s) &= \cos\theta(s) \\ \theta''(s) &= \frac{F_N \cos\theta(s) + (\mu F_N + \rho A g l - \rho A g s)\sin\theta(s)}{EI} \end{aligned} \tag{4.5}$$

where E is the modulus of elasticity, I the second moment of area, ρ is mass per unit length, l is the length of the soft finger, g is gravitational

acceleration, A is cross sectional area, and F_N is the normal force. Substituting $F_f = \mu F_N$ and accounting for the rotated coordinate frame for θ with respect to (X. Zhou et al., 2015) (switching sin with cos), these equations can be rearranged to match that of Equation 4.2, again providing a relationship between the bending angle θ and the grasping force F_N, now for multiple fingers and with the additional relationship between the displacement in $X'(s) = \sin\theta$ and $Z'(s) = \cos\theta$. This provides us with a relationship between the displacement of arc length s, caused by the bending of the soft finger, with θ. Rearranging the equivalence $\theta = sin^{-1}X'(s)$ implies that the greater the displacement along the X axis, the larger the bending angle θ, which is also visually shown in Figure 4.7. (Haibin et al., 2018) poses that there is no analytical solution to these equations due to non-linearity and multiple possible solutions. Instead, they provide a simulation to determine a solution to this set of equations and validate it with experimental data.

Relationship between Input Air Pressure and Grasping Force

While we can provide a relationship between the bending angle θ and the grasping force F_N for the soft fingers, the work of (H. Zhang et al., 2025) allows us to expand our theoretical modelling to include a relationship between the input pressure P_{in} for a pneumatically actuated soft gripper with both the bending angle θ and grasping force F_N. (H. Zhang et al., 2025) uses Pseudo-Rigid Body Modelling (PRBM) to model their pneumatically activated gripper. We map their diagram for a compliant beam-shaped soft finger to our soft fingers in Figure 4.8. The bending of the soft finger is modelled by a torsional spring at point o at a distance γl from the fingertip for a set length ratio γ. The gripping force exerted is denoted here as F_e to match the figure in (H. Zhang et al., 2025), but is equivalent to F_N used in previous equations. P_{in} denotes the pressure input into the soft finger, and θ in this case is the bending angle of the pseudo-rigid body. The effect of the bending angle is equivalent to that in Equation 4.5.

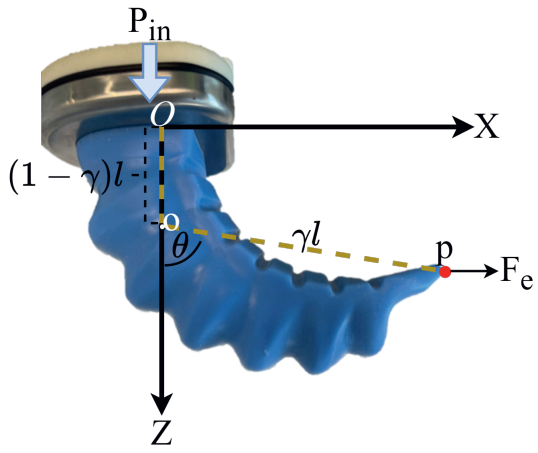


Figure 4.8: Pseudo-Rigid Body Model (PRBM) used in (H. Zhang et al., 2025) visualized for our soft finger. The finger is modelled as two pseudo-rigid segments split by a ratio γ of the total length and a joint at point o, where a torsional spring models the bending characterised by angle θ. The force F_e acts upon the fingertip p when pressing against a rigid surface.

(H. Zhang et al., 2025) derives a transfer function of the output bending angle θ as a function of input pressure P_{in}, starting from the Lagrange equation $L = E_k - E_P$, where E_K is kinematic energy and E_P is potential energy, arriving at Equation 4.6:

$$\frac{\theta(s)}{P_{in}(s)} = \frac{\frac{N}{A}}{s^2 + Ds + \frac{K}{A}} \tag{4.6}$$

where θ is the bending angle, P_{in} is the pressure input, A is a constant resulting from the computation of energy in Equation 4.8, N is defined in Equation4.9 as the product of the cross sectional area and distance between centre of area and centre of rotation, K is a stiffness coefficient, and D is a damping coefficient, and arc length s becomes the variable of the characteristic equation for the differential equation $\theta'' + D\theta' + K\theta = \frac{N}{A}P_{in}$ derived from total energy of the system. The additional variables

are defined as follows:

$$K = \frac{k}{A} \tag{4.7}$$

$$A = \frac{7}{12} m\gamma^3 l^2 \tag{4.8}$$

$$N = \int_{a+l}^{a+b+l} (2e - a)hdh \tag{4.9}$$

where k is a stiffness coefficient, m is the mass of the soft finger, γ is the length ratio, e is the width of the soft finger, a is the width of the inner wall, b is the inner length, h is the total length, and l is the distance from the fixed end to where grasping force is exerted. Using these and Equation 4.6, (H. Zhang et al., 2025) produces the following relations for input air pressure P_{in} with the grasping force exerted upon a held object $F_e = [F_x \quad F_z]$ (Equation 4.10) and the special case when no force is exerted at the finger ($F_e = \vec{0}$) (Equation 4.11).

$$P_{in} = \frac{A(K\theta - J^T F_e)}{N} \tag{4.10}$$

$$P_{in} = \frac{AK\theta}{N} \tag{4.11}$$

where $J = \left[\frac{\gamma l}{2}\cos\theta \quad \frac{\gamma l}{2}\sin\theta\right]$ is the Jacobian relating angular velocity θ' to the end effector's velocity, where we see correspondence to the system of Equations 4.5 for $X'(s)$ and $Z'(s)$. (H. Zhang et al., 2025) further offers controllers for both position θ of the system and force F_e, arriving in a formulation 4.12 where the expected grasping force F_{exp} is computed based on input pressure P_{in} and a measured real bending angle θ_{real} (the angle has to be measured otherwise the set of equations has 2 unknown variables and multiple solutions). Here $J^{+^T} = \frac{2}{\gamma l}[\cos\theta \quad \sin\theta]$ is the Moore-Penrose inverse of J^T:

$$F_{exp} = J^{+^T} \left(\frac{N}{A} P_{in} - K\theta_{real} \right) \tag{4.12}$$

We use the specifications for the Soft Gripping GorillaFingers to compute the constants A and N (Equations 4.8 and 4.9), which allows us to compute the stiffness coefficient k for Equation 4.10. The GorillaFinger is documented as exerting 11.0N at 1.0bar input pressure. Assuming this force is exerted at the tip of the finger $l = 0.104$m, we obtain $k \approx 0.228$.

Relationship between Distance-to-Object and Bending Angle

The hybrid design of our end effector allows us to dynamically adjust the opening of the RG6 to create a larger grasping envelope around materials. We depict this in Figure 4.9. Opening the RG6 increases the tolerance to placement errors in non-highly controlled environments, allowing the soft fingers to wrap around materials of different shapes and sizes and comply with their geometry to establish a grasp despite perturbation. We show the flexibility of the gripper with experiments in Section 4.4.1, where we measure flexibility by introducing offsets and counting successful grasps.

However, reducing the RG6 opening width brings the soft fingers closer together (Figure 4.9a), typically resulting in more stable grasps in experiments. We attempt to explain this phenomenon using the series of equations derived for the kinematics of soft fingers (Equation 4.5) and the relationship between input air pressure and bending angle (Equations 4.11 and 4.10).

(X. Zhou et al., 2015) defines the distance from the soft finger to a contact surface with variable H, which is depicted in Figure 4.10. While there is no direct formulation for a relationship between grasping force F_N and the distance H, (X. Zhou et al., 2015) provides a series of finite element method (FEM) (Morita, 2021) simulations with their soft finger

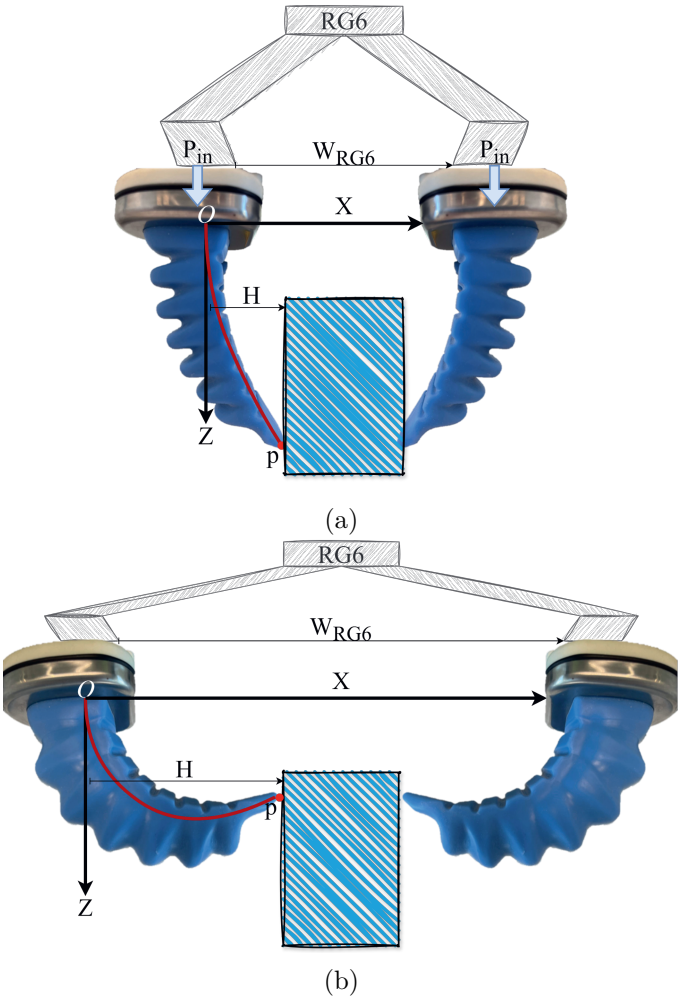


Figure 4.9: Diagram for the effect of closing and opening core RG6 to change the distance between the mounted soft fingers. The opening width of the RG6 is shown by W_{RG6}. The blue box represents a held rigid body. (a) When the RG6 is closed, the distance H from the mounting point O of the soft fingers is smaller, resulting in less bending of the finger. (b) When the RG6 opens by increasing W_{RG6}, the distance H increases, causing more bending and a vertical displacement in the contact point p with a held object.

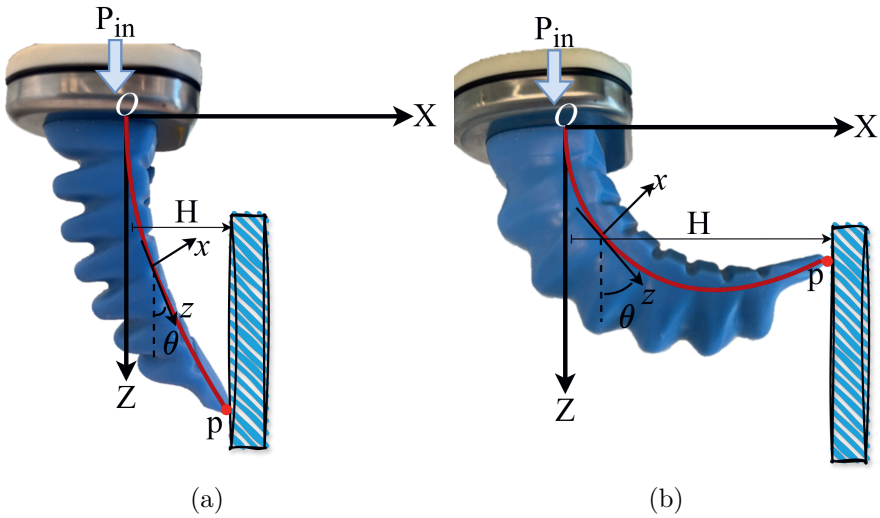


Figure 4.10: Diagram relating the distance to a held item H with the bending angle θ. (a) When the rigid body (blue) is closer to the soft finger, noted by the shorter H, the bending angle θ is also smaller. (b) The distance H increases, leaving more empty space for the soft finger to bend before coming into contact with the rigid body, resulting in a larger θ.

where the distance H is varied, resulting in a lower F_N when increasing H. We confirm this with our own experiments in Section 4.4.1.

Intuitively, when the finger is less bent, a larger portion of its surface is in contact with the held object. Equation 4.4 is a simplified relationship between normal and friction forces, which parametrises surface area and its effects under the friction coefficient μ. However, this does not necessarily hold for soft surfaces, the friction of which becomes significantly more complex at a molecular level (Klaassen et al., 2019; Liang et al., 2021) and when considering non-rigid surfaces of objects [1].

[1] This depends on the actual/real contact area, which is typically smaller than the apparent surface area (Liang et al., 2021). We deduce that the soft material of the fingers will likely have a more complex relationship with the actual contact area due to surface irregularities and flattening (Klaassen et al., 2019).

Effectively, the increased contact surface between the soft fingers when the bending angle θ is smaller is expected to contribute to a stronger grasping force.

In addition to this, there is an effect of the distance-to-object H on the grasping force F_N as an indirect result of the bending angle θ. This stems from the 'critical' situation when the grasping force is just enough to hold the object (in a pinching grasp, such as Figure 4.10), exerting the lowest necessary force. To explain this, we use the formulations of Equations 4.5, 4.10, and 4.12 to define an indirect relationship between the distance H and the grasping force F_N. First, we relate the bending angle θ to the distance to the object H, where both will increase when the object is placed further from the mounting point of the soft finger. We show this visually in Figure 4.10, and support it with Equations 4.5 using the relationship $X'(s) = \sin\theta$. We determine that $\theta \propto H$, as the soft finger will bend further for larger H before contact is established with the object and the normal force F_N starts acting upon the fingertip. Since we are using a pneumatically actuated soft finger, we turn to Equation 4.10 to show that $F_N = \frac{N}{A}P_{in} - \frac{k}{A}\theta$ (matching Equation 4.12). An intuitive way to increase the grasping force and bending angle is to increase the input air pressure P_{in}. However, if we assume the input air pressure P_{in} is set as a constant, $\frac{N}{A}P_{in}$ becomes a constant. We can deduce that $F_N \propto -\frac{k}{A}\theta$. Therefore, the grasping force F_N at the contact point p is expected to be lower when θ is larger (Figure 4.10b), and F_N will increase when the finger bends less (Figure 4.10a). Therefore, through $\theta \propto H$, when the object is placed further from the mounting point (origin O), we expect a larger bending angle and lower grasping force, which is confirmed by the results of FEM simulation (X. Zhou et al., 2015) as well as in our experiments (Section 4.4.1). We deduce that we can use the opening width of the RG6 as a tradeoff between additional tolerance in grasping placed objects and the grasping force exerted.

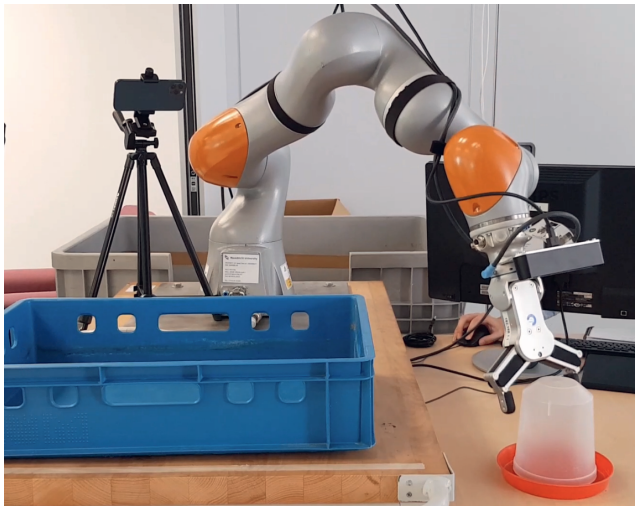


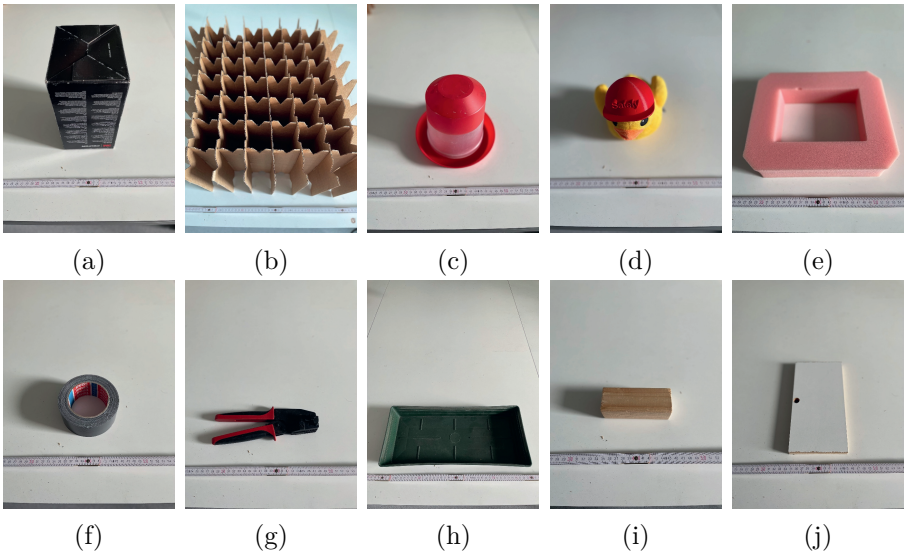
Figure 4.11: RG6 mounted on KUKA iiwa 14 used in initial requirement analysis of the end effector for CoRoSect. The gripper is used to pick items from the insect farming industry to determine the operational range across various materials. A ZED2i camera is mounted atop the flange.

4.4 Experiments and Results

4.4.1 Experiment Setup

Initial RG6 Experiments

We use the RG6 mounted to a KUKA iiwa 14 (Figure 4.11) to perform initial attempted grasps of materials used in insect farming (Chapter 2). We test the limitations of the RG6 to determine which objects can not be reliably picked and placed. The RG6 is limited to pinching grasps, which we show to be problematic for deformable objects, such as the cardboard structures for cricket rearing and filled trays. Additionally, the minimum gripping force of 25N is too high for handling of delicate and soft materials in close proximity to living insects (Requirement 4, Chapter 2).



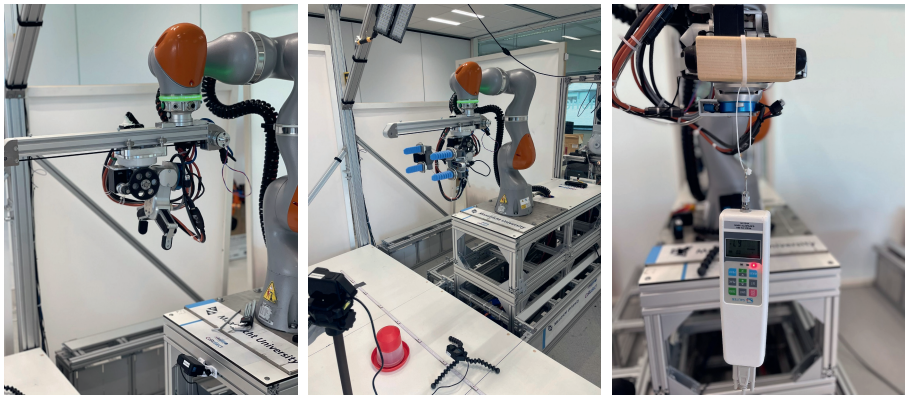
(a) (b) (c) (d) (e)

(f) (g) (h) (i) (j)

Figure 4.12: Materials for handling in experiments. (a) A common cardboard box. (b) A cardboard structure used in cricket rearing. (c) A water container, or drinking device, used in cricket rearing. (d) A plush duck (with a hat). (e) A foam packing insulator. (f) A roll of duct tape. (g) A tool. (h) A food tray used in cricket rearing. (i) A 116mm wide wood block. (j) A 116mm wide, flat wooden plate.

Hybrid End Effector Experiments

We use the entire robotic system (Chapter 5), mounting the end effector to the robot extension (Chapter 3), to perform experiments in a laboratory environment over a large workspace (Figure 4.13). We evaluate the hybrid end effector by testing grasps on 10 diverse objects shown in Figure 4.12. We include both standard shapes, such as a cardboard box, as well as items specific to the insect farming industry. Among various protocols of evaluating end effectors and grasp quality (Falco et al., 2020), we evaluate the grasps by quantifying *resistance*: the resilience of the grasp to external perturbation, and *dexterity*: the precision involved when grasping an object as defined in (Shimoga,

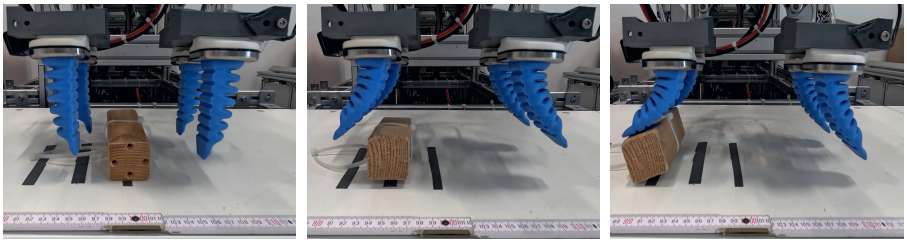


(a) (b) (c)

Figure 4.13: CoRoSect end effector experiment setup. (a) The RG6 end effector in *downward* orientation, used to emulate an industrial gripper. (b) The full end effector in **upright** orientation, featuring a set of two soft fingers on each arm of the RG6. (c) The Sauter FH500 force gauge (Figure 4.13c) was used to measure the pulling force exerted on objects held by the end effector, in this case the wooden block (Figure 4.12i).

1996; Zechmair & Morel, 2021).

We test *resistance* by measuring the force needed to pull the object downwards and cause it to slip out. A gripper with high *resistance* to outside perturbation will require a high force to release a held object (Figure 4.13). We use a Sauter FH500 force gauge (Figure 4.13c), pull on each item from below, and record the exerted downward force until we exceed the friction force keeping the object grasped. We stop pulling at $\approx$ 40N to prevent damage to the brakes. Two orientations of the gripper are tested, with orientation 1: *upright* facing the gripper parallel to the workspace surface (Figure 4.13b), and orientation 2: *downward* facing the gripper down towards the workspace surface (Figure 4.13a). As a baseline, we first use the RG6 (Figure 4.13a) to grip each object with closing forces of 25N, 50N, and 100N. We then test each object when held by the soft fingers (Figure 4.13b). Since the soft fingers are



(a) (b) (c)

Figure 4.14: CoRoSect end effector offset experiment setup, before gripping. (a) Wooden block with no offset. (b) Wooden block with 50mm offset. Vacuum was used to open the soft fingers outwards and an RG6 opening width of 80mm. (c) Wooden block with 100mm offset, barely in range of the soft fingers at RG6 opening width of 80mm.

unaffected by the closing force of the RG6, we measure the downward force for opening widths of the RG6 of 40mm, 60mm, and 80mm, which affects the geometry of the grasp and the magnitude of the grasping force (F_N, Section 4.3.2). The input air pressure is not changed and set at 1bar. We repeat each grasp 3 times. We record visual data for the deformation caused to non-rigid items when grasped by both the RG6 and the soft fingers.

Furthermore, we test *dexterity* by introducing a $25 - 100$mm offset to the item and performing a repeatable motion plan of the robot cell to attempt a grasp from the workspace surface (Figure 4.14). Each motion plan positions the end effector at a pre-pick pose and then descends along the Z axis to reach a feasible grasping location. The change in the relative position of the object to the end effector simulates placement errors in non-highly-controlled workspaces. Each grasp is performed at 25N with the RG6 and 11N (at 1bar) with the soft fingers. Each item is lifted (if grasped), and we repeat the *resistance* test to determine how the offset affects the quality of the grasp. We first use the RG6 to perform baseline grasps. We initially perform a grasp with no offset (0mm). Next, we increase to 50mm. If a grasp is successful at 50mm offset, we further increase the offset and attempt a grasp at 100mm.

Otherwise, if the grasp fails at 50mm (or if the grasp cannot support the force gauge and fails), we decrease the offset to 25mm and perform a final attempt. We then repeat each grasp using the soft fingers and vary the opening width of the RG6 to achieve successful grasps on objects out of range for the baseline RG6. Each test is repeated 3 times. We apply displacement along the opening axis for the RG6, because this is where we add additional tolerance by varying the opening width of the RG6. Naturally, a perturbation in the workspace can occur along all axes as well as in the rotation of the placed object. The symmetry of the end effector and held objects (particularly the rectangles or cylinders) allows us to decrease the number of repeated tests, but a full exploration of the offset and rotation is warranted as future work.

4.4.2 Results

RG6 Baseline Grasping and Offset Results

Each grasping experiment produces a measurement of force over time, such as that plotted and labelled in Figure 4.15. Here, we show a sample of the data for grasps produced with the RG6 gripper at 100N grasping force on the cardboard box. There are four key features of each plot: A) the plateau when the force meter exerts its own weight on the held item ($\approx$ 9N), B) a decrease in force or slope when the item first starts slipping, C) a peak when the item drops out of the gripper either by slipping out, or is released when we exert over 40N (for safety of the robotic components), and D) if the grasp was aborted, the force meter is still attached and returns back to $\approx$ 9N, otherwise, the item slipped out of the grasp and the force becomes 0. We first focus on extracting the peak where the held item was released, with the differentiation between grasps which exceeded $>$ 40N being aborted by the experimenter, and those released at $\leq$ 40N due to slipping.

Figure 4.16 shows the results for the peak force (mean over 3 repetitions) before the slipping/releasing of a held object occurs when using the RG6 end effector in *downward* orientation. The figure shows three values per

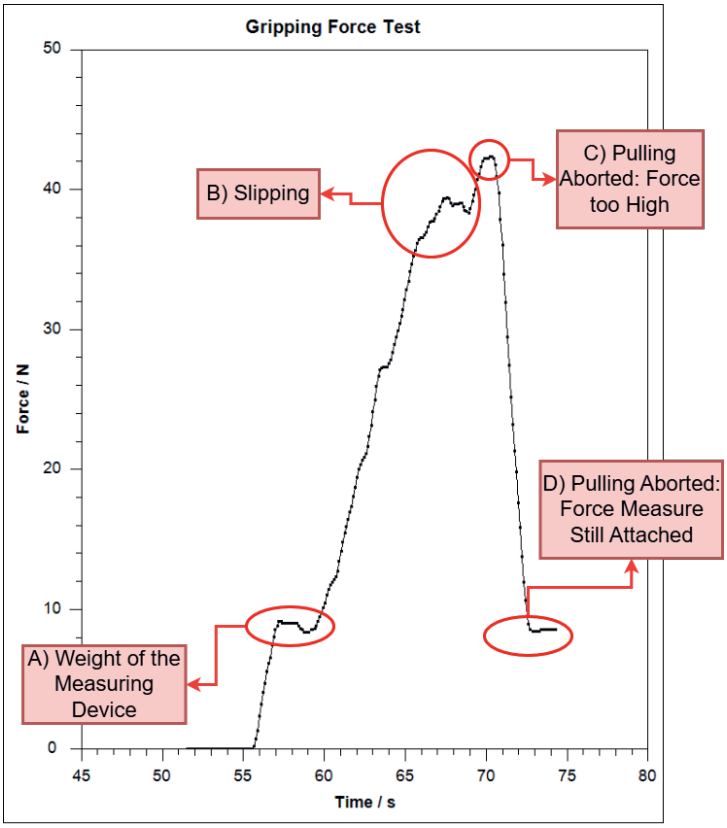


Figure 4.15: Force over time measured while pulling on the cardboard box gripped by the RG6 at 100N. (A) A plateau occurs when the full weight of the force meter is exerted by hanging it on the held object, adding to the force of gravity pulling it out of the grasp. (B) Slipping occurs when the slope of the steady increase in pulling force applied by the experimenters decreases. The object is still held, but dislocates along the pulling direction. (C) When the pulling force exceeds 40N, the experimenters stop the test to prevent overloading the robot joints. (D) If the object is released, the force meter remains attached, ending with the plateau. If the object slipped out of the grasp, it is no longer affected by the pulling of the force meter, and the measurement returns to 0.

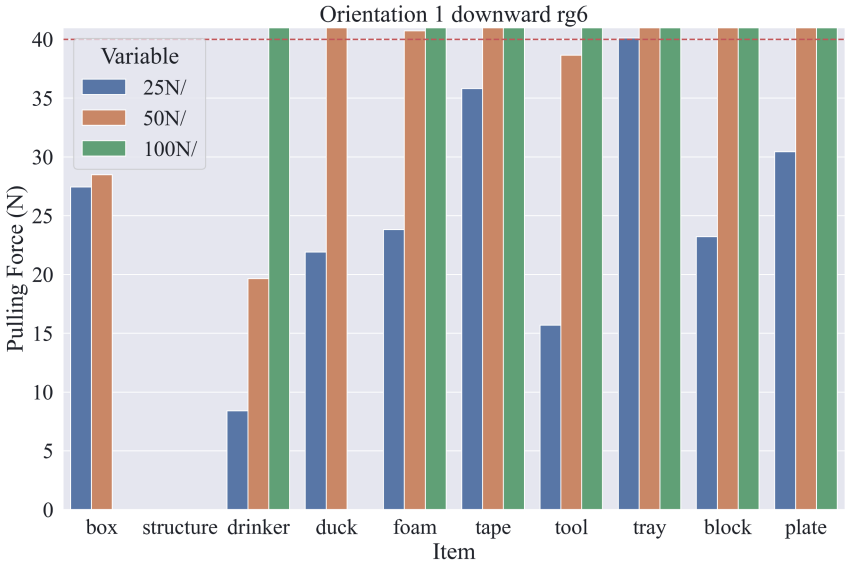


Figure 4.16: Gripping results RG6 end effector in *downward* orientation. The peak pulling force is averaged over 3 repetitions, shown for grasping forces of 25N, 50N, and 100N in coloured columns blue, orange, and green, respectively, for each object. A grip could not be established on the cardboard structure at this orientation. The box and duck were not gripped with 100N to prevent permanent deformation of the items.

item, representing three grasping force settings on the RG6: 25N, 50N, and 100N, respectively. The grasp of the large cardboard structure (Figure 4.12b) in this orientation was not feasible. We also omitted using 100N on the cardboard box and plush duck to prevent destroying the items in our first tests. The expected trend for a higher pulling force required to cause slipping when the grasping force is increased is seen for most rigid items in Figure 4.16. This follows from equation 4.4 where the static friction coefficient μ is constant for the contact between the gripper and the object while the gripping force F_N is increased. We see from 4.16 that a gripping force of 50N and 100N with the RG6 provide a secure grasp on all tested items in this position, while using a lower

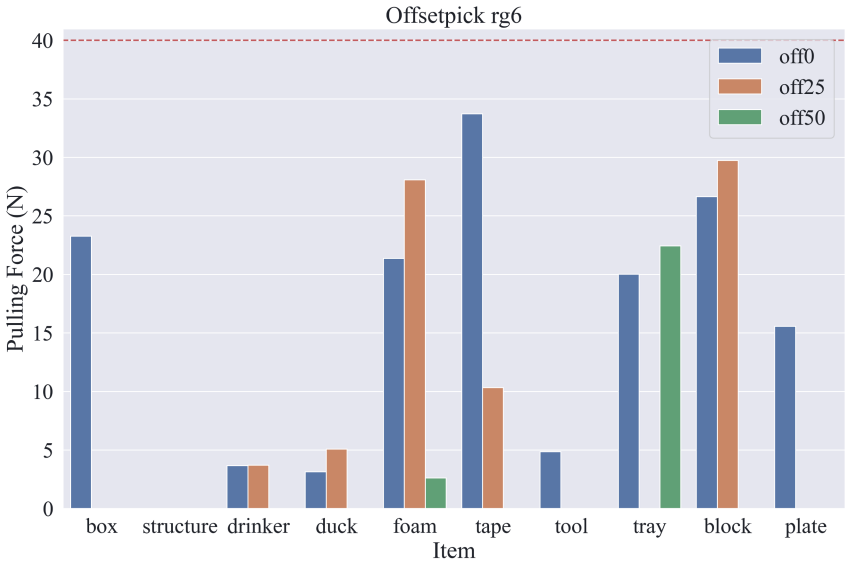


Figure 4.17: Offset results RG6 end effector in downward orientation. Peak measured pulling forces are shown for offsets of 0mm, 25mm, and 50mm in coloured columns blue, orange, and green, respectively, for each object. Only 2 out of 10 objects could be grasped at a 50mm offset: the foam and food tray. 5 out of 10 objects are successfully grasped at 25mm offset.

grasping force of 25N causes lower *resistance* to outside disturbance, particularly on non-flat surfaces such as the cylindrical 'drinker' (Figure 4.12c).

Figure 4.17 shows the results of the quality of the grasp with the RG6 when placing the item at 0mm, 25mm, and 50mm offsets, respectively. The RG6 could not perform a grasp at 100mm offset, hence we defaulted to 25mm for follow-up grasps. A natural observation is the effect of the size of each object on the grasp quality. With no offset, objects that fit tightly into the opening width of the RG6 (such as the box in Figure 4.18g) can be grasped stably. Smaller items were more likely to be grasped at increasing offsets, being pulled along the workspace

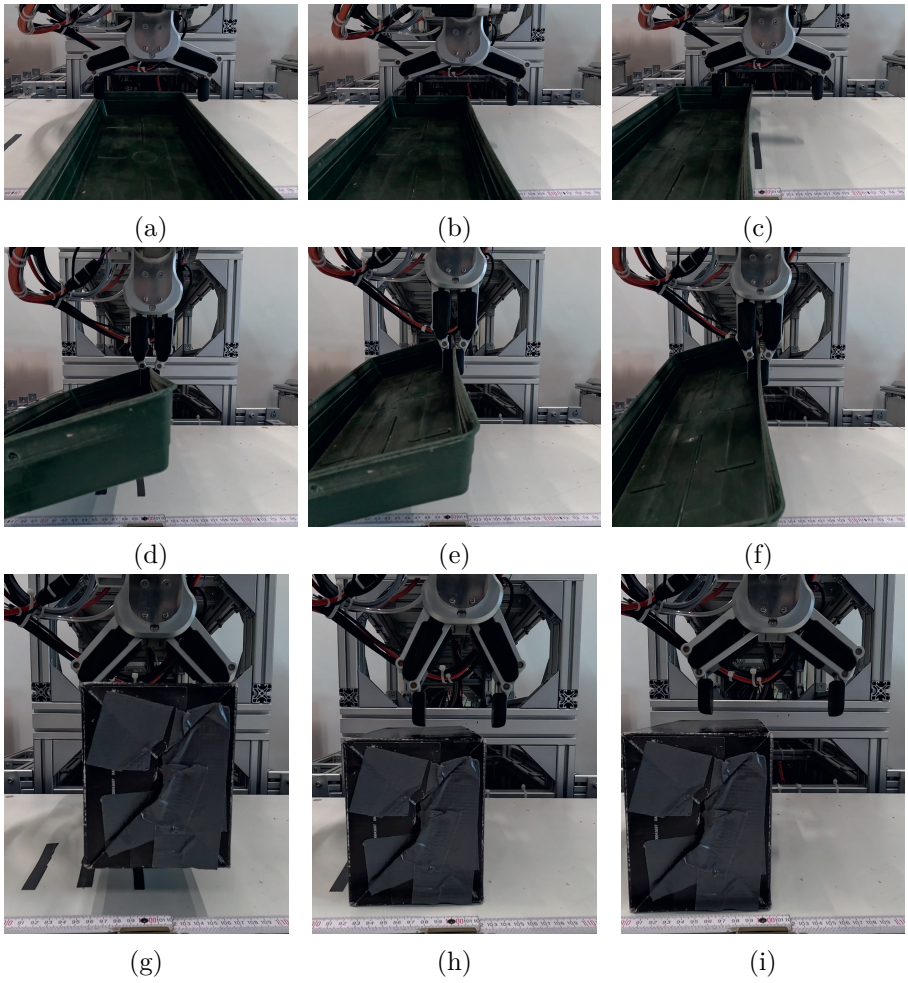


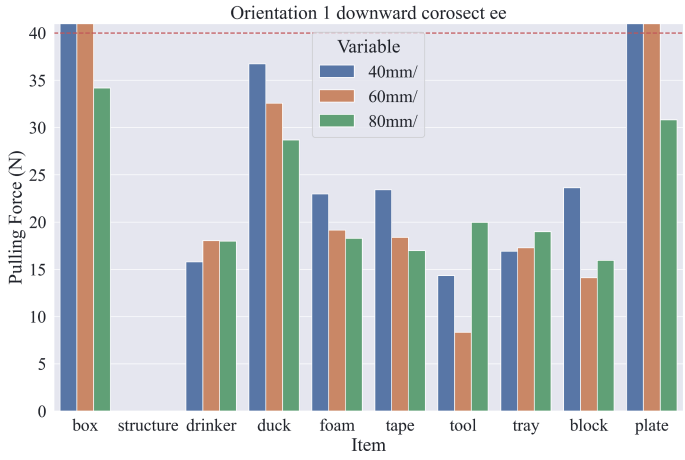
Figure 4.18: RG6 end effector offset case with the food tray item and box. (a)-(c) A food tray at offsets of 0mm, 25mm, and 50mm, respectively, before being grasped. (d)-(f) A food tray at offsets 0mm, 25mm, and 50mm, respectively, after being grasped. As the only successful item, the wall lining of the tray was within the stroke of the RG6 in all experiments. (g)-(i) A cardboard box at offsets 0mm, 25mm, and 50mm, respectively, where the offset places the box outside the stroke of the RG6, making grasping impossible without adjusting the orientation or positioning of the end effector.

to fit into the grasping envelope. We observe that larger objects pose a challenge to being gripped off the workspace already at 0mm offset and do not reach their maximum potential pulling forces from Figure 4.16.

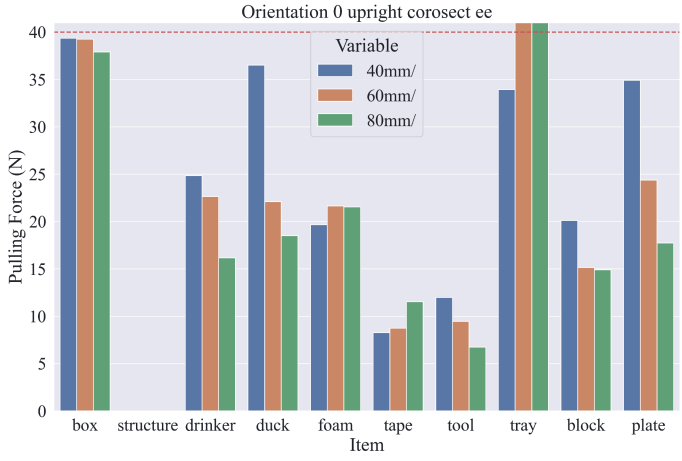
Images of the setup and example grasps are shown in Figure 4.18. The RG6 has a stroke large enough to encompass objects in a pinching grasp in certain orientations. For example, the 'box' is too wide when placed sideways, or the 'drinker' tightly fits into the opening. The outlier is the 'tray' (Figure 4.12h), which can be pinched by the side wall lining as long as it is within the stroke of the gripper (Figures 4.18a to 4.18f). However, the RG6 does not feature the dexterity to still grasp most offset items. The missing bars in Figure 4.17 designate those items that could not be picked at an offset. This is further explored in Figure 4.18g, 4.18h, and 4.18i, for the cardboard box, showing that the RG6 has no way to grasp the box without being repositioned. Overall, if an item is outside the stroke of the RG6, it cannot be pinched, and there is no tolerance to push along edges for items to slot into the gripper. In contrast to Figure 4.16, when grasping from the workspace surface after a set of motions, 25N grasping force does not secure a resistant grasp on some items: both the cylindrical 'drinker' (Figure 4.12c), tool (Figure 4.12g), and the soft 'duck' (Figure 4.12d) were dropped below 5N of pulling force. With the soft fingers, we seek to improve on the RG6 in terms of both the quality of these grasps and enable those that could not be established.

Soft Finger Grasping and Offset Results

Figures 4.19a and 4.19b show the results of grasping the items with the soft fingers while altering their separation by opening/closing the RG6 width to 40mm, 60mm, and 80mm, respectively, split between the two tested orientations. The RG6 gripping strength was set to 25N. The rated grasping force of the soft fingers is 11N at 1bar (Section 4.3.2).

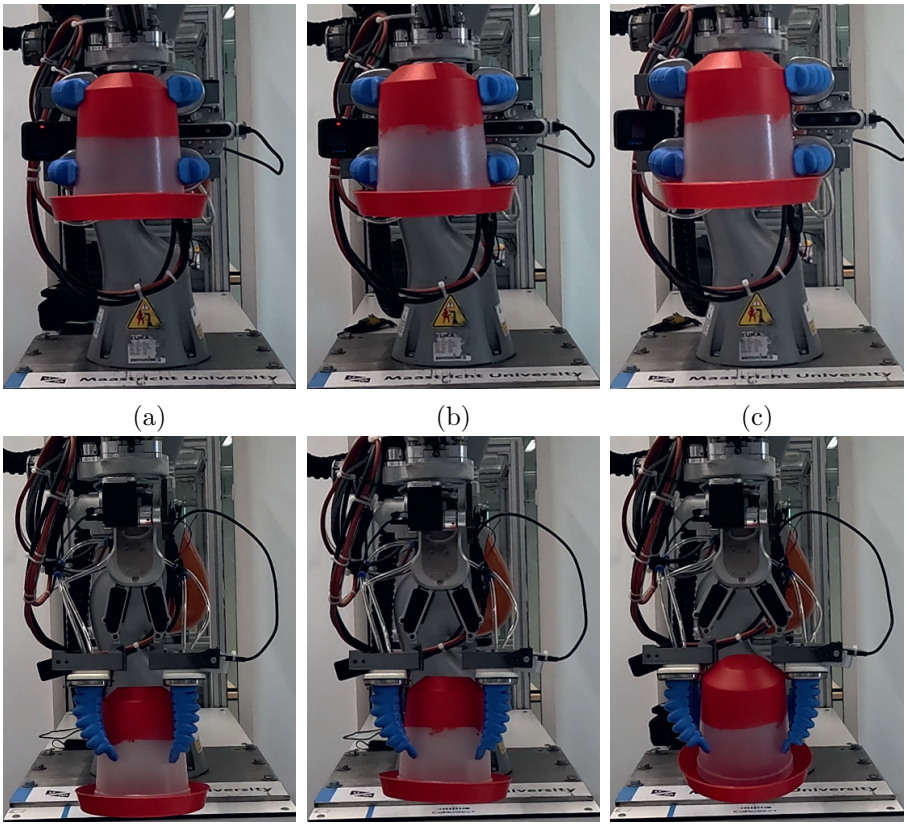


(a)



(b)

Figure 4.19: Gripping results hybrid end effector and soft fingers. The peak pulling force is averaged over 3 repetitions, shown for opening widths (distances between opposite soft fingers) of 40mm, 60mm, and 80mm in coloured columns blue, orange, and green, respectively, for each object. (a) *Downward* orientation. (b) *Upright* orientation. A grip could not be established on the cardboard structure at this orientation.



(a) (b) (c)

(d) (e) (f)

Figure 4.20: hybrid end effector and soft fingers orientation case for drinking device (Figure 4.12c). (a)-(c) Opening widths of 40mm, 60mm, and 80mm, respectively, in the *upright* orientation. The drinker is enveloped by the soft fingers, creating a Grip III (rotated outward). (d)-(f) Opening widths of 40mm, 60mm, and 80mm, respectively, in the *downward* orientation. Not all four soft fingers are able to touch the cylindrical surface, destabilising the grasp.

The orientation of the gripper influences the quality of the grasp. We focus on this for the 'drinker' item in Figures 4.20a to 4.20c, showing the grasp achieved in the *upright* orientation while 4.20d to 4.20f in the *downward* orientation. The soft fingers allow compliance with the geometry of the object, securing an embracing grasp (Grip III in Section 4.3.2) for the *upright* orientation and a pinching (Grip I) in *downward* orientation. When referenced with the force in Figures 4.19a and 4.19b, we can see that a greater pulling force is required when the gripper is able to embrace the cylindrical shape, indicating a stable grasp. In cases where the force exceeded the safety margin of 40N, the item was held at a corner by the ridges on the surface of the soft fingers, effectively locking it in place.

From the theoretical modelling in Section 4.3.2, we expect to see a larger pulling force necessary to release held items when the distance between the soft fingers is decreased, which is shown for most items in Figure 4.19. Although the equations derived in (Haibin et al., 2018; H. Zhang et al., 2025; X. Zhou et al., 2015) assume a rigid contact surface, we can show this is also the case for some deformable and soft surfaces such as the 'duck' or 'foam'. This implies that larger objects, which fit tightly into the grasping envelope, are expected to have a larger pulling force. However, because of the bending of the soft fingers and the geometry of the contact surface, we see high pulling forces exerted on smaller objects which the soft fingers can wrap around (Figure 4.19). The outliers, such as 'drinker' or 'tray', are caused by perturbations in the grasp geometry when an item is fully embraced (Grasp III) or is held by an asymmetric configuration of soft fingers. This is particularly the case of the cylindrical 'drinker', for which each attempt yields a slightly different grasp based on the exact positioning of the walls with the soft fingers (Figures 4.20d to 4.20f). In such cases, the grasp is not stable and requires a lower pulling force to release the held items. In cases of tightly fitting objects, such as the 'box' in Figure 4.19a at 40mm and 60mm, the grasping force is at its highest.

Figure 4.21 shows the results of attempted grasps at offsets of 0mm, 50mm, and 100mm using the hybrid gripper. In contrast to Figure

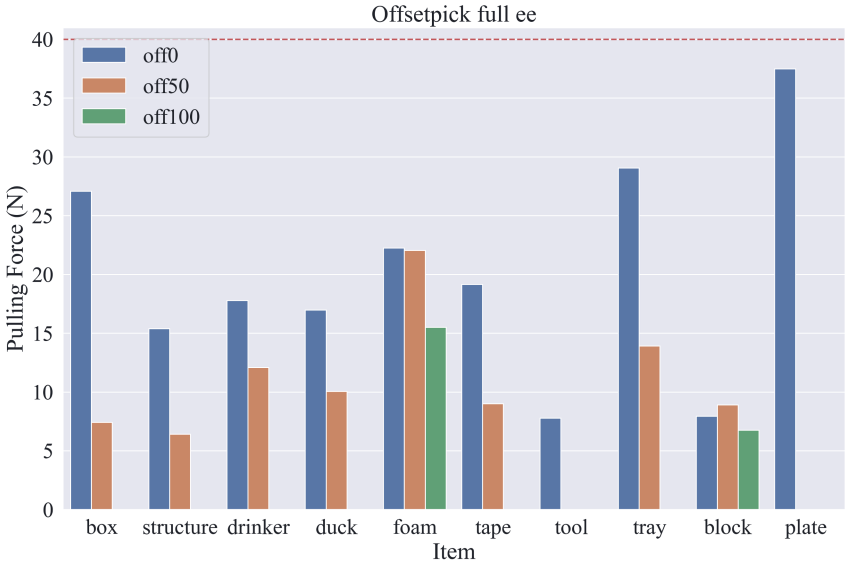


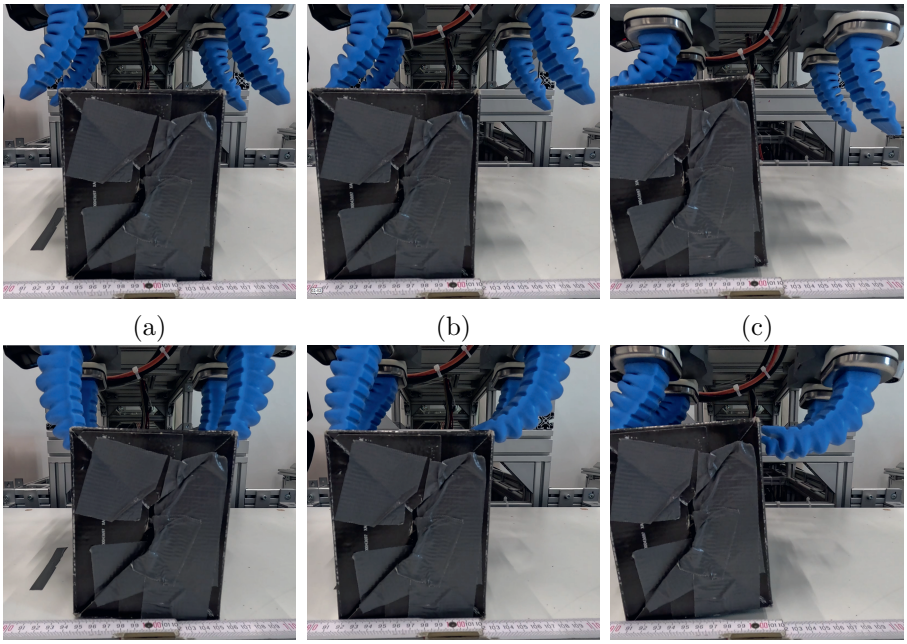
Figure 4.21: Offset results hybrid end effector and soft fingers. Peak measured pulling forces are shown for offsets of 0mm, 50mm, and 100mm in coloured columns blue, orange, and green, respectively, for each object. 2 out of 10 objects could be grasped at a 100mm offset: the foam and wood block. 8 out of 10 objects are successfully grasped at 50mm offset. Held items have a higher average force necessary to cause dropping than with the RG6 in Figure 4.17.

4.17, grasps on items except the 'tool' and 'plate' were successful at 50mm, hence the distance was increased to 100mm to test the upper bound.

Overall, the forces required to pull an object out of the soft fingers are lower than those of the RG6, comparable only to when the lowest grasping force of 25N is used. This is expected, as the rated grasping force of the soft fingers is 11N at 1*bar* (Section 4.3.2). However, we can establish a reliable grasp on larger objects that are out of range for the RG6 already at 0mm offset, showing an increase in the grasping envelope. We can also dynamically change this envelope with the RG6

opening width to suit the specific object, at the cost of grasping force (Figure 4.19). Considering the offset objects, the force required to pull the item out of the grasp is lower for offsets of 50mm, meaning the resistance of the grasp decreases. We can establish a grasp on the 'foam' and 'block' at up to 100mm offset at the furthest. This is because their cross-section along the grasping axis was the smallest, allowing them to easily fit into the grasping envelope. However, through increasing the stroke by opening the RG6 and pushing the soft fingers outwards through vacuum (Figures 4.22a to 4.22c), grasps of up to 50mm offset are reliably achieved. Hence, the hybrid gripper provides additional tolerance to placement errors at the cost of grasp quality, which we attribute as increased *dexterity*.

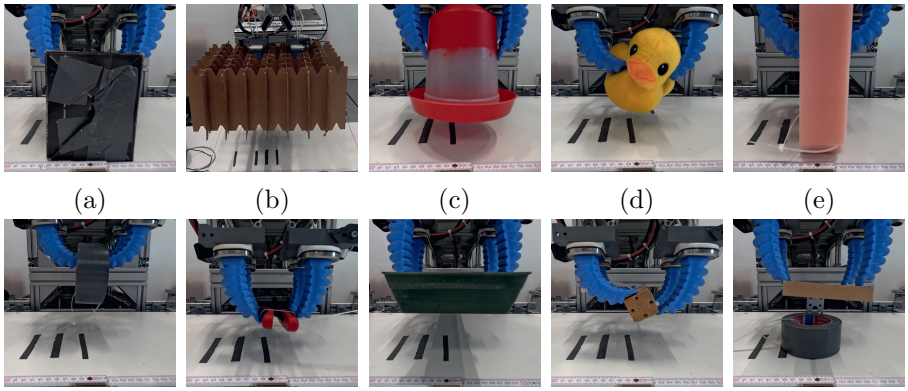
Figure 4.22 demonstrates how the offset influences the grasp for the cardboard box and how it becomes unstable. While half of the fingers are able to envelop the box on the offset side, the other side can only reach once the box is shifted towards them by the closing of the fingers (Figure 4.22e). However, although the box is grasped, once lifted, the item is no longer aligned with how it was picked up. Figure 4.23 further demonstrates the dexterity of the gripper in performing a stable grasp on each item.



(a) (b) (c)

(d) (e) (f)

Figure 4.22: Hybrid end effector and soft fingers offset case for the cardboard box. (a)-(c) A box at offsets of 0mm, 50mm, and a repetition of 50mm with a larger RG6 opening width of 120mm, respectively, before being grasped. (d)-(f) A box at offsets of 0mm, 50mm, and a repetition of 50mm with a larger RG6 opening width of 120mm, respectively, after being grasped. The soft fingers succeed in the grasp, but the asymmetry of their positioning to the box's surface causes an unstable grip and a loss of alignment with the workspace.



(a) (b) (c) (d) (e)

(f) (g) (h) (i) (j)

Figure 4.23: All materials grasped with the hybrid end effector and soft fingers. (a) A common cardboard box. (b) A cardboard structure used in cricket rearing. (c) A water container, or drinking device, used in cricket rearing. (d) A plush duck (without their hat). (e) A foam packing insulator. (f) A roll of duct tape. (g) A tool. (h) A food tray used in cricket rearing. (i) A 116mm wide wood block. (j) A 116mm wide, flat wooden plate. The roll of tape was used as a platform to place the plate upon to be level with the workspace surface.

4.5 Discussion

While the RG6 is intended for high precision grasping, with up to 125N grasping forces for stability, it requires a controlled placement of items to achieve a stable grasp. This holds for common rigid and industrial grippers (Hughes et al., 2016). When an offset is introduced in the placement of the object beyond $\approx 25mm$, achieving a successful grasp becomes difficult or fails for the current configuration (Figure 4.17). While the required precision is tolerable within highly controlled environments, this becomes a challenge in dynamic workspaces or when involving human workers. A common solution is a sufficiently precise robot vision system, which helps alleviate this issue through object localisation (which we implement in Chapter 6). However, sensors and computer vision software are not perfect and include errors in

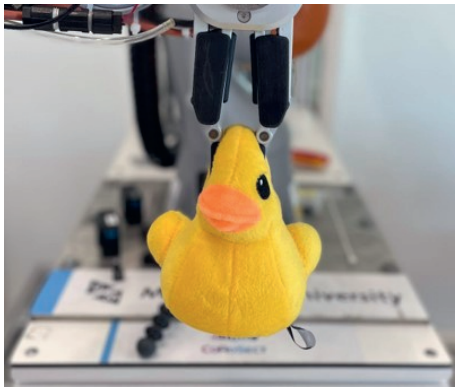


Figure 4.24: Deformation of the plush duck under 25N force of the RG6 gripper.

localisation and calibration, meaning a gripper reliant on high precision positioning is still vulnerable to failed grasps. Therefore, in industries, it is easier to control variables in the workspace by enforcing consistency and control over material placement. Reaching a high level of precision in the insect farming workspace is challenging because each crate is non-uniformly filled (for example, by a human worker), and we can not assume objects are placed consistently in the same positions in the workspace. This reveals a trade-off between establishing a secure grip on diverse types of materials and the ability of the robot to handle errors and inconsistencies in the workspace. The RG6 is capable of highly stable grasps at high force, but is limited by the grasping envelope and the need for precise positioning. It is also rigid and does not conform to the geometry of soft/deformable objects.

The issue of grasping at offsets and diverse sizes of materials can be addressed with a larger industrial gripper, one that provides additional tolerance in object placement by having a larger stroke and is designed for higher payloads. However, this may not be a practical solution for a collaborative robot with limited payload capacity, such as the KUKA iiwa 14. This option induces additional costs and may no longer fit within the confined spaces occurring in insect farming (for which

we already add additional degrees of freedom in Chapter 3). With larger industrial grippers, we also consider that the exerted forces are too large. The minimal force of $25N$ with the RG6 is already too high around delicate materials (Figure 4.24), and the rigid structure does not conform to object geometry, potentially causing permanent deformation. We also consider insect well-being (Requirement 4, Chapter 2), where larger industrial grippers are indelicate compared to a smaller, soft counterpart. In experiments, we have demonstrated that the enhanced gripping capabilities gained from soft elements, particularly their compliance to object geometry, increase the dexterity of the end effector. This is a desirable property when considering an industry that deals with diverse and developing materials. Our approach to a hybrid end effector takes advantage of both the rigid and soft elements, allowing grasping of various objects, and retaining the high payload capacity of the RG6 if necessary. Additionally, we retain the possibility of dynamically altering the grasping envelope using the opening width of the RG6.

Furthermore, we use a soft finger configuration to provide flexibility in grasping with additional tolerance to misplacement, which can comply with the geometry of complicated shapes (Hughes et al., 2016) and to avoid computing complex grasp synthesis. However, the typically lower grasping forces (Soft-Gripping, 2024; Tian et al., 2022; H. Zhang et al., 2025; X. Zhou et al., 2015) on soft grippers/fingers lead to less resistant grasps (Shimoga, 1996; Zechmair & Morel, 2021). In practice, most of the gripping is performed by the soft fingers. We are able to dynamically change the width between them to manipulate the quality of the grasp (Figures 4.19 and 4.19a) and achieve success at larger placement errors and misalignment (Figure 4.21). We also retain the rigid and high grasping force properties of the RG6 if necessary. While the hybrid design does not exceed the grasp resistance of the RG6, it is meant to increase dexterity and invariability to material geometry in a non-highly-controlled workspace. The results of picking offset objects show an increase over the RG6 in handling larger items with a wider grasping envelope and an increased tolerance to positional errors with

our hybrid approach. In practice, this end effector can be coupled with a visual servoing (or similar) system to ensure objects are within the grasping envelope. For example, our system is equipped with a mounted RealSense camera for visual feedback at the TCP.

4.5.1 Future Work

We propose a more thorough analysis of the dexterity of the hybrid gripper through follow-up experimentation with 3D orientation to explore the effect of object geometry on the quality of the grasp. A higher resolution of offset and rotation would allow refinement of exact boundaries for a grasping envelope, while rotation of items tests the extent of invariability to object geometry. This should additionally include further measurement of the quality of the grasp by pulling the object until slipping, which deserves its own analysis on detecting the point at which slipping occurs.

4.5.2 Grasping in Insect Farming Use Cases

Figure 4.25 demonstrates additional baseline grasps for comparison of practical material handling performed in insect farming. Figures 4.25a and 4.25b show the feeding tray (Figure 4.12h) with additional weights (simulating feed). We demonstrate how a pinching grasp with the RG6 may cause an imbalance of the held item, causing contents to spill when filled. The RG6 does not have a stroke large enough to grasp on either side of the tray, meaning a larger gripper is necessary to handle it. Figures 4.25c to 4.25e show a process of lifting the 'drinker' item out from a tall cricket crate in a laboratory setting. The only possible orientation is grasping from above, which has been shown to be unstable at low grasping forces in Figure 4.16, especially when misplaced (Figure 4.17).

While the definition of insect farming use cases is in Chapter 6, we use some of the materials involved to demonstrate additional capabilities of the hybrid end effector in a warehouse setting. Figure

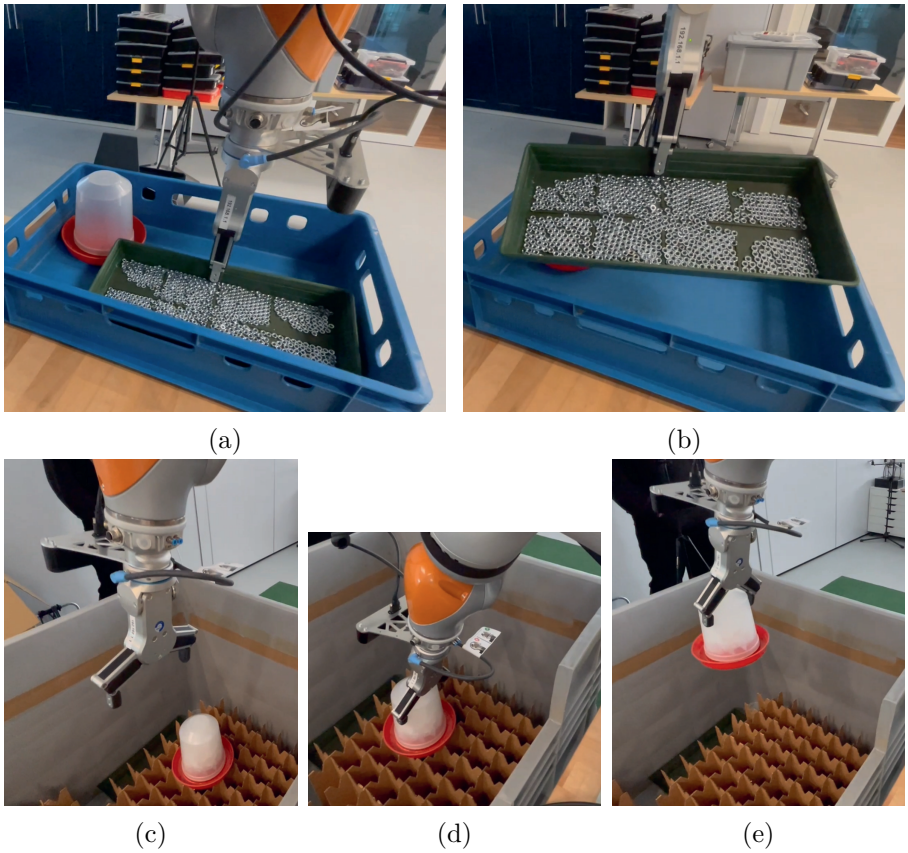
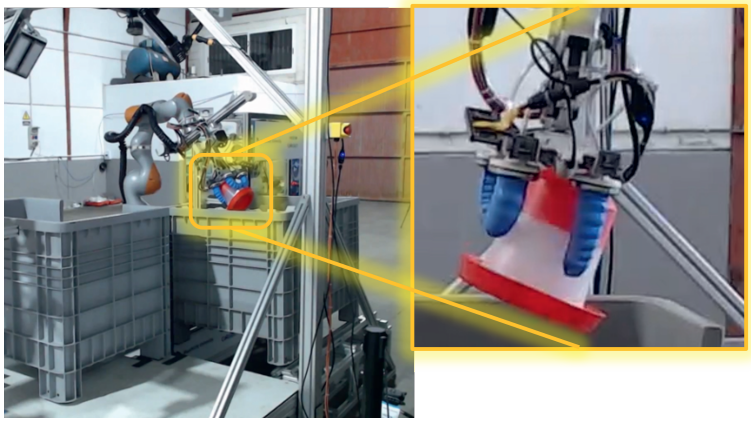


Figure 4.25: RG6 initial experiments with picking insect farming material. (a) A food tray, carrying small metal nuts to emulate additional weight, pinched the wall by the RG6. (b) The food tray after being lifted. The additional weight of the nuts causes the tray to be lifted unevenly, causing misalignment when placed back. (c)-(e) The RG6 is used to pick a drinking device from inside a cricket crate. The cylinder is placed atop the cardboard structure. Gripping the drinking device is only possible from above in practical use cases.

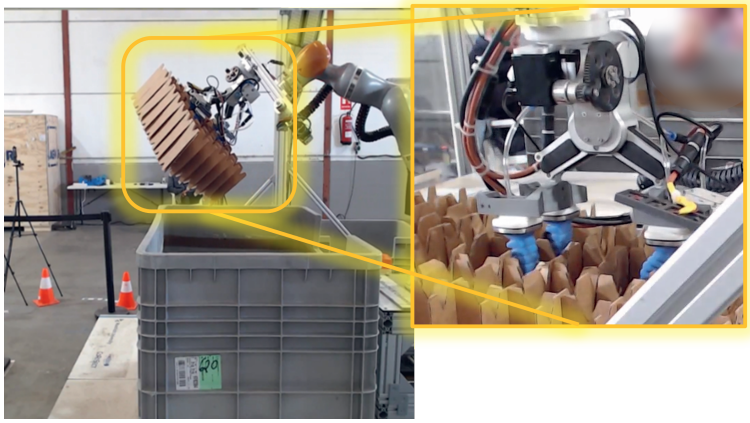
4.26 highlights the grasps achieved on materials involved in cricket management. In particular, the soft fingers allow stable handling of the cardboard structure (Figure 4.12b) by inserting them into openings before pressurising (Figure 4.26b). Without all four fingers, or using a pinching grasp, the cardboard structure folds, and placement cannot be solved without human intervention. Although the grasp on the cardboard is not highly resistant to outside forces (Figure 4.19), it is sufficient to prevent the structure from dropping during the motion of the robot cell.

Figure 4.27 demonstrates grasping an oviposition plate of comparable dimensions to the wooden plate in our experiments in Figure 4.12j. We ensure the stability of the held plate by gripping with all four fingertips and minimising the bending of the soft fingers to exert a larger grasping force. Plates are deposited within a rack (Figure 4.27c) and picked from within a large tent or from a stack (Figure 4.27b).

Finally, some objects were too large to pinch or envelop with the soft fingers. Figure 4.28 shows the end effector reconfigured with modular 3D printed side brackets (Figure 4.5d) to achieve a grasp on a tightly fitting inlay (white) that is extracted from a crate (blue) and placed within another. The side brackets enable grasping the inlay from inside, applying pressure to the inside walls by opening the RG6. Longer brackets allow fitting the soft fingers still upon the end effector (Figure 4.5d).



(a)



(b)

Figure 4.26: Picking cricket farming materials during CoRoSect use cases. (a) A focus on the grasping of the drinking device by the hybrid end effector. A grasp is established with two of the four soft fingers, leaving the other two for alignment stabilisation when the drinking device is moved. (b) A focus on the grasping of the cardboard structure, where the soft fingers are inserted into the openings for a proper grasp. Using four soft fingers, pressure is applied from within the cardboard, preventing folding and providing sufficient grasping force to move the item into cricket containers.

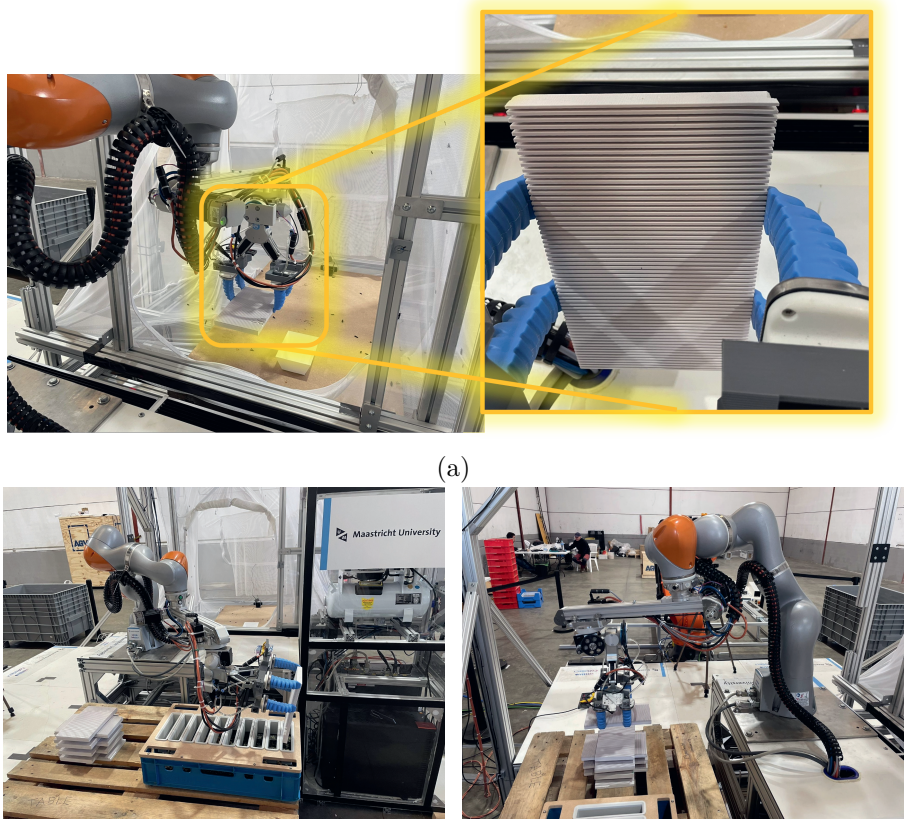
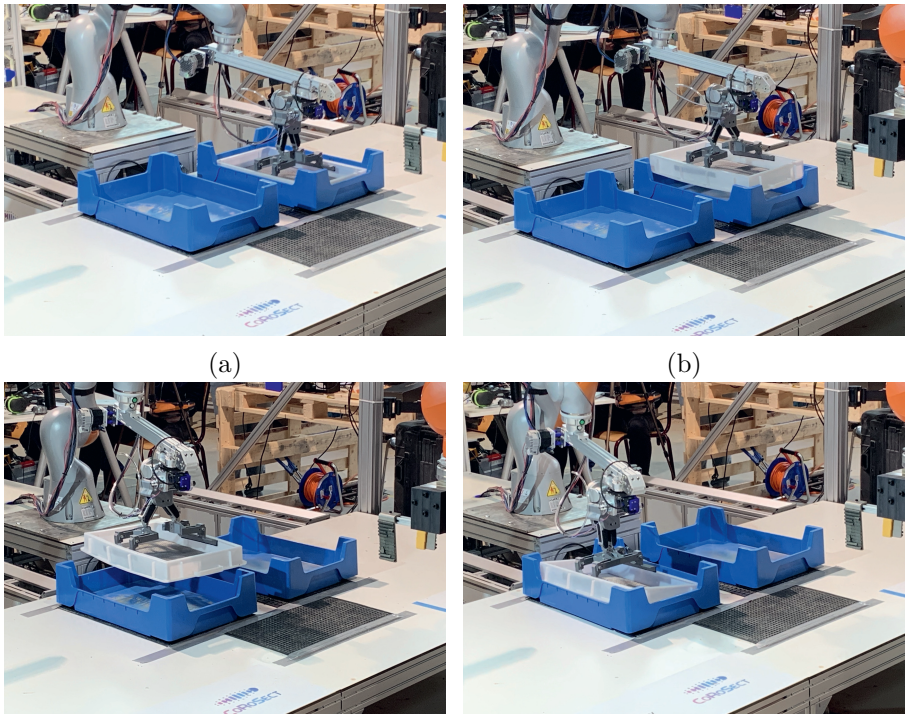


Figure 4.27: Picking oviposition plates for larvae management CoRoSect use cases. (a) A focus on the grasp of the oviposition plate, held at the fingertips by the soft fingers. The plate contains delicate eggs, meaning only a low-pressure, soft actuator was permissible. Four soft fingers provide enough stability to orient the plate to be extracted from within a mating cage and place it safely within a rack. (b) The oviposition plate is placed within a tightly fitting rack. (c) An empty oviposition plate is picked up from a stack of fresh material.



(a) (b)

(c) (d)

Figure 4.28: Picking oviposition inlay for larvae management CoRoSect use cases. An order of operations for picking and placing the oviposition inlay using modular side brackets on the end effector. The brackets apply force from the inside of the inlay, allowing it to be held by friction against its inner walls. (a) The end effector fitted with side brackets is positioned at the detected centre of the inlay. (b) The RG6 is opened outwards with the side brackets pushing against the inside of the inlay, allowing it to be lifted. (c) The entire inlay is positioned above the secondary crate for insertion. (d) The process ends with the inlay being placed within a separate insect crate (blue container).

4.6 Conclusion

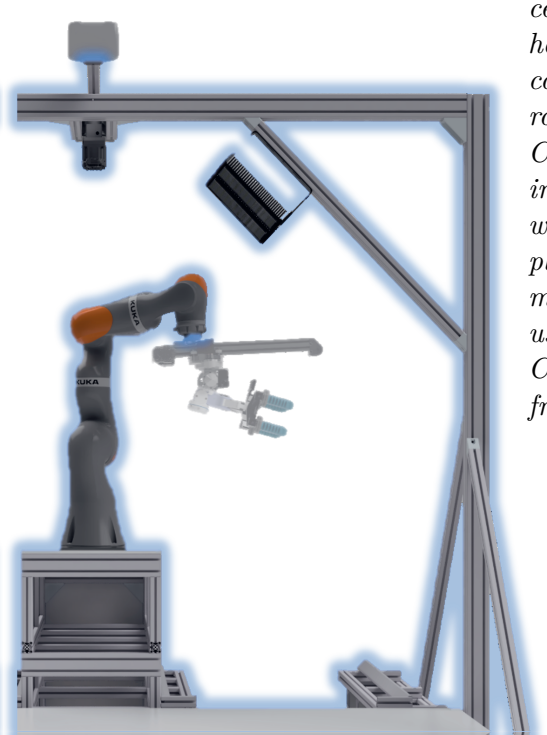
In this chapter, we presented the design and evaluation of a hybrid end effector that extends the capabilities of the RG6 gripper through the integration of modular and soft robotic elements. The adjustable opening width of the RG6 allowed dynamic control over the spacing between soft fingers, facilitating a tradeoff between a broad gripping range and stable, higher-force grasps. While the soft fingers do not exert as much force as an industrial gripper, they are more suited to delicate material handling in insect farming.

We developed a theoretical model informed by existing work in soft robotics to better understand the impact of finger spacing. Our experimental results confirmed that this spacing affects both the grasping force and the contact surface (Grip I vs. Grip III). The hybrid gripper demonstrated better performance than the RG6 in non-highly-controlled conditions, maintaining higher resistance to external perturbations when handling offset or misaligned objects. Additionally, the soft fingers effectively conformed to irregular and deformable objects, as confirmed through visual documentation.

To broaden its utility, we augmented the end effector with modular 3D-printed components capable of safely manipulating hard or abrasive items, further enhancing its versatility. The final prototype was successfully validated in an insect farming context, which requires handling a diverse array of sensitive and irregular materials. Chapter 6 contains demonstrations and results for successfully completing entire insect farming processes using the hybrid end effector in diverse workspace configurations. Overall, this work demonstrates a practical approach to increasing the flexibility of robotic manipulation through the strategic combination of rigid and soft elements in a modular design.

5

CoRoSect Robot Cell: Hardware Design, Motion Planning, and Software Architecture



In this chapter, we present the CoRoSect robot cell for versatile manipulation and material handling in insect farming. The robot is composed of a KUKA LBR iiwa 14 collaborative robot arm, the extension rail described in Chapter 3, and the hybrid end effector described in Chapter 4. A surrounding support structure was developed that accommodates a workspace platform and mounted 3D vision sensors. We motivate the design choices for the robot cell using the CoRoSect requirements defined in Chapter 2. In this chapter, we propose a control framework for the robot cell, at the core of which

is motion planning in MoveIt!. We use CAD models to implement a virtual planning scene resembling real conditions at an insect farm. To demonstrate the capabilities of the robot cell operating in enclosed spaces in insect farming, we perform motion planning for the extended robot arm in a virtual planning scene. With the additional degrees of freedom, surrounding support structure, and obstacles in the planning scene, there is a 100% *success rate of computing a trajectory in under* 5*s in constrained workspaces and within enclosures. Finally, we present a software architecture as a result of practically implementing the robot cell, which connects the motion planning to low-level controllers and high-level task management systems.*

5.1 Introduction

In this chapter, we propose an autonomous robot cell that addresses the shortcomings of industrial robots for versatile manipulation in the insect farming industry. The robot cell consists of a KUKA LBR iiwa 14 collaborative articulated robot with a surrounding support structure for sensors and lighting. The KUKA iiwa carries an extension rail (Chapter 3) for increased reachability over the workspace and a hybrid end effector (Chapter 4) for gripping various materials encountered in insect farming. Furthermore, we present the control framework developed to enable motion planning of the robot cell in MoveIt! (Coleman et al., 2014). A digital twin is used to test the feasibility of performing coordinated motions within a virtual motion planning environment resembling real conditions. The resulting software architecture, inspired by the work of (Hennersperger et al., 2017) and centred around high-level motion planning, is presented at the end of this chapter. The integration of an extension rail, hybrid end effector, 3D sensors, and motion planning systems is aimed at improving the versatility of the collaborative robot arm, making it more adaptable across tasks and domains (Rahman et al., 2024). While the robot cell is designed to fit the specific setting of insect farming, the systems are more widely applicable. Computer vision

and additional strategies for versatile manipulation are discussed in Chapter 6, which also demonstrates the capabilities of the robot cell in the CoRoSect pilot studies.

The research question addressed in this chapter follows from the need to design a robot cell that meets the requirements posed in Chapter 2 and implement an underlying control framework that enables its use.

Research Question 4

How can control and motion planning for a robot cell be achieved for the purpose of versatile manipulation in the insect farming industry?

We approach this research question from two perspectives. (1) The integration of an off-the-shelf motion planner, MoveIt!, with the extended kinematic chain of our robot cell. Motion planning is first performed in a virtual planning scene, where collision-free trajectories are computed based on a virtual representation of the workspace. We test the motion planner's performance in enclosed spaces and workspaces tailored to resemble insect farming to determine the effect of workspace complexity on the computation time. (2) Achieving a practical implementation of the robot cell by connecting a virtual motion planning scene to the physical articulated components. A final result in this chapter is a software architecture that enables two-way communication between hardware components, which together give the robot its versatile capabilities.

The first contribution in this chapter is a self-contained robot cell for the versatile automation of day-to-day tasks in the insect farming industry. While research relating to collaborative robotics in the insect farming industry remains limited, insights from fields such as agriculture, automation, and manufacturing offer a basis to approach the issues faced in insect farming (Pietrantoni et al., 2024; Tziolas, Karapatzak, Kalathas, Karampatea, et al., 2023; Tziolas, Karapatzak, Kalathas, Lytridis, et al., 2023). Collaborative robots are extensively used within the Industry 4.0 framework and are shown to provide

added utility in terms of safety and adaptability to processes, but are also typically slower and not necessarily well regarded for automation (Galin & Meshcheryakov, 2019; Kragic et al., 2018). The need for versatile robots that can correct errors and adapt to dynamic environments is growing in the insect farming industry as much as in other industries (Madau et al., 2020; Ortiz et al., 2016; Qadeer et al., 2024).

The second contribution is the control framework needed to perform high-level motion planning of the robot's extended kinematic chain. Control frameworks govern the behaviour of robots, dictating how they perceive, interpret, and respond to their environment and task requirements (Brogårdh, 2007). The development of robust robot control frameworks is necessary for the seamless interaction of autonomous robotic systems in insect farming operations and for providing scalable solutions to automation (Bertoli et al., 2024; El Zaatari et al., 2019).

Finally, the third contribution is the software architecture resulting from the control framework and structural components of the robot cell. The software architecture connects the hardware components, such as the end effector or mounted sensors, with the central high-level control systems that orchestrate the robot's motions. By enabling robots to autonomously navigate, manipulate, and interact with their environment in a cognitively aware manner, these frameworks have the potential to enhance the efficiency, productivity, and sustainability of insect farming operations (Galin & Meshcheryakov, 2019; Kragic et al., 2018).

This chapter begins with a motivation of the design choices for hardware components of the robot cell and compares them against similar approaches taken in related research (Section 5.2). This is followed by the control framework proposed for the robot cell and focuses on the central component of motion planning (Section 5.3). Experiments then test the feasibility of performing motion planning on the robot cell's kinematic chain in a virtual workspace (Section 5.4).

The resulting software architecture that enables control and high-level operation of the real robot cell concludes the chapter (Section 5.5).

5.2 Robot Cell Design and Hardware

5.2.1 Structural Components

The cognitive robot cell, introduced as the M-Robot in Chapter 2, is required to handle multiple insect species, multiple stages of life cycles, and the different types of materials, including insect crates, used by insect farming industries (Chapter 2). While the robot cell is designed to accommodate the needs of an insect farm, principles of versatility in automation in different industries (Duckett et al., 2018; Giusti et al., 2018; Lytridis et al., 2021; Oliveira et al., 2021) can be applied to its design. We propose a robot cell that combines an articulated collaborative robot with the developed extension rail (Chapter 3) and a hybrid end effector (Chapter 4). We develop a workspace platform and a surrounding support structure to accommodate these systems.

Modular Support Structure

An articulated robot requires a platform for handling the different types of materials introduced in Section 2.2, namely food trays, drinking devices, cardboard lattices for crickets, two types of ovipositioning devices for mealworm and BSF larvae, as well as performing delicate manipulation within their container crates. We developed a modular support structure, such as designs in (Cho et al., 2020; Schütz et al., 2014; R. Xu & Li, 2022). This support structure is composed of 4 main components shown in Figure 5.3. The structure is re-configurable to the specific setting at an insect farm.

The main platform of the robot cell, dedicated as a workspace for articulated robots, needs to be large enough to allow Human-Robot Collaboration (HRC) (Requirement 2, Chapter 2). Collaborative

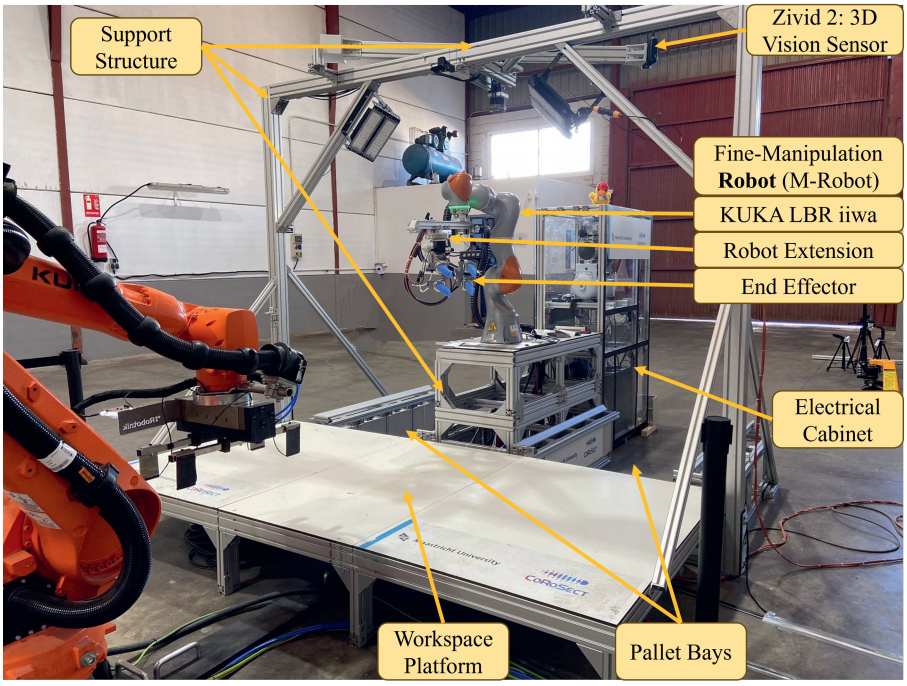


Figure 5.1: An annotated diagram of the robot and its support structure. The robot consists of three articulated components: a KUKA LBR iiwa 14, the robot extension, and the hybrid end effector. The support structure provides a central platform for mounting the KUKA iiwa and additional sensors, such as the Zivid 2 L100, on an articulated joint. The support structure also accommodates the workspace platform and two pallet bays where Automated Guided Vehicles (AGVs) deposit pallets of materials.

industrial robots typically ensure the safety of nearby human workers through an abundance of internal sensors, lower operational velocities, and compliance to touch (Chacón et al., 2021; Michalos et al., 2015). With these safety features, the workspace does not need to be restricted by physical barriers/fences, as it is for larger industrial robots. However, to comply with the requirement for HRC, it does need to be large enough to accommodate enough space for larger

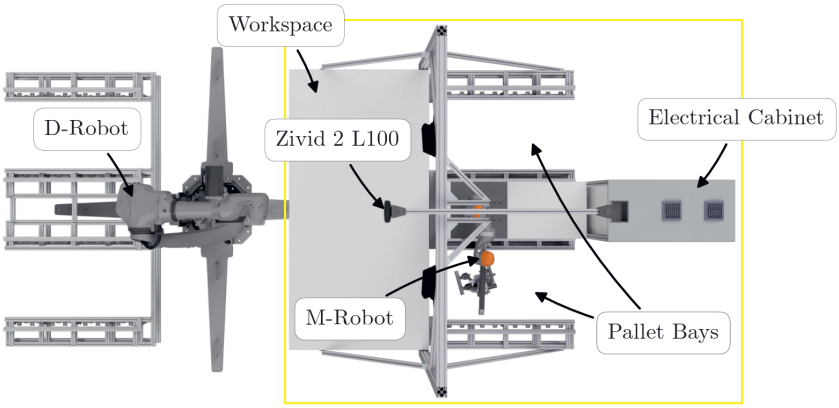
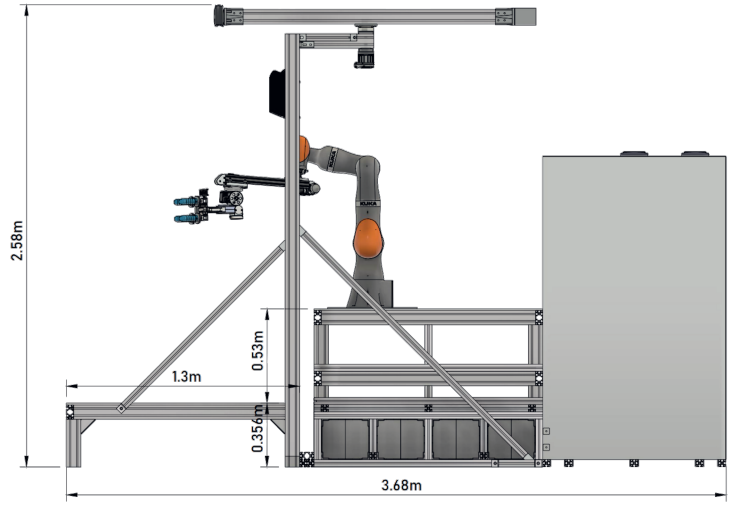


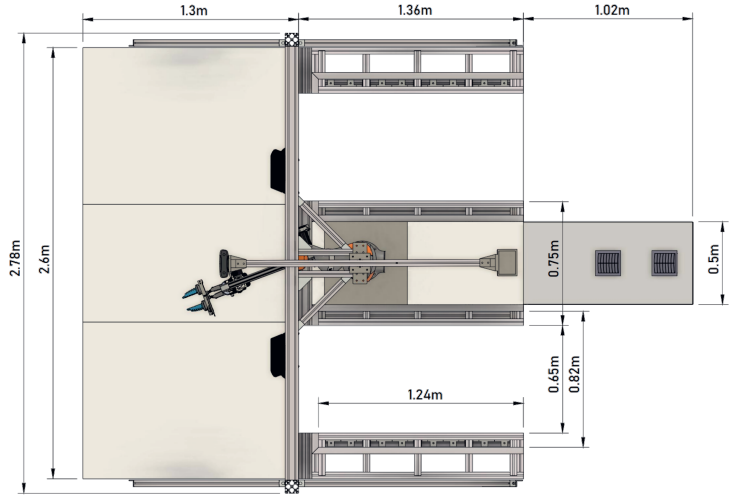
Figure 5.2: An annotated CAD render of the CoRoSect robot cell, with placement of the CoRoSect D-Robot (Chapter 2) for context. AGVs place pallets in the pallet bays. The Zivid sensor is mounted above the workspace on an articulated joint to enable rotation to the pallet bays. The electrical cabinet stores all electrical modules required to send and receive digital and analogue signals between robot components.

cricket crates and a potential co-worker. As such, it spans a width of 2.6 meters and a length of 1.3 meters. This encompasses a sufficient area for placing large cricket crates and the maximum reachability of a mounted collaborative robot arm, following from a reachability simulation (Chapter 3). This platform is the main workspace where the robot manages crates filled with insects and handles materials. The surface of the workspace is finished with HPL, providing a durable and easy-to-clean area for operations. Two programmable 100W LED lights illuminate the workspace, which are mounted on the camera support structure to ensure adjustable lighting conditions for robot vision systems, described in Section 5.2.2.

The support structure is a mounting space for a collaborative articulated robot. The main robotic component, a KUKA LBR iiwa



(a)



(b)

Figure 5.3: An overview of the robot cell and its dimensions, with (a) a side elevation and (b) a top view.

14 R820 (Section 5.2.1), is mounted on a central box constructed of durable standard aluminium extrusions and high-pressure laminate (HPL), chosen for its durability and resistance to wear. A stainless steel plate is placed atop the mounting platform to distribute the operational loads of the robot evenly through the structure. The height of the mounting platform (0.88 meters) is also determined in a reachability simulation (Chapter 3) to provide the greatest coverage of the workspace while still maintaining manipulability within tall cricket crates. Additional height stems from the space needed by AGVs.

The implementation of AGVs in CoRoSect requires the existence of docking bays where the AGVs deposit pallets of materials within the reachability envelope of the robot. AGVs are widely used in industry for material handling (Dabic-Miletic, 2024; Deacon, 2017). In combination with articulated robots, AGVs perform tasks of material transport (Bogue, 2023), mobile platforms (B. Li et al., 2022), and flexible systems (Martinez-Barbera & Herrero-Perez, 2010). On either side of the central mounting platform, we place two pallet bays that can accommodate standard Euro pallets (L-1.2m, W-0.8m, H-0.144m, used universally by industries) at a height of 0.336m within aluminium extrusion alignment rails. Additional tolerance in the width of the workspace and pallet bays is required to accommodate the navigational needs of AGVs, leaving the floor-level width of each bay at 0.65m. These bays serve as both input and output stations, with their modular construction allowing for reconfiguration to handle material intake from multiple directions and pallets that exceed the dimensions of Euro pallets.

Considering the working conditions at insect farms, electrical components need to be protected from damaging environmental conditions, such as humidity and dust (Ortiz et al., 2016). Proper protection increases the longevity of robotic systems (Trevelyan et al., 2016). While the KUKA iiwa is rated for limited industrial use (IP54 (Bloch, 2009)), some of the custom-created extensions and their controllers need to be similarly durable inside insect farms. We place electrical components in an enclosure at the back of the cell.

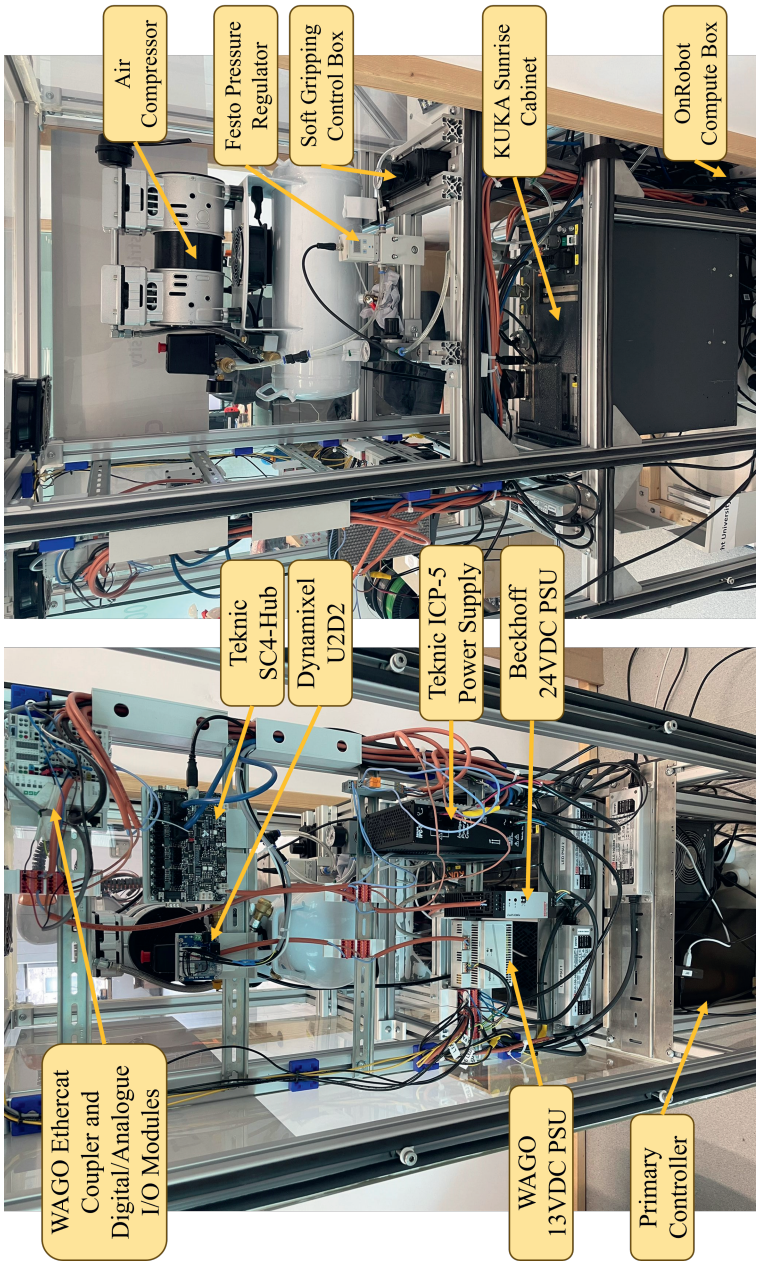


Figure 5.4: An annotated image of the electrical cabinet, featuring labels for each component housed within the protective enclosure. The functionalities of these components are described in Section 5.2.3.

It serves as a hub that contains all necessary electrical components, an air compressor for pneumatic operation of the end effector, and main computers for control and programming. Fans placed atop the cabinet provide ventilation and heat dispersion for the more intensive computational assets. The electrical components are detailed in Section 5.2.3, while the electrical cabinet can be seen in Figure 5.4.

Additionally, the requirement to perform versatile manipulation on various geometries is approached by incorporating a robot vision system (Golnabi & Asadpour, 2007). Similar approaches to robot vision in industries implement robot-mounted cameras (D'Avella et al., 2023) or 3D scanners (Kuts et al., 2018; Pérez et al., 2016). Overhead camera systems provide a wide view of the robot's workspace for material handling (Golnabi & Asadpour, 2007; Pérez et al., 2016). The cell's central vision sensor, a Zivid 2 L100 camera, is mounted above the workspace on a camera support structure connected through a motorised revolute joint. The revolute joint allows the Zivid sensor to be rotated for precise scans of the workspace as well as both pallet bays. This allows object detection and material handling at all locations without using multiple sensors.

KUKA LBR iiwa 14 R820

A collaborative robot, although typically smaller and limited in payload capacity, introduces a new level of versatility to industries, allowing the execution of a broader range of complex and delicate tasks alongside human workers Dmytriyev et al., 2024; Dusadeerungsikul and Nof, 2019; Galin and Meshcheryakov, 2019; Kragic et al., 2018. In contrast, a larger robot arm, with a higher payload capacity, would not be practical in confined spaces within an insect crate (Section 5.4)(D'Avella et al., 2023; Dmytriyev et al., 2024; Galin & Meshcheryakov, 2019), and would be unsafe for HRC schemes (Hentout et al., 2019; Vysocky & Novak, 2016). The KUKA LBR iiwa 14 is a collaborative robotic arm built for industry with 7 degrees

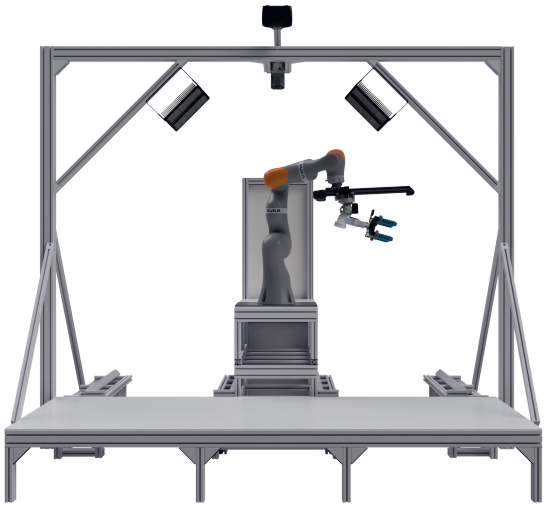


Figure 5.5: The robot cell mounted on the support structure for insect farming is configured to begin operations in the workspace. The ranges of the iiwa's joints are limited when the extension rail and end effector are attached, resulting in the L-shaped orientation of the robot cell.

of freedom, designed specifically for human-robot collaboration, and was chosen following the requirements for sophisticated and safe human-robot collaboration while maintaining a payload capacity of 14 kilograms. The robot cell utilises the *media-flange touch pneumatic* configuration, which features user-interface buttons for human-robot interaction. The integration of force/torque sensors along each axis enhances the iiwa's safety by providing real-time feedback and allows dynamic force control and sensitivity, which are utilised to perform error correction (Chapter 6). These sensors are vital in the placement of inlays where force feedback is used as an indicator of contact with a surface. Although reachability and payload capacity are common limiting factors of collaborative robots (Chutima, 2023; Taesi et al., 2023), the iiwa is a highly precise robot intended for industrial use (Mokaram et al., 2017; Stürz et al., 2017). KUKA cobots have been found to provide the highest payload/weight ratio and the highest

efficiency among other cobot manufacturers (Amiri et al., 2024), implying a favourable return on investment (Requirement 1, Chapter 2). However, with the continued development of new cobot models, multiple will likely be suitable. Hence, the work in this thesis is not dependent on the presence of the KUKA iiwa, but is an extension and framework generalisable to cobots in industry.

We use the extension rail (Chapter 3) to extend reachability at a low cost. Although reducing the total payload capacity for handling material, the moments exerted by the extension rail on the joints of the KUKA iiwa are minimised by mounting in an L-shaped configuration, as shown in Figure 5.5. This L-shaped configuration keeps the exerted moments from exceeding hardware limits at a full extension of the robot arm, meaning reachability can be maintained over the workspace and pallet bays. The modular end effector (Chapter 4) is then mounted at the sledge using a mounting interface made of lightweight aluminium. The end effector is designed to provide a soft contact surface for delicate operations and variable pressure when a firm grip is necessary (Requirement 3, Chapter 2).

5.2.2 Sensors

A challenge for performing versatile material handling is that the consistent placement of objects and materials cannot be assumed (D'Avella et al., 2023; Kuts et al., 2018; Pérez et al., 2016). The overview of materials involved in insect farming is in Section 2.2, with additional insights into gripping in Chapter 4. In a largely human-oriented industry (Buerkle et al., 2023; Ortiz et al., 2016), misalignment of workspace elements occurs in the task process (Tsay et al., 2010; Y. Zhang & Lu, 2020). While industrial machines can consistently place tools or materials with low errors, they also need precise calibration to operate (Asif & Webb, 2022; T. Chen et al., 2021; Z. Li et al., 2021). Adding additional error tolerance using pre-fabricated alignment features on the trays, inlays, or crates would not be enough to ensure consistent operation and is not a cost-effective

solution for larger industries. A versatile robot needs to detect the poses of relevant objects in its environment (Buerkle et al., 2023; Chutima, 2023; Kuts et al., 2018; Tsay et al., 2010). Furthermore, the use of visual sensors is necessary to give the robot a virtual representation of human co-workers (Pietrantoni et al., 2024; Sandini et al., 2024).

Therefore, there are three motivations for a vision system. (1) Firstly, performing precise object localisation is needed for positioning the end effector such that a secure grip can be established on materials. This entails both identifying the right object of interest and locating it in 3D space relative to the robot's base. (2) Secondly, dynamic collision avoidance requires the robot to perceive the workspace before moving, allowing it to update its digital twin, a virtual representation of its workspace where it performs motion planning, with actual information of its current state. This includes obstacles that it should avoid and materials that are of interest to the completion of a task. (3) Finally, visual sensors enable control strategies, such as visual servoing, which allow reactive control of the robot to conditions observed in the environment, for example, the presence of insects in a sample.

We use visual sensors and 3D scanners for environment registration and object localisation. For the purpose of versatile manipulation, our 3D robot vision performs identification of occupied space for collision avoidance and precise object localisation for material handling. The key requirements for a 3D vision solution that produces a high-quality point cloud are as follows:

Field of View. Encompassing the entire workspace area $[2.78, 1.3]$m at a height of at least 2.5m.

Accuracy. Producing a point cloud that has enough resolution to be used to extract locations of objects inside the workspace, with the precision necessary to align the objects with the end effector.

Point Precision The error in the position of a point is low ($<$ 1mm) between independent captures. This produces consistent

depth (z-axis) measurements with reduced noise in the observed point cloud between captures.

Processing Time The time required to process depth data and fuse it with RGB images to output a 3D representation of the imaged surface as a point cloud.

Robustness. Robust to occlusion, transparent materials, and very thin/small structures such as cardboard sheets.

	Zivid 2 L100	**ZED 2i**	**RealSense D435**
3D Method	Structured Light	Stereo	Stereo
Optimal Distance (mm)	$800 - 1400$	$300 - 3000$	$300 - 12000$
Field of View (at Distance)	1147mm ×680m	$87° \times 58°$	$110°(H) \times 70°(V) \times 120°(D)$
Depth Accuracy	$< 0.3\%$	$< 2\%$	$< 0.8\%$
Point Precision	100μm	—	—
Frames per Second (highest resolution)	2	30	15
Capture Time (ms)	60-100	—	10
Weight (g)	945	73	230
Environmental	IP65	—	IP66

Table 5.1: An overview of relevant camera parameters, compiled into a table. Some missing data is not computed or made available by manufacturers.

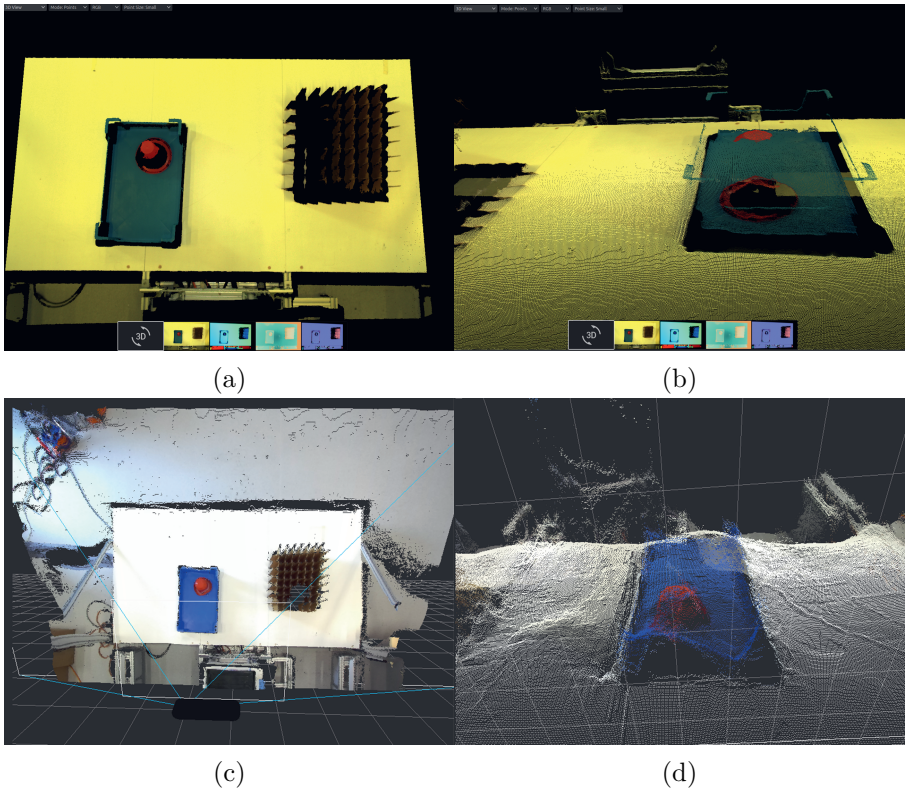
To this end, a selection of imaging devices is made, prioritising versatility and domain-agnostic information acquisition capabilities. Specifically, the Zivid 2 L100, Stereolabs ZED 2i, and RealSense D435 cameras were identified as suitable choices due to their complementary features. Their relevant parameters are summarised below and in Table 5.1.

Zivid 2 L100: A pattern-projector-based 3D imaging device used for generating highly accurate point clouds, enabling effective environmental mapping and object recognition within the robot's operational vicinity. This is a prerequisite for material handling. The Zivid 2 has a framerate of 2 frames per second (FPS) (depending on the image acquisition parameter configuration for a particular application) and produces a highly detailed point cloud. Mounted on the articulated joint at the top of the support structure, the Zivid camera is used to identify material in the workspace and both pallet bays.

Stereolabs ZED2i: Although lacking the high precision of the Zivid, the Zed2i's wide field of view and higher image capture rate make it a good choice for the registration of occupied space within the workspace and for producing an occupancy map for dynamic collision avoidance, making the Zed2i a good choice for human-robot collaborative workspaces.

RealSense D435: Mounted on the robot's end-effector, the RealSense D435 produces less detailed point clouds than the Zivid 2 but is more effective at shorter distances and its lightweight design and higher image capture rate (30 FPS) make it highly suitable for real-time visual feedback applications, such as visual servoing and sieving tasks.

UI-3884LE: Additionally mounted on the robot's extension rail, or held as a tool by the end effector, this high-resolution camera was used exclusively for visual inspection of insect crates (Papadopoulos et al., 2024).



(a) (b)

(c) (d)

Figure 5.6: Point Cloud Comparison Zivid 2 L100 to Zed 2i. (a) and (b) The point cloud output of the Zivid 2 L100, showing a stable point cloud with insignificant variance between captures and smooth surfaces in detail. (a) and (d) Tthe same scene from the Zed2i.

Collectively, these cameras constitute a suitable vision system, offering broad task adaptability. While some industrial setups choose a trade-off between robot-held versus mounted camera systems, the CoRoSect robot cell requires both to handle the broad array of tasks presented by insect farming. The Zivid 2 L100 and Zed2i cameras have a field-of-view (FOV) wide enough to capture the entire workspace platform. Figure 5.6 shows a side-by-side comparison of the quality of both point

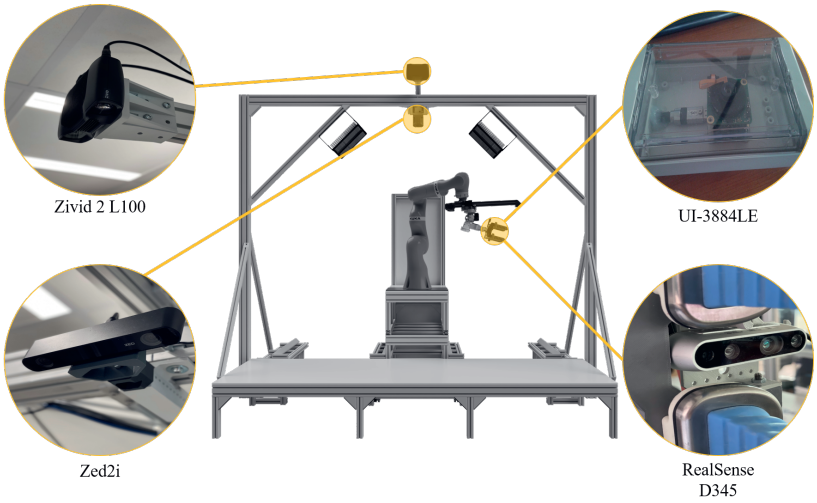


Figure 5.7: Workspace and robot mounted cameras.

clouds captured by the cameras mounted over the workspace. Precisely modelling the workspace is important in positioning the end effector to grasp objects and avoid collisions with the insect crates. In particular, the point precision of the Zivid 2 is $\approx$ 130μm when positioned at the mounting height of 2.58m. The Zivid 2, generating a consistent and precise point cloud with each capture, was selected for the object localisation pipeline in Chapter 6. On the other hand, the Zed2i is used for registering the general workspace environment and generating an occupancy map. Such maps are representations of 3D space as both occupied and free space, common in robotics for autonomous navigation (Elfes, 1989; L. Zhao et al., 2024). A virtual representation of a workspace is necessary for collision avoidance, where a robot can plan its motions virtually before executing them on real hardware, further described in Section 5.3.2 and in Chapter 6.

5.2.3 Electrical Components

To finalise the robot cell as a self-contained system, all electrical components need to be placed within the scope and cable reach of their corresponding hardware. Each mechanical component of the robot cell requires an infrastructure of power supply, controllers, and I/O devices. As such, most are placed within the electrical cabinet. Within this cabinet, motion control hubs, power supply units, and various input/output modules are routed to endpoints in the robotic arm, linear extension, end effector, and mounted sensors. At the heart of this system lies a Primary Controller (PrC), which coordinates a wide array of tasks ranging from trajectory generation to task execution and image processing. The PrC houses the core control framework discussed in Section 5.3. Below is a detailed overview of these key components, their functions, and how they integrate into the broader system, along with the interconnection in Figure 5.8.

PrC (Primary Controller): Individually, each dedicated controller only manages its dedicated piece of technology, and cannot synchronise with other devices without a high-level overview of the entire robot cell. The Primary Controller runs the ROS Master, orchestrating the interoperation of each component on Ubuntu 20.04 (5.15.067) and ROS Noetic. It is a central hub which manages communication between all embedded systems. In addition, it processes generating trajectories for the robot and its linear extension, conducts image processing, and oversees task-level management and execution. Essentially, it handles the bulk of high-level computational duties. The PC maintains a series of connections to other critical components, including the Zivid 2 L100, RealSense D435, the Teknic SC4-Hub for motion control, the Dynamixel U2D2 for additional joint control, the OnRobot Compute Box for gripper operation, and the KUKA Sunrise.

Teknic SC4-Hub: This component controls the prismatic joint of the linear extension and the revolute joint of the Zivid camera

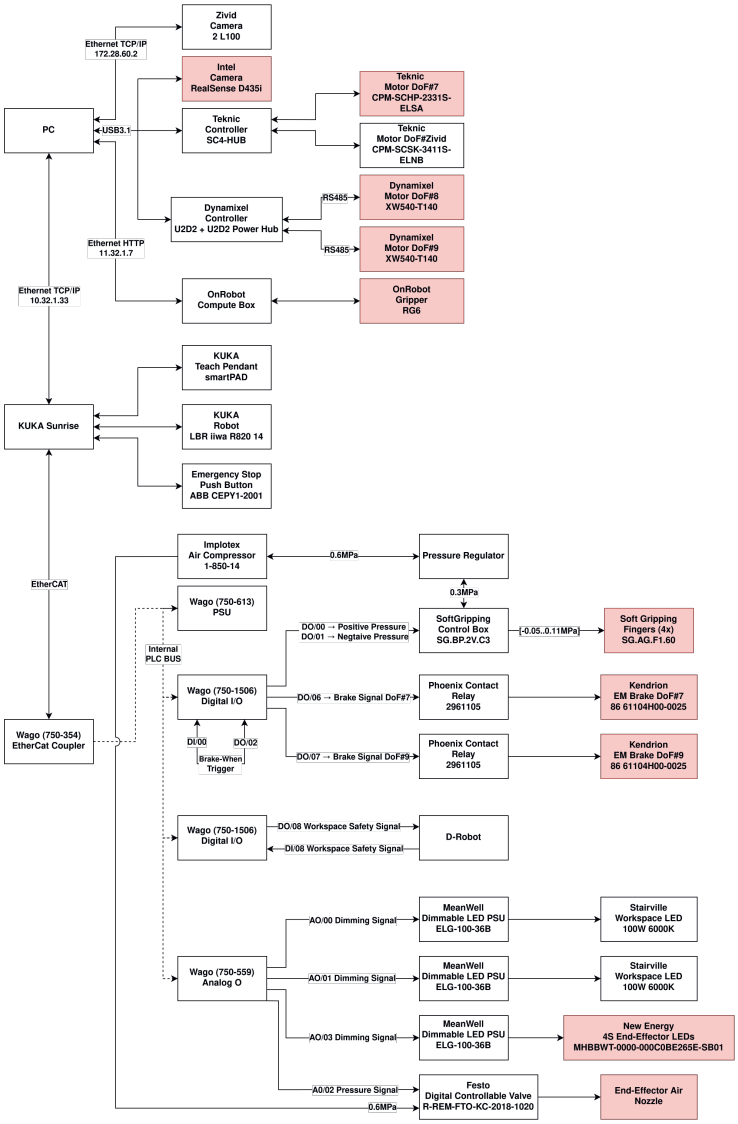


Figure 5.8: Overview of electrical components and their connections to enable communication between all hardware components and their respective controllers.

mount. It does so through two motors: the Teknic CPM-SCHP-2331S-ELSA for the prismatic joint and the Teknic CPM-SCSK-3411S-ELNB for the revolute Zivid joint. The SC4-Hub is powered by a 24VDC supply from a Beckhoff PSU, and the motors receive 75VDC from the Teknic IPC-5 power supply.

Dynamixel U2D2: This component is responsible for the control of two revolute joints located on the linear extension, commanding two Dynamixel XW540-T140s motors. The U2D2 receives its power from a 13VDC supply provided by the Wago PSU (787-1221).

OnRobot Compute Box: Dedicated to the control of the OnRobot RG6 Gripper, and serving as the communication interface between the PC and the gripper.

KUKA Sunrise: The KUKA Sunrise controls the KUKA LBR iiwa R820 14 robot arm and ensures safety through monitoring two emergency stop buttons - one located on the KUKA smartPAD and another external ABB CEPY1-2001 button connected to the X11 safety interface, specifically to the CIB_SR.1 port. Additionally, it interfaces with the Wago EtherCat Coupler to control the Wago Programmable Logic Controllers (PLCs).

Wago EtherCat Coupler (750-354): The EtherCat Coupler facilitates communication with the KUKA Sunrise. It is connected to a series of modules, including a Wago PSU, Digital Input and Output Modules, and an Analogue Output Module.

Wago PSU (750-613): This power supply unit is providing the necessary power to all the following PLC components.

Wago Digital Input and Output Module (750-1506): This module is tasked with managing digital signals for controlling the airflow to soft grippers and the Electromatic brakes on the linear extension. It also monitors and controls the safety coordination between robots, managing the safety signals between the m-robot

and d-robot, which indicate the occupancy status of the workspace as a backup.

Wago Analogue Output Module (750-559): The module controls dimming signals for LED power supplies and operates a Festo Controllable valve. It is responsible for the illumination within the workspace, controlling the intensity of LEDs mounted on the workspace and the end-effector, as well as managing a controllable pneumatic valve that provides air to an optional air-nozzle on the end-effector.

Wago 13VDC PSU (787-1221) The power supply is solely responsible for providing power to the two Dynamixel actuators on the linear extension. It supplies 8 amperes at 13VDC.

Beckhoff 24VDC PSU (PS1061-2405-0000) This power supply provides up to 5 amperes at 24VDC to the Wago EtherCat Coupler, Wago PSU, Teknic SC4-Hub, and the two Kendrion 81 61104H00-0025 electromagnetic brakes through the two Phoenix Contact 2961105 relays.

5.2.4 Hardware Safety Features

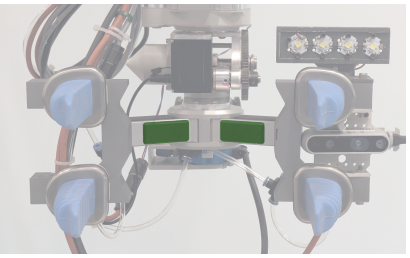
The robot cell is required to operate in a human-robot collaborative environment (Requirement 4, Chapter 2). The extension of the kinematic chain and adding custom components necessitates additional safety mechanisms for safe human-robot interaction (Dmytriyev et al., 2024). Without incurring extra costs, safety mechanisms can be obtained by selecting technologies that are already mindful of collaborative workspaces (Bi et al., 2021; Michalos et al., 2015; Schepp et al., 2022). Engineered to operate near humans, the KUKA iiwa avoids pinch points and sharp edges in its design, significantly reducing the potential for accidental injury. The KUKA iiwa was chosen for the CoRoSect project as it is one of the few industrial-grade collaborative robots (Amiri et al., 2024) where all joints are equipped with a torque sensor, with further distinction between internal and

external torques. These joint sensors enhance the robot's sensitivity to unexpected contact and enable it to detect collisions with human operators. The end-effector incorporates a gripper chosen in part for its safety-enhancing properties. Due to the natural occurrence of pinch points in such mechanisms, it includes sensors that actively monitor these points and, upon activation by pressure, command the robot to halt all motion immediately (Figure 5.9a).

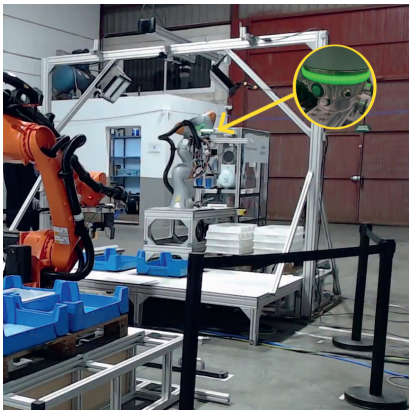
We implement additional safety features to complement the tactile safety mechanisms. Visual cues convey the robot's status to surrounding personnel (Figures 5.9b and 5.9c). The flange of the iiwa features a light system that broadcasts the operational state of the robot: a static green light signifies an idle state, awaiting task assignments, while a flashing red light warns of imminent or ongoing movement. Furthermore, there may be instances where the motion of the robot must be stopped immediately. The system includes emergency stop buttons designed to directly signal the robot to halt its operations immediately. The KUKA SmartPad has an integrated emergency stop button for immediate deactivation of the robot's functions. In addition to this, an external emergency button is integrated into the system, offering a supplementary stopping mechanism mounted on the cell structure.

Shared Workspace Safety

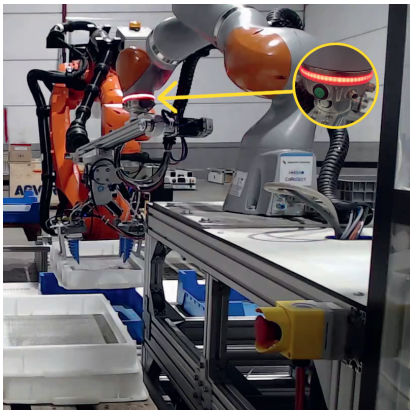
The CoRoSect workspace is shared between the large industrial stacking robot and the smaller collaborative robot cell (Chapter 2). Coordination between these two components is required to make the most use of the workspace as well as avoid collisions that would damage equipment. Coordination of multiple robots in a single workspace can take the form of coordinating trajectories (Akella & Hutchinson, 2002), partitioning the workspace (Agarwal et al., 2007), or other multi-agent strategies (Gautam et al., 2017). Since our robot cell is meant to collaborate with a human worker, we implement a



(a)



(b)



(c)

Figure 5.9: Safety mechanisms included in the robot cell. (a) The safety sensors on the RG6 lock the end effector when triggered through undesirable grasps. (b) and (c) The signalling the robot is capable of while operating a task.

method to ensure the larger industrial robot is never operating inside the workspace at the same time.

We coordinate the occupation of the workspace using a hard-wired safety connection to signal the availability of the shared workspace, routed through the WAGO Programmable Logic Controllers (PLCs). This system is facilitated through two distinct signals serving as an indicator of the workspace's availability, one for each robot. A HIGH signal denotes the workspace is free, while a LOW signal implies it is

currently engaged. A HIGH signal was selected to signify an available workspace, ensuring that in the event of a power outage or damaged wire, the signal defaults to LOW as power is physically required to maintain a HIGH signal, therefore ensuring that the system fails safely. Bidirectional communication ensures each robot is constantly aware of the other's operational state, independent of any other system coordination system, improving the overall robustness of the system. Before initiating any new task, and throughout its execution, the m-robot verifies that the workspace is not simultaneously being utilised by the d-robot. In the event of a detected conflict, signified by both signals being LOW, an immediate emergency stop is triggered. Given the robots' lack of mutual state awareness, any such occurrence necessitates intervention by a human operator to resolve the impasse currently. Moreover, the collaborative robot is programmed to defer the commencement of its task: it will wait until the workspace is available.

5.3 Robot Control and Motion Planning

5.3.1 Robot XML Specification

A crucial component for motion planning is a description of the robot's physical configuration and kinematics. This is typically done using an interpretable file that contains the main structural links and the joints between them (Coleman et al., 2014; Dong et al., 2023; Hennersperger et al., 2017; Tola & Corke, 2023). Such a description file is used to define and model the kinematics or dynamics of a robot, particularly for use in simulation and motion planning (Tola & Corke, 2023). It provides a model that contains the relevant information to use inverse kinematics for reaching a point in Cartesian space and performing coordinate transformations on relevant parts of the robot.

We use the Unified Robot Description Format (URDF) to define our robot model, which is an XML file format for the description of robot kinematics and their eventual simulation (Tola & Corke, 2023).

We use URDF because it is commonly used in robotics and hence well-documented and compatible with ROS and MoveIt! motion planner. A URDF presents a hierarchical description of links and joints that create the kinematic chain, where the relative position and orientation of each following element are defined. The format enables accurate correspondence between the motion planning scene and the real robot cell. Links hold a reference to the CAD model for that structural segment of the robot, which is used in collision checking. Joints specify the type of connections existing between links (rotational for the articulated robot and prismatic for the extension rail). The URDF includes the joint limits and internal parameters for safety limits and dynamics. Our robot description includes CAD models of all links and physical components (visualised in Figure 5.12). The robot description file has been extended with the three additional joints of the extension rail, an accurate model of the end effector, and the surrounding support structure of the CoRoSect cell. Including the support structure enables fast collision checking with the elements that remain static with respect to the robot. Figure 5.10 depicts the simplified hierarchical structure of the robot's URDF.

The success of control and motion planning executed on a real robot depends on an accurate description file. For this reason, we use CAD models of each link, using those from (KUKA, 2013) for the KUKA iiwa and include our designs of the robot extension and end effector. A detailed summary of the kinematic chain in Figure 5.10 follows. The 'world' link is located at the top of the hierarchy and serves as the absolute reference frame for the robot cell. The 'base_link' is the beginning of the robot structure and the main reference point from which all other robot links are positioned. Since the iiwa uses its own coordinate system internally, it is important to align these two coordinate frames if operating in Cartesian coordinates. The 'support_structure' extends from the 'base_link' and serves as a static mounting point for the 'm_robot_link_0', which represents the base of the robot. The model for the extensive surrounding support structure is included in the URDF for fast collision checking between

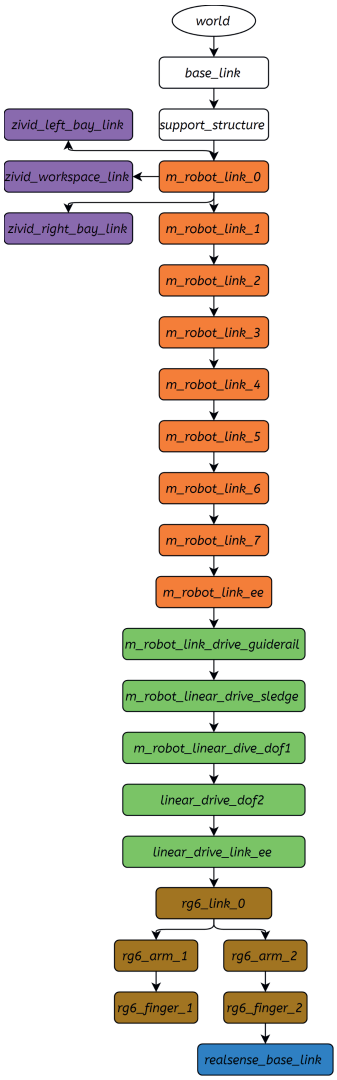


Figure 5.10: The structural hierarchy of the m-robot's components. White frames are static in the world. The KUKA iiwa R820 14 is represented in orange, the linear extension in green, and end effector in brown. Purple frames are defined by the Zivid calibration process. The blue vertex is the frame of the D435 (Section 6.3.2).

the moving robot and the static workspace elements. This also provides a comprehensive mounting point for the overhead Zivid 3D scanner. Further, a series of interconnected links ('m_robot_link_1' through 'm_robot_link_7') represent the joints and segments of the KUKA iiwa R820 14. These links provide the robot with 7 degrees of freedom, culminating in the 'm_robot_link_ee', which is the flange of the KUKA. This part of the URDF is based on the robot description used in (Hennersperger et al., 2017) with accurate 3D meshes and specified joint parameters for all 7 revolute degrees of freedom. These parameters do not necessarily correspond with reality but can be obtained through experimentation. The robot is further extended by the extension rail to include a prismatic joint as the linear drive and 2 additional revolute joints. The 'rg6_link_0' serves as the base of the gripper, which is mounted to the flange of the linear drive. The 'zivid_workspace_link' is a branch from the support structure, from which 'zivid_left_bay_link' and 'zivid_right_bay_link' extend. These positions are where the Zivid camera generates point clouds for the left and right bays. The coordinate transformations from the base link are obtained through a calibration process. Finally, the 'realsense_base_link' is positioned at the base of one of the RG6 fingers where the Intel RealSense D435i camera is mounted. In total, the motion planner handles a planning group of 10 articulated joints for the main robot, plus the extension and 4 additional joints for an end-effector sub-group.

5.3.2 Motion Planning in MoveIt!

Comprised of multiple independently controlled components, the robot cell needs a control framework to coordinate motions for the KUKA iiwa, the extension rail, and the end effector. Motion planning accounts for the surrounding environment for collision avoidance, and distributes high-level trajectories to the corresponding low-level controllers (D'Avella et al., 2023; Hennersperger et al., 2017). We extended the description of the KUKA iiwa with the addition of 3

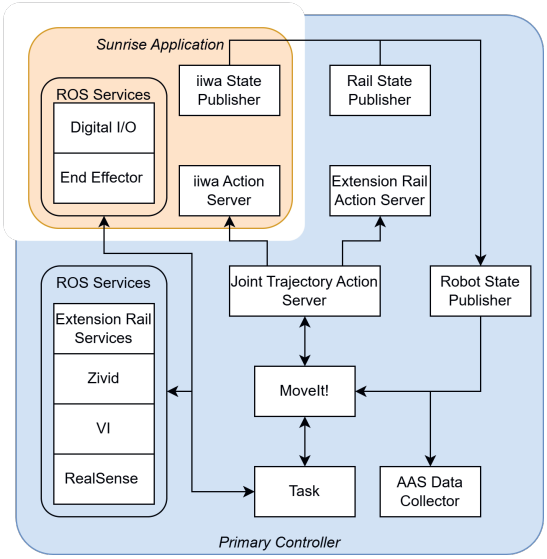


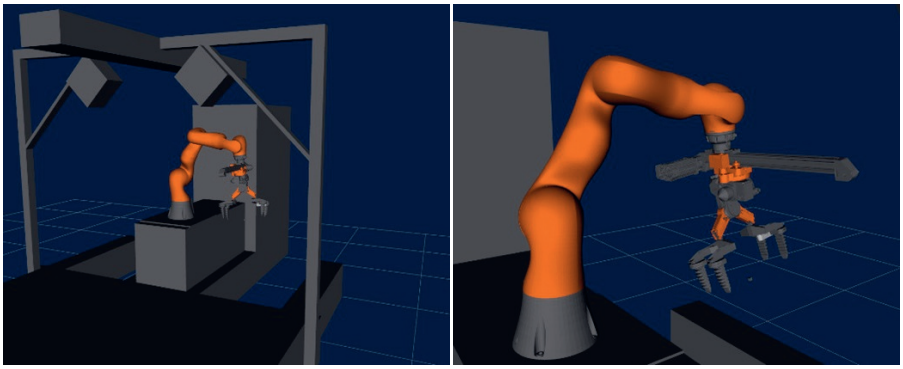
Figure 5.11: The components of the robot cell that utilise ROS to communicate have arrows marking the main lines of communication, such as through ROS topics or services. Motion plans are handled by the core ROS action servers, which distribute a trajectory to the correct hardware controllers. Feedback on the robot's current state is done using a publisher-subscriber architecture. Additional features, such as control of the end effector or the LEDs, are available via ROS services.

degrees of freedom from the robot extension and a kinematically complex gripper. The proprietary motion planning included in KUKA's Sunrise Workbench and on-board software allows for planning common industrial motions (Point-to-Point, Linear, Circular) (Gerget et al., 2022; Hennersperger et al., 2017) and generating splines of smooth compound motions. However, these only encompass the scope of the iiwa's joints and cannot plan for extensions to the robot model. Conversely, the controllers for the extension rail or end effector can not easily compute their pose within the kinematic chain without information about the KUKA iiwa. A solution is to use a central, high-level, motion planning environment (D'Avella et al., 2023;

Hennersperger et al., 2017; Tamizi et al., 2023; C. Zhou et al., 2022) that builds a digital planning scene of the entire robot configuration in a virtual workspace. We adopt this approach to motion planning over, for example, reinforcement learning control (Dong et al., 2023), due to limited resources for training.

We implement motion planning on the primary controller (PrC) using MoveIt! motion planning software (Coleman et al., 2014) and Open Motion Planning Library (Şucan et al., 2012). These allow us to plan coordinated motions for the iiwa 14 and robot extension. The Rapidly-Exploring Random Tree (RRT) (Kuffner & LaValle, 2000) algorithm is used within MoveIt! to plan collision-free paths within the virtual workspace. A planned trajectory is broadcast to all low-level controllers through ROS. The entire robotic system (KUKA iiwa, extension rail, and end effector) is considered a single kinematic chain that extends past the 7 degrees of freedom of the KUKA iiwa (Section 5.3.1). These trajectories are split to their corresponding hardware controllers to be executed synchronously at a lower level. The visualisation of the motion planning scene is shown in Figure 5.12 using the RViz plugin (Kam et al., 2015).

The robot cell needs to be able to plan trajectories when being placed in various workspace configurations (Requirement 3, Chapter 2). The materials and containers that are placed upon the workspace platform become obstacles that need to be considered when motion planning and performing tasks. CoRoSect additionally introduces confined areas with occlusions, limited operational space, and low tolerances for collision, such as the cricket crates and mating cages in Section 2.2. In particular, the length of the cricket crate is 800mm, leaving $\approx$ 100mm tolerance to the placement of the robot extension from either edge, but no tolerance if the end effector is at maximum extension, and no possibility of rotation. Food trays, drinking devices, and cardboard structures are placed irregularly and close to the crate's corners. Carried materials need to be hoisted over the crate's edges without collision. Furthermore, mealworm inlays fit tightly into their crates, leaving $\approx$ 1mm of positioning error before it is pushed against a



(a) (b)

Figure 5.12: Two perspectives on the motion planning scene visualised in RViz. The robot cell is comprised of the support structure, the iiwa, the extension rail, and the end effector, all integrated into a single description file.

solid surface when being inserted. Additionally, the oviposition plates removed from BSF mating cages are placed within 10mm of each other when stored in racks for maturation. Such problems require motion planning that can handle limited information and dynamic changes in the workspace (Brito et al., 2020; Burget et al., 2013; Michaux et al., 2024; Nayl et al., 2017). Failure to plan one step in a sequence of motions required for a task will affect the entire task process.

We use volumetric information of occupied space and CAD models of objects within the motion planning scene to represent the sensed workspace environment. Volumes of occupied space are taken into account during collision detection (Coleman et al., 2014). Mapping occupied space is described in Chapter 6. We use CAD models of important objects detected inside the workspace to avoid sensing errors of known geometries that are expected during a specific task. These models are added autonomously when detected through a surface matching procedure (Chapter 6). This allows us to perform object localisation and rely on the virtual planning scene in tightly enclosed spaces, such as the cricket crates and BSF mating cages (Section 5.4).

Tightly constrained areas require additional processing time to find a planning solution (Section 5.4). A trajectory is valid when it avoids collisions with workspace elements, the support structure, and any of the robot's links. Coordinated motion planning for the entire robot cell ensures no collisions between any part of the robot and large structural elements.

Furthermore, to address the efficient use of robots (Requirement 1, Chapter 2), a single insect-farming task may involve handling various objects (Requirement 3, Chapter 2). An example is filling a cricket crate with two cardboard structures, drinking devices, and food trays in order. In research, these are handled as sequences of operations that the robot is given (Dong et al., 2023), learns (Dong et al., 2023; Zhu & Hu, 2018), or optimises (Caccavale & Finzi, 2016; Rovida et al., 2017). The use cases defined for insect rearing in Chapter 2 are mostly sequential operations, particularly when considering the M-Robot, which allows us to identify certain high-level atomic operations for the robot. We define sets of objects and poses relevant to the completion of a task for the robot to autonomously locate (object localisation is covered in Chapter 6). MoveIt! facilitates the planning of trajectories from a start pose (typically the robot's current state) to a goal pose, a visualisation of which is provided in Figure 5.13. A single task can then be characterised as a set of target poses to reach (Alatartsev et al., 2015; Dong et al., 2023). Additional operations, such as gripping material or sampling insects, are intermediate actions by dedicated components in between the sequence of poses (Alatartsev et al., 2015). Within the CoRoSect use cases, tasks are defined by sequences of start and end poses for material to be moved, or a pose to be reached by inspection cameras.

Each pose is a compound of a position $[x, y, z]^T$ and an orientation quaternion $[x, y, z, w]^T$. Start and end states are defined in Cartesian space as the 3D pose of an object of interest in the workspace, a favourable gripping position, or a desired offset from a target point. This formulation allows for later input of 3D poses that are obtained using an object localisation procedure, described in Chapter 6. To perform handling of a located object, the end-effector of the robot model

has to reach a pose relative to the object from which a grasp is possible, hence a pose with an offset

$$\vec{p}_{\text{target}} = \vec{p}_{\text{object}} + \vec{p}_{\text{offset}} \tag{5.1}$$

$$\vec{p}_{\text{target}} = [x_{\text{object}} + x_{\text{offset}}, y_{\text{object}} + y_{\text{offset}}, z_{\text{object}} + z_{\text{offset}}]^T \tag{5.2}$$

from the object location $\vec{p}_{\text{object}}$ and offset $\vec{p}_{\text{offset}}$. A motion plan has to take the robot from its current state $\vec{S_0} = [j_1, j_2, j_3, j_4, j_5, j_6, j_7, \text{rail}_1, \text{rail}_2, \text{rail}_3]$ to a target pose $\vec{p}_{\text{target}}$. Using inverse kinematics, solutions such as $\vec{S_0}$ are found for joint positions needed to reach a point in Cartesian space. A joint trajectory is hence defined as the series of joint positions

$$\vec{T} = [\vec{S_0}, ..., \vec{T_i}, ..., \vec{T_n}] \tag{5.3}$$

where

$$\vec{T_i} = [j_1, j_2, j_3, j_4, j_5, j_6, j_7, \text{rail}_1, \text{rail}_2, \text{rail}_3] \tag{5.4}$$

denotes the trajectory at time point i, needed to be reached in a timed sequence from the robot's current position to the target goal pose.

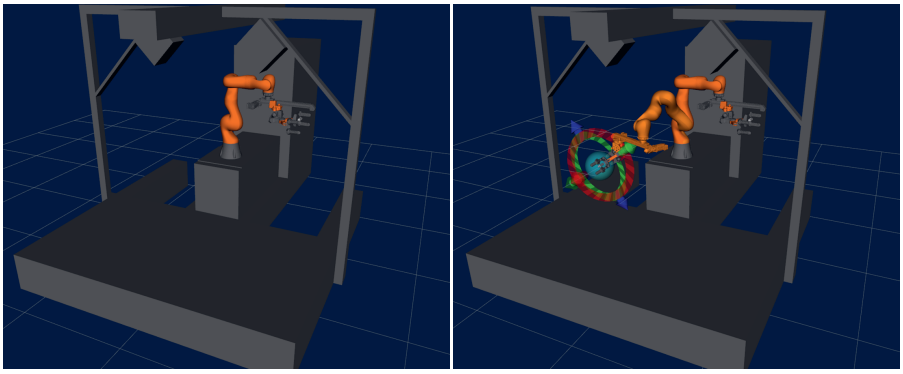
To create a final control framework, the virtual planning scene in MoveIt! is connected to a ROS action server, which distributes the trajectory to hardware controllers. Figure 5.11 shows the proposed ROS infrastructure around the planning scene, which is used to distribute trajectories and update the internal state of the robot cell. The output of the planning scene is a planned trajectory, which is distributed to the corresponding hardware controllers by ROS action servers. The input is the state information of each robotic component that, together, comprises the state of the entire system. Additional input is the target pose from a defined task. Additional hardware elements, such as the end effector and mounted sensors, are linked through dedicated controllers and ROS services.

5.4 Experiments and Results

Using the URDF robot description (Section 5.3.1) and control framework (Section 5.3.2), a digital twin of the robot cell is tested in a virtual workspace. The objective of the test is to place the robot cell in an environment that resembles potential conditions at an insect farm. We measure the time taken to find a motion plan in increasingly obstructed workspaces to quantify the complexity of these workspaces and provide an indication of how obstructions will slow down the robot under real conditions. In particular, we tested the limitations of the control framework once the workspace is filled with obstacles and containers. The efficiency of the entire system depends on the processing time spent on motion planning. The robot reaches into containers and enclosed spaces, avoiding collisions while still finding a feasible route to a target pose. While classical control relies on pre-defined trajectories, we require the robot to operate within a dynamic and unstructured workspace, meaning that, when a new object/container is placed in the workspace, its location, orientation, and geometry are not consistent with previous placements. Therefore, motion planning has to be repeated when there is a change in the workspace. The focus of these experiments is to determine the load on the system when performing repetitive motion planning in increasingly complex workspaces. We test in a simulation first to prevent collisions between the real robot and the workspace elements, which additionally relies on the implementation of an object localisation system described in Chapter 6. The RRT algorithm ((Kuffner & LaValle, 2000)) is used to compute trajectories in each experiment.

5.4.1 Experiment Setup

Tests were performed using the MoveIt! motion planning scene and visualised in RViz (Kam et al., 2015). Objects and obstacles are introduced into the planning scene to fit scenarios expected under the conditions in insect farms, particularly to test operations within small enclosures such as the rearing structure shown in Figure 5.14c



(a) (b)

Figure 5.13: Planning scene start conditions for experiments. (a) and (b) The initial conditions and the control experiment with an empty workspace. The target pose (the blue orb) and resulting orientation of the robot arm to reach it are shown in (b).

and a tall cricket crate in Figure 5.14a. These figures show the larger structures from Chapter 2 that need to be entered by the robot arm in green highlight, namely the cricket crates (Figures 5.14a and 5.14a) and the BSF mating cage (Figure 5.14d). The starting (home) position is constant throughout all tests (Figure 5.13a).

Experiment conditions 1 through 5 progressively introduce new obstacles into the workspace as shown in Figure 5.14. Each experiment has the robot planning to the same target pose, which simulates a position where a sample of insects taken from a crate is held below an inspection camera (Quality Management in Section 2.2). Condition 1 acts as the control with an empty planning scene, whereas condition 2 aims to prove that adding arbitrary objects to the scene does not inflate the computation time. Conditions 3-5 test increasingly complex planning problems using insect farming workspace elements as obstacles. Conditions 6, 7, and 8 consider the motion planning for reaching into and operating within a tall cricket crate, starting at the defined home position (Figure 5.13a) but reaching for a target inside

the crate (Figure 5.15). Conditions 7 and 8 introduce an obstacle in the direct path of the robot as it moves into the crate, where condition 8 is meant to be unsolvable. All conditions have a feasible goal state, meaning there are no inherent collisions between the elements of the workspace and the end pose (although there is no path between the start and end states in the case of condition 8). Motion planning for each condition is repeated 20 times with a 5s upper time limit and up to 10 attempts on a failure.

Condition 1: Empty workspace as depicted in Figure 5.13.

Condition 2: Empty workspace with obstacles not in the direct path, to test whether simply adding objects to the planning scene inflates planning times. Figure 5.14a.

Condition 3: One tall cricket crate inside the workspace, placed as a direct obstacle. Figure 5.14b.

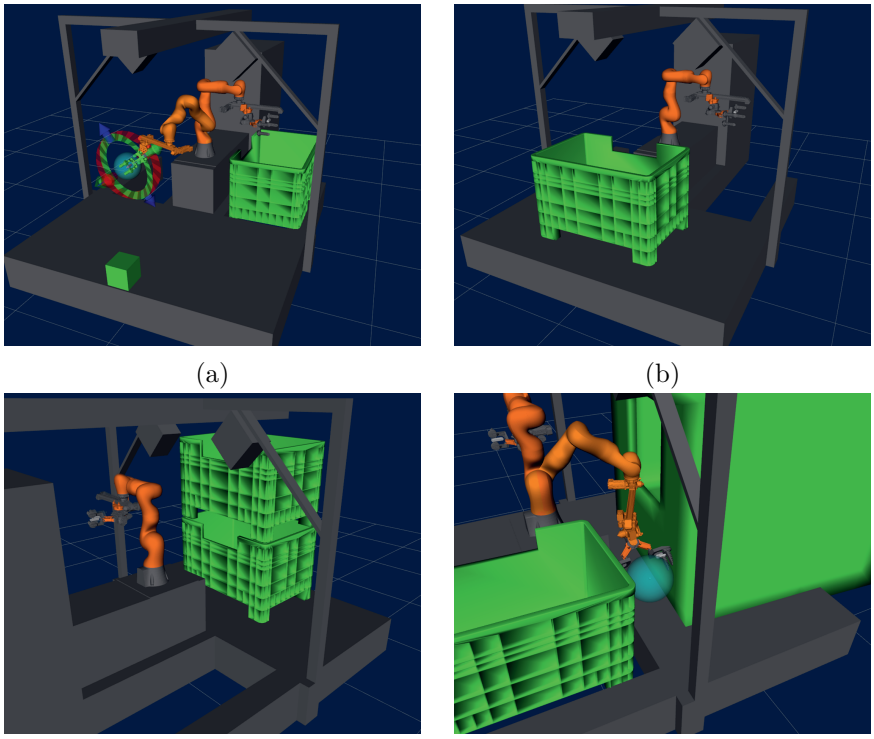
Condition 4: Two stacked cricket crates inside the workspace, creating one large barrier on the most direct path. Figure 5.14c.

Condition 5: A large rearing tent inside the workspace and a tall cricket crate blocking the right pallet bay. Figure 5.14d.

Condition 6: Reaching inside an open cricket crate. Figures 5.15a and 5.15b.

Condition 7: Reaching inside an open cricket crate with a small obstacle box. Figure 5.15c.

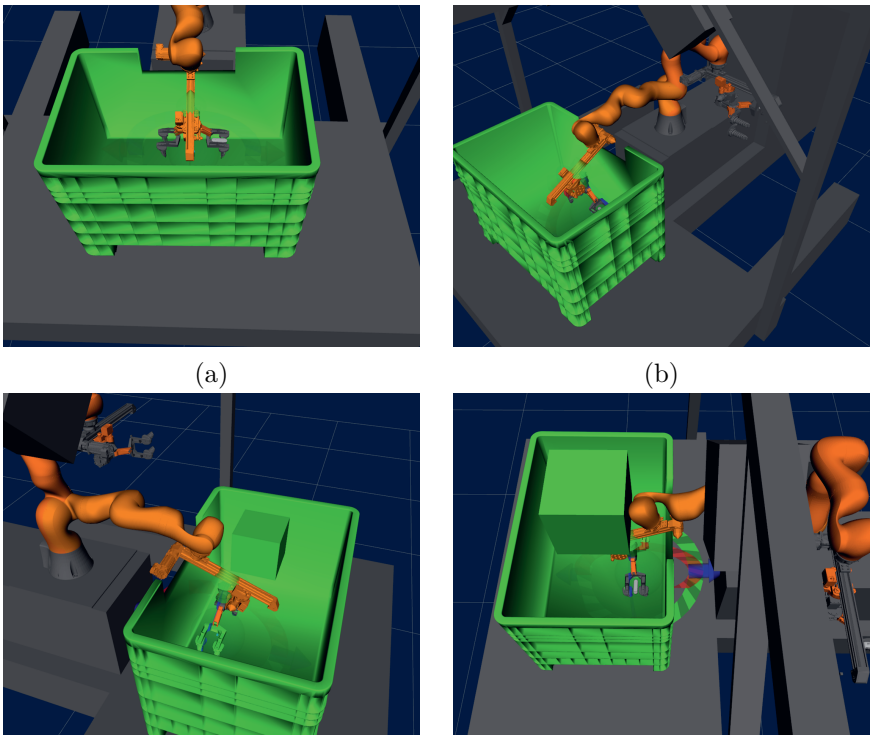
Condition 8: Reaching inside an open cricket crate with a large obstacle box. Not enough space to reach the target pose, meaning the task should be unsolvable. Figure 5.15d.



(a) (b)

(c) (d)

Figure 5.14: Planning scene with virtual objects as materials. Each figure shows the starting pose of the robot arm, and Figures (a) and (d) additionally depict the target pose with a robot arm holding a blue-highlighted ball in the end effector. (a) Workspace condition 2, where the environment contains obstacles not along the direct path of the robot, meaning they should not have an impact on the motion plan. The green box represents an arbitrary workspace element. (5.14b) Condition 3, containing an insect crate in the direct path of the robot, is trying to reach the same target as condition 2. This workspace configuration is used in cricket quality management (Section 2.2). (c) Condition 4, containing stacked crates to block the simple approach of going above a crate. (d) Condition 5, confining the target between an insect crate in the side pallet bay and a large structure inside the workspace. This is a potential workspace configuration for BSF oviposition management (Section 2.2).



(a) (b)

(c) (d)

Figure 5.15: Planning scene with an insect crate. (a) and (b) The starting and target poses for reaching inside the tall cricket crate. The end effector is positioned in a vertical alignment to simulate operating within the crate. (c) and (d) A cube obstacle in the way, simulating a workspace element that needs to be planned around. The final condition is not reachable from outside, but tests whether the motion planner will attempt a partial solution or successfully recognise that the problem cannot be solved.

Cond.	1	2	3	4	5	6	7
Time (s)	0.03 ± 0.003	0.03 ± 0.003	0.05 ± 0.02	0.13 ± 0.04	0.20 ± 0.07	0.09 ± 0.02	3.89 ± 1.14

Table 5.2: This table presents the mean time taken to compute a motion plan in each of the experimental conditions with workspace setups. The 8^{th} setup is left out as the task was infeasible and hence took no time.

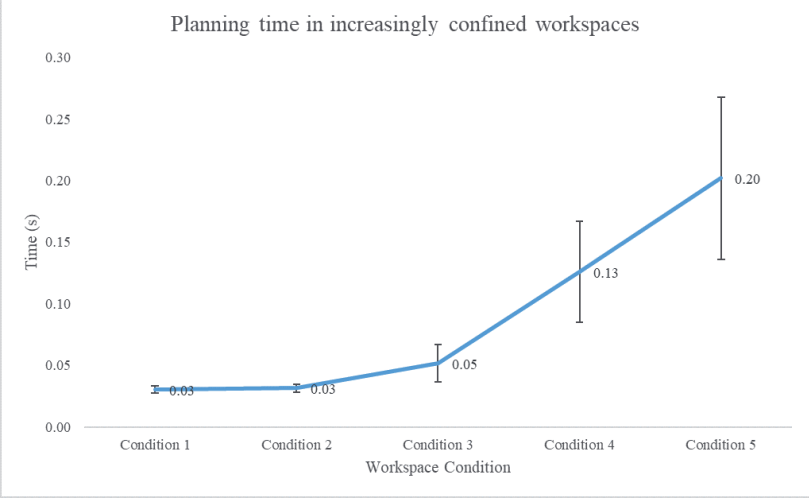


Figure 5.16: Time taken to generate motion plan in experiment conditions 1-5. Tasks with no additional complexity, such as condition 2 where objects were not obstacles, do not show an increase in time taken. The Introduction of obstacles in the direct path of the robot cell, or the creation of confined spaces within which the robot must operate, increases the planning time.

Cond.	1	2	3	4	5	6	7
Steps	35.0 ± 0	35.0 ± 0	52.3 ± 9.2	67.3 ± 17.5	68.9 ± 16.1	51.8 ± 7.5	110.3± 118.1

Table 5.3: This table presents the mean number of waypoint poses (steps) comprising a computed motion plan in each of the experimental conditions. The 8^{th} setup is left out as the task was infeasible, and hence took 0 steps.

5.4.2 Robot Motion Planning Results

Table 5.2 shows the mean and standard deviation of planning time for each experiment setup, which are also plotted for conditions 1-5 in Figure 5.16. Table 5.3 shows the mean and standard deviation of the number of waypoints involved in each trajectory, which directly affects the computation time. Preliminary results on the processing time of path planning in an empty workspace were calculated within a mean of $0.030s \pm 0.003s$ over 20 repetitions. In more challenging environments, such as in condition 2 (Figure 5.14a) and condition 6 (Figure 5.15a), the motion planner takes up to $0.200s \pm 0.066s$ and $3.890s \pm 1.141s$ planning time, respectively, especially when reaching into confined spaces. This suggests the motion planning system will not become a processing time bottleneck during operation.

5.4.3 Discussion

Research question 4 specifically addresses the need for versatile manipulation, where the robot is able to operate in various workspace configurations and handle unstructured environments. We determined that changes to the workspace require a dynamic re-computation of a motion plan, for which we measured the computation time under multiple workspace configurations matching insect farming. Feasible trajectories are consistently computed below the upper time limit of $5s$ (Table 5.2). Condition 2 suggests that the increase in processing time is not simply the effect of additional objects inside the workspace.

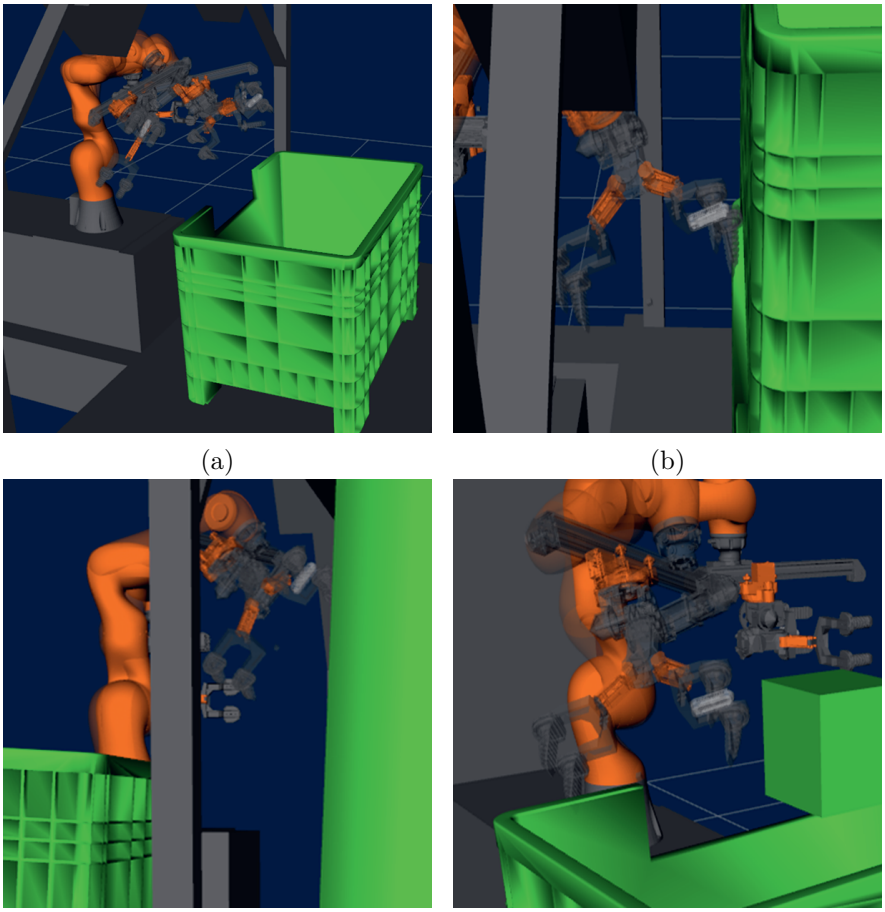
The increased processing time can instead be explained by the increased length of computed motion plans (Table 5.3). With more obstacles in the direct path of the robot, the motion planner has to compensate by creating trajectories around these objects, which takes the RRT algorithm additional time to expand the solution space (and in general, processing collision detection). The trend of increasingly long trajectories follows that of Figure 5.16. Although these test scenarios were limited to $5s$, it is possible to create workspaces where the trajectories are too convoluted and take increasingly longer to compute. However, a collision-free path will be computed unless no solution exists. Except for experiment condition 8, in which the task was unsolvable, the motion planner achieved a 100% success rate across all trials. Moreover, a partial plan is not output for infeasible scenarios. This means that the robot will not move into unfavourable poses in complex workspaces. Additionally, MoveIt! and OMPL sufficiently encompass all extended joints of the robot cell to execute synchronous motion to the target pose in simulation.

Fast motion planning enables reactive and close to real-time re-planning in dynamic environments. It is an important feature that increases the versatility of a robotic manipulator, per Requirement 3 (Chapter 2). We deduce that increased computation time is necessary for convoluted workspaces, implying that challenging use cases, such as operating within a mating cage for BSF oviposition management (Section 2.2), require more time allocated. Meanwhile, short motions through open workspaces require minimal planning time and can be repetitively performed for dynamic workspaces, especially when changes to the workspace are also small.

Figure 5.17 shows visualisations of selected motion plans along challenging paths that the planner was able to compute. This highlights how a precisely modelled URDF (used in the motion planning scene) is vital to computing efficient and collision-free paths. The end effector can be positioned very close to workspace elements without being considered in a collision state. This provides insight into how the motion planner can handle tightly enclosed spaces, showing

the capability to compute a feasible trajectory close to collision boundaries. However, to replicate this with a real robot, an accurate correspondence between the URDF and the real robot is required. This means that the closer the proportions, dimensions, joint limits, and joint configurations of the URDF are to the real robot's parameters, the more likely it is to succeed in planning within enclosures. Another aspect of this is the precise localisation of obstacles in the workspace. Detection of obstacles and placement of objects in the workspace is outlined in Chapter 6. Moreover, it is necessary to connect the virtual planning scene with the real robot through a hierarchy of software interfaces that enable two-way communication: (1) providing planned trajectories to all physical articulated components, and (2) providing the robot and workspace states to the virtual planning scene. The final result is a software architecture which achieves control and motion planning for the extended kinematic chain, per research question 4.

The largest limiting factor in motion planning has been the need for sufficient space to orient the robot extension (Chapter 3) while avoiding obstacles. While the effect on the operational space gained with the robot extension is documented in Chapter 3, here it is introduced into a constrained environment. The robot extension allows reaching target poses that would otherwise be infeasible for the base KUKA iiwa, especially when having to reach into enclosures (such as the cricket crates in Figure 5.15). Commonly, the robot had to compensate for the additional protrusion with the use of its core joints. This creates trajectories which first position and orient the robot extension before moving it linearly into the final position. As a result, this contributes to the complexity of the search space, which influences the computation time for motion planning. However, as none of the experiment conditions exceeded the allocated $5s$ planning time, there is no need to reduce the kinematic chain to simplify the search space.



(a) (b)

(c) (d)

Figure 5.17: Specific highlights of the motion planning scene. The multiple robot poses are sequential steps in a trajectory, captured in a snapshot. (a) The robot cell trajectory steps along a motion path over the tall cricket crate inside the workspace, before moving down towards the target state. (b) and (c) The precision with which the robot can avoid obstacles while computing a collision-free path in test conditions 3 and 4, respectively. (d) The robot cell first moves to the far side of the obstacle before positioning the end effector within the insect crate from a more favourable opening in test condition 6.

5.5 Resulting Software Architecture

The previous section tested the performance of motion planning on the extended kinematic chain of the robot in a virtual environment. To test the motion planner on hardware and achieve similarly synchronous control of the physical robot, a hierarchy of software layers is identified as: (1) the low-level hardware components, (2) the software components involved in motion planning, and (3) software interfaces needed to integrate sensors, manage tasks, and communicate externally (Figure 5.18). The structure of this architecture results directly from the virtual and physical components described as part of the robot cell so far.

In this section, we integrate the motion planning scene (Section 5.2) and the low-level robot control frameworks (Section 5.3) into a single software architecture that facilitates control of the physical robotic components. This software architecture addresses the practical implementation of robot control, which is encapsulated in research question 4. The architecture achieves control of the developed robot cell from a high-level task management layer to the low-level hardware interfaces (Figure 5.18). Both need to be connected to the corresponding hardware assets of the robot cell through software interfaces in order to achieve control of the physical robot. We integrate the robot cell with connected CoRoSect management systems using an Asset Administration Shell (AAS) introduced in Chapter 2. The resulting

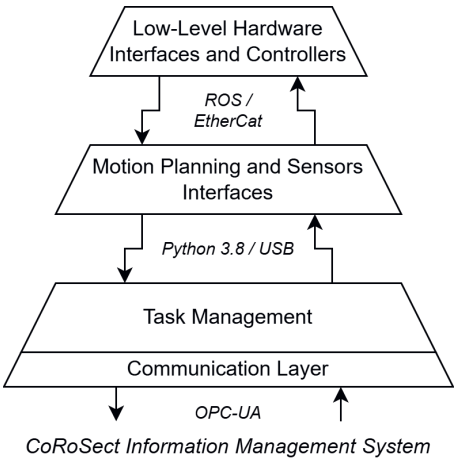


Figure 5.18: Hierarchical overview of the main implementation layers and the lines of communication between them.

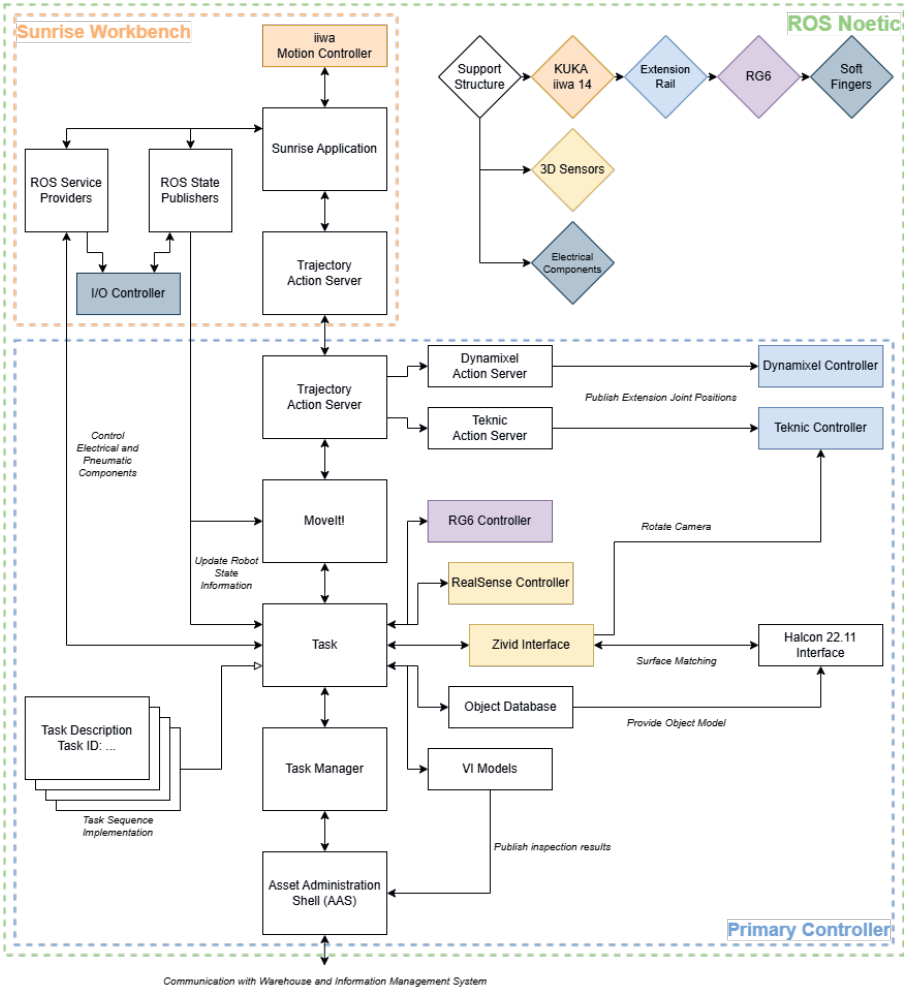


Figure 5.19: Software architecture overview and connection to hardware components. Each hardware component has a dedicated controller, denoted by the coloured components and the legend in the top right. The software architecture is split between the Sunrise Workbench, which controls the KUKA iiwa 14, and the Primary Controller, which facilitates system integration and motion planning and distributes low-level commands.

software architecture is presented in Figure 5.19.

Together with CoRoSect partners at CERTH and ATOS (CoRoSect Deliverable 2.3, 2021; CoRoSect Deliverable 2.4, 2022), a service-driven architecture model is developed (Ahmad & Babar, 2016; Veiga et al., 2009) using Robot Operating System (ROS) (Quigley et al., 2009) to connect the hardware components and make their capabilities available to higher-level management systems. Our high-level task management, vision, AI-model integration, and AAS are built on object-oriented architecture principles (Ahmad & Babar, 2016) to allow the modularity of our system and the seamless addition of future components. We create a hierarchy of software layers to organise the primitive functions of our robot cell (Choi et al., 2014). The hierarchy is visualised in Figure 5.18.

The communication layer communicates with the CoRoSect Information Management System (IMS). It is available to publish status data about the robot cell and accept new tasks through an OPC-UA server (Section 5.5.3). The communication layer hosts an AAS typically needed by modern industrial robots (Nagrath et al., 2022; X. Ye et al., 2021).

The task-oriented management layer keeps a high-level overview of a task that the robot is performing. During operation, the task manager monitors the sequence of steps that characterise a task, for example, a sequence of motions to perform a visual inspection on an insect crate. The next layer in the hierarchy is the control framework, including the motion planning environment and a package of functions that enable the use of hardware components and sensors. This layer also includes interfaces for operating the end effector with variable force and robot vision implemented in Chapter 6. Part of this layer is a ROS action server that broadcasts motion plans to the low-level controllers for the KUKA iiwa 14 and the extension rail. The main functional hardware components of the KUKA iiwa 14, extension rail, end effector, and 3D sensors are all integrated into a single system using ROS Noetic and EtherCat as middleware.

5.5.1 Sunrise Workbench

The KUKA iiwa 14 hosts its proprietary internal robot operating system on the Sunrise Controller. Programming on the iiwa uses the Sunrise Workbench, a Java-based development environment, where robot applications can be written. Applications utilise pre-installed Java packages that translate commands written in the Sunrise Workbench development environment into low-level operations understandable by the KUKA hardware. However, integrating outside features such as AI models, 3D sensors, and complex collision-avoiding motion planning cannot easily be done in the Sunrise Workbench, as it requires integrating multiple external packages that are not inherently compatible (Mokaram et al., 2017). Instead, the Sunrise hosts multiple robot operating system (ROS) nodes, based on (Hennersperger et al., 2017). These nodes enable two-way communication between the KUKA systems and a high-level controller denoted as the Primary Controller (PrC) in Section 5.2.3, where all the components for AI, task management, and robot vision can be integrated. The most important node in the Sunrise robot application is a group of ROS action servers that accept trajectories and convert these into a sequence of motion primitives, such as point-to-point (PTP), that the robot executes. Smooth and continuous motion along the entire trajectory is achieved by converting the list of waypoints into a spline in the Sunrise application, resulting in velocity-efficient movements of the robot arm. It is possible to queue multiple trajectories, which are executed in sequential order, eliminating the necessity to wait for a motion to complete before pre-processing or planning the next steps in a task. Each type of motion, PTP, linear, circular, or spline, has its dedicated action server implemented, allowing a range of motion types depending on the requirements of specific tasks. These action servers are the core of operating the KUKA iiwa, allowing motion commands to be sent from a high-level controller.

In addition, the Sunrise application hosts nodes that provide ROS services for functionalities beyond the movement of the robot arm.

Integration of electrical components is done through the Sunrise Controller EtherCat interface. When a ROS message is received by the service host, the functionality of the referenced module is activated by sending a digital or analogue signal routed through EtherCat. Digital signals are used for activating brakes on the extension rail, activating positive or negative pressure for the soft fingers, and workspace safety signals. Analogue signals are used to dynamically change the pressure on the soft fingers and control the intensity of the LEDs. The background architecture that routes signals to the appropriate ports maps the output signals from the KUKA systems to the input signals of the WAGO Modules. ROS services are in the Sunrise application, and these functionalities are then opened to the Primary Controller. Setting end effector opening width, LED intensity, extension rail position, and pressure for pneumatic elements are then available to the high-level controller.

5.5.2 ROS Interfaces and Task Descriptions

We use ROS as the main middleware for connecting hardware components with their controllers and establishing communication between each operational component. The centralised motion planning software components have an interface to access their functionalities written in Python 3.8, based on (Coleman et al., 2014; Görner et al., 2019). Each motion plan contains trajectories for the joints of the iiwa and extension rail, which are broadcast to the correct controllers using a chain of ROS action servers in Figure 5.19. The format of the trajectory output message from the motion planner is compatible with the action server on the Sunrise application. The Teknic and Dynamixel motors of the extension rail have dedicated ROS action servers to control the extension and additional degrees of freedom. ROS publishers on the Sunrise application and extension rail nodes publish the state of the robot arm (joint positions, velocities, safety variables, and internal/external forces/torques). This feedback provides the latest robot state to the motion planning scene for

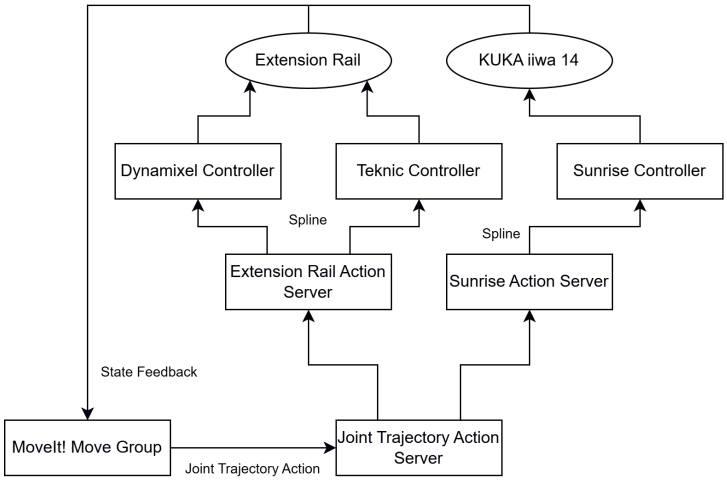


Figure 5.20: Dissemination of a motion plan made up of a trajectory of joint positions to the relevant hardware interfaces through ROS action servers.

accurate correspondence with the real robot cell. The update cycle is shown in Figure 5.20. Additional ROS services enable control of external devices, such as mounted LEDs and the end-effector, through the EtherCat interfaces on the Sunrise Workbench.

We connect the ROS interfaces to the core applications that handle the robot's functionalities on a task and process level, namely the task descriptions. A task description is a script consisting of sequences of operations that control the functionality of the robot (Figure 5.21). Tasks are defined at a high level of abstraction. Each task description inherits the main functionalities from a core package, which contains functions for communication with each of the robot's components, denoted as *Task* in Figure 5.19. This core package allows the design of abstract tasks for the robot in a natural way inspired by Görner et al., 2019. This core package is extendable to include new modules for robot vision and AI models (Chapter 6). We add cognitive functionalities through direct integration in Python or by

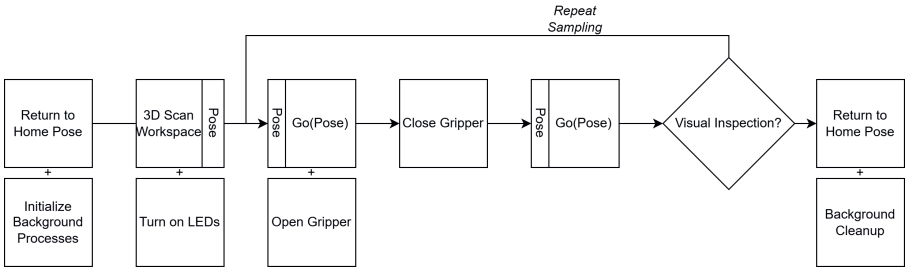


Figure 5.21: A task script represented as a block diagram. Each block represents a function or script coded to perform the named operation with the robot. A task sequence becomes an appropriately ordered sequence of blocks that achieve some meaningful operations. Some blocks will require input either from other blocks or from a configuration of this particular task, for example, a detected pose to reach in the workspace. This sequence represents a mock process of sampling and visual inspection at an insect farm, querying the management system to re-sample. Some operations can be performed in parallel, as shown by stacked blocks.

creating ROS nodes that provide the new functionalities as services. Task management is performed using a set of ROS publishers and subscribers launched in the *Task Manager* layer in Figure 5.19. These create requests for new tasks to be started and wait for incremental updates of the task status while it is being performed. The same approach is used for collecting data about the robot state to be published over the OPC-server (Section 5.5.3).

5.5.3 Asset Administration Shell

We developed an Asset Administration Shell (AAS) in the form of an Open Platform Communications Unified Architecture (OPC-UA) server (Cavalieri & Chiacchio, 2013; Leitner & Mahnke, 2006). This server connects the robot cell to the CoRoSect warehouse and information management systems. The server facilitates the publishing of process-critical data. It opens the functionalities of the robot to high-level management layers that coordinate CoRoSect robotic systems. The

AAS is located at the communication layer of the process chain in Figure 5.19. Individual tasks are identified by an integer ID. This convention is used for each use case involved in the CoRoSect pilots. This provides a simple interface for warehouse management systems, where initialising a task for the robot cell is done by calling its ID through the AAS. Once the sequence of robot operations is complete, the AAS signals a 'done' signal, and the entire process can move to the next stage. During operation and while idle, the robot cell provides a heartbeat through the AAS that notifies the high-level management systems of the robot's state. The state is a compound of the task ID currently being performed (or is available for new tasks), whether the robot is actively moving, and the latest trajectory for visualisation in virtual reality (Chapter 2). Finally, the AAS also publishes data from visual inspection models to the CoRoSect information management system, from which it is made available to experts at the insect farms.

5.5.4 Discussion

The software architecture uses ROS as middleware to ensure stable and reliable communication between various embedded systems, as is commonly done in robotics (D'Avella et al., 2023; Quigley et al., 2009). We use ROS1 instead of ROS2 due to the prevalence of documentation and supporting material at the time of developing the robot cell. The Sunrise Workbench is only programmable in Java, limiting the options for integrating the KUKA iiwa to the ROS-Java distribution (Hennersperger et al., 2017). We use ROS1 to ensure compatibility with ROS-Java, despite ROS-Java no longer being maintained or developed. Furthermore, ROS-Industrial libraries (Edwards & Lewis, 2012) are specifically developed and recommended for industrial robotics. However, their support for KUKA platforms is still at an experimental stage. The choices behind the communication middleware were made out of necessity for a practical infrastructure and compatibility with all the hardware components. Under ROS, each hardware component is treated as an independent system and

is provided two-way communication: (1) publishing its internal state and (2) subscribing to actions it is told to perform. For this reason, the lowest level in the hierarchy is a set of hardware interfaces in the form of action servers. To align with this paradigm, we create similar interfaces for sensors, VI models, and the end effector, instead of integrating them directly into a central program/script. The functionalities of all these components can be accessed independently, allowing a high-level manager to utilise resources as needed, without loading unnecessary systems. The system can be modularly extended with additional hardware by creating a corresponding ROS interface.

Moreover, the architecture of multiple independent embedded systems under ROS requires a central manager that synchronises the functioning of the entire system. We rely on MoveIt! and the intermediate action server to distribute trajectories to the articulated components. To reduce the computational load, we use MoveIt! solely for motion planning and storing a virtual representation of the workspace (which is augmented through sensor observations in Chapter 6). Task-level management is performed at a higher level. An alternative approach is to use MoveIt! Task Constructor (MTC) (Görner et al., 2019), which allows for the creation and execution of sequential operations for a robot to follow, including end effector control and grasp generation. However, the articulated components of the KUKA iiwa, robot extension, and end effector are not the only systems in the robot cell. While MoveIt! does allow for sensor integration and task construction, it does not encapsulate all the systems we require, such as object localisation (Chapter 6), decision-making, or integration of machine learning models. For this reason, we need a higher-level task manager that communicates with MoveIt!, sensors, and cognitive components through ROS and Python. While this solution may not be as efficient or secure as using existing libraries, it provides the flexibility of utilising all ROS-integrated components of our robot cell from a single location. We can define a task as a sequence of operations, similar to how it is done in MTC, with the additional possibility to include conditions based on sensor

data, parallel processing of sensor data through machine learning models, and micro-management of individual digital/analogue signals if necessary. Computationally expensive processes are parallelised where possible, but some operations still require sequential execution: the robot needs to know the pose of a located item before it can plan motions.

A particular challenge is in providing MoveIt! with a valid input to perform motion planning. The MoveIt! Python Interface outputs a trajectory to a defined target pose of joint or Cartesian coordinates, meaning the target pose has to be known beforehand. This means relevant poses need to either be pre-defined or computed in the Task Manager stage. We show how this can be fused with object localisation in Chapter 6, to input the poses of nearby materials as targets, so that a trajectory places the TCP of our robot within grasping reach of an object. A limitation of the current implementation is the lack of a stop trigger for planned trajectories, meaning that once a trajectory is output by MoveIt! and distributed to the Sunrise and robot extension controllers, the robot will move along this trajectory to its end. While the motion can be stopped by releasing enabling switches, the trajectory is stored as active until the program is reset. While our experiments have shown that MoveIt! is suitable for dynamic re-planning and versatile motion through an obstructed workspace, the practical implementation of this requires a stop trigger on the Sunrise application. An implementation we considered here is conditional motion, which ends a trajectory when a pre-defined condition is met, for example, a signal sent through ROS. However, sending this signal cannot be computed through MoveIt!, meaning even if the workspace is re-observed and the previously planned motion causes a collision, this has to be detected and signalled externally. Observation of the workspace is a topic in Chapter 6.

Additionally, with the integration of multiple extensions of the KUKA iiwa, we consider the safety of the collaborative system. Additional safety configurations are added on top of these preset constraints. Atomic safety conditions are set that enable the robot to perform an

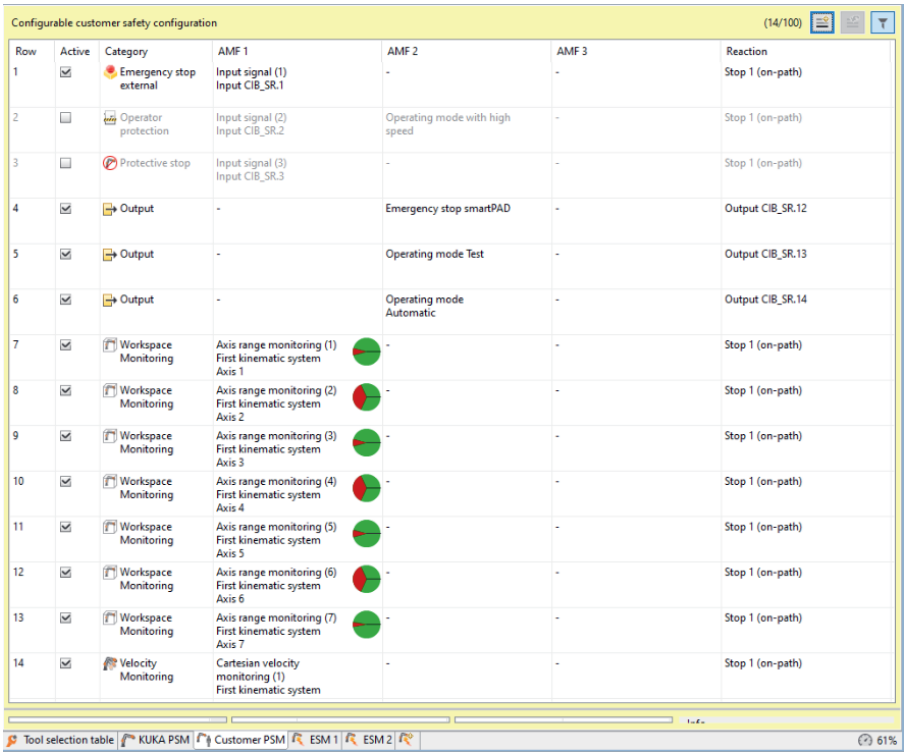


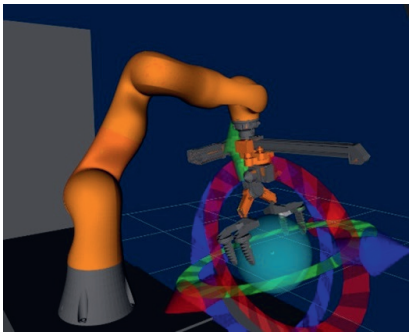
Figure 5.22: Sunrise workbench safety configuration for the robot cell project. Software limits for each joint are hand-set to 5 degrees before the hardware limits, giving the breaks additional tolerance. Safety stop conditions dictate the reaction of the robot when a condition is breached. In this case, the robot ceases motion but with the possibility of resuming motion. In more extreme cases of emergency stops, the robot needs to be manually reset out of a violating state.

emergency stop based on pre-configured rules. The Sunrise application features a low-level safety configuration required by industrial robotics (Bi et al., 2021; Buerkle et al., 2023; Pietrantoni et al., 2024). The setup of safety features is a vital step in operating an industrial robot and is important in a collaborative workspace to prevent physical harm

to human co-workers. Such configurations are used on the KUKA iiwa in (Hennersperger et al., 2017). Within this configuration, the system has pre-established safety modes that are always active while the robot is operating and cannot be changed. Common pre-defined rules include exceeding a joint or velocity limit or reaching a certain peak in an internal sensor reading (indicating a collision). By default, the KUKA iiwa will stop operating upon collision, performing an emergency stop. The emergency stop is also linked through ROS to the extension rail and end effector, meaning the entire system executes a stop command. Software limits for each joint are set to 5^o before the hardware limits to give the breaks extra tolerance. Upon exceeding a hardware limit for a joint, a process of mastering needs to be performed, which is infeasible with the extension rail mounted.

Finally, the media flange touch features a compliance mode where the robot can be guided to positions by hand. This feature is used for human-robot collaboration purposes, such as learning-from-demonstration (J. Chen et al., 2017; Ko et al., 2016). This compliant mode is enabled by holding the user interface button on the media flange touch and having an ESM safety configuration for the media flange. The robot needs to be told how to react in the event of a hand-guiding device being released by the operator. The important aspect of a safety configuration is the ability to customise the robot's motion-stop modes and emergency stops based on user-defined conditions, such as the inclusion of the external emergency switch in Section 5.2.4. This allows for versatile adaptation of the safety rules depending on the target application.

The resulting software architecture allows the execution of trajectories planned in the virtual planning scene using the real robot cell (Figure 5.23). A system for defining sequences of operations as task scripts allows the implementation of CoRoSect use cases. The architecture is extendable to include robot vision, AI models, and additional control strategies (Chapter 6). The robot cell can be modularly rearranged, but is demonstrated in multiple workspace configurations and can handle diverse sequences of operations, with additional sensors and flexible



(a)



(b)

Figure 5.23: The motion planning scene during testing. (a) and (b) The correspondence between the planning scene and the real robot, respectively.

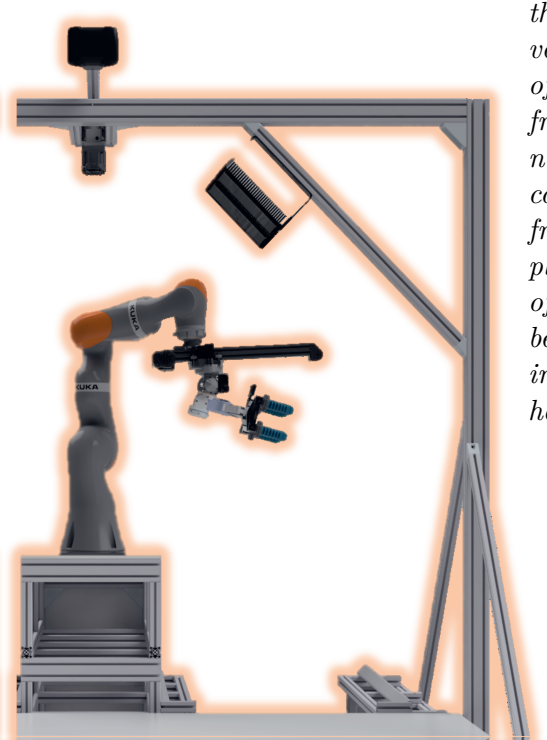
tools at its disposal. This allows an industry to reuse the same robot cell at different stages of internal processes, increasing the added value of the robot cell beyond a single task, demonstrating versatility.

5.6 Conclusion

The focus of this chapter has been the design and development of a robot cell for insect farming. We address the research question of how to achieve control and high-level planning of our robot cell by presenting a control framework and service-oriented software architecture that centres around a virtual motion planning scene. We used the virtual planning scene to perform experiments on operating the robot to demonstrate its capabilities under expected real conditions. The design decisions involved in the support structure and the mounting of the collaborative robot arm are directly motivated by the general requirements for versatility and human-robot collaboration. Accomplishment of specific insect farming use cases is described in Chapter 6. The focus of this chapter has been on highlighting the core components of the robot cell and demonstrating its capabilities for industrial use.

6

CoRoSect Robot Cell: Use Cases, Visual Inspection, and Material Handling in Insect Farming



In this chapter, we present work on developing the capabilities of the CoRoSect robot cell for versatile manipulation. The base capabilities of a collaborative robot arm to plan collision-free trajectories and grasp diverse materials are not yet enough to operate in a non-highly-controlled workspace, such as in insect farming, from which we derive use cases. Material placement is not predefined, and the consistency of obstacles such as crates and enclosures cannot be assumed. Additionally, the possibility of incorrect observations or offsets in material handling calls for systems that allow the robot

to handle such errors without the need for human intervention. Without such control over the robot's surroundings, we face a challenge in sensing and interpreting which elements of a workspace are important objects or obstacles. We present a novel pipeline for accurate object localisation using industrial tools for visual sensing and surface matching, which is used to build a virtual representation of the workspace within the robot's motion planning environment. Furthermore, each individual use case entails high-level operations that each pose unique challenges, such as motion planning in an enclosed space, tightly fitting insertion tasks, sensor occlusion, or the need to handle multiple objects in one sequence. To address these problems, we implement practical strategies for material handling, error correction, and sensing and manipulation within enclosures. We demonstrate how the combination of these strategies increases the versatility of our robot cell in handling diverse materials and operations in real-world pilot studies at insect farms. The robot cell reaches up to 93.7% *average success rate across all tasks during repetitive runs of use cases.*

6.1 Introduction

CoRoSect proposes a versatile robotisation solution for material handling and quality management tasks in different paradigms of insect farming without extensive reconfiguration or re-programming. In the previous chapter, we presented an autonomous robot cell for insect farming, motivated by the industry's requirements for versatile manipulation and process adaptability (Chapter 2). The extension rail (Chapter 3) and versatile end effector (Chapter 4) enable handling diverse materials, but this is not yet enough for task/object agnostic operations.

Each use case defined in Chapter 2 is a collection of unique processes under specific insect farming paradigms. Each full process involves logistics, fine-manipulation, and may require decision-making based on perceived parameters. The focus of our robot cell is automation of tasks

for insect nursing and material handling, tasks which are commonly human-centric. Hence, we first redefine the processes from Chapter 2 into the relevant sequential robot operations in Section 6.2.

Furthermore, implementing a robot cell in an industrial setting requires overcoming practical challenges (Dean-Leon et al., 2017; Pedersen et al., 2016; Tantawi et al., 2019), namely in perception, grasping, and error correction. A particular challenge in insect farming and other industries (Tantawi et al., 2019) is that assumptions about consistency in the workspace do not apply, and the robot's environment is not highly controlled. Not only does the size of the insect crates and their placement create a challenge in collision-free motion planning (Chapter 5), but the contents, possibly filled by a human co-worker, are subject to occlusion and perturbation. This makes it difficult to ensure a secure grasp on objects in the workspace and risks collisions unless obstacles are perceived. Thus, there is a need to use mounted sensors and computer vision for object localisation and workspace observation. The use of 3D cameras and scanners is common in industry (Nilsson, 2010; Robinson et al., 2023), along with algorithms and software solutions such as MVTec Halcon (Eckstein & Steger, 1999). However, difficulty lies in integrating these stand-alone systems into a single robotic platform in order to provide the robot with additional capabilities and decision-making. Additionally, this introduces additional errors with incorrectly located materials, misrepresented obstacles, or false-positive observations (Robinson et al., 2023), which is why automation typically favours highly-controlled environments where poses for materials are pre-set (Andersson et al., 2021; Galin & Meshcheryakov, 2019). In this chapter, we address the need for solutions in the areas of precise robot vision, error correction, and flexible control strategies for material and insect handling. We show how we integrate off-the-shelf industrial solutions into a cognitive and versatile robotic system that consistently handles diverse tasks in insect farming. Finally, we demonstrate the capabilities of the robot cell by accomplishing the use cases defined by the CoRoSect project in repetitive testing.

The following research question is addressed in this chapter:

Research Question 5

How to achieve versatile manipulation in a confined environment?

The work in this chapter builds upon the foundations laid out in Chapter 5 for a versatile robot cell. The first major contribution in Section 6.3 is a computer vision system that is integrated with the extended KUKA iiwa 14 robot to enable accurate localisation of objects in the workspace. This fusion of sensors with a set of algorithms solves the need for perception in the dynamic workspace and is extensively used to perform material handling and insect sampling use cases. The second major contribution is the extension of the control framework from Chapter 5 to accommodate multiple control strategies, including error correction. These strategies (Section 6.4) address the unique requirements of each use case, namely the need to handle diverse materials, reach into enclosed spaces, perform rigorous oscillation, and operate a high-resolution camera for visual inspection. They are demonstrated in tasks of inserting tightly fitting inlays (Chapter 2), harvesting insects, sieving material, or operating in a tent-like enclosure.

This chapter is structured as follows. We first re-frame the CoRoSect use cases from Chapter 2 into sequences of primitive operations for a robot and identify the unique obstacles to automation (Section 6.2). Further, we present the robot vision system developed for the robot cell in Section 6.3. This is followed by the extension of the control framework with additional implemented capabilities in Section 6.4, namely strategies for material handling (Section 6.4.1), error correction (Section 6.4.2), and quality management (Section 6.4.4). We then present results of repetitive testing and data gathered during the CoRoSect pilot studies in Section 6.5, and provide a discussion of the robot cell's performance. Conclusions are in Section 6.7.

6.2 CoRoSect Use Case Requirements and Processes

In this section, we isolate the tasks from the use case processes defined in Section 2.2 that are relevant for our robot cell for insect nursing. We reframe these as sequences of primitive robot operations that can be implemented in software using the task descriptions proposed in Section 5.5.2. This is important because the use case definitions are high-level representations of ideal processes that do not describe how each task is actually accomplished. Instead, we translate the internal processes of the insect farms into well-defined programmable operations for the robot, which allows us to identify unique operations and subtasks involved in the completion of each step. Each sequence is then made accessible to the CoRoSect Manufacturing Execution System (MES) to be used in high-level process management. Each sequence of operations is given to the robot by a process designer, in this case, the insect farm (Section 5.5).

6.2.1 Cricket Quality Management

Cricket quality management requires visually inspecting crickets to measure growth parameters and detect pathogens inside the rearing crate (Chapter 2). The tall walls of the crate necessitate the use of overhead cameras (Figure 6.2). However, since crickets reside within tightly packed cardboard structures, they may remain occluded from an overhead camera. During standard operations, a human worker has better perception capabilities and can resort to gently lifting the cardboard structure. However, due to occlusion, a robot cannot grip the cardboard without the high risk of crushing insects. Additionally, carrying an inspection camera into the container limits the options for establishing a grasp on the cardboard.

To alleviate the issue of occlusion, a visual inspection is performed above filled food trays, which lures the crickets to the crate's surface. Images are taken of the food trays placed on the top of the cardboard structure, where crickets are visible. The Ueye camera (Chapter 5) is positioned

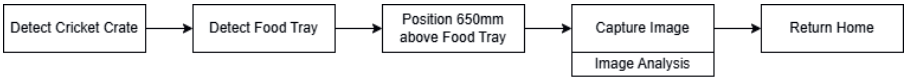


Figure 6.1: Cricket quality management sequence of robot operations.



Figure 6.2: Cricket quality management. The robot is grasping the Ueye camera to position it for visual inspection.

650mm above the food trays. The sequence of robot operations required to perform this task repetitively is in Figure 6.1. The sequence of steps is straightforward and relies on the accurate localisation of food trays to dynamically find the correct position for the inspection camera. The setup of the robot cell is shown in Figure 6.2. Due to their dimensions, a single cricket crate is handled at a time inside the workspace, with 2 feeding trays inside as the targets of the inspection process.

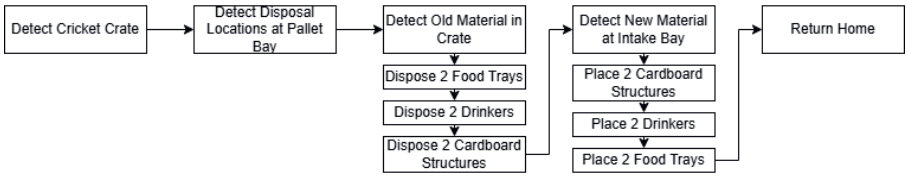


Figure 6.3: Cricket management sequence of robot operations. The initial step of disposing of old material is optional, conditional on its presence.

6.2.2 Cricket Management

The cricket management use case, as a series of material-handling-intensive operations, highlights the requirements for versatile robots in insect farming. The variety of materials involved in rearing crickets requires multiple gripping strategies for deformable and rigid objects. A robust robot vision system is needed to handle transparent material and identify gripping poses. The depth of the crate necessitates tolerance to manoeuvre gripped objects from different approaches and orientations. Materials need to be held steady to prevent spilling water or feed, further constraining the motion planning. Per the requirements of the cricket farm, each cricket crate is filled with 2 cardboard structures, 2 round drinking devices, and 2 feeding trays, in this order. A sample of the materials is shown in Figure 6.4.

The robot operations are presented in Figure 6.3. The sequential nature of these operations makes this task ideal for automation. However, to be cost-effective (Requirement 1, Chapter 2), the robot should handle all materials without reconfiguration. A secondary process in this use case involves first disposing of old materials. Food trays and drinking devices inside a crate are carried to a disposal crate on one of the pallet bays. A versatile robot allows the filling and disposal of materials to be modularly scaled up. It also provides adaptability to new developments in crate types, new materials, and changes to the sequence of operations.

Another objective for cricket management is to assist in harvesting a



Figure 6.4: Cricket management setup inside the crate. Filling the crate this way is the objective of the robot cell.

crate. The above-mentioned cardboard structures, as the living spaces of the crickets, are vigorously shaken to drop crickets into the crate, most effectively by colliding with a solid surface to dislodge crickets quickly. Articulated robots are typically averse to collisions to prevent damage to the internal hardware. As a highly valuable step in the industrial process, the automation of harvesting requires soft elements to dampen collisions but enough intensity to be effective at removing crickets. Requirements 1 and 4, concerning efficiency and insect well-being, respectively, also apply to prevent killing the insects during the harvesting process.

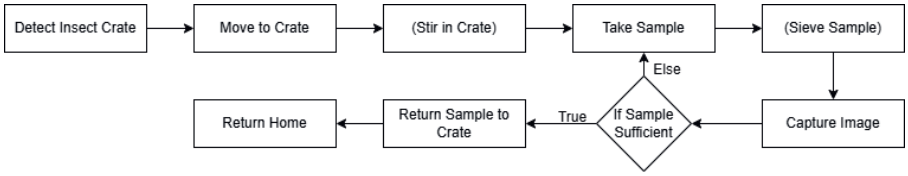
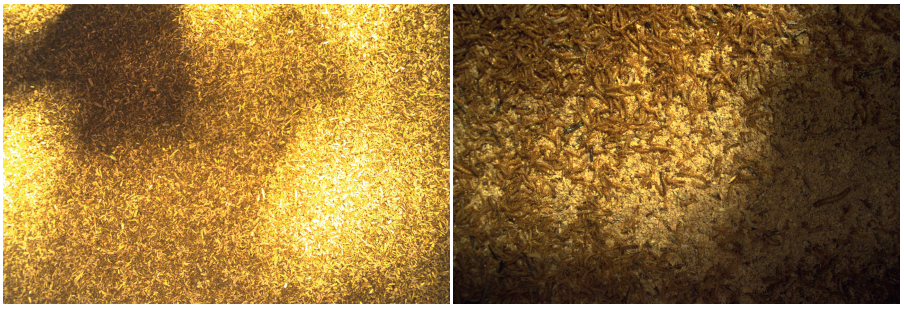


Figure 6.5: Mealworm quality management sequence of robot operations.

6.2.3 Mealworm Quality Management

The following use case involves visual inspection of larvae of the Tenebrio Molitor species. Most aspects and requirements of this use case also apply to the quality management of black soldier fly (BSF) larvae (Section 6.2.5). Three age groups are selected to measure the development of mealworms, namely 5, 7, and 9-week-old larvae. Quality management for larvae is normally a repetitive and tedious process, the automation of which allows fast anomaly detection in individual crates. The approach to quality management is through a visual inspection using a high-resolution camera (Chapter 2). AI models analyse the images to determine specific growth parameters of larvae and detect pathogens. This is valuable feedback for the insect farm. However, the larvae commonly burrow into frass and organic material inside their crates. This is an obstacle for industrial systems with mounted cameras or overhead imaging, as in cricket quality management (Section 6.2.1). Images captured by an overhead camera capture only excess material and contain too much noise for a reliable estimation of insect parameters (Figure 6.6) (Papadopoulos et al., 2024). This is typically handled at insect farms by manually taking a sample for analysis and filtering using an industrial sieving machine to separate the larvae from excess materials by an ensemble of sieves.

To be minimally effective, a robot must be capable of replicating the process of separating the larvae from the excess material. Industrial sieving is common in agriculture (Modrzewski et al., 2022; H. Zhao et al., 2021) and can be approached with dedicated industrial or robotic instruments (Legner et al., 2021). Considering that quality management



(a) (b)

Figure 6.6: Mealworm and BSF larvae visual inspection input image. The insects commonly burrow into the organic material in the crate that comprises their feed and waste. (a) An example surface image of a crate of 5-day-old BSF larvae. (b) An example surface image of a crate of 5-week-old mealworms.

is only part of the industrial process, a dedicated industrial sieve is not a cost-efficient option for the robot cell. The same configuration used for oviposition management (Section 6.2.4) needs to be applied here with adaptability across tasks. Adaptability is also necessary to handle larvae at the progressing stages of development. Given the necessity of operating within a crate filled with insects, gathering a sufficient sample of living larvae requires a delicate approach with a soft/compliant robot. Additionally, visual feedback is needed to determine the quality of the sample, instructing a resampling if necessary. The resulting process flow for the robot is shown in Figure 6.5. Effective sieve sizes and sampling strategies will differ for small or large larvae.

6.2.4 Tenebrio Molitor Oviposition Management

Adult beetles are reared in insect crates containing oviposition inlays where they lay eggs (Chapter 2). The inlays separate frass and eggs from the beetles, which are placed into new crates or sorted out with an industrial sorting machine. The specific process depends on the

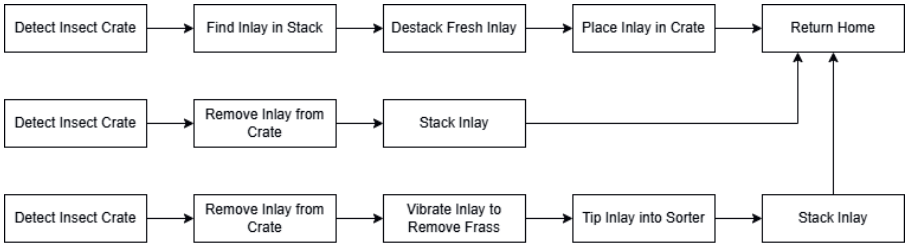


Figure 6.7: Mealworm management sequence of robot operations.

batch's stage of development. The use case is divided into three subtask sequences in Figure 6.7.

The task for the robot cell is the handling and placement of a tightly fitting inlay into an insect crate (Figure 6.8). Insertion and precise peg-in-hole problems are common in automation and are popular for robot learning and learning-from-demonstration (LfD) (H. Chang et al., 2024; Schoettler et al., 2020; K. Wang et al., 2023). Misalignment in the insect farming workspace stems from crate placement and perturbations during operation. To be cost-effective (Requirement 1, Chapter 2), the robot cell must consistently place inlays into crates at various orientations and poses without human intervention. This necessitates accurate object localisation and error correction strategies to handle missed placements of inlays. Finally, tipping inlays into sorting machines is challenging for a robot in both stable motion planning and securing a proper grip for tipping.

6.2.5 Black Soldier Fly Larvae Quality Management

The requirements for quality management and sampling of BSF larvae closely resemble those of mealworms in Section 6.2.3. The diagram for the task sequence is shown in Figure 6.5. While the same overall strategies apply, the living conditions of BSF vary from those of mealworms. Developing a single robotisation solution to quality management for both insect species (Requirement 3, Chapter



(a) (b)

Figure 6.8: Inlay management setup. The white inlay fits tightly into the blue insect crate. (a) The inlay is inside the crate in the workspace. (b) The inlay is gripped by an early version of end effector side brackets designed to handle these inlays.

2) highlights the need for a versatile system that adapts to those species' unique rearing methods. Effective sieve meshes and sampling strategies need to be applicable across insect species.

6.2.6 Black Soldier Fly Oviposition Management

Oviposition management for BSF requires operation within an enclosure of a mating cage, a tall tent structure shown in Figure 6.10a. This use case involves the delicate handling of egg-filled oviposition plates, depositing them in a storage rack, and placing a fresh plate into the mating cage (Chapter 2). Figure 6.9 presents the sequential robotic operations derived from the description of insect farm processes. This use case is a challenge due to the limited space in the enclosure of the tent. The small opening and lack of manoeuvrability inside the tent (Figure 6.10b) pose challenges to classical robotisation. While a human worker can proficiently open the tent and gently lift the egg-filled oviposition plate, a classic industrial robot is too bulky and indelicate to operate inside. A collaborative robot, while better suited to the tent

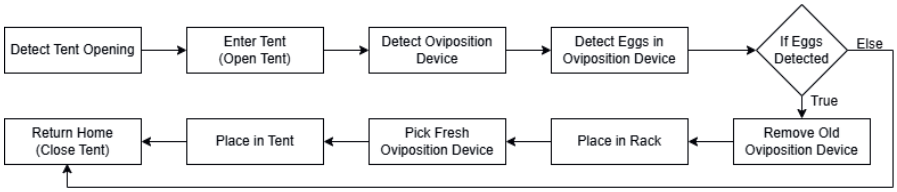


Figure 6.9: BSF Management sequence of robot operations.

opening and need for force feedback, may not have sufficient reachability to grasp an oviposition plate and place it in a storage rack.

Additionally, the outer dimensions of the tent and the fabric it is made of prevent the use of an overhead/external camera, limiting the range of solutions to a mounted sensor. The gripping options for the oviposition plate are limited to prevent crushing eggs, which is a financial loss for the insect farm. The gripping force must be variable to establish a good contact surface to carry the plate without crushing eggs. The orientation of grippers/fingers needs to avoid the egg-filled surfaces. Compared to previous use cases, this use case poses novel challenges to object handling and flexibility, requiring the robot to undertake and adapt to unique strategies.



(a) (b)

Figure 6.10: BSF mating cage and robot cell configuration. (a) The full mating cage is shown next to the robot cell (on its right) and the CoRoSect AGV (on its right). At full extension, the cage and tent-mesh reach up to 3m height. (b) The robot cell reaches into the small opening in the mating cage. The end effector and linear extension fit tightly into the opening after the door is slid open. To achieve this motion, the KUKA iiwa needed to be rotated by 90° on its mounting platform to still be within range of the oviposition plate within the cage.

6.3 Robot Vision and Virtual Workspace Representation

Visual sensors and robot vision systems are typically stand-alone technologies to be integrated into a robotic system to increase its capabilities. A common industrial or collaborative robot arm, such as the KUKA iiwa 14, does not feature its own implementation of visual sensing. Instead, these have to be integrated separately. We present a novel pipeline that automates the process of observing the robot's surroundings (workspace and pallet bays described in Chapter 5), locating obstacles and objects relevant to the completion of tasks, and populating a virtual motion planning environment in MoveIt! with information necessary to plan collision-free trajectories. This pipeline allows the robot to begin each task by perceiving its workspace, isolating task-relevant elements in the point cloud through a surface matching algorithm, and identifying grasping positions for materials, which it then moves to grasp. Our pipeline attempts to minimise task failures caused by errors in object localisation, leading to unsuccessful grasps, and is robust enough to handle various insect farm configurations. To ensure high-precision observation of the workspace, we integrate existing solutions to robot vision in MVTec Halcon software (Eckstein & Steger, 1999) with off-the-shelf sensors such as the Zivid 2 L100.

Commonly, in rigid industrial settings, it is preferred for the workspace to be highly controlled, structuring the workspace so the robot does not necessarily need to observe the positions of relevant materials to accomplish a task (Pérez et al., 2016), hence eliminating sensor errors. However, with the move towards flexible automation, where a significant portion of the workspace is dynamic and cannot be controlled, the need arises for the robot to perform its own observations (Golnabi & Asadpour, 2007; Kuts et al., 2018; Pérez et al., 2016). In particular, visual sensors are implemented when the workspace is not predefined and has to be observed, providing a method to measure the robot's environment and use that data for decision-making and planning systems (Nilsson, 2010; Robinson et al., 2023). A solution

for autonomous robots in dynamic environments typically involves a 3D vision-based sensor that can compute depth information either through a lidar scan, stereo vision, or other approaches (for example, pattern-projection). The 3D vision approach relies on building a virtual representation of the environment, where the robot plans future motions before performing them in the real world. Such a representation commonly takes the form of a point cloud, surface map, or voxel map. In related research and industries, various types and configurations of sensors are used for different tasks (Devalla et al., 2012; Robinson et al., 2023), for example, overhead cameras in (Tsarouchi et al., 2013) or mounted/integrated cameras, such as in (Pretlove & Chen, 1995). While observing the workspace with highly accurate sensors is an important step, another challenge is the accurate interpretation of this data into useful information, such as the 3D coordinates of relevant objects or the detection of obstacles and errors (Nilsson, 2010; Robinson et al., 2023). This is challenging because even small errors in object detection/localisation can lead to failed grasps or tasks, and introducing more systems grows compounding errors (i.e. errors in sensor readings add to the uncertainty of where an object is detected). For consistent operation in insect farming, the robot needs a visual sensor with high enough resolution and point precision to detect small openings for the placement of oviposition devices or cardboard structures and robust object localisation for positioning inlays within crates and even detecting transparent materials (Chapter 2). An additional challenge is the integration of systems that are not necessarily compatible into a single platform. The CoRoSect robot cell features both overhead camera systems and one on the end effector (Chapter 4), providing multiple options for observing various parts of the workspace. The 3D vision cameras mounted on the robot and the surrounding structure are:

Zivid 2 L100: a pattern-projector-based 3D imaging device for generating highly accurate point clouds, enabling effective environmental mapping and object recognition within the robot's operational vicinity.

Stereolabs ZED2i: Although also lacking the high point cloud quality of the Zivid, the ZED2i's wide field of view and higher image capture rate make it a good choice for the registration of larger objects within the entire workspace.

RealSense D435: Mounted on the robot's end-effector, the RealSense D435's lightweight design and higher image capture rate (30 frames per second, compared to Zivid's 2 frames per second with our specific image acquisition settings) make it highly suitable for real-time visual feedback applications, such as visual servoing and sieving tasks.

UI-3884LE: A high-resolution camera dedicated to tasks involving visual inspection of insects.

6.3.1 Occupancy Map for Workspace Registration

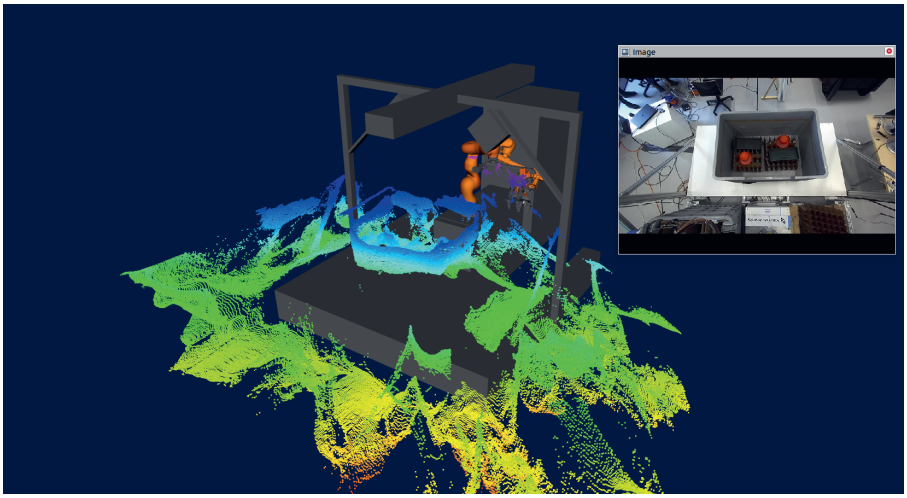
Collision avoidance is a key concept in both autonomous robotics (Cai et al., 2007; Haddadin et al., 2017; Hu et al., 2009) and human-robot collaboration (Martínez-Salvador et al., 2003; A. Mohammed et al., 2017; L. Wang et al., 2013). Articulated robots are vulnerable to collisions, which cause damage along the kinematic chain. Such robots use strictly collision-free motion planning, which is a well-researched field (C. Chang et al., 1990; Haddadin et al., 2017; Rahmanian-Shahri & Troch, 1995; Schwarzer et al., 2005). This collision-averse approach necessitates the use of virtual motion planning environments (Chapter 5) where trajectories are first checked for collisions before being approved for the real world (Martínez-Salvador et al., 2003). The prerequisite for collision avoidance is an accurate virtual representation of the robot's surrounding environment (Claes & Tuyls, 2018; Martínez-Salvador et al., 2003). This approach relies on building a virtual, three-dimensional representation of the workspace for the robot to process before and during its operation. In the context of human-robot collaboration, it is necessary to dynamically update the robot's representation of occupied space to avoid collisions with

moving humans (Martínez-Salvador et al., 2003). A vision system also allows the robot to be robust to perturbations of the workspace during its operations if objects are displaced.

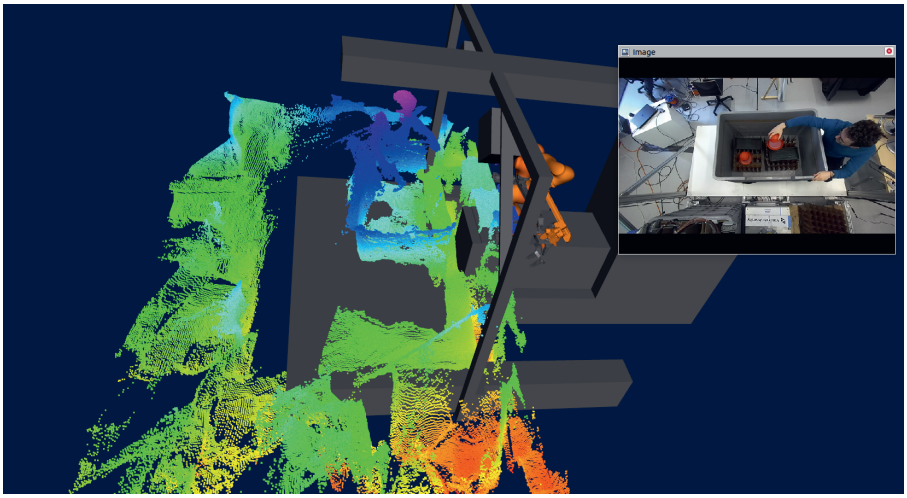
We use 3D-vision sensors and off-the-shelf software to register the environment actively (Figures 6.11a, 6.11b). We construct a dynamic representation of the robot's surroundings instead of operating on predefined assumptions. MoveIt! allows the integration of 3D sensors to generate a volume map of occupied space in the workspace to allow collision avoidance with an observed environment, which is visualised in Figure 6.11.

Both the Zivid 2 and Zed2i 3D sensors are compatible options. The trade-off between vision systems is the update rate of the occupancy map. The Zed2i has a higher capture rate and hence is appropriate for a dynamic workspace. Although it will update the workspace less often, the Zivid outputs a high-quality point cloud with high point precision (Chapter 5). The occupancy map features a colour-coded heatmap of the distance from the camera and is updated at a frequency inversely proportional to the granularity of the map. A higher resolution will slow down the update rate. This system allows the workspace to be observed and translated into information for the virtual planning scene.

A limitation of the current setup is that a trajectory cannot be updated during execution. Once the robot starts moving along a trajectory, it only stops upon detecting a collision. To produce real-time collision avoidance while in a collaborative workspace, such as (A. Mohammed et al., 2017; Schwarzer et al., 2005; L. Wang et al., 2013), the software interface on the KUKA iiwa needs to be adapted to allow updating a trajectory mid-execution, which is possible with conditional motion programming. A ROS signal, used to trigger the path-maintaining stop, can be sent to the Sunrise interface depending on a collision-avoidance strategy within the motion planning scene. Without these, we instead execute shorter trajectories in a dynamic environment, re-observing the workspace in increments.



(a)



(b)

Figure 6.11: Occupancy map in planning scene. (a) One perspective of the occupancy map visualised in RViz. (b) Another perspective, this time with a person operating within the crate, is also represented in real-time updates to the occupancy map.

6.3.2 Surface Matching for Object Localisation

The occupancy map of the observed workspace (Figure 6.11) is sufficient for obstacle avoidance with static objects. However, to accomplish meaningful tasks within an insect farming process, the robot needs to autonomously locate task-relevant objects and identify correct targets for material handling operations. Object detection is a wide field of research that helps solve some of the challenges of versatile robotics (Devalla et al., 2012; Du et al., 2021; Sumi et al., 2007). However, this needs to be coupled with object localisation to extract meaningful coordinates for the robot to autonomously find target poses to perform grasps (Farag et al., 2019). Common approaches utilise deep learning methods, such as YOLO (W. Gao, 2024; Mei et al., 2025), and techniques for object tracking (Banerjee et al., 2018). While it is possible to extrapolate the depth and map pixels to real-world distances from RGB and depth images, such methods are highly reliant on the sensor's calibration and the mapping from image to reality, either of which introduces errors in the transformation of coordinates. Methods based on deep learning, such as those in (Cong et al., 2023), need to be trained for non-standard geometries of objects.

A challenge in handling material at an insect farm is the abundance of occlusions and transparent elements, which cause virtual representations of objects in point clouds to be incomplete or partially covered. This can adversely affect the robot's operations when detecting objects in the wrong pose or with an offset, leading to failed grasping attempts or dropping. The versatile design of the end effector (Chapter 4) adds some tolerance with the soft pneumatic fingertips, providing an additional margin of error. However, the implementation of accurate object localisation is the basis of performing material handling at different stages and configurations of insect farming. We develop an object localisation pipeline (Figure 6.12) that is integrated into the robot cell's software architecture (Chapter 5). The high-resolution point cloud from the Zivid 2 sensor is processed with a

surface-matching algorithm from an off-the-shelf robot vision solution: MVTec Halcon Eckstein and Steger, 1999. We use surface matching to ensure consistent localisation of materials with a geometry-based approach (which is largely deterministic apart from an initial sampling) with a minimal amount of training, and one which allows us to fully take advantage of the 3D point cloud representation of the workspace. Only a CAD model of known objects is a prerequisite to perform surface matching, meaning the robot can easily be transferred between tasks by updating the set of known models.

Surface-matching identifies the points in a point cloud that comprise an object (Paral et al., 2019; Sallade & Philpott, 1997; Skotheim et al., 2012). Once located, the object is represented inside the virtual planning scene in MoveIt! using its original CAD model at the detected pose. The poses of task-relevant materials are used as targets for motion planning. Figure 6.13f shows a located cricket crate placed within the motion planning scene. The virtual models accurately represent occupied space in the workspace, compared to the volatile outline in an occupancy map in Figure 6.11. Adding information to the virtual environment in this way helps reduce the presence of occlusions by filling in information about known objects. Correspondence between the virtual planning scene and the real workspace is determined by the point precision of the Zivid and an accurate camera calibration matrix (Section 6.3.2).

Our pipeline provides interfaces for generating a 3D mesh from the output point cloud of the Zivid and locating known objects within the workspace. The surface matching algorithm samples an observed surface model of the workspace generated from the point cloud. The procedure scores potential matches for a known object based on the local geometry of that object with a model of the observed workspace. It returns a 3D pose with a confidence score. The process is visualised in Figure 6.13 from frame (a) showing the point cloud to the observed crate and drinking devices appearing inside the motion planning scene in Figure f. Locating objects and placing them in the virtual planning scene is a prelude to establishing a grasp (H. Cheng et al., 2022; Sumi

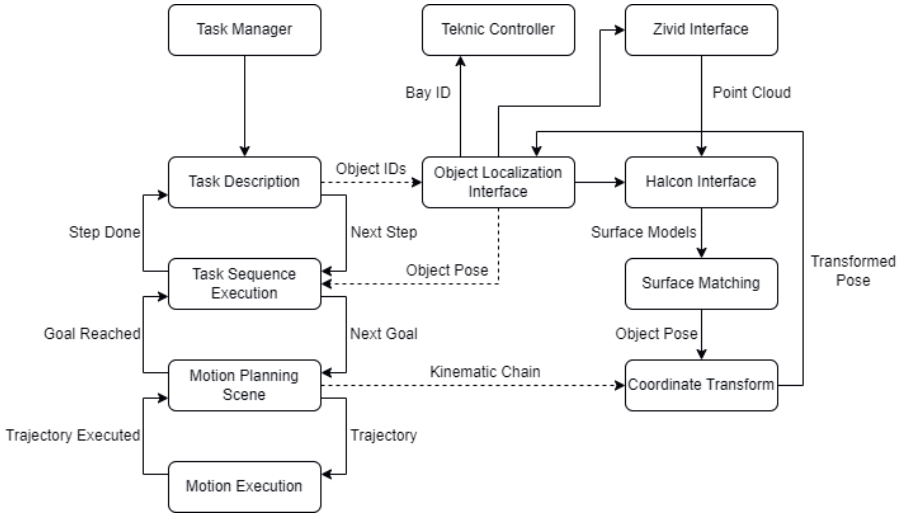


Figure 6.12: Object localisation pipeline at task execution.

et al., 2007). Comparable methods in robotics are taken to object-agnostic grasp synthesis (Bodenhagen et al., 2014; H. Cheng et al., 2022; Newbury et al., 2023).

The localisation of objects begins at the start of the task sequence (Section 6.2), where the models of task-relevant objects are asynchronously provided to the object localisation interface. Therefore, when a task involves handling multiple objects in a sequence, the poses of the material can be computed while the robot is already operating on prior material. Our pipeline (Figure 6.12) parallelises the process of object localisation with the execution of robot actions where possible. Each task definition includes a set of objects that need to be handled for the task to be accomplished. The surface matching algorithm receives as input a surface model generated from the point cloud captured by the Zivid, a CAD mesh of the object to be matched in this environment, and the desired confidence threshold and sampling percentage. The sampling percentage determines the number of individual points sampled from the surface models. The confidence

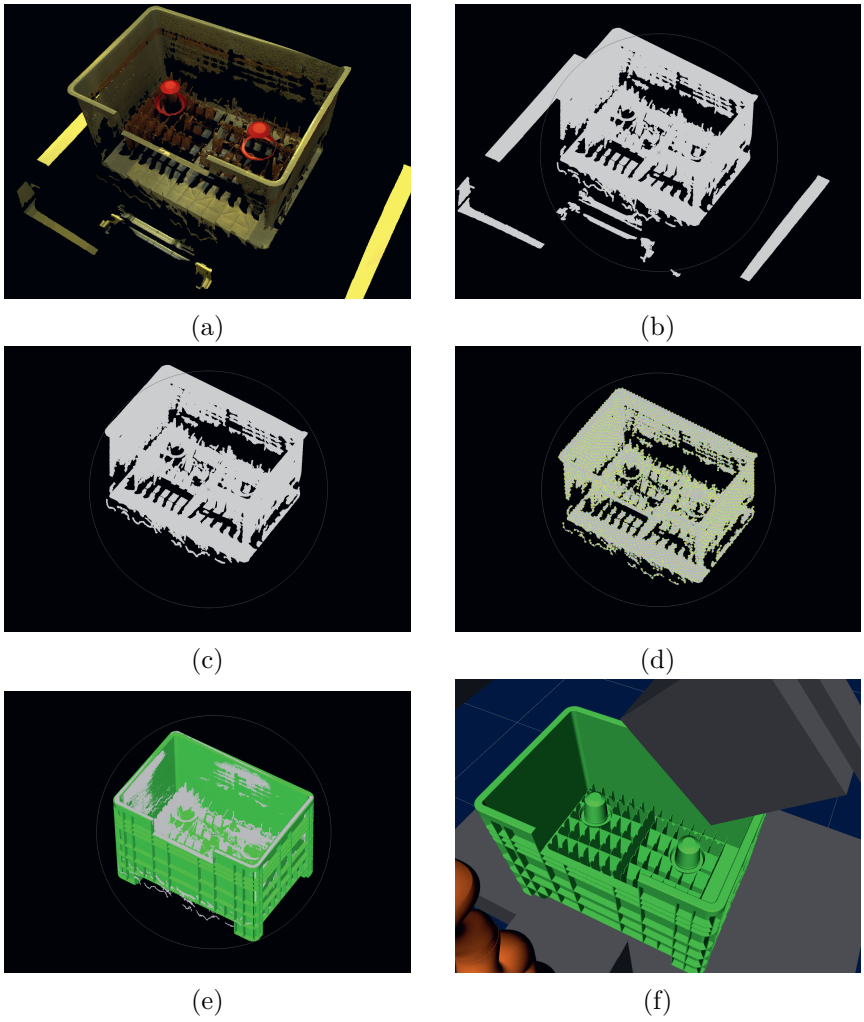


Figure 6.13: (a) 3D scan with Zivid L100. The output is a point cloud. (b) The point cloud is then processed as a data structure compatible with surface matching in Halcon. (c) Removing background and segmenting objects of interest using Zivid Region of Interest (ROI). (d) Sampling 3D points for Surface Matching. (e) Surface Matching result outputs a 3D pose. (f) Object spawned within the motion planning environment. Visualised in RViz.

threshold indirectly affects how many of the sampled points need to match for the object to be located at a candidate pose. A limitation of this approach is the lack of dynamic re-observation. If the workspace configuration changes during a task, the area has to be re-scanned by the Zivid, and the robot has to wait for the next object to become available at the interface. In a deterministic setting, the workspace is re-observed after a complex operation, such as moving an object. Conversely, continuous re-observation is necessary in dynamic settings with moving elements and potentially human co-workers.

Camera Calibration

The articulated joint atop the robot's support structure allows the Zivid sensor to be rotated above either the workspace or the left/right pallet bays. Material intake and disposal are performed by AGVs and accommodated by two pallet bays on either side of the robot cell (Chapter 2, Chapter 5). The robot cell needs to autonomously place new material in the workspace and place old/used material for disposal at a pickup location. New intake material is located using the surface matching procedure, and the poses are stored for when the robot is done operating in the workspace. Each region has a transformation matrix M associated with it for coordinate transformation. This matrix is obtained by performing the Zivid calibration sequence at each area. The pose output from Halcon contains the position and orientation of the matched object in the camera's frame of reference.



Figure 6.14: Calibration Setup.

$$\vec{p_c} = [x, y, z] \tag{6.1}$$

$$\vec{o_c} = [x, y, z, w] \tag{6.2}$$

where $\vec{p_c}$ is the position and $\vec{o_c}$ is the orientation quaternion of an object in the coordinate frame of the camera. The pose of the object, particularly the position, can be transformed into the coordinate frame of the robot's base link by multiplying by the calibration matrix M.

$$\vec{p_r} = \vec{p_c}M \tag{6.3}$$

Motion plans always use the robot's base link as the reference point for trajectories. Hence, a plan can be computed for the newly obtained object's location as long as it is within operational range.

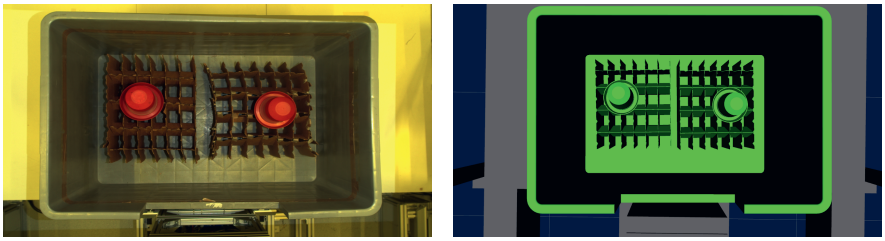
Hand-to-eye calibration is needed for the Zivid 2 and Zed2i cameras, which are mounted on the support structure. Although the Zivid is mounted on an articulated joint, its range of motion is limited to 3 defined positions (above the central workspace and both pallet bays). The calibration of the Zivid is hence performed to obtain three transformation matrices, one per position. The process involves attaching a calibration plate to the robot's end-effector, followed by the robot executing a sequence of predefined poses. Each pose is captured by the camera, and the collected data is utilised to calculate a homogeneous transformation matrix. This matrix defines the camera's spatial relation to the robot's base and is then included in the robot's description file. A similar approach can be taken for the Zed2i. Calibration of the RealSense sensor is conducted using the MoveIt Calibration toolbox, utilising a hand-in-eye calibration approach since the camera is held by the robot. This involves placing a calibration pattern within the workspace and manoeuvring the robot through various poses to gather data necessary for computing the transformation matrix between the RealSense sensor and the RG6 gripper's finger joints, where it is attached. Each calibration procedure results in a transformation matrix M_k from the camera's coordinate frame to the frame of reference of the robot's base link, which is used when performing object localisation to obtain an object's coordinates aligned with the robot's internal frame of reference.

6.4 Strategies for Flexible Manipulation

The next challenge in versatile manipulation is that basic robot functionalities of executing trajectories and grasping objects are not yet enough to ensure the completion of diverse use cases. Each use case is characterised by a unique sequence of operations and corresponding crates, tools, or materials (Section 6.2 and Chapter 2). While some of these operations are common, such as returning to a home position, which is a basic motion capability of the robot, others, such as applying oscillation for sieving or placing the correct trays in a crate, require refined/specialised operations. This means that, when the abstract sequential operations are defined as they have been in Section 6.2, these low-level robot operations need to be individually implemented. In this section, we outline the additional functionalities implemented in the control software of the robot as additional capabilities needed to accomplish insect farming use cases. In this way, we expand on the scope of our robot cell to provide novel operations available to the end user. In particular, we focus on the techniques used to ensure stable grasps on regular and irregular objects, performing error correction with tightly fitting inlays, and exploring various sampling strategies for quality management applications.

6.4.1 Strategies for Versatile Material Handling

Material handling is encountered in most insect farming tasks (Section 6.2). A single task can involve handling various materials or manipulating the same material in different ways. A versatile approach that enables a single robot to operate on all available materials remains a cost-effective method of scaling up existing farm processes. Such a robot requires invariance to the geometries of objects it grasps and the ability to identify them autonomously. Our approach to automated material handling begins with the surface matching procedure to determine the poses of objects of interest in the workspace (Section 6.3). Once located, poses of important materials are stored, and their models are placed in the virtual planning



(a) (b)

Figure 6.15: Locating materials for collision avoidance and material handling. (a) The RGB image of the workspace by the overhead Zivid 2 L100. The capture is accompanied by a point cloud that is used in the surface matching. (b) The same view after surface matching and loading the CAD models for detected objects into the virtual planning scene.

scene to process collisions (Figure 6.15). The robot uses this virtual representation of the workspace to plan collision-free trajectories. Common to all use cases is the detection of the insect container crate (Figure 6.15). Information in the virtual scene can be updated using repeated scans from the Zivid sensor. However, this costs computation time and risks occlusions if done while the robot is operating. A limitation of this approach is the need for re-identification of objects if the workspace is changed during a use case.

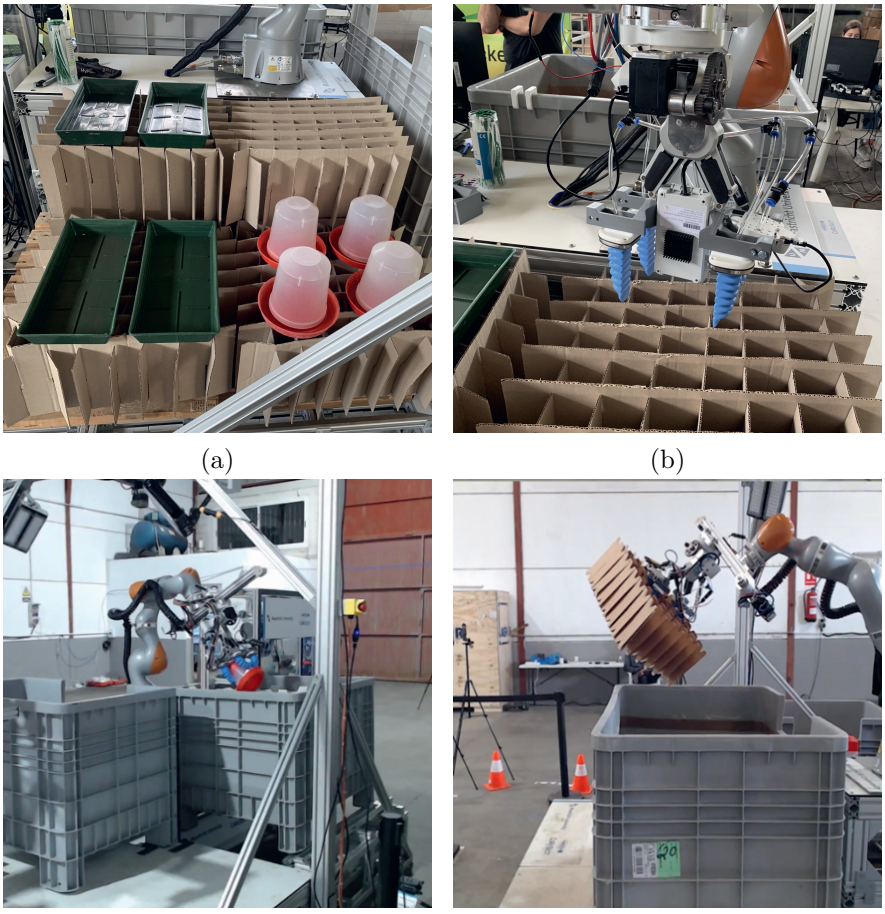
Target poses, from where grasping is attempted, are described in relation to the located objects. The tool centre point (TCP) for our end effector (Chapter 4) is positioned at an offset from the position of an object. With an object inside the gripping envelope of the end effector, the pneumatic fingers are closed to establish a grasp. The soft elements provide a pinch or enveloping grasp, conforming to the object's geometry. We adjust the size of the contact surface with the soft fingers by introducing an offset into the position of the TCP, or the opening width of the RG6. We position the TCP further from the target object to pinch-grip with the fingertips. Conversely, we can position the TCP closer to create a greater envelopment grasp, or grip with the rigid surface of the RG6 (Chapter 4).

The soft fingers provide sufficient gripping strength to lift insect farming materials with different contact surfaces (Figure 6.16). Cylindrical drinking devices are gripped with soft fingers wrapping around the geometry. Rectangular trays and oviposition devices (Figures 6.17 and 6.25c) are pinched between two sets of soft fingers. The compliance from using a soft end effector provides the versatility to grasp various geometries of materials without the need to pre-compute complex grasp synthesis. Opening the fingers using negative pressure increases the tolerance and allows the gripping of larger objects (Figure 6.17a). We also use the RG6 opening width to increase or reduce the size of the grasping range for the soft fingers. This accommodates even wider objects and is used to increase the contact surface around cylindrical materials. A stable orientation while carrying objects (to prevent spilling feed and water) is introduced as a constraint on the end joint in the motion planner.

The combination of surface matching and versatile end effector allows the solid material involved in cricket management to be handled without changing the robot configuration (Figures 6.16, 6.31). Similar grasp strategies are used for the oviposition device placed within BSF mating cages (Figure 6.17).

Autonomous insertion of held material into slots or containers uses surface matching to identify target poses. Target containers, such as the disposal container in Figure 6.16c or racks in Figure 6.17b, are placed in the virtual planning scene. The point-precision of the Zivid sensor allows us to identify individual slots in the rack in Figure 6.17b. The instructions for the order of disposing of and inserting materials are defined in the task sequence. Sequentially placed materials, such as the drinking devices on top of cardboard structures in Figure 6.15, are handled by re-observing the crate after each placement. Cardboard structures are first placed based on the pose of the crate. Target locations for the drinking devices are relative to the detected poses of the cardboard structures.

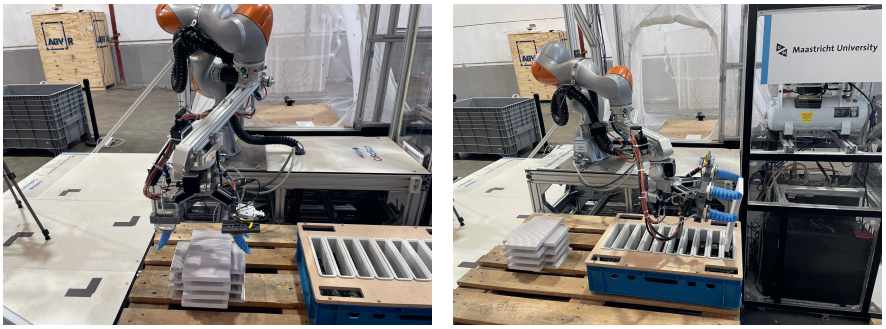
We also use the end effector to handle non-standard and deformable



(a) (b)

(c) (d)

Figure 6.16: Cricket management materials and examples of handling. (a) The intake material at the pallet bay is placed by an AGV. The materials are organised strategically to match the sequence of placement. (b) The cardboard structure is approached by the end effector's soft fingers, which will be inserted into the empty slots to establish a grasp. (c) The disposal of a drinking device that was taken out of the central crate. (d) The cardboard structure is being hoisted over the edge of the tall cricket crate to avoid collisions.



(a) (b)

Figure 6.17: Gripping strategy for oviposition trays of BSF. (a) New oviposition trays are picked up. Negative pressure is used in the soft fingers to increase the tolerance of the grasp, allowing the fingers to get close to the stack without disturbing it. (b) A used oviposition tray is being placed in a storage rack. The tray is held at the tips of the fingers to prevent crushing eggs.

objects. The cardboard structure in Figure 6.16b folds upon being picked by a single pinch point. It is also too large for an embracing grasp. Placing it in an unfolded state is achieved by inserting the soft fingers into openings and applying shear force in the opposite direction of the fold. This keeps the cardboard open until it is placed inside the insect crate (Figure 6.16d). Gripping cardboard requires significantly more time (table 6.1). This extra time was spent visual servoing to find openings for the soft fingers (Figure 6.16b). Visual servoing is done using the RealSense D435 camera on the end effector and short linear motions of the KUKA iiwa.

The crickets in the cardboard structure add significant weight to the KUKA iiwa beyond its torque limits. Figure 6.18 shows the harvesting process using a reduced cardboard structure (half the size). The pressure of the pneumatic soft fingers is increased to secure a grasp inside the cardboard. An open tube of air from the same pneumatic system is attached to the end effector to blow crickets away from the contact surfaces to prevent crushing. The cardboard is collided

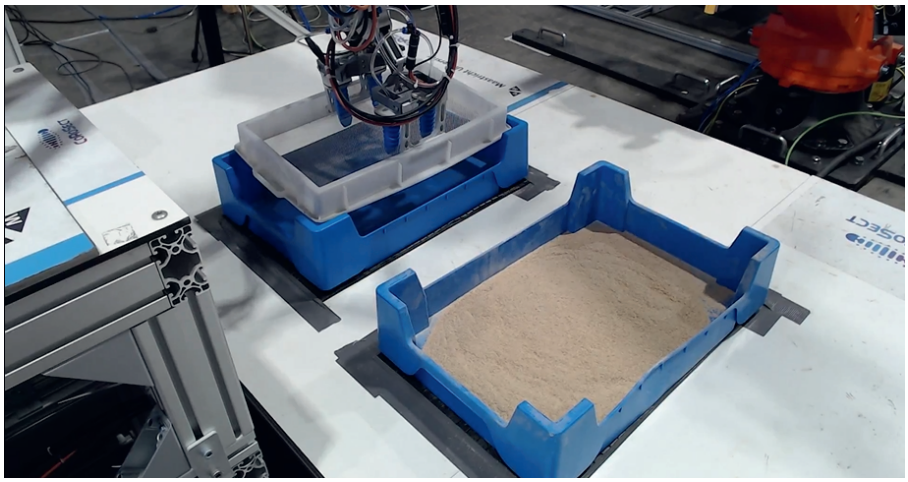
with the wall of the crate by accelerating it along the extension rail, resembling the harvesting procedure done by workers (Figure 6.32).

A pinch or embracing grasp cannot be applied to all materials. Objects with open surfaces, such as inlays (Figure 6.8), are grasped by applying outward pressure to the inside walls. To achieve this, we equip the end effector with modular side brackets that fit against flat surfaces (Figure 6.19). The exerted force is controllable by opening and closing the RG6 gripper (Figure 6.19a). Using rigid brackets prevents the soft fingers of the end effector from being cut by the sharp edges of the inlay. This gripping strategy is tested with inlays for oviposition management of Tenebrio Molitor. Motions for picking inlays (Section 6.2.4) are planned in relation to the pose of the insect crate. The robot performs these operations regardless of the placement of the crate within the workspace, as long as it is within reach. Example grips are shown in Figure 6.19. The use case is broken into 3 sub-processes, each involving placing or removing an inlay into a crate or pallet (Figure 6.33). Sorting is done by transplanting an inlay from a crate to a supplementary crate (Figure 6.19). The supplementary crate is then tipped by the larger (de)stacking robot (Chapter 2).

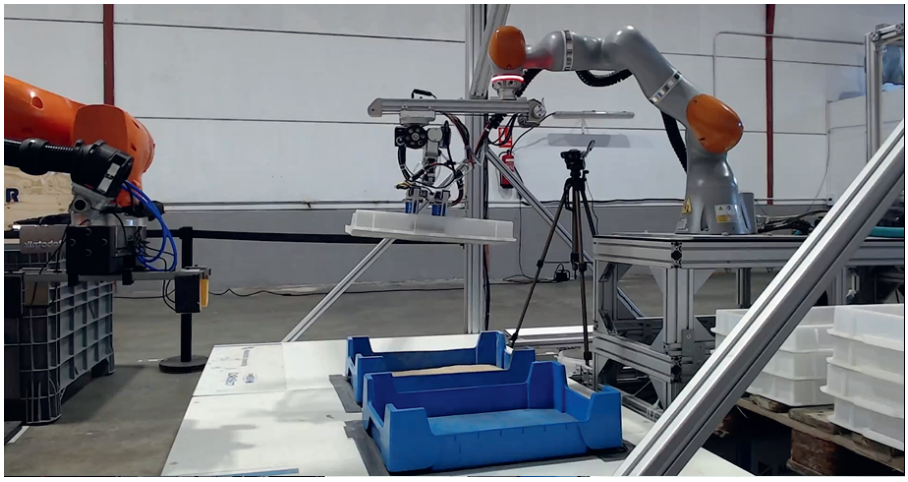
We also consider grasping delicate objects that are subject to damage or crushing. This is a common problem for robotics in agriculture, where soft end effectors are popular (Vrochidou et al., 2022; W. Ye et al., 2023). We achieve a delicate grasp by lowering the pressure in the pneumatic soft fingers. A limitation of our approach is the lack of pressure sensors and force feedback at the fingertips. Implementation of such sensors would allow the robot to reactively control the finger pressure based on the profile of the held object. Without this feedback, we rely on using low pressure in the soft fingers when handling delicate elements. This is used for grasping oviposition plates from BSF mating cages (Figure 6.17). While the plate is rigid, the eggs within the ridges are subject to crushing. Crushing is prevented by gripping on the sides and with low pressure to avoid the edges of the fingers from entering the ridges. This also loosens the grip on the oviposition plate, making it compliant to gentle placement inside the making cage (Figure 6.17a)



Figure 6.18: Automated cricket harvesting. Top Left: the extension rail and the grasp on the cardboard structure. Top Right: the bottom of the crate where crickets drop during harvesting. Bottom Left: overhead view of the workspace. Bottom Right: side view of the workspace.

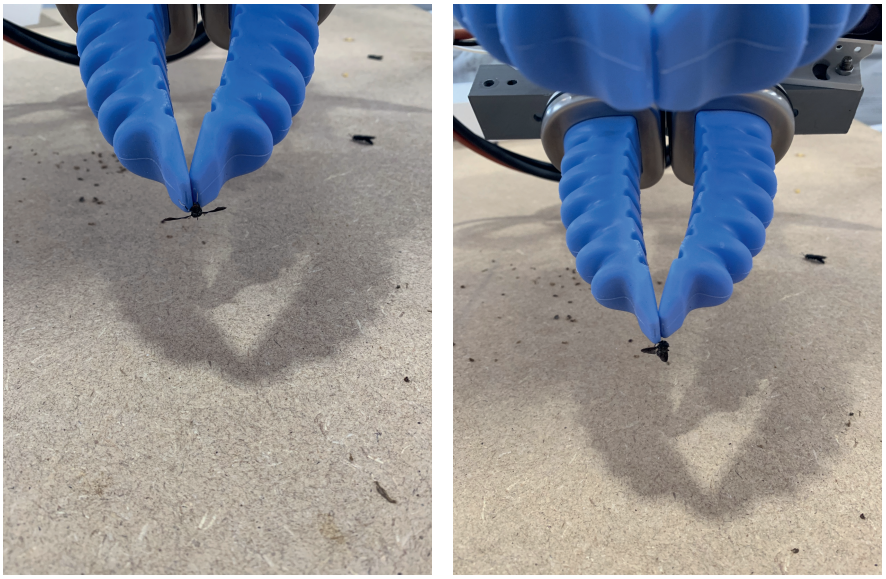


(a)



(b)

Figure 6.19: Side brackets used for handling inlays are mounted to the end effector. (a) An inlay is being picked up from inside a crate with the end effector gripping from within. (b) The inlay is lifted above the workspace during operation.

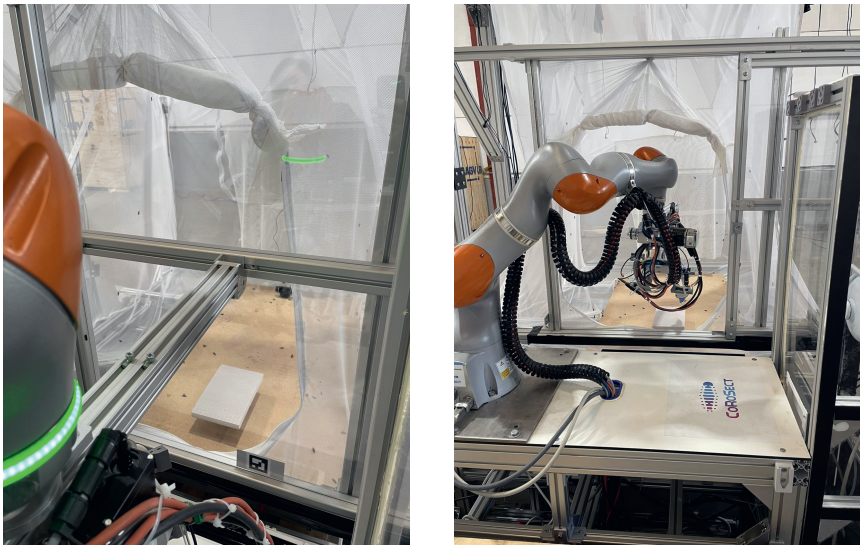


(a) (b)

Figure 6.20: Delicate gripping strategy used to pick individual (dead) insects with low air pressure in the soft fingers. Contact surfaces were established with extremities or limbs, not crushing the insects but exerting sufficient pinching force to lift. (a) and (b) Dead BSF being picked and cleaned out of a mating tent.

or storage racks (Figure 6.17b). A further test of delicate grasps is performed by picking dead BSF from within the mating cage (Figures 6.20a, 6.20b), in a cleaning process. The use case involves cleaning mating cages by picking out dead flies after they are identified. This is possible by minimal closing pressure on the soft fingers to avoid crushing the dead insect during picking. While this is not an industrially scalable strategy, it is intended to showcase the robot's capability to perform gentle operations.

Strategies for versatile manipulation are not limited to handling objects. Obstacles in the workspace represent physical barriers that



(a) (b)

Figure 6.21: The opening in the tent is sealed using a sliding door to prevent insects from passively escaping. The robot uses the extension rail and a rigid contact surface to slide the tent with linear motion. (a) The tip of the extension rail is positioned against a bracket on the door. Pushing this bracket slides the door open. (b) The robot is entering the opening of the mating tent after having opened the door.

limit the operational capacity of the robot cell. However, some obstacles prevent robots from performing tasks and need to be overcome instead of avoided. An example is the door mounted to the BSF mating cage that covers the opening, preventing insects from escaping. It also prevents the robot from reaching directly inside. We use the rigid structure of the extension rail to push against brackets attached to the door frame. A series of linear motions slides the door, revealing the tent opening. The door is closed using the same operations in the opposite direction. With this approach, we take advantage of the reachability added by the extension rail and do not risk damage to the soft elements of the end effector.

6.4.2 Error Correction

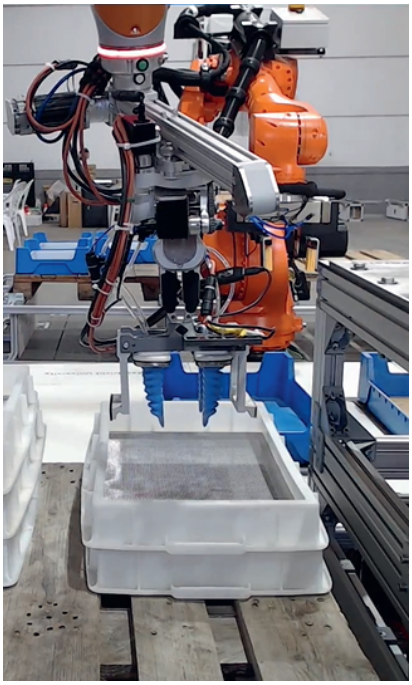


Figure 6.22: The robot slowly moves down at the observed location of the stack. The force sensors in the KUKA iiwa detect a peak exceeding a set threshold once the robot is in contact with the top. The soft fingers absorb some contact force by bending, meaning the robot does not push against a rigid surface and hence will not be damaged.

The adaptability of the robot cell to errors in object placement is a critical feature. The workspace is not highly controlled (Tantawi et al., 2019), and there are no alignment features for object placement or visual aids. We address error correction with visual and force feedback. Error detection is performed using the joint torque sensors integrated in the KUKA iiwa. During a placement manoeuvre, the robot monitors the torque measured by the internal torque sensors for any indication of abnormal resistance or collision with a surface. If a spike in force is detected before positioning is finalised along the Z axis, the robot infers improper contact with a surface. The process is depicted in Figure 6.23. This force-feedback system is also used for detecting the heights of stacks when placing or collecting material from pallets, such as inlays in Figure 6.19. Once a torque threshold is exceeded, the top of the stack is in contact with the end effector. At this point, the top object can be gripped (Figure 6.22).

We use this strategy for consistent inlay placement (Figure 6.19). The robot faces the challenge of aligning the inlay with a margin of error as

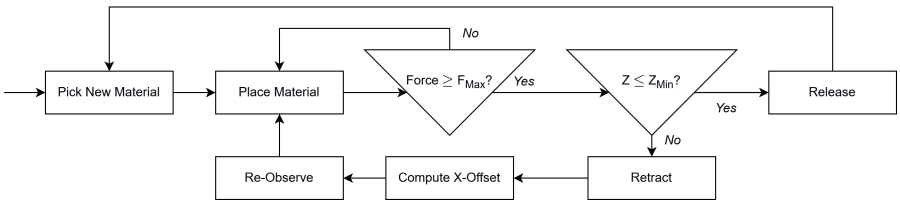


Figure 6.23: Error correction strategy for inlay and material placement shown as a diagram. The robot continues placing material until a maximum force threshold is exceeded. It then tests whether the object is placed based on its position in the vertical axis relative to the workspace. If the object has not yet been placed, the workspace is re-observed, and the offset between the held inlay and the target container is updated so that another attempt can be made.

slim as ±1.5mm and ±4mm along the short and long axes of the crate, respectively. Offsets in this task originate from the pick of the inlay, errors in the crate's placement, or are introduced when a worker stops the robot to manually inspect the crate. Figure 6.24a illustrates an exaggerated scenario of misplacement to clarify the underlying principle. In conventional automated setups, an assumption is often made that objects will be positioned within a negligible distance from their designated spots, eliminating the need for corrective actions. However, given the robot's design for a versatile and less restrictive workspace, it must consistently evaluate its actions and environment to ensure an uninterrupted operation.

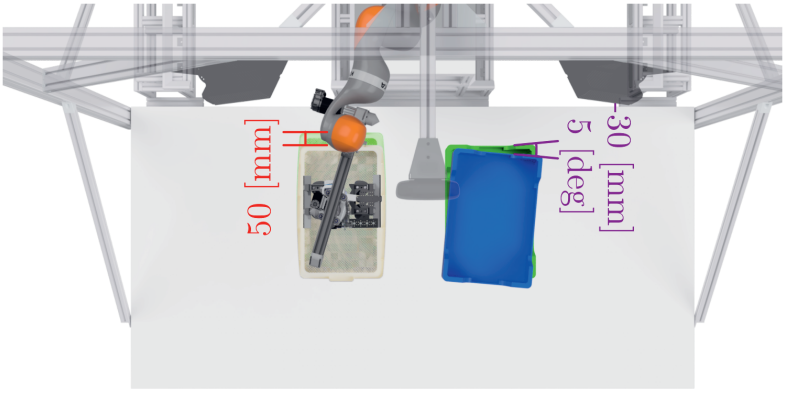
Post-pickup of the inlay, the robot uses the Zivid 2 L100 for visual feedback to confirm the inlay's actual orientation in relation to the end effector's coordinate frame. Concurrently, it performs surface matching on the target crate to pinpoint its location within the workspace. With this data, the motion planning software computes a motion trajectory for the inlay placement, which is then executed. When a placement error is detected, the robot aborts the insertion attempt to prevent damage. It retracts to perform another environmental scan, reassessing the situation and re-planning its approach. The

Zivid sensor and surface-matching (Section 6.3) are used to re-observe the workspace. Naturally, errors and the need to repeat insertion attempts inflate the time needed to complete a task (Figure 6.33a). The error correction strategy allows for consistent success in a task that would otherwise need alignment correction or human intervention (Figure 6.33b). Future developments in the robot's adaptability could potentially streamline this process by developing algorithms to intelligently estimate the contact point during a collision and obtain a force vector for the surface profile. The robot could then adjust its placement strategy without needing to re-observe the workspace, thereby reducing cycle times.

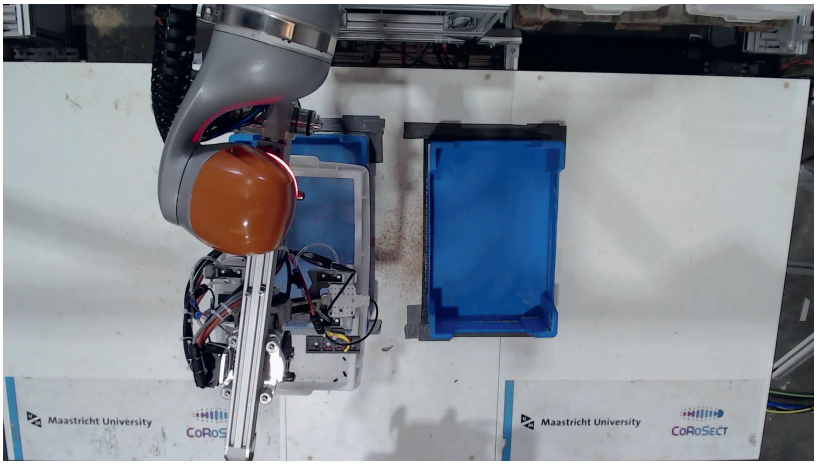
Additionally, we use visual feedback to correct errors in the quality management strategies (Section 6.4.4), particularly when sampling larvae. The sample must be large enough to be representative of the population of the crate. We implement this on the robot cell through feedback from the AI visual inspection (Papadopoulos et al., 2024). Resampling is performed until a sufficient count ($\geq$ 100) of larvae is detected. The process autonomously repeats until a representative sample is taken (Figure 6.28).

6.4.3 Operating in Enclosures and with Constraints

Enclosed spaces pose the risk of collisions with rigid surfaces as the robot operates inside. Collision detection is needed for the entire kinematic chain so that no link collides during operation. Occlusions and lack of sensor coverage hinder accurate correspondence between the real workspace and the virtual motion planning scene. An overhead camera cannot be used to dynamically update the state of a crate within the workspace if the robot is in the way. The presence of occlusions and incompletely observed objects is also detrimental to the accuracy of surface matching. We improve the capabilities of operating inside enclosures using the RealSense D435 sensor mounted to the end effector (Chapter 4).



(a)



(b)

Figure 6.24: Error correction based on force and visual feedback. (a) Demonstrates how the m-robot can compensate for an offset when picking up an inlay (offset by 50 mm) and accurately placing it into a misaligned blue crate (offset by 30 mm and rotated by 5 degrees) compared to the ideal positioning marked by the green outlines. (b) The real robot, while attempting to place the inlay in the blue crate on the right.

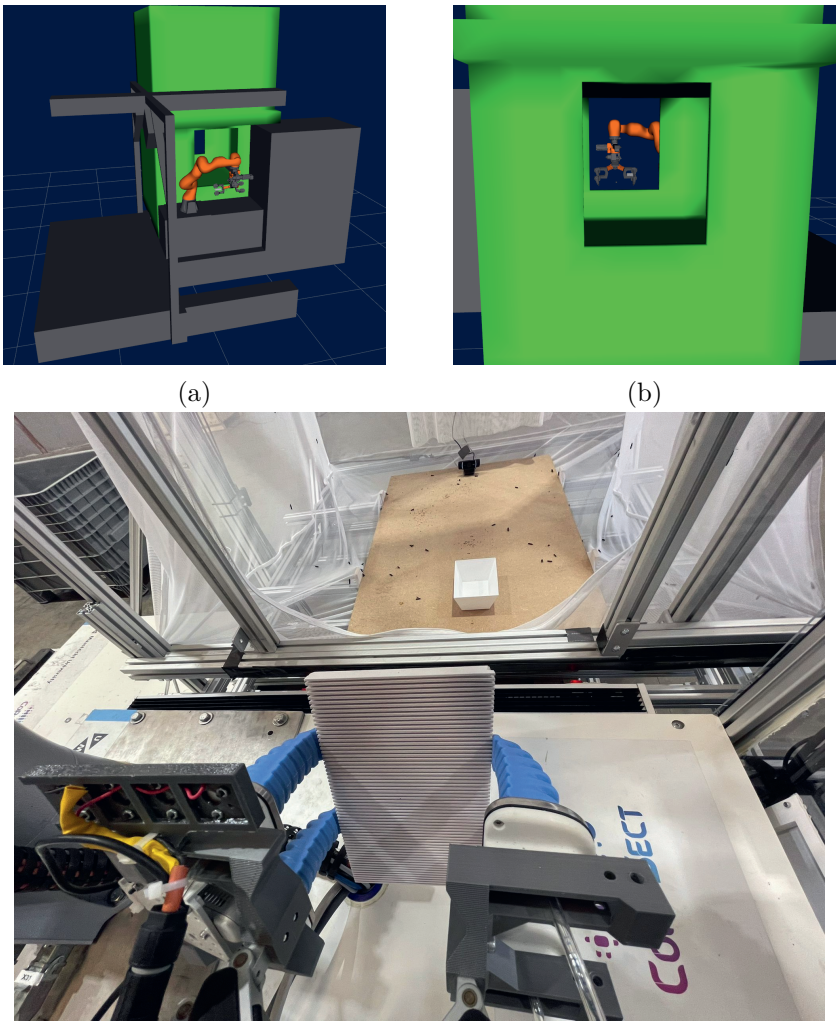
We use ArUco marker (Kalaitzakis et al., 2021) detection to position objects in the workspace that are too large to be fully observed, such as the BSF mating tent (Figure 6.25). This allows us to use the CAD model of enclosed spaces to process collisions in the virtual planning scene. An alternative approach, when the geometry of the enclosed area is unknown, is to generate an occupancy map (Section 6.3) using the RealSense sensor output. However, this becomes inaccurate when dealing with a semi-transparent meshed material that introduces errors in the point cloud. We use a CAD model to handle BSF mating tents to prevent observation errors from appearing inside the planning scene and blocking the available operational space. The virtual tent is positioned based on a detected ArUco marker that the robot actively looks for at the start of the task. The robot cell is shown entering the BSF mating cage in Figure 6.21b.

In cases where the overhead Zivid sensor is completely obstructed, we use classical computer vision techniques of contour detection and shape matching to locate materials (Brahmbhatt, 2013). These are also used when the full object cannot be observed by 3D vision. The oviposition plate inside is located using contour detection and mapped to 3D coordinates using a transformation matrix determined using ROS. Figure 6.25c shows the lifting and grip of the oviposition plate as it is inserted into a tent. The placement of the plate relies on the calibration of the RealSense sensor, and force feedback is used to determine contact with the placement surface (Figure 6.25c).

6.4.4 Sampling Strategies for Quality Management

Visual inspection poses the challenges of optimal camera positioning and obtaining a sample from inside an insect crate. In this paradigm, imaging for visual inspection requires both a stable and high-resolution image, where insects are visible without occlusion.

In the case of crickets, we address the problem using a high-resolution camera gripped by the robot. Crickets are visible atop food trays



(a) (b)

(c)

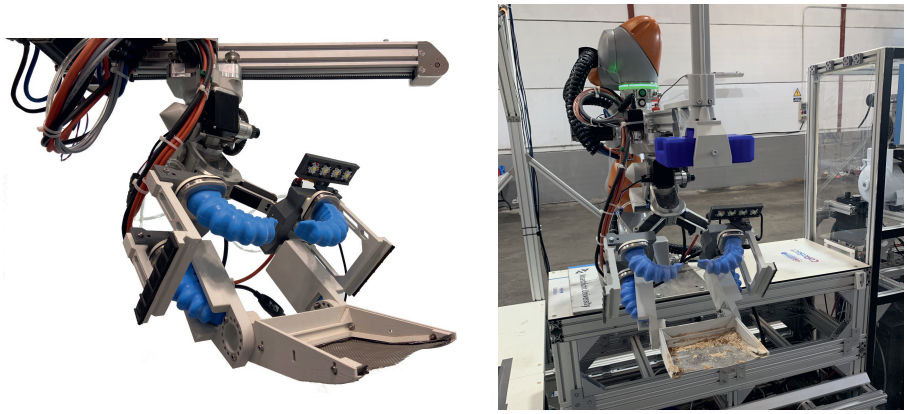
Figure 6.25: Mating cage inside the virtual planning scene. (a) and (b) The BSF mating tent CAD model is placed inside the planning scene from two perspectives. The CAD model approximates the shape and opening of the tent but is sufficient in a simple form (Figure 6.34b). (c) The robot is handling the oviposition plate to be placed on top of the white structure inside the tent.

exposed to an overhead view. These trays are imaged from a height of 650mm. The Ueye camera used for visual inspection is held in an IP66 protective case by the rigid contact surface of the RG6. Autonomy is achieved using the surface matching procedure (Section 6.3.2) to position the motion planning target at a point 650mm above the detected location of each food tray. The robot dynamically positions the camera in a favourable pose for imaging as long as the crate is within reach. Figure 6.2 shows the robot taking a surface image of crickets above a crate, while Figure 6.4 is a view of the inside.

Performing quality management of mealworms and BSF larvae requires a sampling strategy. The insects burrow into the frass and organic material inside the crate, meaning a top-down camera is ineffective at finding actual insects in the images. A standard approach to handling excess material is to use an industrial sieving machine, which utilises multiple mesh sizes to remove particulate matter, leaving only the insects in a sample. To match existing quality management operations, the robot carries a sampling tool (Figure 6.26a) to sieve excess material from a sample, and the high-resolution Ueye camera is mounted on the extension rail (Figure 6.26b). Required to be adaptable across various insect species and warehouse setups, the robot cell first uses the surface matching procedure (Section 6.3.2) to identify a crate within the workspace. The sequence of motions for sampling is relative to the identified pose of the crate, allowing the robot to adapt to different crate depths and orientations across rearing methods.

We propose multiple modalities of automated sampling to accommodate a variety of insect farming standards and demonstrate the versatility of the robot cell. Each process is a trade-off between the time taken and the complexity of operations shown in Figure 6.27:

- **Surface Image**: a top-down image of the crate where larvae are visible at the surface. This is the quickest method (Figure 6.36) but is unsuitable for small (young) larvae that burrow under the surface.



(a) (b)

Figure 6.26: Sampling tool and visual inspection camera mounting. (a) A close-up image of the sampling tray held by the end effector's soft fingers. (b) An image in real-world conditions inside an insect farming warehouse. The visual inspection camera is mounted to the tip of the robot extension and is shown here by a blue box case above the sampling tray.

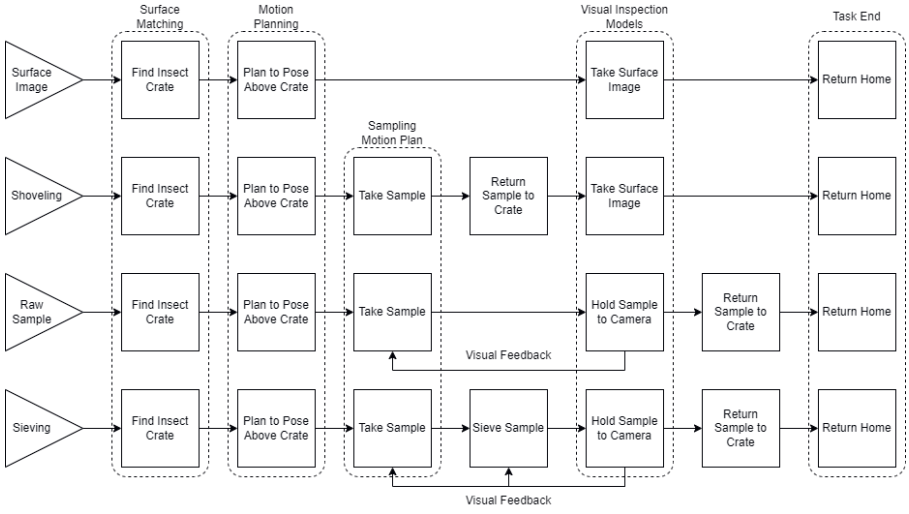


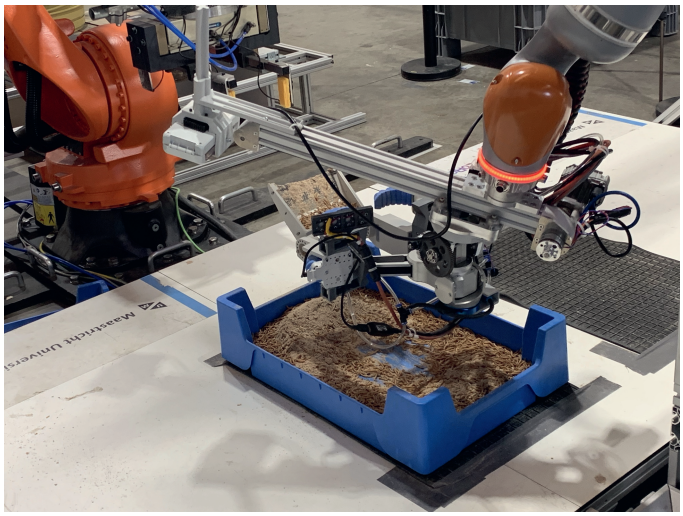
Figure 6.27: Sampling strategies process flow.

- **Shovelling**: the sampling tool held by the robot is used to scoop a volume of material (frass and larvae) and deposit it directly back into the crate before a surface image is taken. The extra operation uncovers burrowed larvae, making more insects visible for visual inspection (Figure 6.38).

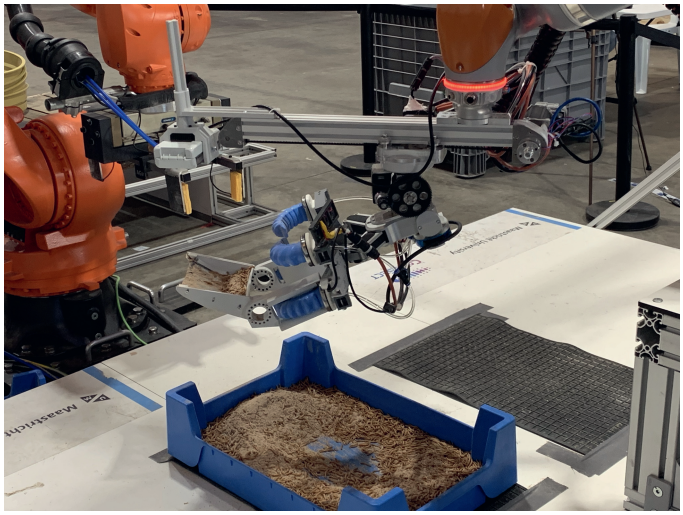
- **Sample without Sieving**: a sample of the insect population is taken using the sampling tool and is shown directly to the visual inspection camera mounted on the extension rail. The sample can be weighed using the torque sensors in the KUKA iiwa. The sample is returned to the crate after imaging.

- **Sieving**: additional material that will affect both a weight measurement and create false-positive results for the visual inspection models is present in a sample. The sample is first sieved using the mesh surface of the sampling tool. The sieve mesh size can be exchanged in the sampling tool to accommodate different frass and larvae sizes. The RealSense camera mounted on the end-effector provides visual feedback for when the sample is sieved sufficiently. We use a threshold on the average colour of the RGB image to determine whether excess material is sufficiently sieved out.

The required intensity and frequency of vibration to effectively sieve a sample are beyond the capabilities of an articulated robot arm. Sieving is viable (Figure 6.37) using the extension rail (Chapter 3) by oscillating the position of the sledge along the rail. An amplitude of 10-25mm is rigorous for sieving out particulate frass, and up to 100 oscillations are done before the larvae become visible. A sieve size of 1.5mm is used for 5-week-old mealworms and 5-day-old BSF larvae. A sieve size of 2.0mm is used for 7 and 9-week-old mealworms and 16-day-old BSF larvae. A smaller sieve is not effective for frass, and a larger one would have the larvae falling through. Figure 6.28 shows the process of sampling performed during the CoRoSect pilot studies. During experimentation, up to 3 repetitions of the sieving process are performed.

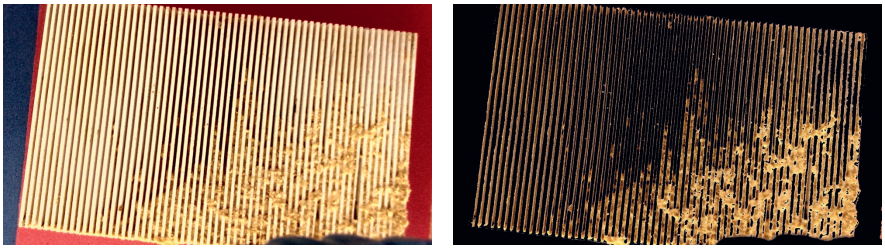


(a)



(b)

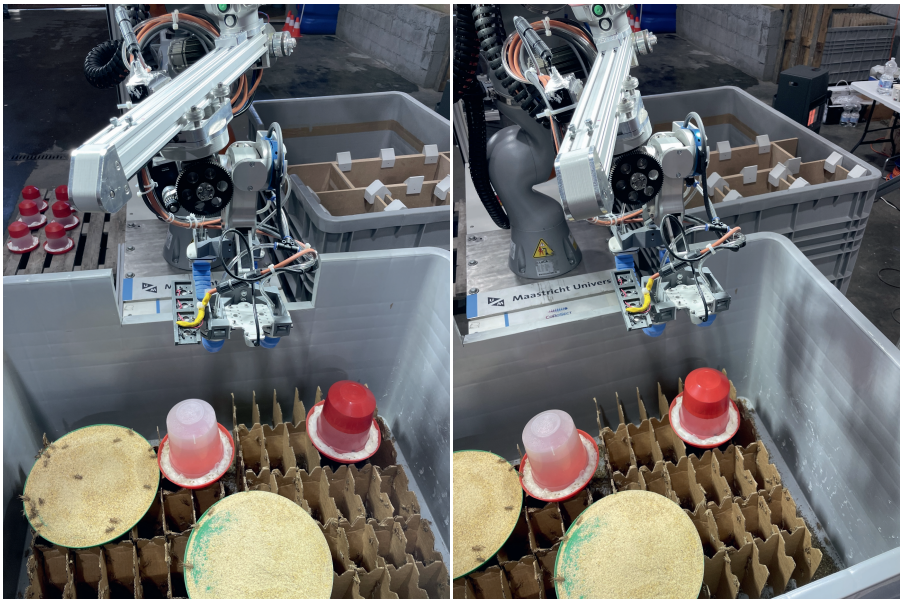
Figure 6.28: (a) The robot after performing motions to scoop a sample from inside a mealworm crate. The sample is shown to the camera mounted at the end of the extension rail in (b).



(a) (b)

Figure 6.29: Visual inspection of BSF oviposition plate. (a) The raw RGB image. (b) The image was filtered to determine the percentage of eggs (yellow).

Finally, the RealSense D435 is used in an auxiliary role to provide visual feedback when other sensors are occluded. Inside BSF mating cages, visual inspection is used to determine whether eggs are present in ovipositioning plates (Figure 6.29). The robot autonomously decides whether a replacement of the plate is necessary (Figure 6.9) based on the coverage of eggs. We perform visual servoing using RealSense to find openings in the cardboard structures to fit the soft fingers of the end effector for a grasp (Figure 6.16b). The limitation of velocity control on our KUKA iiwa configuration forces us to use small increments of position control to emulate visual servoing. Full scans of cricket crates are performed using a linear motion along the crate (Figure 6.30).



(a) (b)

Figure 6.30: Linear motion used to scan the contents of a cricket crate in detail.

6.5 Use Case Results

We use data collected during repetitive testing at the CoRoSect pilot studies to analyse the performance of our robot cell. Performance metrics consist of the robot's success rate and the time taken to complete tasks. We use these metrics to validate both the vision system and the additional capabilities of our robot in ensuring the successful completion of a task sequence. An incorrectly observed obstacle or large element in the workspace incurs a possible collision, causing an emergency stop of the robot and a failure of the task sequence. An incorrectly located material results in a failed grasp and an error in completing the task sequence. Cricket and BSF management use cases demonstrate our strategies for gripping materials and operating in enclosed spaces. Error correction is used

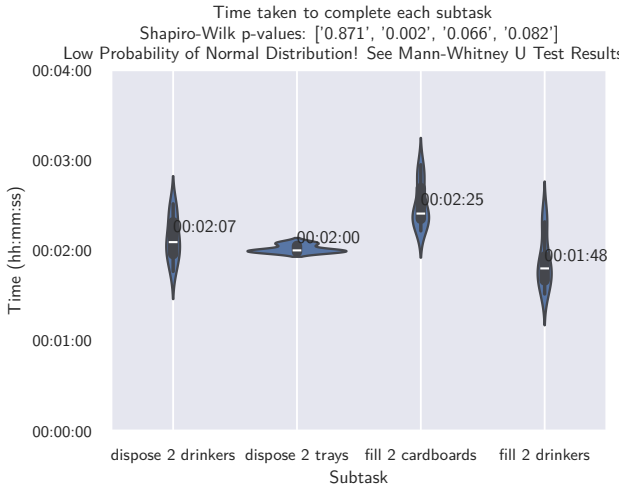
in mealworm oviposition management, as the inlays involved required the most precise placement with little tolerance for offset. Finally, visual inspection for all insect species demonstrates the delicate and versatile capabilities of the robot cell. All use cases are broken down into generalizable subtasks for analysis.

Success rates are measured in repeated runs for each use case. The repeated runs feature a cutoff point after which the system is no longer being tested and autonomously repeats tasks. The overall success rate is the percentage of task repetitions the robot autonomously completed. This is further broken down into a '**completion**' rate that measures when the robot completes a task despite errors (for example, using error correction), a '**no-error**' rate that measures when the robot encounters no errors that would case a failure, and a '**no-interference**' rate that measures the successful completion of tasks without the need for small adjustments by the experimenter (caused by factors outside the robots control, such as perturbations in the workspace), hence fully autonomous.

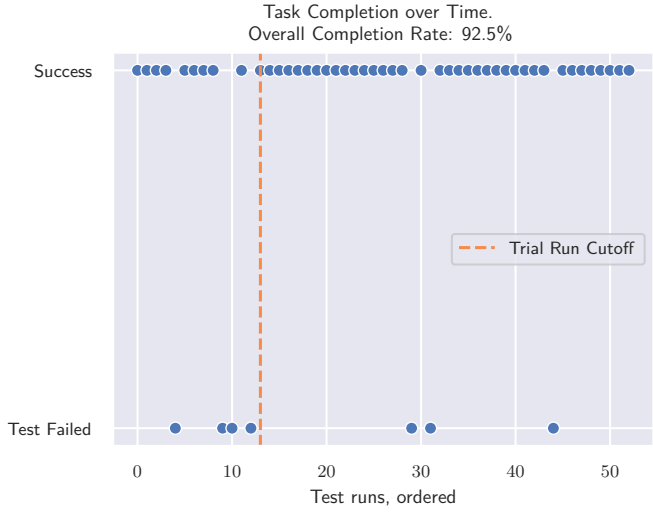
Time is measured at three stages of use case processes: independently for the robot (the M-Robot), for the full robot cell, including de-stacking (the D-Robot), and the entire CoRoSect system, including AGV transportation (Chapter 2). We present KDE plots of the distributions in violin plots. Where relevant, the distributions for certain subtasks are compared to related tasks using a Mann-Whitney U test. The Shapiro-Wilk test is used to determine whether data is drawn from a normal distribution. A t-test or ANOVA is used for normally distributed data. The Bonferroni correction is used to adjust the significance level of repeated tests.

6.5.1 Material Handling and Cricket Harvesting

Material handling for cricket management is broken down into handling of each material involved, namely drinking devices, food trays, and cardboard structures. Repeated testing involved filling



(a)



(b)

Figure 6.31: Time and success rate figures for cricket management. (a) Time taken for cricket management. (b) Success rate over time for the full cycle of cricket management.

an empty crate with two cardboard structures and drinking devices, followed by emptying two food trays and drinking devices in preparation for material replacement. Since each crate is filled with two of each object, the tasks are decomposed into the time taken to fully process each pair (Figure 6.31). The robot cell handles all three materials with a difference of up to 30s in operating time depending on the complexity of gripping the object. Table 6.1 compares the p-values for which subtasks take significantly longer than others, making them stand out as more difficult to handle.

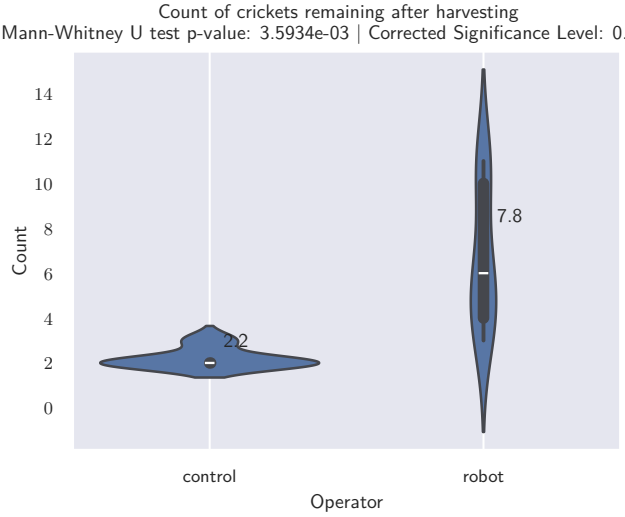
Bonferroni Corrected significance level $\alpha = 0.008$				
	dispose 2 drinkers	dispose 2 food trays	fill 2 cardboards	fill 2 drinkers
dispose 2 drinkers	—	0.287	0.006	0.069
dispose 2 food trays	0.287	—	0.000	0.083
fill 2 cardboards	0.006	0.000	—	0.001
fill 2 drinkers	0.069	0.083	0.001	—

Table 6.1: Mann-Whitney U test p-values. Cricket management.

We tested the harvesting of crickets with live insects. The initial conditions are shown in Figure 6.32a. A control test was done by having an experimenter physically shake and collide the cardboard (as instructed by experts). After the crickets crawled back into the cardboard, the robot replicated the process, first gripping the cardboard. Oscillatory motions with the extension rail were used to drop crickets from the cardboard structure into a crate. The count of crickets remaining in the cardboard after shaking was determined through visual inspection by an experimenter (Figure 6.32b). Although the difference in distributions of remaining crickets is statistically



(a)



(b)

Figure 6.32: Setup and results for cricket harvesting. (a) The setup image and initial conditions were taken for cricket harvesting. (b) The remaining count of crickets within a cardboard structure after harvesting by humans (control) and the robot after one full cycle of cricket harvesting.

significant (Figure 6.32b), compared to the initial conditions (Figure 6.32a), the harvesting process is considered successful.

6.5.2 Mealworm Oviposition Management

Handling of oviposition inlays is broken up into subtasks for repetitive testing. The subtask 'tipping inlay' was done in coordination with the CoRoSect de-stacking robot (Chapter 2). The inlay was first oscillated along the robot extension (Chapter 3) to remove excess material, then inserted into a secondary crate (Figure 6.19) to be tipped into a sorting machine. Inserting an inlay into a crate used force feedback to correct errors. Figure 6.33a shows KDE plots for the distribution of time taken for each subtask after extensive experiments with the force-feedback system.

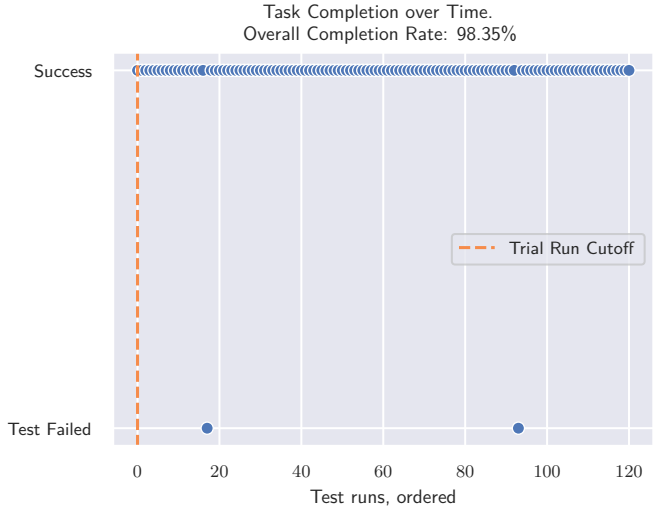
The success rate of repeated iterations of the use case is shown in Figure 6.33b with no initial testing period. Error correction ensured a 98.35% autonomous completion rate. This is further broken down in Table 6.3. The 'no-interference' rate is in this case the percentage of runs repeated fully autonomously without minor adjustments to the inlay orientation when misaligned (Figure 6.24a). Table 6.2 shows the p-values for which subtasks take significantly longer than the others, attributed to their complexity. Table 6.3 shows the breakdown of success rates to show how close the system is to full autonomy.

Bonferroni Corrected significance level $\alpha = 0.017$			
	placing inlay	removing inlay	tipping inlay
placing inlay	—	0.358	0.001
removing inlay	0.358	—	0.000
tipping inlay	0.001	0.000	—

Table 6.2: Mann-Whitney U test p-values. Comparing the time taken to complete the subtasks of Tenebrio Molitor oviposition management.



(a)



(b)

Figure 6.33: Time taken for Tenebrio Molitor oviposition management. (a) Time taken for oviposition management. (b) Success rate over time for the full cycle of oviposition management.

Success Rate Breakdown			
	placing inlay	removing inlay	tipping inlay
Completion	97.92	100.00	96.77
No-Error	97.92	95.83	94.59
No-Interference	89.58	87.50	83.78

Table 6.3: Success rates breakdown. Tenebrio Molitor oviposition management.

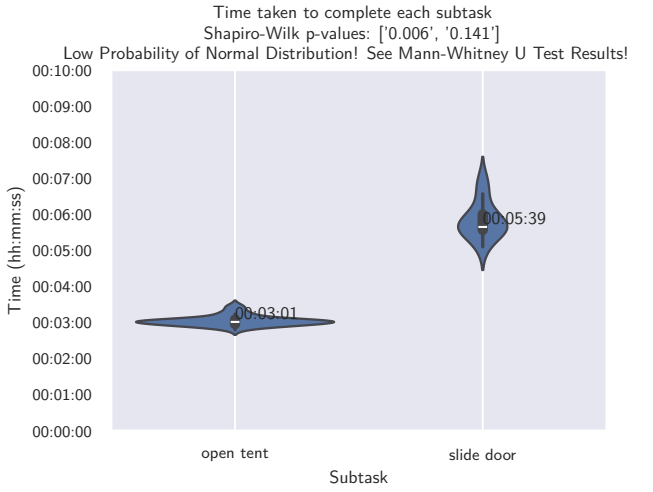
6.5.3 BSF Oviposition Management

Ovipositioning management for BSF is split into operating inside an open mating tent compared to opening the sliding door (Figure 6.21). The distribution of time taken to complete a full pickup and replacement of an oviposition device is shown in Figure 6.34. Opening and closing the door takes significantly more time (Mann-Whitney U test p-value $3.417e^{-7}$).

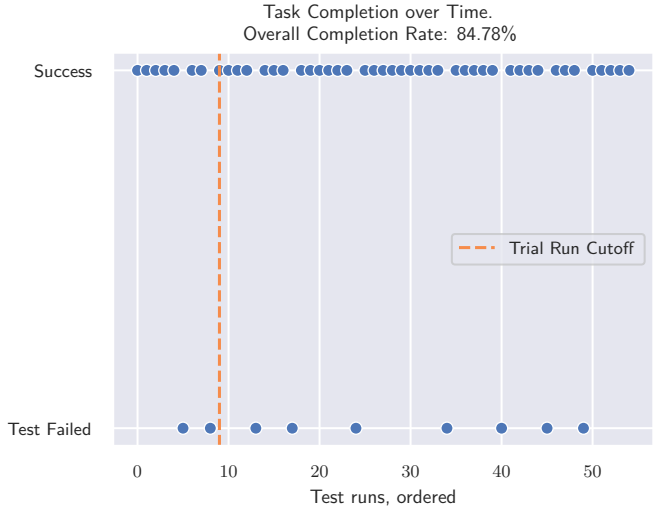
6.5.4 Sampling and Visual Inspection

Figure 6.35 presents the results of visual inspection of crickets based on 7 full repetitions of the entire use case process. The process was timed from the start of all CoRoSect components and is decomposed in Figure 6.35a. Here we show a violin plot for the distribution of time taken to complete the use case. The three plots show the time taken by the robot cell, the time taken including placement of the crate in the workspace, and including crate transport, respectively. A single crate is transported for each use case repetition. Figure 6.35b shows the success rate of the planning and motions of the robot cell, with no test runs.

Quality management for Tenebrio Molitor and BSF involves sampling. The robot cell takes samples in four sampling modalities: surface image, shovelling, sampling without sieving, and sieving (Section 6.2). Figure 6.36a shows the distribution of time taken for each of the sampling

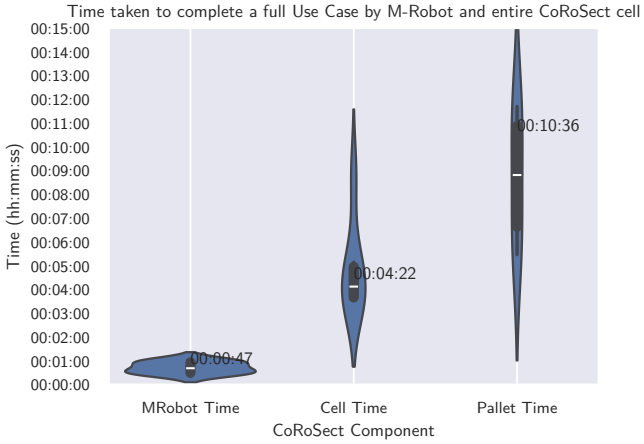


(a)

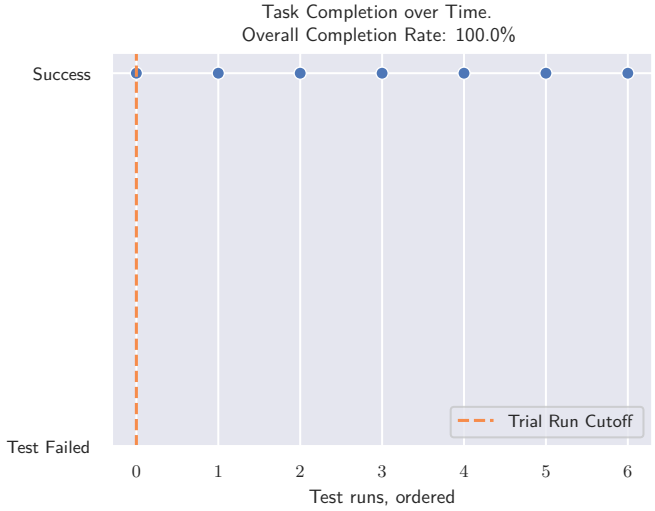


(b)

Figure 6.34: Time taken for oviposition management of BSF. (a) Time taken for oviposition management. (b) Success rate over time for the full cycle of oviposition management.

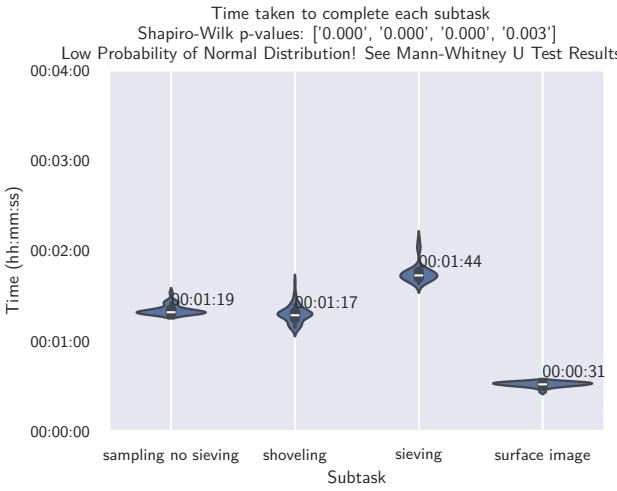


(a)

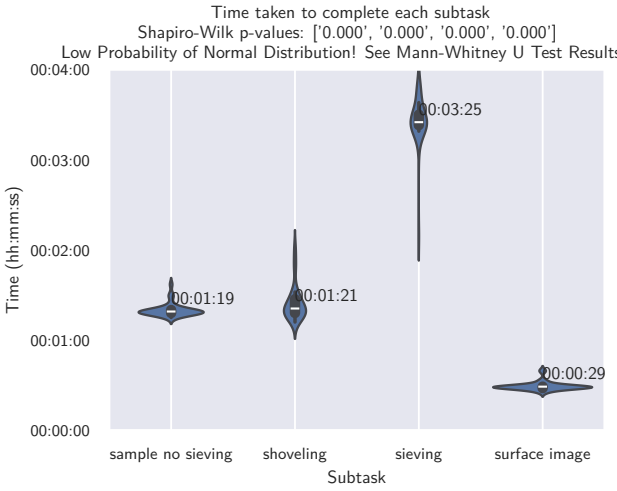


(b)

Figure 6.35: Time and success figures for cricket quality management. (a) Time taken for quality management. (b) Success rate over time for the full cycle of quality management.



(a)



(b)

Figure 6.36: Time figures for sampling mealworm and BSF larvae. (a) Time taken for sampling modalities for mealworm larvae. (b) Time taken for sampling modalities for BSF larvae.

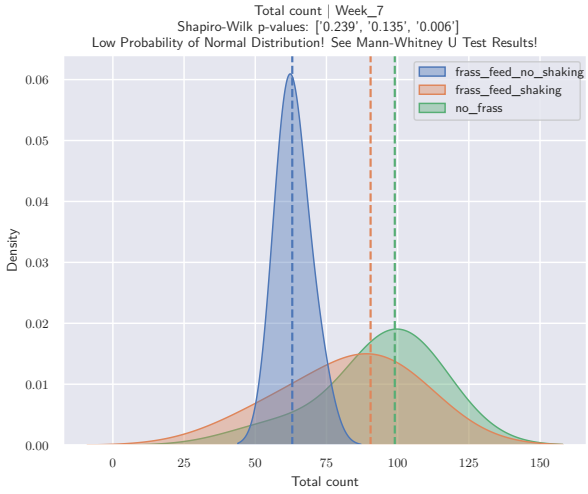
modalities for Tenebrio Molitor. Figure 6.36b does the same for BSF. Figure 6.36 suggests that taking a surface image is significantly the most time-efficient sampling modality (Tables 6.4 and 6.5) with a cycle time median of 31 seconds.

Bonferroni Corrected significance level $\alpha = 0.008$				
	sampling no sieving	shovelling	sieving	surface image
sampling no sieving	—	0.068	$1.045e^{-11}$	$6.396e^{-25}$
shovelling	0.068	—	$1.243e^{-25}$	$7.064e^{-59}$
sieving	$1.045e^{-11}$	$1.243e^{-25}$	—	$4.447e^{-47}$
surface image	$6.396e^{-25}$	$7.064e^{-59}$	$4.447e^{-47}$	—

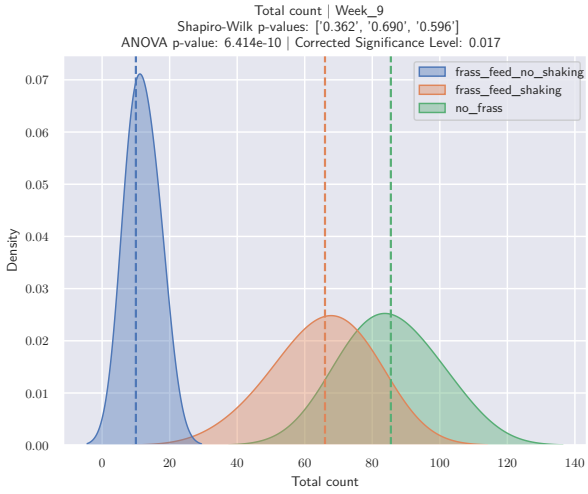
Table 6.4: Mann-Whitney U test p-values. Comparing the time taken when sampling Tenebrio Molitor Larvae under the four different modalities

Bonferroni Corrected significance level $\alpha = 0.008$				
	sampling no sieving	shovelling	sieving	surface image
sampling no sieving	—	0.278	$3.500e^{-32}$	$1.453e^{-26}$
shovelling	0.278	—	$1.436e^{-32}$	$4.125e^{-25}$
sieving	$3.500e^{-32}$	$1.436e^{-32}$	—	$6.144e^{-36}$
surface image	$1.453e^{-26}$	$4.125e^{-25}$	$6.144e^{-36}$	—

Table 6.5: Mann-Whitney U test p-values. Comparing the time taken when sampling BSF Larvae under the four different modalities.



(a)



(b)

Figure 6.37: (a) Count of predicted individuals taken for the control sample for mealworm larvae at week 7. (b) Count of predicted individuals taken for the control sample for mealworm larvae at week 9.

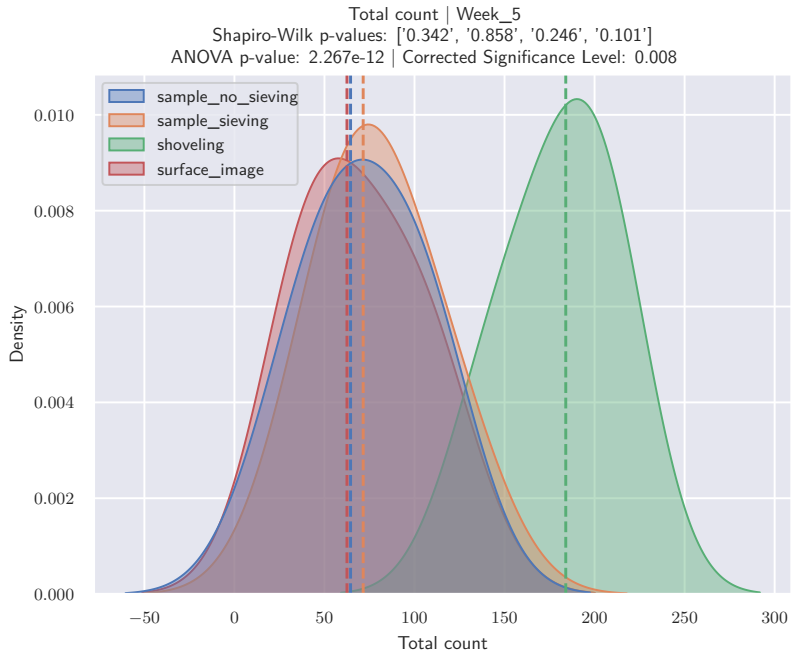
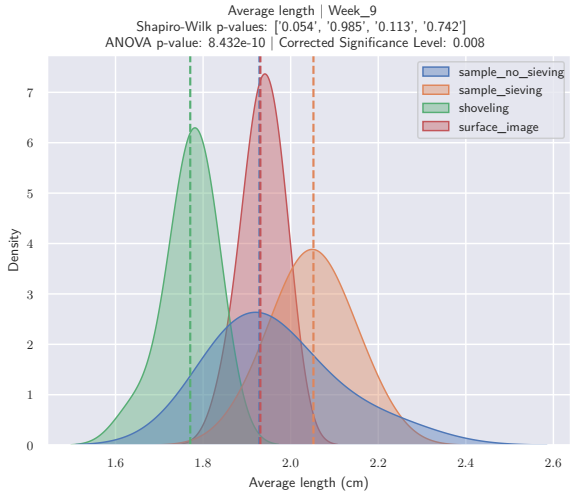


Figure 6.38: VI Larvae Count Week 5 Tenebrio Molitor Real Condition under all sampling modalities.

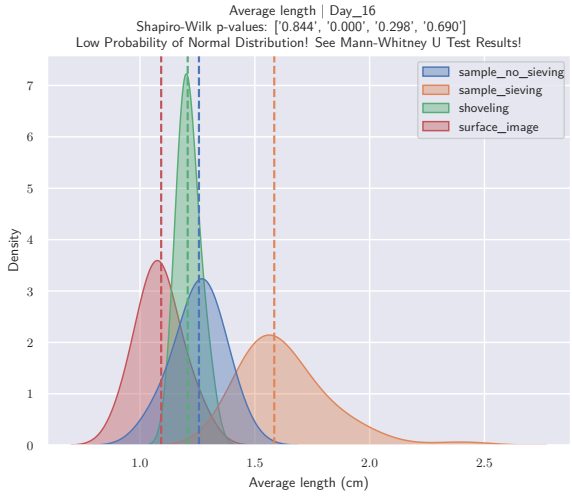
6.5.5 Quality of Visual Inspection

The quality of the visual inspection and the sampling/sieving procedure was further investigated. First, the effectiveness of sieving samples was tested. A control experiment was performed by taking exactly 100 larvae for 3 age groups: 5, 7, and 9 weeks old. An experimenter placed the sample on the scoop held by the robot, which was then shown to the visual inspection camera. This was repeated with additional frass to create occlusion and noise in the image. Finally, the noisy samples were sieved using robot motions to test the effectiveness of removing excess material to get a clearer view of the larvae.

The count of larvae detected is compared with the ground truth (100)



(a)



(b)

Figure 6.39: (a) Count of predicted mealworm larvae under real conditions for all sampling modalities at week 9. (b) Count of predicted BSF larvae under real conditions for all sampling modalities at day 16.

in Figure 6.37. This figure shows the distribution of counts of detected larvae over repetitions of the control experiment. It shows how close the visual inspection system is to count the correct number of larvae under perfect conditions (no frass), when partially obscured by material (frass), and when the additional material is sieved out by the operation of the m-robot (frass, sieving). Figure 6.37 suggests that the process of sieving has a positive effect, as the VI system identifies a count of larvae closer to the ground truth. The distribution of larvae counts that are not sieved is significantly different from the sieved samples (p-value $1.150e^{-7}$) at 9 weeks. The difference in distributions of the unsieved samples (blue) stems from the misidentification of the frass as larvae (Papadopoulos et al., 2024).

Furthermore, the sampling modalities (Figure 6.36) were tested under real conditions of sampling from a filled insect crate. Counting a ground truth is infeasible under real conditions because there is no good way to count or measure that many insects. The distribution of larvae counts is shown in Figure 6.38 for 5-week-old mealworms. Figure 6.39 shows the distributions of lengths of estimated larvae at 9-week-old Tenebrio Molitor and 16-day-old BSF, sampling under real conditions. Each distribution represents one of the four sampling modalities.

6.6 Discussion

In this chapter, we presented a novel pipeline for object localisation based on a highly precise Zivid 3D visual sensor and an industrial-standard surface matching procedure, which we integrated into our robot cell to allow observation of the workspace and represent it virtually in a motion planning environment. This pipeline satisfies our requirements to detect both obstacles in the workspace and find task-relevant materials with enough accuracy to complete use cases. The evidence for this is the rate of successes for all use cases. All use cases were performed in a non-highly-controlled workspace, meaning the detection pipeline was utilised in each repetition. While the

accuracy of the vision system makes grasping consistent, we also gain additional tolerance to offset errors from the design of our end effector, making it difficult to decouple the individual yield in versatility between the two components. However, the compound effect is a robot that can reliably find objects of interest and can consistently grasp materials. A main limitation of the 3D vision system is its inability to quickly re-observe the workspace in a highly dynamic setting. Without outside influence, single observations upon changing states of the workspace are sufficient to complete tasks. However, in a setting with multiple agents (robot or human), the Zivid sensor and surface matching algorithm would not keep up with updating the motion planning environment to prevent collisions with objects in motion. At most, we are able to parallelise the detection of multiple objects at once and update their poses, but this requires a trigger to begin re-observation, for which we currently use the state of the task sequence. Another point of discussion is the need to provide a CAD model of the relevant object for surface matching to find in an observed point cloud. This method requires minimal effort to introduce new materials to the robot, as long as a CAD model is made, but it is not entirely object-agnostic, meaning programming effort is required when use cases change. On the other hand, object localisation methods based on deep learning also require training data for items that they are not already trained on (Cong et al., 2023; W. Gao, 2024; Mei et al., 2025), and a method for consistent grasp synthesis of unknown objects without prior samples is an ongoing field of research (Bohg et al., 2013).

Furthermore, we presented strategies and tools to expand the capabilities of the robot for flexibly handling various materials, correcting errors when picking and placing tightly fitting objects, and exploring approaches to quality management. The diversity of materials involved in insect farming allows us to test both standard and non-standard geometries, some of which require specific approaches or additional feedback (i.e. visual servoing to locate openings in cardboard structures). Cricket management involved handling three

different materials within one use case, which created the potential of multiple points of failure. The success rate in repetitive full runs reaches up to 92.5% (Figure 6.31). However, since this use case was broken up into subtasks, not all combinations of filling and disposing of material were feasibly tested. In Chapter 4, we showed the potential for our end effector to grasp diverse objects. Complemented by the results of the use cases, we demonstrate versatile material handling.

The use case on mealworm oviposition management allows us to test error correction and further demonstrate capabilities in grasping. The force feedback system allows inlays to be consistently placed into crates, stacked, and de-stacked on pallets, with a 98.35% success rate over repetitive trials, although misalignment significantly inflates the time taken (Table 6.2). This is evident by comparing the tasks of removing an inlay with those of placing it. Both tasks consist of the same robot motions (reversed), but the distribution of placing an inlay in Figure 6.33 tends towards a higher mean for those trials that required repeated placement. Due to the tight fit, no trial was completed in one shot without using error correction (although it is theoretically possible), meaning this use case would not have been consistently accomplished without the error correction strategy. This is most likely because the system needed to compute the offset between the held inlay and the target crate at least once to succeed. While we only used error correction in cases where highly precise placement was necessary, the system is more widely applicable. However, this system can further be improved by refining the error detection conditions to involve a profile of how a force is being applied at the TCP instead of relying on the altitude of a held item. While consistent, the determination of when an error occurs can instead be performed visually through cameras or using more detailed heuristics. Our system is, in this case, a working prototype to demonstrate how correcting errors leads to high rates of success in non-highly-controlled workspaces.

6.6.1 Evaluation of Quality Management

We additionally include data gathered from visual inspection use cases to validate the usefulness of the system for quality management. We provide a comparative analysis of the four sampling and inspection strategies to show how each strategy affects the insect parameter estimation described in (Papadopoulos et al., 2024). We use a control experiment to establish a baseline metric for the inspection pipeline and compare it to experiments under real conditions, showing the distribution of larvae counts and parameters (Figure 6.39 shows estimated lengths).

Each distribution is obtained by repeatedly performing each sampling strategy and using the VI models to perform predictions. The differences in the distributions stem from different levels of noise in the image. Sources of noise are most commonly caused by misidentified frass in a surface image or the sampling tool. The close correspondence between distributions of 'no frass' and 'frass feed shaking' (when the sample was filtered by sieving) under control conditions in Figure 6.37 suggests that the sieving process is effective at returning the sample to a noise-free state. Further, when no sieving is performed, seen as the blue distribution labelled 'frass feed no shaking', the distribution is at a clearly different location. This is the result of small bits of grass being misclassified as larvae, leading to a distribution of smaller identified individuals in the sample (Papadopoulos et al., 2024).

Considering the predicted measurements of larvae in Figures 6.39, the lengths of larvae can be compared against the expected growth parameters in the insect farm (Rodjaroen et al., 2020; Tinder et al., 2017). Although the ground truth depends on the internal growth cycles of the insect farm, expected values for ground truth are 2.4cm for mealworms in Figure 6.39a and 1.5cm in Figure 6.39b. From Figure 6.39, it is apparent that sampling with sieving attains the closest mean to the expected ground truth, validating the need for intricate sieving motions with our robot cell. This can be balanced against the sample size from estimated counts and tailored to the quality management

requirements of individual insect farms. In practice, an image taken with a sampling strategy will contain fewer larvae than a surface image of the crate, as there are many more larvae within the crate. However, since these larvae burrow into the frass, shovelling the crate reveals more individuals, hence the distribution for the 'shovelling' sampling modality has a higher mean.

6.6.2 Robot Speedup Analysis

During the initial pilot studies and the majority of testing, the KUKA iiwa was operated in its safest, albeit slowest, mode to build confidence in all the newly developed systems and software. In the intended application, the KUKA iiwa would be set to run at its full speed in automation mode. The operating speed was limited to 24% of the theoretical maximum during the pilot studies and follow-up experiments for safety reasons. This decision led to longer cycle times but ensured the reliability of the full system throughout the pilot studies. When increasing the permissible speed, Figure 6.40 analyses the potential speedup of operating the CoRoSect use cases in an industrial setting.

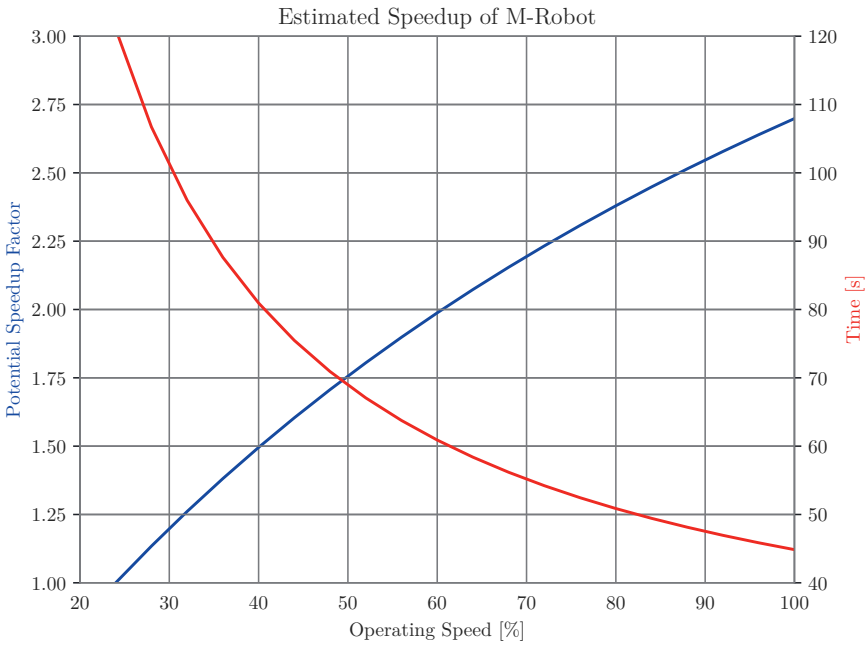


Figure 6.40: The figure presented is based on experimental data collected at the UM Robotics Lab, testing the retrieval of two drinking devices from a cricket-rearing crate. At the baseline level of 24%, the robotic operation takes approximately 120 seconds to complete the task. Increasing the operational speed could potentially improve the cycle time for this task by approximately 2.6 times. Additional improvements can be made by optimising the custom RG6 driver, reducing the Zivid joint motion time, and combining/optimising consecutive trajectories. This speedup would apply to all use cases, meaning cycle times for full automation would be increased by a comparable factor.

6.7 Conclusion

In this chapter, we presented work on developing the cognitive and operational capabilities of the CoRoSect robot cell for versatile manipulation (Chapter 5). We presented further work on incorporating robot vision, error correction, and flexible strategies for material handling. We address the research question of how to achieve versatile manipulation by presenting various use cases with unique requirements that our robot is capable of automating without extensive reconfiguration. We show that we handle grasps on various geometries of materials, as well as deformable objects. We tested motion planning inside enclosures such as cricket crates and BSF mating cages. We demonstrate the versatility of the robot cell to accommodate a variety of insect farming standards and demonstrate that the robot can adapt to different crate depths and orientations across rearing methods.

We provided evidence for the versatility and adaptability of our robot cell by having it operate in real conditions in insect farming use cases. The robot cell is capable of performing a variety of insect and material handling tasks, making it a promising prototype. It is intended for small and medium-sized farms, but is also applicable for large insect farms that are looking for versatile and scalable solutions. The robot cell has been carefully tested at four insect farms handling three different insect species. The robot is not extensively reconfigured for any use case. Each use case provided a unique challenge that we defined in machine-understandable task sequences.

7

Discussion and Conclusions

This chapter serves as a general discussion of the cognitive robot developed throughout this dissertation, outlining high-level insights and achievements in the context of the CoRoSect ecosystem defined in Chapter 2. The significant contributions of each chapter are referenced to address the main research questions. Finally, it contains a general outlook and proposes future work in related fields.

7.1 Capabilities, Versatility, and CoRoSect Use Cases

This section provides the general discussion of the technologies and prototypes that are components of the overall CoRoSect robot cell for quality and insect management. The entire final system was intensively tested during the CoRoSect pilot studies, allowing an evaluation of its capabilities in the context of the CoRoSect ecosystem and cognitive robotics in general. Here, we decompose the system into its individual components, as was done between the thesis chapters, and provide a high-level discussion.

The cognitive robot for insect farming and versatile material handling is one of the core achievements of the CoRoSect framework. The purpose of its development was to provide insight into the role and components of a cognitive robot in a non-deterministic industrial setting, and to contribute to the framework for a digitised insect farm with Industry 4.0 developed by the CoRoSect project (Bauer & Mäkiö, 2023; Larrinaga, 2024). As part of a work cell (Chapter 2), the cognitive robot cell is a self-standing, networked component of the CoRoSect ecosystem that has capabilities in motion planning, perception, and decision-making over the scope of its workspace.

In Chapters 1 and 2, the insect farming use cases were described as a complex test scenario for robotisation. While solutions for logistics and large-scale insect management were identified on the market (Better Insect Solutions, 2025; Ortiz et al., 2016; Viscon Group, 2025), handling the day-to-day insect nursing processes is not uniformly addressed across the industry (Madau et al., 2020; Ortiz et al., 2016). Overall, we consider the cognitive robot cell to have successfully handled multiple configurations of farming three different insect species under separate conditions. While its capabilities have been discussed in the scope of each chapter, in this section, we consider its components against the general requirements, related literature, and research objectives in Chapters 1 and 2.

The design and implementation of the robot cell combines: requirement definitions (Chapter 2), a extension with additional degrees-of-freedom (Chapter 3), an end effector (Chapter 4), structural design and motion planning (Chapter 5), and perception, versatility, and integration into a coherent system that addresses complex real-world challenges (Chapter 6). Each component increases the scope of the robot's capabilities, either mechanically or cognitively, and hence contributes to the completion of tasks.

Robot Extension

In Chapter 3, we presented work in extending the operational range of a KUKA LBR iiwa 14 through a custom-made open-source articulated robot extension. We developed the robot extension for increased reachability and manipulability while maintaining a high number of degrees of freedom for operating within confined spaces. The extension proved successful in enabling a larger operational reach and sufficient degrees of freedom to operate around corners of crates and enclosures (Chapter 3). It addressed a limitation of the reach and lower manipulability envelope of collaborative articulated robots compared to industrial counterparts (Galin & Meshcheryakov, 2019; Pietrantoni et al., 2024; Tziolas, Karapatzak, Kalathas, Karampatea, et al., 2023), which proved necessary for the confined spaces of insect crates and the black soldier fly enclosures.

With the robot extension, we retain the versatility and collaborative features of the KUKA iiwa 14 with a larger reach over the workspace, taking advantage of additional rotational degrees of freedom for operation within enclosures. In comparison, industrial robots offer high manipulability for large-scale automation over an open workspace and a high payload (Kragic et al., 2018; Makulavičius et al., 2023; Sandini et al., 2024). However, particularly large industrial robots will require a highly controlled environment and may be limited by their degrees of freedom or bulk within enclosures. The design of the extension was bounded by Requirement 1, revealing a trade-off between an industrial manipulator and an extended collaborative system. Ultimately, the versatility of the collaborative robot, combined with additional degrees of freedom, was demonstrated to manoeuvre without collisions in the constrained insect farming workspaces, operate within containers and handle some unique, rigorous operations for harvesting. Addressing limitations in reachability was described in the research objectives in Chapter 1, but comes at the cost of an already constrained payload capacity of collaborative robots. Limitations in payload capacity can be addressed by advancements in collaborative robotics (Dmytriyev

et al., 2024; Kragic et al., 2018), but joint torque for a KUKA iiwa 14 is at the upper limit when handling insect farming materials with the mounted extension and end effector.

End Effector for Versatile Material Handling

In Chapter 4, we presented the design and evaluation of a hybrid end effector that extends the capabilities of the RG6 gripper through the integration of modular and soft finger elements. The adjustable opening width of the RG6 allowed dynamic control over the spacing between soft fingers, facilitating a trade-off between a broad gripping range and stable, higher-force grasps. While the soft fingers do not exert as much force as an industrial gripper, they are more suited to handling delicate material in insect farming (Hughes et al., 2016). The handling of small, fragile organisms introduces requirements for fine motor control and gentle manipulation that have not been fully addressed in prior automation efforts (Tai et al., 2016). Placing this contribution within the context of related work, research in agricultural robotics recognises the challenge of variability and unpredictability, as well as the need for soft end effectors, for instance, in fruit harvesting, greenhouse management, and livestock monitoring (Duckett et al., 2018; Schütz et al., 2014). Our design for a soft-rigid hybrid gripper addresses the research objective for a versatile robotic system that handles diverse rigid and soft materials, as well as Requirements 3 and 4 on versatile insect management and insect well-being. The main achievements are the development of a prototype end effector and the exploration of its *resistance* and *dexterity* when performing grasps on various objects.

First, we demonstrated an increased tolerance to errors/offsets in object placement, which is common in a non-highly-controlled workspace. Reaching a high level of precision in the insect farming workspace is challenging because each crate is non-uniformly filled (for example, by a human worker), and we can not assume objects are

placed consistently in the same positions in the workspace. When an offset is introduced in the placement of the object beyond $\approx 25mm$, achieving a successful grasp becomes difficult or fails for the current configuration (depending on the object's geometry). For the overall system, this offset is relative to the gripper TCP, meaning the tolerance applies to errors in the surface-matched pose of objects. Such offsets can occur due to occlusions, transparency, or perturbations in the point cloud, leading to the matching of the target object to a different surface. In cases where the object is detected incorrectly in a different part of the workspace, there is no way for an end effector to account for a high-level error. However, we can show that our end effector is robust to small-scale perturbations, up to an extent of $25 - 50$mm. We can not draw strong conclusions concerning the tolerance to rotational perturbations, except that the end effector is robust and compliant to object geometry and hence can handle diverse orientations. Treating a rotated object as a separate instance, geometrically, suggests that the compliance of the soft fingers provides enough versatility to establish a grasp with limited gripping strength. However, this requires systematic validation. The issue of grasping at offsets and diverse sizes of materials can instead be addressed with a larger industrial gripper, one that provides additional tolerance in object placement by having a larger stroke and is designed for higher payloads (Birglen & Schlicht, 2018; Samadikhoshkho et al., 2019). However, this may not be a practical solution for a collaborative robot with limited payload capacity, such as the KUKA iiwa 14. This option induces additional costs and may no longer fit within the confined spaces occurring in insect farming (for which we already add additional degrees of freedom in Chapter 3). We also consider insect well-being (Requirement 4, Chapter 2), where larger industrial grippers are indelicate compared to smaller, soft counterparts (Hughes et al., 2016; Tai et al., 2016).

The end effector is a proof of concept for the combination of both rigid and soft gripping capabilities into a single gripper, including a modular design for additional elements needed for specific tasks. Traditional industrial grippers are typically specialised designs

for precision and strength, but risk damaging fragile or irregular items (Hughes et al., 2016). At the same time, there is significant research in the development of soft grippers, which offer compliant and gentle handling at the cost of stability and load capacity (Hughes et al., 2016; Tai et al., 2016). Our requirement to provide versatile modalities of gripping is achieved by the hybrid design, but results in no specialisation for high-efficiency material handling. To broaden its utility, we augmented the end effector with modular 3D-printed components capable of safely manipulating hard or abrasive items, such as the mealworm inlays and a sampling tool for quality management. This costs additional payload, but expands on the potential tasks the end effector can be applied to, increasing its versatility as per the research objectives. In experiments and real-world testing, we have demonstrated that the enhanced gripping capabilities gained from soft elements, particularly their compliance to object geometry, increase the dexterity of the end effector. This is a desirable property when considering an industry that deals with diverse and developing materials, per Requirement 3. In practice, most of the gripping is performed by the soft fingers. While the soft elements do not exceed the grasp resistance of the RG6, they provide invariability to object geometry in a non-highly-controlled workspace. We are able to dynamically change the width between them to manipulate the quality of the grasp and achieve success at larger placement errors and misalignments. We also retain the rigid and high grasping force properties of the RG6 if necessary.

Robot Cell Design

The design decisions involved in the support structure and the mounting of the collaborative robot arm are directly motivated by the general requirements for versatility, adaptability, and eventual Human Robot Collaboration (HRC). Structurally, the workspace is designed specifically to match the insect farming use cases, although the sensor setup, electrical components, and the support structure

are generalisable to a work cell that fits in industrial processes (Aghazadeh et al., 2011; Gautam et al., 2017). In environments with collaborative tasks shared between robots and human workers (or between multiple robots (Akella & Hutchinson, 2002; Cai et al., 2007)), or with Autonomous Guided Vehicles (AGVs) handling logistics, the developed robot cell includes necessary amenities, such as the intake/output of materials through pallet bays, overhead cameras, electrical connections, and safety devices. This fits with practical deployment of robotics in industrial settings, such as those described by (Bogue, 2023; Rauch, 2020; Tantawi et al., 2019).

The robot cell can be modularly rearranged, but is suitable for multiple workspace configurations and can handle diverse sequences of operations, with additional sensors and tools at its disposal. This potentially allows an industry to reuse the same robot cell at different stages of internal processes, increasing the added value of the robot cell beyond a single task (Aghazadeh et al., 2011). This is further strengthened by the versatility we add to the system, increasing its scope of capabilities in material handling, perception, and decision-making without the need for re-training or re-programming to match specific use cases. Related literature supports that versatility is an important progression within the Industry 4.0 framework (Galin & Meshcheryakov, 2019; Leng et al., 2022).

Software Architecture

The result of Chapter 5 was the design and development of a software architecture that controls the cognitive robot cell. The software architecture is extendable to include robot vision, AI models, and additional control strategies (that are implemented in Chapter 6). The integration of cognitive capabilities ensures that the robot is usable across a range of insect handling tasks without major reconfiguration or re-programming, and can handle inconsistencies, errors, and changes in the workspace. Moreover, the software architecture defined

the communication between modules, the handling of sensor data, and the execution of high-level task planning in ways that adhered to the requirements established in the use cases. While it is based on common practices in developing industrial robotics software (Ahmad & Babar, 2016; Bertoli et al., 2024), it is tailored to the integration of cognitive decision-making systems and high-level functions in perception and motion planning. The off-the-shelf motion planner (Coleman et al., 2014) is capable of taking into account an extended kinematic chain with additional degrees of freedom, a mounted end effector with carried materials, and obstacles in the workspace. We achieve integration of the core motion planning software, allowing the robot to generate trajectories that account for the environment.

A limitation of the current implementation is the lack of a stop trigger for planned trajectories, meaning that once a trajectory is output, the robot will move along this trajectory to its end. While the motion can be stopped through safety conditions, the trajectory is stored as active until the program is reset. While our experiments have shown that MoveIt! is suitable for dynamic re-planning and versatile motion through an obstructed virtual workspace, the practical implementation of this requires a method to identify stopping conditions autonomously. Stopping such trajectories dynamically with the real robot remains untested without human intervention.

In the context of the research objectives in Chapter 1, the software architecture is a basis for controlling the primitive operations of the robot and a platform for expanding its capabilities with cognitive systems. We tested motion planning inside enclosures such as cricket crates and BSF mating cages, showing success at the cost of operating time to avoid multiple collisions in cluttered workspaces. We demonstrated the versatility of the robot cell to accommodate a variety of insect farming standards and showed that the software architecture does not need to be changed to different insect crates, workspaces, or rearing methods. This aligns with the research objective in creating a versatile robotic system and testing it in real-world conditions and Requirement 3. The robot can complete diverse use cases without

major reconfiguration, able to reach all necessary materials and handle them according to the requirements of the task specifications. The final compound effect of additional software and hardware is an increase in the capabilities of our robot cell over that of the base KUKA iiwa 14.

Perception

In Chapter 6, we presented a novel pipeline for object localisation based on a Zivid 3D visual sensor and an industrial-standard surface matching procedure (Eckstein & Steger, 1999), which we integrated into our robot cell to allow observation of the workspace and represent it virtually in a motion planning environment. A challenge in autonomous motion planning is identifying and quantifying valid target positions. Relevant poses need to either be pre-defined or identified through workspace observation and interpretation, which we address with object localisation. This approach is specific to material handling, and it depends on the accurate localisation of items in a potentially cluttered workspace (Doignon et al., 1994; Sumi et al., 2007). However, this remains highly vulnerable to occlusions and partial information. This is alleviated with additional sensors (Qadeer et al., 2024), but remains an issue for robotic manipulation (Du et al., 2021; Nilsson, 2010).

Vision is a well-researched area in robotics, and is extensively used to provide robots with autonomy in various environments and industries (Bodenhagen et al., 2014; H. Cheng et al., 2022; Kuts et al., 2018). Commonly, approaches use deep learning methods (W. Gao, 2024; Hussain, 2023; Mei et al., 2025) and have been shown to provide accurate detection and localisation of materials. We opted for a geometric approach using surface matching to eliminate the need for re-training and allow the accurate representation of the workspace in the virtual motion planning scene using CAD models of located objects. This also allows the system to use CAD models to fill in

incomplete information in the observed point cloud. Our pipeline satisfies our requirements to autonomously detect both obstacles in the workspace and find task-relevant materials with enough accuracy to complete use cases. Robot vision is essential in enabling cognitive decision-making and motion planning by providing the perceptual input about the state of the workspace (Pretlove & Chen, 1995). In practice, it allowed the robot to locate all relevant materials in CoRoSect use cases and navigate within containers and enclosures. In the scope of the research objectives and the overall challenges in cognitive robotics described in Chapter 1, computer vision is a vital component to handle non-highly-controlled environments (H. Cheng et al., 2022; Du et al., 2021; Kuts et al., 2018). The versatility gained from object localisation depends on the potential to add more object models to the library of known objects, which can easily be done with CAD software. Since the surface matching algorithm will locate materials based on geometric properties of the CAD model, this does not require re-training or re-programming.

However, there are still limitations to this system, partially general challenges with computer vision, but also some capabilities which do not generalise. The vision system remains a sensitive component, vulnerable to environmental variability, noise, and occlusion, which are common in real-world workspaces (Golnabi & Asadpour, 2007; Nilsson, 2010). The Zivid camera system handles varied light conditions, but the point-cloud quality depends on the intrinsic settings. Transparent objects, such as the drinking devices used with crickets, are difficult to identify because their points are underrepresented in point clouds[1]. Additionally, multiple instances of the same items have no precedence in the surface matching procedure, meaning the one with more sampled points will be processed first. For example, in the case of two drinking devices to be removed from a cricket crate, it is irrelevant which is picked first. No use case required ordering identical

[1]The Zivid 2+ system improves on the detection of transparent objects (Zivid, 2023), but this system was not yet available to us at the time of the CoRoSect pilot studies.

materials, which is not accounted for in surface matching. In these situations, where a specific ordering is assigned to identical parts, the system requires additional help to identify the correct object first, for example, by setting regions-of-interest or pre-defined spatial context. From a general perspective, another limitation is the inability to quickly re-observe the workspace in a highly dynamic setting. In a setting with multiple agents (robot or human), the Zivid sensor and surface matching algorithm would not keep up with updating the motion planning environment to prevent collisions with objects in motion. At most, we are able to parallelise the detection of multiple objects at once and update their poses, but this requires a trigger to begin re-observation, for which we currently use the state of the task sequence.

Use Case Deployment

Overall, the use cases were meant to represent challenging tasks that defeat industrial automation due to a lack of consistency, structure, the presence of occlusions and delicate living organisms, and highly dynamic processes. While dedicated solutions to each insect farming setup are available on the market (Better Insect Solutions, 2025; Viscon Group, 2025), CoRoSect proposes a framework proof-of-concept that has been shown to handle the process of three different insect species within four different insect farms. It does this not by introducing standardisation across the industry, but by creating cognitive systems that support existing processes and adapt across workspaces. The unstructured environment served as a stress test, exposing limitations of robotic and industrial technologies: limited reachability and degrees of freedom in enclosed spaces, specialised approaches to gripping introduced to delicate tasks, vulnerability to noise in visual data, incorrect observation/localisation, and the need for frequent low-level decision making. Overcoming such limitations is addressed in various avenues of research in robotics, focused on increasing their versatility in industrial processes (Galin &

Meshcheryakov, 2019; Grau et al., 2020; Mohamed, 2018). In Chapter 6, we provided evidence for the flexibility and adaptability of our robot cell by having it operate in real conditions in insect farming use cases. Each use case provided a unique challenge to test a robotisation solution for insect farming. As the topic of this dissertation, the cognitive robot cell for fine manipulation and insect handling was capable of performing a variety of insect and material handling tasks, making it a promising prototype.

In Chapter 6, we presented further work on incorporating error correction and strategies for material handling. Error correction enables a robot to compensate for unpredictable effects in the workspace, such as deformations (Woodside et al., 2021), delays (Asif & Webb, 2023), or observation errors (Borenstein, 2002; Borenstein & Feng, 1995). Such systems are increasingly implemented in industrial settings to ensure consistent operations (Sandini et al., 2024; Woodside et al., 2021). Our system is, in this case, a proof of concept to demonstrate how correcting errors based on force and visual feedback leads to rates of success in non-highly-controlled workspaces. Cricket management involved handling up to three different materials within one process, which created the potential of multiple points of failure. The use case on mealworm oviposition management allowed us to test error correction and further demonstrate capabilities in grasping. The force feedback system allows inlays to be consistently placed into crates, stacked, and de-stacked on pallets at the cost of time taken to correct errors. Errors resulted from imperfect object localisation or deviations along the trajectory. Finally, operating within a BSF mating cage tested the robot's capabilities in operating in confined spaces, while having to both enter and exit the enclosure without assistance and perform manipulation within. This is made possible by the robot extension, providing an extended envelope of motions within the enclosure, and the use of the RealSense D435, because other workspace sensors were occluded. Overall, the effect of introducing these functionalities increases the scope of tasks our robot cell can be applied to. Complemented by the results of Chapter 4, we

demonstrated versatile material handling.

However, it must be acknowledged that the evaluation did not include a systematic comparison with an equivalent system lacking these cognitive capabilities. Many of the operations that a robot is expected to perform within the insect farm would not have been possible without the extension of the kinematic chain, the soft and rigid hybrid end effector design, the implementation of perception and object localisation, or error correction strategies. Each of the chapters in this thesis presents the relevant components individually to contribute additional capabilities to the overall robot cell. However, the success of the use cases is a compound effect. We presented a proof-of-concept implementation and tools to expand the capabilities of a robot for versatile handling of various materials, correcting errors when picking and placing tightly fitting objects, and exploring approaches to quality management.

In terms of the research objectives defined in Chapter 1, we consider the contribution of testing our cognitive robot cell in a highly unstructured environment to provide insight into the necessary components, their integration into a single system, and the implications for the field of cognitive robotics. From the perspective of the requirements in Chapter 2, the overall cognitive robot cell illustrates how requirements shape the architecture of our robotic system, although the implementation can also be generalised to broader contexts beyond insect farming. The requirements were used to design and evaluate the robot cell, starting from explicit use case definitions and iteratively building towards an integrated solution. This framework demonstrates how cognitive robotics can be systematically applied to dynamic, non-highly-controlled real-world workspaces and what cognitive components are needed for versatility. This contributes to the framework stemming from the CoRoSect project as a whole, supported by related publications (Bauer & Mäkiö, 2023; Papadopoulos et al., 2024). The material handling use cases allowed us to test the fusion of various industrial systems (perception, motion planning, and gripping) to achieve complex tasks with an

articulated robot arm. We were also able to perform an extensive exploration of quality management use cases and compare four different methods for automated sampling of living organisms specific to insect farming.

7.2 Addressing the Research Questions

This section contains concise answers to the research questions defined in Chapter 1, briefly summarising the approaches and developments involved in addressing each one.

Research Question 1

How to quantify and measure the reach of an articulated robot over its workspace for the purpose of testing different robot configurations and extensions?

The first research question stemmed from the limited reach of the KUKA iiwa 14 over the necessary workspace for insect farming use cases. In order to address this limitation, it was first necessary to determine measurements/experiments that quantify the reach of an articulated robot arm, such that this reach could be improved through extension of the kinematic chain. This was done in Chapter 3, where the variables of *reachability* and *manipulability* were introduced based on related literature. *Reachability* measures whether there exists an inverse kinematic solution to a target point in any orientation by a robot configuration, which is defined by a URDF description (Tola & Corke, 2024). *Manipulability* measures the ratio of orientations of the end effector that are reachable at a target point.

With this quantification, a simulation was developed and presented in Chapter 3 to determine the operational envelope of a robot placed within a grid of linearly spaced points, which it tries to reach. Each point in the grid was assigned a reachability and manipulability score based on the ratio of successfully reached orientations. A virtual robot

extension featuring up to three degrees of freedom was attached to the KUKA iiwa 14, to determine the effect a linear extension and additional joints have on the operational envelope of the robot arm. Simulations were performed in both an open workspace to provide a general representation of the reachable workspace and in confined spaces of insect crates to demonstrate additional capabilities gained with respect to the use cases.

Research Question 2

How to achieve an extension for a collaborative robot arm to increase reachability in the workspace and within enclosed spaces?

The second research question constitutes the practical implementation of a robot extension in Chapter 3. To address this research question, a prototype extension was developed, documented, and tested under real conditions within insect farming use cases. The design of the extension was motivated by simulation results included in the chapter.

The robot extension is compatible with industrial and collaborative robot arms. It adds three degrees of freedom: a prismatic joint that extends along a linear rail, providing up to 0.33m reach, and two revolute joints to actuate yaw and pitch of the end effector. The extension is actuated by two sets of motors and is controlled at a low level through proprietary controllers, which are integrated with a KUKA iiwa 14 through ROS. The complete prototype design and demonstration in insect farming use cases were covered in Chapter 3, including simulation results for the theoretical additional capabilities gained. It achieves a 210% increase in the total number of reachable positions in an open workspace and 302% increase in the total number of highly manipulable points compared to a baseline unextended KUKA iiwa 14. Within use cases, the robot extension enabled operation inside enclosed spaces, such as insect crates and mating cages, where the baseline robot arm did not have sufficient degrees of freedom to enter and retain sufficient range of motion to perform manipulation.

Research Question 3

How to achieve a hybrid end effector for the versatile manipulation of both rigid and delicate materials in the insect farming industry?

A core research objective was to develop versatile capabilities in material handling, where a robot arm is able to operate with diverse objects involved in insect farming and retain a delicate approach to insect handling and deformable objects. The gripping capabilities of a robot arm are encapsulated within the design of the end effector, which is addressed by the third research question in Chapter 4. To answer this research question, an end effector was designed using a hybrid approach of both soft and rigid gripping surfaces to increase the scope of objects that fit within the grasping envelope. Versatility was achieved by increasing the robot's capabilities in grasping different geometries of materials as well as equipping it for delicate tasks involving biological organisms.

The end effector consists of a core OnRobot RG6 two-fingered gripper with two pairs of Soft Gripping GorillaFinger SoftActuators mounted. While these constitute the main gripping capabilities, there are additional modular slots for brackets and configurable elements to enable new grasping techniques or mount tools and devices. The opening width of the RG6 dynamically changes the grasping envelope between the soft fingers, allowing it to accommodate larger items beyond the scope of the base gripper. The soft fingers conform to the geometry of held objects, allowing a wide variety of items to be held securely without the need for matching surfaces through grasp synthesis techniques. The compound effect is an increase in the potential materials that can be handled with a single end effector, allowing versatile material handling.

The end effector was evaluated with metrics of grasp *resistance* and *dexterity*. *Resistance* was measured by establishing a grasp on an object and determining the pulling force required for it to be relinquished. *Dexterity* was measured by introducing diverse objects and an offset

to the object's placement in the workspace, determining whether the item could still be held and again measuring the resistance of the established grasp. Chapter 4 includes systematic testing of the hybrid end effector at handling various materials of common geometries and those involved specifically in insect handling. These are compared to a baseline two-fingered gripper. The final effect is an increase in the grasping capabilities beyond that of the base RG6, and successful demonstrations of handling materials involved in insect farming.

Research Question 4

How can control and motion planning for a robot cell be achieved for the purpose of versatile manipulation in the insect farming industry?

Chapter 5 describes the structural design of a robot cell for insect farming, which is then used as a platform to address the fourth research question. The research question of how to achieve control and high-level planning of our robot cell is addressed by presenting a control framework and service-oriented software architecture that centres around a virtual motion planning scene, for which off-the-shelf packages in MoveIt! (Coleman et al., 2014) are used. This software architecture integrates the individual mechanical, electrical, and sensor components into a single system that is controllable from a central high-level task management module, enabling the capabilities of each component to be available to the robot.

To achieve autonomous and versatile manipulation in the insect farming industry, the robot cell embeds capabilities in perception, motion planning, and control strategies, which are facilitated by the software architecture. A virtual motion planning environment is the central module where information about the workspace is gathered and digitally represented, such that the robot's motions can be planned for collision avoidance in the real workspace. The motion planning is evaluated in the context of the insect farming workspace with a series of experiments outlined in Chapter 5. Using ROS, the software architecture facilitates two-way communication between

the robot's embedded systems, allowing the execution of trajectories planned in the virtual planning scene using the real robot cell. A system for defining sequences of operations as task scripts allows the implementation of CoRoSect use cases. The architecture is extendable to include robot vision, AI models, and additional control strategies, which are addressed in Chapter 6.

The robot cell can be modularly rearranged, but is demonstrated in multiple workspace configurations and can handle diverse sequences of operations, with additional sensors and flexible tools at its disposal. This allows an industry to reuse the same robot cell at different stages of internal processes, increasing the added value of the robot cell beyond a single task, demonstrating versatility.

Research Question 5

How to achieve versatile manipulation in a confined environment?

The final research question was addressed in Chapter 6. The research question of how to achieve versatile manipulation involved deploying the cognitive robot into various use cases with unique requirements and workspaces, without requiring reprogramming or extensive reconfiguration. These use cases were defined in Chapter 2, and were first re-framed into sequences of automatable robot operations that become task scripts within the robot's software architecture. Use cases were focused on presenting a single robot configuration with diverse tasks to test its versatility when handling materials involved in rearing three separate insect species and performing sampling of living insects and larvae for quality management.

To achieve versatile manipulation, additional cognitive capabilities in perception and error correction were covered in Chapter 6. A pipeline for object localisation based on a Zivid 3D visual sensor was presented, including an industrial-standard surface matching procedure using Halcon software (Eckstein & Steger, 1999). This system was integrated into the robot cell to allow observation of the workspace and represent

it virtually in a motion planning environment. The challenge in identifying and quantifying valid target positions was addressed with object localisation through surface matching, using CAD models to fill in information in the virtual planning scene. This approach was specific to material handling and depended on the accurate localisation of items in a potentially cluttered workspace. A force feedback system allowed consistent placement of materials, stacking, and de-stacking on pallets, with a 98.35% success rate over repetitive trials. Operating within a BSF mating cage tested the robot's capabilities in operating in confined spaces while performing an extended sequence of tasks. This was made possible by the robot extension and additional mounted sensors, providing an extended envelope of motions within the enclosure despite occlusions. Overall, the effect of introducing these functionalities increases the scope of tasks the robot cell can be applied to, achieving versatility. The robot can complete diverse use cases without major reconfiguration, able to reach all necessary materials and handle them according to the requirements of the task specifications. The final compound effect of additional software and hardware is an increase in the capabilities of the robot cell over that of the base KUKA iiwa 14.

7.3 General Outlook

The field of cognitive robotics is an effort to unify various elements within robotics, namely mechanical design, sensing, control, and artificial intelligence, into systems capable of functioning in complex environments that are inherently difficult to control. In this thesis, we address several of these elements and identify particular limitations that prevent a robot from operating within an unstructured workspace, using the insect farming industry as a case study. This work outlines the structure of a cognitive robot work cell to make it fit into an industrial setting, and underlines the critical components that enable operation within a constrained and non-highly-controlled workspace. Specifically, we address challenges in extending the robot's reach,

handling diverse materials, operating within enclosures, observing the workspace, and in general systems that increase a robot's ability to adjust its behaviour dynamically in response to variability in the workspace or environment. However, the lack of controlled baselines, such as non-cognitive implementations on the same hardware, limits the ability to measure the exact added value of cognitive approaches. Without shared benchmarks within the use cases, it remains difficult to compare systems or generalise insights across studies. Hence, we consider the general implications of the contributions outlined in each chapter.

Mechanical design and degrees of freedom define the robot's physical capabilities, which were found to be limited for a collaborative robot such as the KUKA iiwa 14. Higher degrees of freedom increase manipulability, redundancy, and the ability to approach objects from multiple kinematic configurations, which are essential properties when object shape, pose, and accessibility are uncertain. In the insect farming use cases, completing certain tasks within containers and enclosures would have been out of scope without the additional robot extension, while using a larger robot instead limits the operational space further. The possibility of extending an articulated robot arm, in particular collaborative robots, is generalisable also to other use cases, where operating space is obstructed or limited, for example, in greenhouses or warehouses (Duckett et al., 2018). Although it would be expected that added kinematic complexity imposes heavier demands on real-time planning and state estimation, the motion planning software was capable of handling the extended kinematic chain within an expected time threshold. Although our simulations show that industrial robots retain higher manipulability in an open workspace, an effect also shown in (Kuhlemann et al., 2016), work on extending the KUKA iiwa 14 serves as a proof of concept that extending the reach and manipulability of a collaborative robot arm is a viable approach to handling enclosed and obstructed workspaces. While related work in the field shows marginal benefits of using an increased number of degrees of freedom (Kuhlemann et al., 2016), the

situation where the majority of the robot's joints become obstructed or locked while reaching around and over obstacles implies there is still a need for tailoring the kinematic chain to match the workspace.

The material handling requirements in insect farming are closer to precision manipulation than bulk material transfer, which differentiates it from some related work in agricultural automation, such as those mentioned in (Duckett et al., 2018; Lytridis et al., 2021). The literature on soft grippers shows improved versatility, but also highlights unresolved issues in force control, wear, and sensing integration (W. Ye et al., 2023; Y. Zhang & Lu, 2020; X. Zhou et al., 2015). However, the need for manipulation of both delicate and rigid structures remains an area with challenges. Hybrid and modular end effectors, like the one developed in this work, mitigate the trade-off between grasp strength and versatility to handle diverse objects. Our robot cell's gripper worked across different tasks but requires better fingertip sensing and closed-loop force control to ensure a secure grasp, increase reliability under high throughput, and potentially minimise residual damage. Combining rigid structural elements for load-bearing with soft, compliant fingers yields the ability to handle both fragile biological material and robust items without continual tool changes. Modular interfaces that allow task-specific attachments further extend this capability, enabling the same manipulator to support a wider set of behaviours with minimal downtime. This trend of end effector research leads towards a universal gripper that is applicable for a wide range of tasks (Liu et al., 2018; Reddy & Suresh, 2013), to which we contribute with our gripper design. However, this currently implies a trade-off between versatility and specialised end effectors made for precision and high-throughput in manufacturing and automation, which is difficult to reach with a flexible design (Hughes et al., 2016; Samadikhoshkho et al., 2019; Tai et al., 2016).

Another contribution is the integration of multiple subsystems into a coherent framework. Related research has often produced specialised advances in areas such as soft robotics for delicate gripping (Firth et al., 2022; Liu et al., 2018), computer vision for object classification

(H. Cheng et al., 2022; Du et al., 2021), or motion planning under uncertainty (C. Chang et al., 1990; Dadvar et al., 2022). These advances are frequently tested on a specific robotic platform and remain isolated, leaving the problem of cross-integration of separate components ambiguous. The CoRoSect cognitive robot cell addresses this by identifying components that are crucial for practical use, providing a framework, and proposing a software architecture that includes perception, material handling strategies, motion planning, and control/actuation into a single system explicitly guided by the requirements and standards of Industry 4.0. The results suggest that progress in cognitive robotics depends as much on individual technological breakthroughs as on frameworks that systematically coordinate existing advances into effective, deployable systems. The integration of these components is achieved through software architectures that support modularity, scalability, and resilience (Ahmad & Babar, 2016; Bertoli et al., 2024; Coleman et al., 2014). They enable the coordination of perception, planning, and action while correcting errors and managing uncertainty. Taken together, the contributions of this thesis extend beyond insect farming. The robot cell serves as a framework for the necessity of cognitive systems in industries that cannot be controlled through workspace structuring. In terms of research in manipulation and perception, it demonstrates the advantages of versatility and adaptability over specialisation. However, our setup matches the particular needs of use cases as they were identified in Chapter 2, in terms of workspace area, material intake, and insect well-being. Furthermore, although the robot cell is equipped with multiple sensors, safety settings, and collaborative features, it remains untested in human-robot collaboration strategies. Hence, in regard to Chapter 2, we can only assert a proof-of-concept in the design of a collaborative platform that is ready for HRC, supported by related studies in worker training in virtual reality (Katranitsiotis et al., 2024), but can draw no conclusions on the robot's performance with human co-workers in the workspace.

Finally, this dissertation contributes to evidence that cognitive systems

and versatility are necessary layers for operation in unstructured environments. In particular, vital systems of perception and adaptability remain fragile when placed into real-world industrial conditions. Even with high-resolution sensors and pre-processing strategies, occlusion, clutter, and variable lighting remain difficult to overcome. This underscores the need for continued research into active perception robots that can plan their sensing actions as deliberately as their motor actions. Agricultural and industrial robotics in general require perception strategies that are robust to unpredictable occlusions and artefacts, and overcome changes in the environment (Duckett et al., 2018; Kuts et al., 2018; Lytridis et al., 2021). Overall, related literature confirms the potential of hybrid, modular hardware and the necessity of active perception and collision-aware motion planning, while also documenting persistent limitations in manipulability, sensing, handling diverse materials, and system-level robustness. Addressing these limitations, as was done in this thesis, opens the door to practical, versatile cognitive robots that operate reliably in complex domains.

7.4 Future Work

The cognitive robot cell presented in this thesis has highlighted the potential of versatile automation in unstructured environments while also exposing the limitations of current methods. Current results demonstrate functionality, but without common baselines, it is difficult to quantify the added value of integrated systems or compare different approaches. Future work should therefore include the development of standardised benchmarks for comparable delicate manipulation tasks to those found in insect farming. This could include datasets, simulation environments, and common performance measures that make it possible to systematically compare systems, similar to comparisons of collaborative and industrial robots in (Birglen & Schlicht, 2018; Cepolina & Razzoli, 2024; Oliveira et al., 2021; Tziolas, Karapatzak, Kalathas, Karampatea, et al., 2023).

One of the most critical areas for future work is the fragility of perception under real-world conditions. Current vision pipelines and sensor fusion approaches, while sufficient for controlled trials, remain vulnerable to occlusion, clutter, contamination, and variable lighting within our use cases. Future research should prioritise active perception strategies in which sensing is treated as an action, enabling robots to dynamically adapt their viewpoints or employ tactile exploration to reduce uncertainty, such as approaches developed in (H. Cheng et al., 2022; Du et al., 2021).

Another avenue for future work lies in learning and adaptation. This includes constrained reinforcement learning, transfer learning across similar industrial tasks, and meta-learning approaches that reduce dependence on large datasets (J. Chen et al., 2017; K. Wang et al., 2023). Developing frameworks that balance the need for exploration with the fragility of biological material is important in advancing cognitive robotics in this domain.

This also relates to the deployment of Human-Robot Collaboration (HRC) schemes where robots and humans share tasks in production chains. Future work should therefore examine how cognitive capabilities affect safe and efficient collaboration, including intuitive communication channels, shared autonomy frameworks, and adaptive role allocation. The cognitive capabilities of the system, particularly in perception, reasoning, and error correction, can be leveraged to anticipate when human intervention is required and to facilitate seamless handovers.

Furthermore, trust, explainability, and safety are measures that contribute to cognitive robotics employing AI tools and human-robot interaction. Deeper explainability through comprehensible justifications for learnt behaviours or perception errors remains limited. Black-box learning components can still produce failures, and developing explainable cognitive modules that are both efficient and interpretable is an open research problem.

Scalability and economic viability were addressed in design choices (modularity, reuse, and attention to throughput) and provide

preliminary evidence that cognitive robotic approaches can be practical outside of prototyping environments. However, significant work remains in reducing per-unit cost, lowering computational and maintenance overhead, and proving long-term reliability in commercial settings. In summary, advancing the field will require progress in active perception, safe online learning, hybrid end effector design, risk-aware motion planning, resilient software architectures, and benchmarking. Addressing these areas will not only improve the applicability of cognitive robots to insect farming but also strengthen the foundations of cognitive robotics to a broader range of industries.

Bibliography

ABB. (2021). *Gofa™ crb 15000*. Retrieved June 12, 2025, from https://new.abb.com/products/robotics/robots/collaborative-robots/crb-15000

Agarwal, A., Hiot, L. M., Joo, E. M., & Nghia, N. T. (2007). Rectilinear workspace partitioning for parallel coverage using multiple unmanned aerial vehicles. *Advanced Robotics*, *21*(1-2), 105–120.

Aghazadeh, S.-M., Hafeznezami, S., Najjar, L., & Huq, Z. (2011). The influence of work-cells and facility layout on the manufacturing efficiency. *Journal of facilities management*, *9*(3), 213–224.

Ahmad, A., & Babar, M. A. (2016). Software architectures for robotic systems: A systematic mapping study. *Journal of Systems and Software*, *122*, 16–39.

Akella, S., & Hutchinson, S. (2002). Coordinating the motions of multiple robots with specified trajectories. *Proceedings 2002 IEEE International Conference on Robotics and Automation (Cat. No. 02CH37292)*, *1*, 624–631.

Akundi, A., Euresti, D., Luna, S., Ankobiah, W., Lopes, A., & Edinbarough, I. (2022). State of industry 5.0—analysis and identification of current research trends. *Applied System Innovation*, *5*(1), 27.

Alatartsev, S., Stellmacher, S., & Ortmeier, F. (2015). Robotic task sequencing problem: A survey. *Journal of intelligent & robotic systems*, *80*, 279–298.

Alexandratos, N., & Bruinsma, J. (2012). World agriculture towards 2030/2050: The 2012 revision. *Food and Agriculture Organization of the United Nations*.

Alison's Montessori. (2025). *Life cycle of meal worm models*. Retrieved May 26, 2025, from https://www.alisonsmontessori.com/Life_Cycle_Set_Earthworm_p/z33.set.htm?1=1&CartID=0

Almurib, H. A., Al-Qrimli, H. F., & Kumar, N. (2012). A review of application industrial robotic design. *2011 Ninth International Conference on ICT and Knowledge Engineering*, 105–112.

Aly, A., Griffiths, S., & Stramandinoli, F. (2017). Metrics and benchmarks in human-robot interaction: Recent advances in cognitive robotics. *Cognitive Systems Research*, *43*, 313–323.

Amiri, P., Müller, M., Southgate, M., Theodoridis, T., Wei, G., Richards-Brown, M., & Holderbaum, W. (2024). A statistical analysis of commercial articulated industrial robots and cobots. *Journal of Manufacturing and Materials Processing*, *8*(5), 216.

Andersson, S. K. L., Granlund, A., Bruch, J., & Hedelind, M. (2021). Experienced challenges when implementing collaborative robot applications in assembly operations. *International journal of automation technology*, *15*(5), 678–688.

Arents, J., & Greitans, M. (2022). Smart industrial robot control trends, challenges and opportunities within manufacturing. *Applied Sciences*, *12*(2), 937.

Arora, N. K. (2018). Agricultural sustainability and food security. *Environmental Sustainability*, *1*(3), 217–219.

Asif, S., & Webb, P. (2023). Managing delays for realtime error correction and compensation of an industrial robot in an open network. *Machines*, *11*(9), 863.

Asif, S., & Webb, P. (2022). Realtime calibration of an industrial robot. *Applied System Innovation*, *5*(5), 96.

Bakhy, S. H., Hassan, S. S., Nacy, S. M., Dermitzakis, K., & Arieta, A. H. (2013). Contact mechanics for soft robotic fingers: Modeling and experimentation. *Robotica*, *31*(4), 599–609.

Bakhy, S. H. (2014). Modeling of contact pressure distribution and friction limit surfaces for soft fingers in robotic grasping. *Robotica*, *32*(7), 1005–1015.

Banerjee, D., Yu, K., & Aggarwal, G. (2018). Object tracking test automation using a robotic arm. *IEEE Access*, *6*, 56378–56394.

Bauer, D. A., & Mäkiö, J. (2023). A lightweight mes using rami4. 0 on the example of smart insect farms. *IECON 2023-49th Annual Conference of the IEEE Industrial Electronics Society*, 1–8.

Berman, S., & Nof, S. (2011). Collaborative control theory for robotic systems with reconfigurable end effectors. *21st International Conference on Production Research: Innovation in Product and Production, ICPR 2011*.

Bertoli, A., Ferraguti, F., & Fantuzzi, C. (2024). An iot-enabled software architecture for user-friendly fault diagnosis and identification: The welding cobot use case. *2024 7th Iberian Robotics Conference (ROBOT)*, 1–6.

Better Insect Solutions. (2025). *Better insect solutions*. Retrieved June 12, 2025, from https://www.betterinsectsolutions.com/en/

Bhavana, N., Kodabagi, M. M., Kumar, B. M., Ajay, P., Muthukumaran, N., & Ahilan, A. (2024). Pot-yolo: Real-time road potholes detection using edge segmentation based yolo v8 network. *IEEE Sensors Journal*.

Bi, Z., Luo, C., Miao, Z., Zhang, B., Zhang, W., & Wang, L. (2021). Safety assurance mechanisms of collaborative robotic systems in manufacturing. *Robotics and Computer-Integrated Manufacturing*, *67*, 102022. https://doi.org/https://doi.org/10.1016/j.rcim.2020.102022

Birglen, L., & Schlicht, T. (2018). A statistical review of industrial robotic grippers. *Robotics and Computer-Integrated Manufacturing*, *49*, 88–97.

Bloch, H. P. (2009). Ingress protection code explained. *World pumps*, *2009*(11), 26.

Bodenhagen, L., Fugl, A. R., Jordt, A., Willatzen, M., Andersen, K. A., Olsen, M. M., Koch, R., Petersen, H. G., & Krüger, N. (2014). An adaptable robot vision system performing manipulation actions with flexible objects. *IEEE transactions on automation science and engineering*, *11*(3), 749–765.

Bogue, R. (2023). The role of robots in the electronics industry. *Industrial Robot: the international journal of robotics research and application*, *50*(5), 717–721.

Bohg, J., Morales, A., Asfour, T., & Kragic, D. (2013). Data-driven grasp synthesis—a survey. *IEEE Transactions on robotics*, *30*(2), 289–309.

Booth, D. T., & Kiddell, K. (2007). Temperature and the energetics of development in the house cricket (acheta domesticus). *Journal of insect physiology*, *53*(9), 950–953.

Borenstein, J. (2002). Experimental results from internal odometry error correction with the omnimate mobile robot. *IEEE Transactions on Robotics and Automation*, *14*(6), 963–969.

Borenstein, J., & Feng, L. (1995). Correction of systematic odometry errors in mobile robots. *Proceedings 1995 IEEE/RSJ International Conference on Intelligent Robots and Systems. Human Robot Interaction and Cooperative Robots*, *3*, 569–574.

Brahmbhatt, S. (2013). *Practical opencv*. Apress.

Bredenbeck, A., Della Santina, C., & Hamaza, S. (2022). End-effector contact force estimation for aerial manipulators. *The 2022 IEEE/RSJ International Conference on Intelligent Robots and Systems (IROS 2022): IROS 2022*.

Brettel, M., Fischer, F. G., Bendig, D., Weber, A. R., & Wolff, B. (2016). Enablers for self-optimizing production systems in the context of industrie 4.0. *Procedia CIRP*, *41*, 93–98.

Brito, T., Lima, J., Costa, P., Matellán, V., & Braun, J. (2020). Collision avoidance system with obstacles and humans to collaborative robots arms based on rgb-d data. *Robot 2019: Fourth Iberian Robotics Conference: Advances in Robotics, Volume 1*, 331–342.

Brogårdh, T. (2007). Present and future robot control development—an industrial perspective. *Annual Reviews in Control*, *31*(1), 69–79.

Buerkle, A., Eaton, W., Al-Yacoub, A., Zimmer, M., Kinnell, P., Henshaw, M., Coombes, M., Chen, W.-H., & Lohse, N. (2023). Towards industrial robots as a service (iraas): Flexibility, usability, safety and business models. *Robotics and Computer-Integrated Manufacturing*, *81*, 102484.

Bujnarowski, K., Krüger, J., Karca, C., Dahl, L., & Möckel, R. (2025). Extension of industrial and collaborative robots for increased work space and operation in confined spaces. *Annual Conference Towards Autonomous Robotic Systems*, 475–488.

Burget, F., Hornung, A., & Bennewitz, M. (2013). Whole-body motion planning for manipulation of articulated objects. *2013*

IEEE International Conference on Robotics and Automation, 1656–1662.

Caccavale, R., & Finzi, A. (2016). Flexible task execution and attentional regulations in human-robot interaction. *IEEE Transactions on Cognitive and Developmental Systems*, *9*(1), 68–79.

Cai, C., Yang, C., Zhu, Q., & Liang, Y. (2007). Collision avoidance in multi-robot systems. *2007 International Conference on Mechatronics and Automation*, 2795–2800.

Cangelosi, A., & Asada, M. (2022). *Cognitive robotics*. MIT Press.

Cavalieri, S., & Chiacchio, F. (2013). Analysis of opc ua performances. *Computer Standards & Interfaces*, *36*(1), 165–177.

Cepolina, F., & Razzoli, R. (2024). Review of robotic surgery platforms and end effectors. *Journal of Robotic Surgery*, *18*(1), 74.

Chacón, A., Ponsa, P., & Angulo, C. (2021). Usability study through a human-robot collaborative workspace experience. *Designs*, *5*(2), 35.

Chang, C., Chung, M. J., & Bien, Z. (1990). Collision-free motion planning for two articulated robot arms using minimum distance functions. *Robotica*, *8*(2), 137–144.

Chang, H., Boularias, A., & Jain, S. (2024). Insert-one: One-shot robust visual-force servoing for novel object insertion with 6-dof tracking. *2024 IEEE/RSJ International Conference on Intelligent Robots and Systems (IROS)*, 2935–2942.

Chen, J., Ren, H., & Lau, H. Y. (2017). Automate robot reaching task with learning from demonstration. *2017 18th International Conference on Advanced Robotics (ICAR)*, 543–548.

Chen, T., Lin, J., Wu, D., & Wu, H. (2021). Research of calibration method for industrial robot based on error model of position. *Applied Sciences*, *11*(3), 1287.

Cheng, H., Wang, Y., & Meng, M. Q.-H. (2022). A vision-based robot grasping system. *IEEE Sensors Journal*, *22*(10), 9610–9620.

Cheng, P., Jia, J., Ye, Y., & Wu, C. (2021). Modeling of a soft-rigid gripper actuated by a linear-extension soft pneumatic actuator. *Sensors*, *21*(2), 493.

Cheng, R. (2021). *Assuring safety under uncertainty in learning-based control systems* [Doctoral dissertation, California Institute of Technology].

Cho, Y., Woo, S. Y., Song, S. H., Hong, H. G., Yun, H., Oh, J. S., Kim, J., Kim, D. W., Seo, K. H., & Kim, D. H. (2020). A study on modular agricultural robotic platform for upland. *The Journal of Korea Robotics Society*, *15*(2), 124–130.

Choi, J., Cho, Y., Choi, J., & Choi, J. (2014). A layered middleware architecture for automated robot services. *International Journal of Distributed Sensor Networks*, *10*(5), 201063.

Chutima, P. (2023). Assembly line balancing with cobots: An extensive review and critiques. *International Journal of Industrial Engineering Computations*, *14*(4), 785–804.

Claes, D., & Tuyls, K. (2018). Multi robot collision avoidance in a shared workspace. *Autonomous Robots*, *42*(8), 1749–1770.

Coleman, D., Sucan, I., Chitta, S., & Correll, N. (2014). Reducing the barrier to entry of complex robotic software: A moveit! case study. *arXiv preprint arXiv:1404.3785*.

Cong, X., Li, S., Chen, F., Liu, C., & Meng, Y. (2023). A review of yolo object detection algorithms based on deep learning. *Frontiers in Computing and Intelligent Systems*, *4*(2), 17–20.

CoRoSect. (2023). *Fiware summit: Corosect showcasing results to the global ecosystem+*. Retrieved September 22, 2025, from https://corosect.eu/fiware-summit-corosect-showcasing-results-to-the-global-ecosystem/

CoRoSect Deliverable 2.1. (2021). *D2.1 use-cases and user requirements* (tech. rep.). CoRoSect Consortium.

CoRoSect Deliverable 2.2. (2021). *D2.2 technical specifications report of the different species in work environments* (tech. rep.). CoRoSect Consortium.

CoRoSect Deliverable 2.3. (2021). *D2.3 initial system architecture* (tech. rep.). CoRoSect Consortium.

CoRoSect Deliverable 2.4. (2022). *D2.4 advanced system architecture* (tech. rep.). CoRoSect Consortium.

CoRoSect Deliverable 7.3. (2023). *D7.3 robot cell for handling crates* (tech. rep.). CoRoSect Consortium.

CoRoSect Deliverable 7.4. (2023). *D7.4 agv for insect farms* (tech. rep.). CoRoSect Consortium.

Coumans, E., & Bai, Y. (n.d.). Pybullet, a python module for physics simulation for games, robotics and machine learning.

Dabic-Miletic, S. (2024). Benefits and challenges of implementing autonomous technology for sustainable material handling in industrial processes. *J. Ind Intell*, *2*(1), 1–13.

Dadvar, M., Majd, K., Oikonomou, E., Fainekos, G., & Srivastava, S. (2022). Joint communication and motion planning for cobots. *2022 International Conference on Robotics and Automation (ICRA)*, 4771–4777.

D'Avella, S., Avizzano, C. A., & Tripicchio, P. (2023). Ros-industrial based robotic cell for industry 4.0: Eye-in-hand stereo camera and visual servoing for flexible, fast, and accurate picking and hooking in the production line. *Robotics and Computer-Integrated Manufacturing*, *80*, 102453.

Deacon, M. M. (2017). *Alternative methods of material handling within a reconfigurable manufacturing station.* [Doctoral dissertation, Stellenbosch: Stellenbosch University].

Dean-Leon, E., Ramirez-Amaro, K., Bergner, F., Dianov, I., & Cheng, G. (2017). Integration of robotic technologies for rapidly deployable robots. *IEEE Transactions on Industrial Informatics*, *14*(4), 1691–1700.

de Lima, J. S., Pittaluga, M. L., de Menezes Lovatto, N., Veiverberg, C. A., Borille, R., & Lazzari, R. (2021). Mealworm (tenebrio molitor) potencial in fish nutrition: A review. *Research, Society and Development*, *10*(16), e269101623229–e269101623229.

Devalla, V., Singh, R., Mondal, A. K., & Kaundal, V. (2012). Design and development of object recognition and sorting robot for material handling in packaging and logistic industries. *International Journal of Science and Advanced Technology*, *2*(9).

Dmytriyev, Y., Carnevale, M., & Giberti, H. (2024). Enhancing flexibility and safety: Collaborative robotics for material handling in end-of-line industrial operations. *Procedia Computer Science*, *232*, 2588–2597.

Doignon, C., Abba, G., & Ostertag, E. (1994). Recognition and localization of solid objects by a monocular vision system for robotic tasks. *Proceedings of IEEE/RSJ International Conference on Intelligent Robots and Systems (IROS'94)*, *3*, 2007–2014.

Dong, L., He, Z., Song, C., & Sun, C. (2023). A review of mobile robot motion planning methods: From classical motion planning workflows to reinforcement learning-based architectures. *Journal of Systems Engineering and Electronics*, *34*(2), 439–459.

Dorna-Robotics. (2023). *Types of robot grippers and their applications*. Retrieved April 10, 2025, from https://dorna.ai/blog/types-of-grippers-for-robots/

Drnevich, J. M. (2003). Number of mating males and mating interval affect last-male sperm precedence in tenebrio molitor l. *Animal Behaviour*, *66*(2), 349–357.

Du, G., Wang, K., Lian, S., & Zhao, K. (2021). Vision-based robotic grasping from object localization, object pose estimation to grasp estimation for parallel grippers: A review. *Artificial Intelligence Review*, *54*(3), 1677–1734.

Duckett, T., Pearson, S., Blackmore, S., Grieve, B., Chen, W.-H., Cielniak, G., Cleaversmith, J., Dai, J., Davis, S., Fox, C., et al. (2018). Agricultural robotics: The future of robotic agriculture. *arXiv preprint arXiv:1806.06762*.

Dusadeerungsikul, P. O., & Nof, S. Y. (2019). A collaborative control protocol for agricultural robot routing with online adaptation. *Computers & Industrial Engineering*, *135*, 456–466.

Eckstein, W., & Steger, C. (1999). The halcon vision system: An example for flexible software architecture. *Proceedings of 3rd Japanese Conference on Practical Applications of Real-Time Image Processing*, 18–23.

Edwards, S., & Lewis, C. (2012). Ros-industrial: Applying the robot operating system (ros) to industrial applications. *IEEE Int. Conference on Robotics and Automation, ECHORD Workshop*.

El Zaatari, S., Marei, M., Li, W., & Usman, Z. (2019). Cobot programming for collaborative industrial tasks: An overview. *Robotics and Autonomous Systems*, *116*, 162–180.

Elfes, A. (1989). Using occupancy grids for mobile robot perception and navigation. *Computer*, *22*(6), 46–57.

Engemann, H., Du, S., Kallweit, S., Cönen, P., & Dawar, H. (2020). Omnivil—an autonomous mobile manipulator for flexible production. *Sensors*, *20*(24), 7249.

Falco, J., Hemphill, D., Kimble, K., Messina, E., Norton, A., Ropelato, R., & Yanco, H. (2020). Benchmarking protocols for evaluating grasp strength, grasp cycle time, finger strength, and finger repeatability of robot end-effectors. *IEEE robotics and automation letters*, *5*(2), 644–651.

FANUC. (2024). *Collaborative robots crx-10ia*. Retrieved June 12, 2025, from https://www.fanuc.eu/be/nl/robots/robot-filter-pagina/collaborative-robots

Farag, M., Abd Ghafar, A. N., & Alsibai, M. H. (2019). Grasping and positioning tasks for selective compliant articulated robotic arm using object detection and localization: Preliminary results. *2019 6th international conference on electrical and electronics engineering (ICEEE)*, 284–288.

Feng, Q. (2021). End-effector technologies. *Fundamentals of agricultural and field robotics*, 191–212.

Firth, C., Dunn, K., Haeusler, M. H., & Sun, Y. (2022). Anthropomorphic soft robotic end-effector for use with collaborative robots in the construction industry. *Automation in Construction*, *138*, 104218.

Foidl, H., & Felderer, M. (2015). Research challenges of industry 4.0 for quality management. *International conference on enterprise resource planning systems*, 121–137.

Frison, E. (2016). From industrial agriculture to diversified agroecological systems. *Indian Journal of Plant Genetic Resources*, *29*(03), 237–240.

Fruggiero, F., Lambiase, A., Panagou, S., & Sabattini, L. (2020). Cognitive human modeling in collaborative robotics. *Procedia Manufacturing*, *51*, 584–591.

Galin, R., & Meshcheryakov, R. (2019). Automation and robotics in the context of industry 4.0: The shift to collaborative robots. *IOP Conference Series: Materials Science and Engineering*, *537*(3), 032073.

Gao, W. (2024). Yolo-based gripping method for industrial robots. *International Journal of Computer Applications in Technology*, *75*(1), 48–57.

Gao, X., Yuan, L., Shu, T., Lu, H., & Zhu, S.-C. (2022). Show me what you can do: Capability calibration on reachable workspace for human-robot collaboration. *IEEE Robotics and Automation Letters*, *7*(2), 2644–2651. https://doi.org/10.1109/LRA.2022.3144779

Gautam, A., Ram, S. A., Shekhawat, V. S., & Mohan, S. (2017). Balanced partitioning of workspace for efficient multi-robot coordination. *2017 IEEE International Conference on Robotics and Biomimetics (ROBIO)*, 104–109.

Gerget, O., Kravchenko, A., Meshcheryakov, R., Lysunets, T., Galin, R., Volf, D., & Mamchenko, M. (2022). Software library for kuka iiwa robot to improve the efficiency of human-robot interaction in robotic medical applications. *International Conference on Interactive Collaborative Robotics*, 284–295.

Ghaly, A. E., & Alkoaik, F. (2009). The yellow mealworm as a novel source of protein. *American Journal of Agricultural and Biological Science*.

Ghobakhloo, M. (2020). Industry 4.0, digitization, and opportunities for sustainability. *Journal of cleaner production*, *252*, 119869.

Giusti, A., Zeestraten, M. J., Icer, E., Pereira, A., Caldwell, D. G., Calinon, S., & Althoff, M. (2018). Flexible automation driven

by demonstration: Leveraging strategies that simplify robotics. *IEEE Robotics & Automation Magazine*, *25*(2), 18–27.

Golnabi, H., & Asadpour, A. (2007). Design and application of industrial machine vision systems. *Robotics and Computer-Integrated Manufacturing*, *23*(6), 630–637.

Görner, M., Haschke, R., Ritter, H., & Zhang, J. (2019). Moveit! task constructor for task-level motion planning. *2019 International Conference on Robotics and Automation (ICRA)*, 190–196.

Grau, A., Indri, M., Bello, L. L., & Sauter, T. (2020). Robots in industry: The past, present, and future of a growing collaboration with humans. *IEEE Industrial Electronics Magazine*, *15*(1), 50–61.

Haddadin, S., De Luca, A., & Albu-Schäffer, A. (2017). Robot collisions: A survey on detection, isolation, and identification. *IEEE Transactions on Robotics*, *33*(6), 1292–1312.

Haibin, Y., Cheng, K., Junfeng, L., & Guilin, Y. (2018). Modeling of grasping force for a soft robotic gripper with variable stiffness. *Mechanism and Machine Theory*, *128*, 254–274.

Hankel, M., & Rexroth, B. (2015). The reference architectural model industrie 4.0 (rami 4.0). *Zvei*, *2*(2), 4–9.

Hennersperger, C., Fuerst, B., Virga, S., Zettinig, O., Frisch, B., Neff, T., & Navab, N. (2017). Towards mri-based autonomous robotic us acquisitions: A first feasibility study. *IEEE transactions on medical imaging*, *36*(2), 538–548.

Hentout, A., Aouache, M., Maoudj, A., & Akli, I. (2019). Human–robot interaction in industrial collaborative robotics: A literature review of the decade 2008–2017. *Advanced Robotics*, *33*(15-16), 764–799.

Hu, Y., Zhao, W., & Wang, L. (2009). Vision-based target tracking and collision avoidance for two autonomous robotic fish. *IEEE Transactions on Industrial Electronics*, *56*(5), 1401–1410.

Hughes, J., Culha, U., Giardina, F., Guenther, F., Rosendo, A., & Iida, F. (2016). Soft manipulators and grippers: A review. *Frontiers in Robotics and AI*, *3*, 69.

Hussain, M. (2023). Yolo-v1 to yolo-v8, the rise of yolo and its complementary nature toward digital manufacturing and industrial defect detection. *Machines*, *11*(7), 677.

Iqbal, J., Islam, R. U., Abbas, S. Z., Khan, A. A., & Ajwad, S. A. (2016). Automating industrial tasks through mechatronic systems-a review of robotics in industrial perspective. *Technical Gazette/Tehnički Vjesnik*, *23*(3).

Javaid, M., Haleem, A., Singh, R. P., & Suman, R. (2021). Substantial capabilities of robotics in enhancing industry 4.0 implementation. *Cognitive Robotics*, *1*, 58–75.

Kagermann, H. (2014). Change through digitization—value creation in the age of industry 4.0. In *Management of permanent change* (pp. 23–45). Springer.

Kalaitzakis, M., Cain, B., Carroll, S., Ambrosi, A., Whitehead, C., & Vitzilaios, N. (2021). Fiducial markers for pose estimation: Overview, applications and experimental comparison of the artag, apriltag, aruco and stag markers. *Journal of Intelligent & Robotic Systems*, *101*, 1–26.

Kam, H. R., Lee, S.-H., Park, T., & Kim, C.-H. (2015). Rviz: A toolkit for real domain data visualization. *Telecommunication Systems*, *60*, 337–345.

Katranitsiotis, P., Zaparas, P., Stavridis, K., & Daras, P. (2024). Leveraging vr and force-haptic feedback for an effective training with robots. *ICPRAM*, 651–660.

Kim, J.-H., Kim, N., & Won, C. S. (2023). High-speed drone detection based on yolo-v8. *ICASSP 2023-2023 IEEE International Conference on Acoustics, Speech and Signal Processing (ICASSP)*, 1–2.

Kimbrell, A. (2002). *The fatal harvest reader: The tragedy of industrial agriculture*. Island Press.

Klaassen, M., De Vries, E., & Masen, M. (2019). Friction in the contact between skin and a soft counter material: Effects of hardness and surface finish. *Journal of the mechanical behavior of biomedical materials*, *92*, 137–143.

Ko, W. K., Wu, Y., & Tee, K. P. (2016). Lap: A human-in-the-loop adaptation approach for industrial robots. *Proceedings of the Fourth International Conference on Human Agent Interaction*, 313–319.

Kragic, D., Gustafson, J., Karaoguz, H., Jensfelt, P., & Krug, R. (2018). Interactive, collaborative robots: Challenges and opportunities. *IJCAI*, 18–25.

Kuffner, J. J., & LaValle, S. M. (2000). Rrt-connect: An efficient approach to single-query path planning. *Proceedings 2000 ICRA. Millennium Conference. IEEE International Conference on Robotics and Automation. Symposia Proceedings (Cat. No. 00CH37065)*, *2*, 995–1001.

Kuhlemann, I., Jauer, P., Ernst, F., & Schweikard, A. (2016). Robots with seven degrees of freedom: Is the additional dof worth it? *2016 2nd International Conference on Control, Automation and Robotics (ICCAR)*, 80–84.

KUKA. (2013). *Lbr iiwa*. Retrieved June 12, 2025, from https://www.kuka.com/en-de/products/robot-systems/industrial-robots/lbr-iiwa

KUKA. (2018). *Mobile robots boost productivity*. Retrieved June 11, 2025, from https://www.kuka.com/en-us/company/press/news/2018/03/verkaufsstart-kmr-iiwa

Kumar, P., & Kumar, V. (2023). Exploring the frontier of object detection: A deep dive into yolov8 and the coco dataset. *2023 IEEE International Conference on Computer Vision and Machine Intelligence (CVMI)*, 1–6.

Kuts, V., Otto, T., Tähemaa, T., Bukhari, K., & Pataraia, T. (2018). Adaptive industrial robots using machine vision. *ASME International Mechanical Engineering Congress and Exposition*, *52019*, V002T02A093.

Larrinaga, F. (2024). Bridging the gap between ids and industry 4.0–lessons learned and recommendations for the future.

Legner, C. M., Tylka, G. L., & Pandey, S. (2021). Robotic agricultural instrument for automated extraction of nematode cysts and eggs

from soil to improve integrated pest management. *Scientific reports*, *11*(1), 3212.

Leitner, S.-H., & Mahnke, W. (2006). Opc ua–service-oriented architecture for industrial applications.

Leng, J., Sha, W., Wang, B., Zheng, P., Zhuang, C., Liu, Q., Wuest, T., Mourtzis, D., & Wang, L. (2022). Industry 5.0: Prospect and retrospect. *Journal of Manufacturing Systems*, *65*, 279–295.

Levesque, H., & Lakemeyer, G. (2008). Cognitive robotics. *Foundations of artificial intelligence*, *3*, 869–886.

Li, B., Cui, G., Tian, W., & Liao, W. (2022). Vibration suppression of an industrial robot with agv in drilling applications by configuration optimization. *Applied Mathematical Modelling*, *112*, 614–631.

Li, L., Stasiak, M., Li, L., Xie, B., Fu, Y., Gidzinski, D., Dixon, M., & Liu, H. (2016). Rearing tenebrio molitor in blss: Dietary fiber affects larval growth, development, and respiration characteristics. *Acta Astronautica*, *118*, 130–136.

Li, Z., Li, S., & Luo, X. (2021). An overview of calibration technology of industrial robots. *IEEE/CAA Journal of Automatica Sinica*, *8*(1), 23–36.

Liang, X., Xing, Y., Li, L., Yuan, W., & Wang, G. (2021). An experimental study on the relation between friction force and real contact area. *Scientific Reports*, *11*(1), 20366.

Liu, C.-H., Chen, T.-L., Chiu, C.-H., Hsu, M.-C., Chen, Y., Pai, T.-Y., Peng, W.-G., & Chiang, Y.-P. (2018). Optimal design of a soft robotic gripper for grasping unknown objects. *Soft robotics*, *5*(4), 452–465.

Lyn, J. C., Naikkhwah, W., Aksenov, V., & Rollo, C. D. (2011). Influence of two methods of dietary restriction on life history features and aging of the cricket acheta domesticus. *Age*, *33*, 509–522.

Lytridis, C., Kaburlasos, V. G., Pachidis, T., Manios, M., Vrochidou, E., Kalampokas, T., & Chatzistamatis, S. (2021). An overview of cooperative robotics in agriculture. *Agronomy*, *11*(9), 1818.

Ma, Z., Poo, A.-N., Ang Jr, M. H., Hong, G.-S., & See, H.-H. (2018). Design and control of an end-effector for industrial finishing applications. *Robotics and Computer-Integrated Manufacturing*, *53*, 240–253.

Madau, F. A., Arru, B., Furesi, R., & Pulina, P. (2020). Insect farming for feed and food production from a circular business model perspective. *Sustainability*, *12*(13), 5418.

Makkar, H. P., Tran, G., Heuzé, V., & Ankers, P. (2014). State-of-the-art on use of insects as animal feed. *Animal feed science and technology*, *197*, 1–33.

Makulavičius, M., Petkevičius, S., Rožėnė, J., Dzedzickis, A., & Bučinskas, V. (2023). Industrial robots in mechanical machining: Perspectives and limitations. *Robotics*, *12*(6), 160.

Martinez-Barbera, H., & Herrero-Perez, D. (2010). Development of a flexible agv for flexible manufacturing systems. *Industrial robot: An international journal*, *37*(5), 459–468.

Martínez-Salvador, B., Pérez-Francisco, M., & Del Pobil, A. P. (2003). Collision detection between robot arms and people. *Journal of Intelligent and Robotic Systems*, *38*, 105–119.

Mei, Z., Li, Y., Zhu, R., & Wang, S. (2025). Intelligent fruit localization and grasping method based on yolo vx model and 3d vision. *Agriculture*, *15*(14), 1508.

Michalos, G., Makris, S., Tsarouchi, P., Guasch, T., Kontovrakis, D., & Chryssolouris, G. (2015). Design considerations for safe human-robot collaborative workplaces. *Procedia CIrP*, *37*, 248–253.

Michaux, J., Li, A., Chen, Q., Chen, C., Zhang, B., & Vasudevan, R. (2024). Safe planning for articulated robots using reachability-based obstacle avoidance with spheres. *arXiv preprint arXiv:2402.08857*.

Modrzewski, R., Obraniak, A., Rylski, A., & Siczek, K. (2022). A study on the dynamic behavior of a sieve in an industrial sifter. *Applied Sciences*, *12*(17), 8590.

Mohamed, M. (2018). Challenges and benefits of industry 4.0: An overview. *International Journal of Supply and Operations Management*, *5*(3), 256–265.

Mohammed, A., Schmidt, B., & Wang, L. (2017). Active collision avoidance for human–robot collaboration driven by vision sensors. *International Journal of Computer Integrated Manufacturing*, *30*(9), 970–980.

Mohammed, M., & Al-Ibadi, A. (2024). Types and applications of soft robot arms and end-effectors: A review. *Journal of Robotics Research (JRR)*, *1*(1).

Mokaram, S., Aitken, J. M., Martinez-Hernandez, U., Eimontaite, I., Cameron, D., Rolph, J., Gwilt, I., McAree, O., & Law, J. (2017). A ros-integrated api for the kuka lbr iiwa collaborative robot. *IFAC-PapersOnLine*, *50*(1), 15859–15864.

Morales-Ramos, J., Rojas, M., & Dossey, A. (2018). Age-dependent food utilisation ofacheta domesticus (orthoptera: Gryllidae) in small groups at two temperatures. *Journal of Insects as Food and Feed*, *4*(1), 51–60.

Morita, N. (2021). Chapter 2 - finite element methods. In N. Morita (Ed.), *Finite element programming in nonlinear geomechanics and transient flow* (pp. 17–27). Gulf Professional Publishing. https://doi.org/https://doi.org/10.1016/B978-0-323-91112-2.00004-5

Nagrath, V., Blender, T., Shaik, N., & Schlegel, C. (2022). Industry 4.0 asset administration shell (aas): Interoperable skill-based service-robots. *arXiv preprint arXiv:2208.01273*.

Nayl, T., Mohammed, M. Q., & Muhamed, S. Q. (2017). Obstacles avoidance for an articulated robot using modified smooth path planning. *2017 international conference on computer and applications (ICCA)*, 185–189.

Newbury, R., Cosgun, A., Crowley-Davis, T., Chan, W. P., Drummond, T., & Croft, E. A. (2022). Visualizing robot intent for object handovers with augmented reality. *2022 31st IEEE International Conference on Robot and Human Interactive Communication (RO-MAN)*, 1264–1270.

Newbury, R., Gu, M., Chumbley, L., Mousavian, A., Eppner, C., Leitner, J., Bohg, J., Morales, A., Asfour, T., Kragic, D., et al.

(2023). Deep learning approaches to grasp synthesis: A review. *IEEE Transactions on Robotics*, *39*(5), 3994–4015.

Nilsson, P. (2010). 3d-vision guided robotics for material handling. *ISR 2010 (41st International Symposium on Robotics) and ROBOTIK 2010 (6th German Conference on Robotics)*, 1–7.

Oliveira, L. F., Moreira, A. P., & Silva, M. F. (2021). Advances in agriculture robotics: A state-of-the-art review and challenges ahead. *Robotics*, *10*(2), 52.

OnRobot. (2025). *Rg6 - flexible 2 finger robot gripper with wide stroke*. Retrieved April 10, 2025, from https://onrobot.com/en/products/rg6-gripper

Oonincx, D. G., Van Itterbeeck, J., Heetkamp, M. J., Van Den Brand, H., Van Loon, J. J., & Van Huis, A. (2010). An exploration on greenhouse gas and ammonia production by insect species suitable for animal or human consumption. *PloS one*, *5*(12), e14445.

Ortiz, J. C., Ruiz, A. T., Morales-Ramos, J., Thomas, M., Rojas, M., Tomberlin, J., Yi, L., Han, R., Giroud, L., & Jullien, R. (2016). Insect mass production technologies. In *Insects as sustainable food ingredients* (pp. 153–201). Elsevier.

Pai, D. K. (2002). Strands: Interactive simulation of thin solids using cosserat models. *Computer graphics forum*, *21*(3), 347–352.

Papadopoulos, A.-M., Melissas, P., Kastellos, A., Katranitsiotis, P., Zaparas, P., Stavridis, K., & Daras, P. (2024). Tenebriovision: A fully annotated dataset of tenebrio molitor larvae worms in a controlled environment for accurate small object detection and segmentation. *ICPRAM*, 187–196.

Paral, P., Chatterjee, A., & Rakshit, A. (2019). Optics-based template matching for vision sensor-based shoe detection in human–robot coexisting environments. *IEEE Transactions on Instrumentation and Measurement*, *68*(11), 4276–4284.

Pedersen, M. R., Nalpantidis, L., Andersen, R. S., Schou, C., Bøgh, S., Krüger, V., & Madsen, O. (2016). Robot skills for manufacturing: From concept to industrial deployment. *Robotics and Computer-Integrated Manufacturing*, *37*, 282–291.

Pérez, L., Rodríguez, Í., Rodríguez, N., Usamentiaga, R., & García, D. F. (2016). Robot guidance using machine vision techniques in industrial environments: A comparative review. *Sensors*, *16*(3), 335.

Piab. (2019). *Picobot® vacuum gripper unit*. Retrieved April 15, 2025, from https://www.piab.com/robot-and-cobot-gripping-solutions/cobots-and-robot-grippers/picobot-vacuum-gripper-unit

Pietrantoni, L., Favilla, M., Fraboni, F., Mazzoni, E., Morandini, S., Benvenuti, M., & De Angelis, M. (2024). Integrating collaborative robots in manufacturing, logistics, and agriculture: Expert perspectives on technical, safety, and human factors. *Frontiers in Robotics and AI*, *11*, 1342130.

Pinstrup-Andersen, P. (2009). Food security: Definition and measurement. *Food security*, *1*, 5–7.

Popp, A., Lotze-Campen, H., & Bodirsky, B. (2010). Food consumption, diet shifts and associated non-co2 greenhouse gases from agricultural production. *Global environmental change*, *20*(3), 451–462.

Pretlove, J. R., & Chen, N. (1995). Integration of active vision and intelligent robotics for advanced material handling. *Intelligent Robots and Computer Vision XIV: Algorithms, Techniques, Active Vision, and Materials Handling*, *2588*, 147–158.

Qadeer, N., Shah, J. H., Sharif, M., Dahan, F., Khokhar, F. A., & Ghazal, R. (2024). Multi-camera tracking of mechanically thrown objects for automated in-plant logistics by cognitive robots in industry 4.0. *The Visual Computer*, 1–20.

Qi, Q., & Tao, F. (2018). Digital twin and big data towards smart manufacturing and industry 4.0: 360 degree comparison. *Ieee Access*, *6*, 3585–3593.

Quigley, M., Conley, K., Gerkey, B., Faust, J., Foote, T., Leibs, J., Wheeler, R., & Ng, A. Y. (2009). Ros: An open-source robot operating system. *ICRA workshop on open source software*, *3*(3.2), 5.

Rahman, M. M., Khatun, F., Jahan, I., Devnath, R., & Bhuiyan, M. A.-A. (2024). Cobotics: The evolving roles and prospects of next-generation collaborative robots in industry 5.0. *Journal of Robotics*, *2024*(1), 2918089.

Rahmanian-Shahri, N., & Troch, I. (1995). Collision-avoidance control for redundant articulated robots. *Robotica*, *13*(2), 159–168.

Rauch, E. (2020). Industry 4.0+: The next level of intelligent and self-optimizing factories. In *Design, simulation, manufacturing: The innovation exchange* (pp. 176–186). Springer.

Reddy, P. V. P., & Suresh, V. (2013). A review on importance of universal gripper in industrial robot applications. *Int. J. Mech. Eng. Robot. Res*, *2*(2), 255–264.

Ritchie, H., Samborska, V., & Roser, M. (2024). Urbanization. *Our world in data*.

Robinson, N., Tidd, B., Campbell, D., Kulić, D., & Corke, P. (2023). Robotic vision for human-robot interaction and collaboration: A survey and systematic review. *ACM Transactions on Human-Robot Interaction*, *12*(1), 1–66.

Rodjaroen, S., Thongprajukaew, K., Khongmuang, P., Malawa, S., Tuntikawinwong, K., & Saekhow, S. (2020). Ontogenic development of digestive enzymes in mealworm larvae (tenebrio molitor) and their suitable harvesting time for use as fish feed. *Insects*, *11*(6), 393.

Romiti, E., Malzahn, J., Kashiri, N., Iacobelli, F., Ruzzon, M., Laurenzi, A., Hoffman, E. M., Muratore, L., Margan, A., Baccelliere, L., et al. (2021). Toward a plug-and-work reconfigurable cobot. *IEEE/ASME transactions on mechatronics*, *27*(5), 3219–3231.

Rovida, F., Grossmann, B., & Krüger, V. (2017). Extended behavior trees for quick definition of flexible robotic tasks. *2017 IEEE/RSJ International Conference on Intelligent Robots and Systems (IROS)*, 6793–6800.

Rucker, D. C., & Webster III, R. J. (2011). Statics and dynamics of continuum robots with general tendon routing and external loading. *IEEE Transactions on Robotics*, *27*(6), 1033–1044.

Safeea, M., Bearee, R., & Neto, P. (2018). End-effector precise hand-guiding for collaborative robots. *ROBOT 2017: Third Iberian Robotics Conference: Volume 2*, 595–605.

Saliba, M. A., Vella Zarb, A., & Borg, J. C. (2010). A modular, reconfigurable end effector for the plastics industry. *Assembly Automation*, *30*(2), 147–154.

Sallade, J., & Philpott, M. (1997). Synthetic template methodology for cad directed robot vision. *International Journal of Machine Tools and Manufacture*, *37*(12), 1733–1744.

Samadikhoshkho, Z., Zareinia, K., & Janabi-Sharifi, F. (2019). A brief review on robotic grippers classifications. *2019 IEEE Canadian Conference of Electrical and Computer Engineering (CCECE)*, 1–4.

Sandini, G., Sciutti, A., & Morasso, P. (2024). Collaborative robots with cognitive capabilities for industry 4.0 and beyond. *AI*, *5*(4), 1858–1869.

Schepp, S. R., Thumm, J., Liu, S. B., & Althoff, M. (2022). Sara: A tool for safe human-robot coexistence and collaboration through reachability analysis. *2022 International Conference on Robotics and Automation (ICRA)*, 4312–4317. https://doi.org/10.1109/ICRA46639.2022.9811952

Schoettler, G., Nair, A., Ojea, J. A., Levine, S., & Solowjow, E. (2020). Meta-reinforcement learning for robotic industrial insertion tasks. *2020 IEEE/RSJ International Conference on Intelligent Robots and Systems (IROS)*, 9728–9735.

Schunk. (2025). *Phl 63 long-stroke gripper*. Retrieved April 15, 2025, from https://schunk.com/de/en/gripping-systems/parallel-gripper/phl/c/PGR_6331

Schütz, C., Pfaff, J., Baur, J., Buschmann, T., Ulbrich, H., & Idea, G. (2014). A modular robot system for agricultural applications. *Proceedings International Conference of Agricultural Engineering, Zurich*.

Schwarzer, F., Saha, M., & Latombe, J.-C. (2005). Adaptive dynamic collision checking for single and multiple articulated robots in

complex environments. *IEEE Transactions on Robotics*, *21*(3), 338–353.

Sheppard, D., Newton, G., Thompson, S., Davis, J., Gasho, G., & Bramwell, K. (1998). Using soldier flies as a manure management tool for volume reduction, house fly control and feedstuff production. *Sustainable agriculture research and education, southern region*, 51.

Shimoga, K. B. (1996). Robot grasp synthesis algorithms: A survey. *The International Journal of Robotics Research*, *15*(3), 230–266.

Siemianowska, E., Kosewska, A., Aljewicz, M., Skibniewska, K. A., Polak-Juszczak, L., Jarocki, A., & Jedras, M. (2013). Larvae of mealworm (tenebrio molitor l.) as european novel food. *Agric. Sci.*, *4*, 287–291.

Simionescu, I., Ion, I., & Vladareanu, L. (2008). Mathematical models of grippers. *Proceedings of the 10th WSEAS International Conference on Mathematical and Computational Methods in Science and Engineering, edited by MM Iliescu, RI Munteanu, and J. FraustoSolis, Mathematics and Computers in Science and Engineering, WSEAS, Bucharest, ROMANIA*, 400–403.

Singh, B., Kumar, R., & Singh, V. P. (2022). Reinforcement learning in robotic applications: A comprehensive survey. *Artificial Intelligence Review*, *55*(2), 945–990.

Skender, F., Ali, I., & Selim, A. (2019). A digitalization and industry 4.0. *International Scientific Journal Vision*, *4*(2), 47–62.

Skotheim, Ø., Lind, M., Ystgaard, P., & Fjerdingen, S. A. (2012). A flexible 3d object localization system for industrial part handling. *2012 IEEE/RSJ international conference on intelligent robots and systems*, 3326–3333.

Soft-Gripping. (2024). *The modular design system for flexible gripping.* Retrieved April 15, 2025, from https://www.soft-gripping.shop/en/two-finger-parallel-softgripper.html

Sogari, G., Amato, M., Biasato, I., Chiesa, S., & Gasco, L. (2019). The potential role of insects as feed: A multi-perspective review. *Animals*, *9*(4), 119.

Stürz, Y. R., Affolter, L. M., & Smith, R. S. (2017). Parameter identification of the kuka lbr iiwa robot including constraints on physical feasibility. *IFAC-PapersOnLine*, *50*(1), 6863–6868.

Şucan, I. A., Moll, M., & Kavraki, L. E. (2012). The Open Motion Planning Library [https://ompl.kavrakilab.org]. *IEEE Robotics & Automation Magazine*, *19*(4), 72–82. https://doi.org/10.1109/MRA.2012.2205651

Sumi, Y., Ishiyama, Y., & Tomita, F. (2007). Robot-vision architecture for real-time 6-dof object localization. *Computer Vision and Image Understanding*, *105*(3), 218–230.

Taesi, C., Aggogeri, F., & Pellegrini, N. (2023). Cobot applications—recent advances and challenges. *Robotics*, *12*(3), 79.

Tai, K., El-Sayed, A.-R., Shahriari, M., Biglarbegian, M., & Mahmud, S. (2016). State of the art robotic grippers and applications. *Robotics*, *5*(2), 11.

Tamizi, M. G., Yaghoubi, M., & Najjaran, H. (2023). A review of recent trend in motion planning of industrial robots. *International Journal of Intelligent Robotics and Applications*, *7*(2), 253–274.

Tang, D., Li, F., Jiang, J., Song, S., & Zeng, Y. (2023). A review on end-effectors of robotic grinding. *Recent Patents on Engineering*, *17*(1), 85–101.

Tantawi, K. H., Sokolov, A., & Tantawi, O. (2019). Advances in industrial robotics: From industry 3.0 automation to industry 4.0 collaboration. *2019 4th Technology Innovation Management and Engineering Science International Conference (TIMES-iCON)*, 1–4.

Tatiana, D. M. P.-S.-Y., Bar, M. E., & Oscherov, E. (1999). Ciclo de vida de tenebrio molitor (coleoptera, tenebrionidae) en condiciones experimentales. *UNNE*.

Tian, Y., Zhang, Q., Cai, D., Chen, C., Zhang, J., & Duan, W. (2022). Theoretical modelling of soft robotic gripper with bioinspired fibrillar adhesives. *Mechanics of Advanced Materials and Structures*, *29*(15), 2250–2266.

Tinder, A. C., Puckett, R., Turner, N., Cammack, J., & Tomberlin, J. (2017). Bioconversion of sorghum and cowpea by black soldier fly (hermetia illucens (l.)) larvae for alternative protein production. *Journal of Insects as Food and Feed*, *3*(2), 121–130.

Tola, D., & Corke, P. (2023). Understanding urdf: A survey based on user experience. *2023 IEEE 19th International Conference on Automation Science and Engineering (CASE)*, 1–7.

Tola, D., & Corke, P. (2024). Understanding urdf: A dataset and analysis. *IEEE Robotics and Automation Letters*, *9*(5), 4479–4486. https://doi.org/10.1109/LRA.2024.3381482

Trevelyan, J., Hamel, W. R., & Kang, S.-C. (2016). Robotics in hazardous applications. *Springer handbook of robotics*, 1521–1548.

Tsarouchi, P., Michalos, G., Makris, S., & Chryssolouris, G. (2013). Vision system for robotic handling of randomly placed objects. *Procedia CIRP*, *9*, 61–66.

Tsay, T. J., Lai, Y.-F., & Hsiao, Y.-L. (2010). Material handling of a mobile manipulator using an eye-in-hand vision system. *2010 IEEE/RSJ International Conference on Intelligent Robots and Systems*, 4743–4748.

Tziolas, E., Karapatzak, E., Kalathas, I., Karampatea, A., Grigoropoulos, A., Bajoub, A., Pachidis, T., & Kaburlasos, V. G. (2023). Assessing the economic performance of multipurpose collaborative robots toward skillful and sustainable viticultural practices. *Sustainability*, *15*(4), 3866.

Tziolas, E., Karapatzak, E., Kalathas, I., Lytridis, C., Mamalis, S., Koundouras, S., Pachidis, T., & Kaburlasos, V. G. (2023). Comparative assessment of environmental/energy performance under conventional labor and collaborative robot scenarios in greek viticulture. *Sustainability*, *15*(3), 2753.

Universal Robotics. (2018). *Medium-sized, versatile cobot*. Retrieved June 12, 2025, from https://www.universal-robots.com/products/ur10e/

Universal-Robots. (2020). *Types of grippers used in manufacturing / universal robots*. Retrieved April 10, 2025, from

https://www.universal-robots.com/blog/types-of-grippers-used-in-manufacturing/

Varghese, R., & Sambath, M. (2024). Yolov8: A novel object detection algorithm with enhanced performance and robustness. *2024 International Conference on Advances in Data Engineering and Intelligent Computing Systems (ADICS)*, 1–6.

Veiga, G., Pires, J., & Nilsson, K. (2009). Experiments with service-oriented architectures for industrial robotic cells programming. *Robotics and Computer-Integrated Manufacturing*, *25*(4-5), 746–755.

Viscon Group. (2025). *Insect farming technology*. Retrieved June 12, 2025, from https://viscongroup.eu/markets/insects/

Vrochidou, E., Tsakalidou, V. N., Kalathas, I., Gkrimpizis, T., Pachidis, T., & Kaburlasos, V. G. (2022). An overview of end effectors in agricultural robotic harvesting systems. *Agriculture*, *12*(8), 1240.

Vysocky, A., & Novak, P. (2016). Human-robot collaboration in industry. *MM Science Journal*, *9*(2), 903–906.

Wang, K., Zhao, Y., & Sakuma, I. (2023). Learning robotic insertion tasks from human demonstration. *IEEE Robotics and Automation Letters*.

Wang, L., Schmidt, B., & Nee, A. Y. (2013). Vision-guided active collision avoidance for human-robot collaborations. *Manufacturing Letters*, *1*(1), 5–8.

Wang, Y. (2010). Cognitive robots. *IEEE robotics & automation magazine*, *17*(4), 54–62.

Widhiada, W., Nindhia, T., & Budiarsa, N. (2015). Robust control for the motion five fingered robot gripper. *International Journal of Mechanical Engineering and Robotics Research*, *4*(3), 226–232.

Womack, J. P., Jones, D. T., & Roos, D. (2007). *The machine that changed the world: The story of lean production–toyota's secret weapon in the global car wars that is now revolutionizing world industry*. Simon; Schuster.

Woodside, M. R., Fischer, J., Bazzoli, P., Bristow, D. A., & Landers, R. G. (2021). A kinematic error controller for

real-time kinematic error correction of industrial robots. *Procedia Manufacturing*, *53*, 705–715.

Xu, R., & Li, C. (2022). A modular agricultural robotic system (mars) for precision farming: Concept and implementation. *Journal of Field Robotics*, *39*(4), 387–409.

Xu, X., Lu, Y., Vogel-Heuser, B., & Wang, L. (2021). Industry 4.0 and industry 5.0—inception, conception and perception. *Journal of manufacturing systems*, *61*, 530–535.

Ye, W., Zhao, L., Luo, X., Guo, J., & Liu, X. (2023). Perceptual soft end-effectors for future unmanned agriculture. *Sensors*, *23*(18), 7905.

Ye, X., Hong, S. H., Song, W. S., Kim, Y. C., & Zhang, X. (2021). An industry 4.0 asset administration shell-enabled digital solution for robot-based manufacturing systems. *Ieee Access*, *9*, 154448–154459.

Zacharias, F., Borst, C., & Hirzinger, G. (2007). Capturing robot workspace structure: Representing robot capabilities. *2007 IEEE/RSJ International Conference on Intelligent Robots and Systems*, 3229–3236.

Zacharias, F., Borst, C., Wolf, S., & Hirzinger, G. (2013). The capability map: A tool to analyze robot arm workspaces. *International Journal of Humanoid Robotics*, *10*(04), 1350031.

Zechmair, M., & Morel, Y. (2021). Assessing grasp quality using local sensitivity analysis. *2021 IEEE/RSJ International Conference on Intelligent Robots and Systems (IROS)*, 3995–4001.

Zhang, H., Heung, K. H., Naquila, G. J., Hingwe, A., & Deshpande, A. D. (2025). A novel parameter estimation method for pneumatic soft hand control applying logarithmic decrement for pseudo-rigid body modeling. *Advanced Intelligent Systems*, *7*(3), 2400637.

Zhang, Y., & Lu, M. (2020). A review of recent advancements in soft and flexible robots for medical applications. *The International Journal of Medical Robotics and Computer Assisted Surgery*, *16*(3), e2096.

Zhao, H., Huang, Y., Liu, Z., Liu, W., & Zheng, Z. (2021). Applications of discrete element method in the research of agricultural machinery: A review. *Agriculture*, *11*(5), 425.

Zhao, L., Wang, Y., & Huang, S. (2024). Occupancy-slam: Simultaneously optimizing robot poses and continuous occupancy map. *arXiv preprint arXiv:2405.10743*.

Zhong, H., Nof, S. Y., & Berman, S. (2015). Asynchronous cooperation requirement planning with reconfigurable end-effectors. *Robotics and Computer-Integrated Manufacturing*, *34*, 95–104.

Zhou, C., Huang, B., & Fränti, P. (2022). A review of motion planning algorithms for intelligent robots. *Journal of Intelligent Manufacturing*, *33*(2), 387–424.

Zhou, X., Majidi, C., & O'Reilly, O. M. (2015). Soft hands: An analysis of some gripping mechanisms in soft robot design. *International Journal of Solids and Structures*, *64*, 155–165.

Zhu, Z., & Hu, H. (2018). Robot learning from demonstration in robotic assembly: A survey. *Robotics*, *7*(2), 17.

Zivid. (2023). *Zivid omni engine: World's first 3d technology for transparent objects*. Retrieved September 24, 2025, from https://www.zivid.com/zivid-omni-engine-transparency

Impact Paragraph

This section contains a general discussion of the societal and scientific impact of this dissertation. The goal is to highlight the main purpose, important results, the potential contributions towards societal and scientific challenges in its field, and for whom this research may be relevant. Concisely, this thesis aims to contribute to the field of versatile robotics and automation, focusing on hand-in-hand hardware and software development, implementation of cognitive systems, and the integration of systems that increase the capabilities of a robot arm. Increasing the scope of tasks a robot arm can handle is hence defined as an increase in its *versatility*.

The main purpose of this thesis is the design and development of a cognitive robot that combines mechanical design, sensors, and informed planning/decision-making to allow a robot to handle complex tasks safely and effectively. This research brings together different scientific fields, including robotics, artificial intelligence, mechanical design, and computer vision, showing how they work together to create more capable machines. A core theme of this dissertation is to provide insight into the versatility of cognitive robotic systems. This is done by addressing the limitations of a collaborative articulated robot arm to increase its scope and capabilities within non-highly-controlled and unstructured environments. This work is performed within the Horizon 2020 project 'Cognitive Robotics for automated and digitised Insect Farming' (CoRoSect). Insect farming is a complex, real-world use case where a robot's capabilities and limitations are tested. The unstructured environment inside an insect farm provides valuable stress tests for cognitive robotic systems, exposing limitations in: reachability and degrees of freedom for operation in enclosed spaces, delicate gripping tasks with diverse objects and living organisms, vulnerability to noise and occlusions in visual data, and the need for frequent low-level decision making.

The main outcomes and contributions, highlighted in each chapter, are namely: the design and control software of a mechanical robot extension for increased workspace and operation in confined spaces (Chapter 3), a soft-and-rigid hybrid end effector for handling diverse materials (Chapter 4), the structural design of the robot cell and its control software implementation (Chapter 5), and the implementation of cognitive capabilities in perception, object localisation, and error correction strategies (Chapter 6). Additionally, this thesis documents experimentation and successful demonstrations of automating real-world insect farming use cases in material handling and quality management.

The robot is prototypically implemented, tested and has been shown to handle processes of three of the most commonly reared insect species in the EU. The intention of demonstrating the versatility of the cognitive robot has been achieved by covering a variety of unique use cases from three different insect species, namely Tenebrio Molitor (Mealworms), Hermetia Illucens (Black Soldier Flies) and Acheta Domesticus (House Crickets).

Each chapter highlights a significant development in hardware and software that contributes to a versatile platform for handling day-to-day operations in insect nursing and quality management. Specifically, the contributions presented in this dissertation are aimed at addressing challenges to the automation of unstructured, human-centred workspaces, where robots handle material, quality management, and fine manipulation tasks. From a scientific point of view, this work aims to help better understand how robots can be made more intelligent and adaptable. While the requirement analysis and validation of systems are performed in the context of insect farming, the research in this thesis is framed as more generally applicable across other industries. In particular, the software architectures, algorithms, mechanical tools, and cognitive systems presented in this thesis are each aimed at addressing the practical challenges of deploying an autonomous robotic system into an unstructured or potentially collaborative workspace.

In Chapter 3, a robot extension for increased workspace and operation in confined spaces is presented. Despite up to seven rotational degrees of freedom typically offered by commercial collaborative (and industrial) robots, the operational reach is often not sufficient. To overcome these limitations, a custom-made, open-source, affordable robot arm extension to be mounted on commercial or custom-made robots has been developed and presented.

Chapter 4 presents a soft-and-rigid hybrid end effector for versatile material handling. Industrial processes are moving toward greater flexibility, customisation, and human-robot collaboration. Therefore, there is a corresponding need for end effectors that can handle a wider variety of objects with minimal reconfiguration. In this chapter, a custom end effector is developed by extending a rigid gripper with two pairs of soft actuators to increase its flexibility for handling diverse materials of different sizes, geometries, and textures.

In Chapter 5, the structural design of the robot cell is developed, and its control software implementation is presented. This transforms the individual mechanical, electrical, and software components into a coherent work cell that is ready to be placed within an industrial process. The final software architecture is presented as an outcome of practically implementing the robot cell, which connects the motion planning to low-level controllers and high-level task management systems. The overall contribution in this chapter is a framework for the development of a robot cell, consisting of multiple embedded systems.

Chapter 6 presents the implementation of cognitive capabilities in perception, object localisation, and error correction strategies. The base capabilities of a collaborative robot arm to plan collision-free trajectories and grasp diverse materials are not yet enough to operate in a non-highly-controlled workspace, such as in insect farming. This chapter also contains demonstrations of the cognitive robot cell performing real-world insect farming use cases, along with an analysis of its performance and results from the CoRoSect pilot studies. This

research benefits industries by demonstrating how cognitive robotics can make automation more adaptable, efficient, and resilient in real-world conditions.

Furthermore, from a societal perspective, the work is closely linked to the need for sustainable food production and more efficient, human-friendly automation. Insect farming is increasingly seen as a sustainable alternative to traditional protein sources, but the work is labour-intensive and involves handling delicate materials. CoRoSect introduces a solution based on the Reference Architecture Model for Industry 4.0 (RAMI 4.0) to support all phases of the insects' rearing cycle inside insect farms. While part of a wider robotisation solution aimed at the automation of insect rearing in the EU, the robotic system developed in this dissertation aims specifically to handle day-to-day, repetitive operations involved in nursing insects during their life cycles, for example, providing feed and water, performing quality inspection, and delicately handling egg containers, while supporting humans in monitoring and higher-level decision making.

Beyond insect farming, the approaches and technologies developed here can be useful in other sectors that require delicate or adaptable automation, such as agriculture, food processing, healthcare or recycling. The focus on human–robot collaboration and adaptability supports the broader shift in technology development towards systems that are not just efficient, but also sustainable and people-centred. This aligns with current European goals for Industry 5.0, which envisions collaborative, intelligent technologies that work alongside humans and contribute to environmental and social well-being.

This research is relevant to a wide range of stakeholders across both academia and industry. Cognitive robotics is a field of research at the intersection of robotics and artificial intelligence (AI), concerned with equipping robotic systems with mechanisms of cognition, enabling them to perceive their environment, process information, and make context-sensitive decisions. This field of research addresses growing limitations of robotics in automation, as traditional robots are effective

at executing pre-programmed tasks in structured environments, but cannot adapt to change, manage uncertainty, or generalise knowledge across contexts. For researchers in robotics, artificial intelligence, and automation, it provides a practical framework for integrating cognitive capabilities into robotic systems and contributes to ongoing discussions about how perception, reasoning, and adaptability can be realised in physical machines. This work also offers insights into structural design and implementation of versatile robotic architectures that can operate in dynamic and unstructured environments. Industrial stakeholders in agriculture, food production, logistics, and manufacturing may find value in how the developed system demonstrates automation solutions for complex, labour-intensive tasks.

The work presented in this thesis will be disseminated through scientific publications, some of which are already available, and others are still planned at the time of writing this section. This is in addition to the dissemination and documentation performed during the CoRoSect project, including public reports, deliverables, outreach, and related scientific publications. The robot cell has been demonstrated at various opportunities, most prominently during the CoRoSect pilot studies, where the direct stakeholders could be involved.

Summary

Cognitive robotics is a field of research at the intersection of robotics and artificial intelligence (AI). It is a field dedicated to equipping robotic systems with mechanisms of cognition, enabling them to perceive their environment, process information, and make context-sensitive decisions (Aly et al., 2017; Cangelosi & Asada, 2022; Levesque & Lakemeyer, 2008). This field of research addresses growing limitations of robotics in automation, as traditional robots are effective at executing pre-programmed tasks in structured environments, but cannot adapt to change, manage uncertainty, or generalise knowledge across contexts (Qadeer et al., 2024; Y. Wang, 2010). Industrial automation, while highly efficient in stable environments, is inherently brittle: deviations from expected inputs can cause failures (Cangelosi & Asada, 2022; Galin & Meshcheryakov, 2019; Javaid et al., 2021). Traditional automation excels in controlled, repetitive, and highly predictable domains, such as assembly-line manufacturing. However, it struggles in contexts characterised by inconsistency, variability, incomplete information, or the need for interaction with humans (Dmytriyev et al., 2024; Galin & Meshcheryakov, 2019).

This thesis presents the design and implementation of a versatile cognitive robotic work cell developed within the Horizon 2020 project 'Cognitive Robotics for automated and digitised Insect Farming' (CoRoSect). CoRoSect aims to develop a framework for the deployment of networked cognitive robotic systems, where insect farming is a use case to test their capabilities and limitations. The unstructured environment inside an insect farm provides valuable stress tests for cognitive robotic systems, exposing limitations in: reachability and degrees of freedom for versatile manipulation in enclosed spaces, delicate gripping tasks with diverse objects and living organisms, vulnerability to noise and occlusions in visual data affecting observation/object localisation, and the need for frequent low-level

decision making. The need to handle living insects introduces quickly changing conditions, which create unique problems depending on the development stages of different insect species, for example, occlusion due to burrowing larvae, fast growth cycles demanding adapted approaches at each stage, or the need for frequent quality inspection. The goal of this dissertation is to provide insight into the versatility of cognitive robotic systems and address the limitations of a collaborative articulated robot arm, to increase its scope and abilities within non-highly-controlled environments. Specifically, the contributions presented in this dissertation are aimed at addressing challenges to the automation of unstructured, human-centred workspaces, where robots handle material, quality management, and fine manipulation tasks. The main outcomes and contributions, highlighted in each chapter, are namely: the development of a framework for a collaborative cognitive robot for insect farming (Chapter 2), the design and control software of an extension of the kinematic chain for increased workspace and operation in confined spaces (Chapter 3), a soft-and-rigid hybrid end effector for versatile material handling (Chapter 4), the structural design of the robot cell and its control software implementation (Chapter 5), and the implementation of cognitive capabilities in perception, object localisation, and error correction strategies, along with experimentation and successful demonstrations of use cases in material handling and quality management (Chapter 6). The robot is prototypically implemented, tested and validated based on end-user requirements. The versatility of the cognitive robot has been demonstrated by covering a variety of unique use cases from three different insect species, namely Tenebrio Molitor (Mealworms), Hermetia Illucens (Black Soldier Flies) and Acheta Domesticus (House Crickets). The outcomes and technologies are discussed in the context of the CoRoSect framework, which proposes a robotisation solution that has been shown to handle processes of three of the most commonly reared insect species in the EU. The chapters are structured to outline significant components in the development of the cognitive robot cell.

Streszczenie

Robotyka kognitywna jest dziedziną badań na styku robotyki i sztucznej inteligencji (AI), zajmującą się wyposażaniem systemów robotycznych w mechanizmy poznawcze, umożliwiające im postrzeganie otoczenia, przetwarzanie informacji i podejmowanie decyzji zależnych od kontekstu (Aly et al., 2017; Cangelosi & Asada, 2022; Levesque & Lakemeyer, 2008). Dziedzina ta odpowiada na rosnące ograniczenia robotyki w automatyzacji, ponieważ tradycyjne roboty są skuteczne w realizacji zaprogramowanych zadań w środowiskach uporządkowanych, lecz nie potrafią dostosowywać się do zmian, zarządzać niepewnością ani uogólniać wiedzy w różnych kontekstach (Qadeer et al., 2024; Y. Wang, 2010). Automatyzacja przemysłowa, mimo wysokiej wydajności w stabilnych środowiskach, jest z natury niedoskonała: odchylenia od oczekiwanych danych wejściowych mogą powodować awarie (Cangelosi & Asada, 2022; Galin & Meshcheryakov, 2019; Javaid et al., 2021). Tradycyjna automatyzacja sprawdza się w miejscach kontrolowanych, powtarzalnych i wysoce przewidywalnych, takich jak produkcja taśmowa. Jednakże napotyka trudności w środowiskach charakteryzujących się niespójnością, zmiennością, niepełnymi informacjami lub koniecznością interakcji z ludźmi (Dmytriyev et al., 2024; Galin & Meshcheryakov, 2019).

Niniejsza rozprawa przedstawia projekt i implementację wszechstronnej kognitywnej komórki robotycznej, opracowane w ramach projektu Horizon 2020 „Cognitive Robotics for automated and digitised Insect Farming" (CoRoSect). Celem CoRoSect jest opracowanie ram dla wdrażania sieciowych systemów robotów kognitywnych, przy czym hodowla owadów stanowi przypadek testowy dla oceny ich możliwości i ograniczeń. Niestrukturyzowane środowisko wewnątrz fermy owadów zapewnia cenne testy obciążeniowe dla poznawczych, ujawniając ograniczenia w: dostępności i stopniach swobody dla wszechstronnego operowania w zamkniętych przestrzeniach,

delikatnym chwytaniu różnorodnych obiektów i organizmów żywych, podatności na zakłócenia i przesłonięcia w danych wizualnych wpływających na obserwację/lokalizację obiektów, oraz konieczności częstego podejmowania decyzji. Konieczność obsługi żywych owadów wprowadza szybko zmieniające się warunki, które stwarzają unikalne problemy zależne od etapów rozwoju różnych gatunków owadów, na przykład przesłonięcia przez zakopujące się larwy, szybkie cykle wzrostu wymagające dostosowanych podejść na każdym etapie czy konieczność częstych kontroli jakości. Celem tej pracy jest dostarczenie wiedzy na temat wszechstronności systemów kognitywnych oraz rozwiązanie ograniczeń współpracującego ramienia robotycznego w celu zwiększenia jego zakresu i możliwości w środowiskach nie w pełni kontrolowanych. W szczególności przedstawione tu badania mają na celu sprostanie wyzwaniom związanym z automatyzacją nieustrukturyzowanych, zorientowanych na człowieka przestrzeni roboczych, gdzie roboty wykonują zadania związane z obsługą materiałów, zarządzaniem jakością i precyzyjną manipulacją. Główne wyniki i analizy, opisane w poszczególnych rozdziałach, obejmują: zaprojektowanie i oprogramowanie sterujące rozszerzeniem łańcucha kinematycznego w celu zwiększenia obszaru roboczego i pracy w ograniczonych przestrzeniach (Rozdział 3), miękko-sztywny hybrydowy efektor końcowy do wszechstronnej obsługi materiałów (Rozdział 4), projekt strukturalny komórki robotycznej i implementację jej oprogramowania sterującego (Rozdział 5) oraz implementację zdolności kognitywnych w percepcji, lokalizacji obiektów i strategiach korekcji błędów, wraz z eksperymentami i udanymi demonstracjami przypadków użycia w obsłudze materiałów i zarządzaniu jakością (Rozdział 6). Robot został prototypowo wdrożony, przetestowany i jego przydatność potwierdzona na podstawie wymagań użytkowników końcowych. Wszechstronność robota kognitywnego została zademonstrowana poprzez realizację różnych unikalnych przypadków użycia dla trzech gatunków owadów: Tenebrio Molitor (mącznik młynarek), Hermetia Illucens (mucha czarna żołnierska) i Acheta Domesticus (świerszcz domowy). Wyniki i technologie omówiono w kontekście ram CoRoSect, które proponują rozwiązanie robotyzacyjne

zdolne do obsługi procesów trzech najczęściej hodowanych gatunków owadów w UE. Rozdziały zostały uporządkowane tak, aby przedstawiać kluczowe komponenty rozwoju kognitywnej komórki robotycznej.

W Rozdziale 3 przedstawiono rozszerzenie łańcucha kinematycznego w celu zwiększenia obszaru roboczego i pracy w ograniczonych przestrzeniach. Pomimo że komercyjne roboty współpracujące (i przemysłowe) zazwyczaj oferują do siedmiu stopni swobody obrotowej, ich zasięg operacyjny często okazuje się niewystarczający. Uniemożliwia to tym robotom sięganie i pracę w zamkniętych przestrzeniach w sposób autonomiczny lub we współpracy z ludźmi. Aby pokonać te ograniczenia, opracowano i zaprezentowano niestandardowe, open-source'owe i niedrogie rozszerzenie ramienia robotycznego, które można zamontować na robotach komercyjnych lub wykonanych na zamówienie. Opracowane rozwiązanie dodaje trzy dodatkowe stopnie swobody, w tym liniowy tor o długości 0.5m. Zostało to zademonstrowane poprzez rozszerzenie współpracującego robota KUKA LBR iiwa 14, wykonującego różne zadania w hodowli owadów, takie jak sięganie do skrzynek hodowlanych, praca w zamkniętych obudowach i obsługa materiałów na większym obszarze roboczym. Ponadto wykorzystano symulacje w celu uzyskania informacji na temat zwiększonego zasięgu robota. Wyniki symulacji pokazują wzrost całkowitej przestrzeni operacyjnej do 110% oraz wzrost o 200% w liczbie pozycji osiągalnych z $\geq$ 50% testowanych orientacji w porównaniu z bazowym robotem KUKA iiwa.

Rozdział 4 prezentuje miękko-sztywny hybrydowy efektor końcowy do wszechstronnej obsługi materiałów. Opracowano niestandardowy efektor końcowy poprzez rozszerzenie OnRobot RG6 o dwie pary Soft Gripping GorillaFinger SoftActuators w celu zwiększenia elastyczności przy obsłudze różnorodnych materiałów o różnych rozmiarach, geometriach i teksturach. RG6 umożliwia dynamiczną regulację odległości pomiędzy parami miękkich palców, co zmienia obszar chwytu i pozwala na uchwyty wykraczające poza możliwości podstawowych chwytaków. Zwinność projektu hybrydowego została zademonstrowana

poprzez podnoszenie obiektów o zróżnicowanych geometriach. Dodatkowo wprowadzono przesunięcie w ich rozmieszczeniu w celu symulacji środowisk nie w pełni kontrolowanych. Aby ilościowo ocenić jakość chwytu, sprawdzono odporność efektora końcowego na zewnętrzne zakłócenia poprzez pomiar siły wymaganej do wyrwania obiektu z uchwytu. Efektor końcowy został zademonstrowany w przemyśle hodowli owadów, który obejmuje zróżnicowane zadania automatyzacyjne związane z delikatnymi owadami, obiektami i materiałami o różnych geometriach i sztywnościach. Ponadto przeanalizowano efektor końcowy w kontekście powiązanych prac nad miękkim chwytaniem, aby opracować model teoretyczny wyjaśniający efekt regulacji odległości między miękkimi palcami.

W Rozdziale 5 opracowano projekt strukturalny komórki robotycznej oraz zaprezentowano implementację jej oprogramowania sterującego. Robot składa się z ramienia współpracującego KUKA LBR iiwa 14, rozszerzenia toru opisanego w Rozdziale 3 oraz hybrydowego efektora końcowego z Rozdziału 4. Opracowano otaczającą strukturę wsporczą, która obejmuje platformę roboczą i zamontowane czujniki wizyjne 3D. Wybory projektowe dotyczące komórki robota uzasadniono przy użyciu wymagań CoRoSect zdefiniowanych w Rozdziale 2. Modele CAD wykorzystano do stworzenia pliku opisu robota rozszerzonego ramienia na potrzeby wirtualnego środowiska planowania ruchu w MoveIt!. W eksperymentach odzwierciedlających rzeczywiste warunki w hodowli owadów zdolności komórki robota zostały zademonstrowane poprzez pracę w zamkniętych przestrzeniach. Dzięki dodatkowym stopniom swobody, otaczającej strukturze wsporczej i przeszkodom w scenie planowania, uzyskano 100% skuteczności w obliczaniu trajektorii w czasie krótszym niż 5s w ograniczonych przestrzeniach roboczych i wewnątrz obudów. Ostateczna architektura oprogramowania została zaprezentowana jako rezultat praktycznej implementacji komórki robotycznej, łącząc planowanie ruchu z kontrolerami niskiego poziomu i systemami zarządzania zadaniami wysokiego poziomu.

Rozdział 6 prezentuje implementację zdolności kognitywnych w zakresie percepcji, lokalizacji obiektów i strategii korekcji błędów.

Podstawowe możliwości współpracującego ramienia robotycznego w zakresie planowania trajektorii wolnych od kolizji i chwytania różnych materiałów nie są jeszcze wystarczające do działania w środowisku nie w pełni kontrolowanym, takim jak hodowla owadów. Rozmieszczenie materiałów nie jest z góry określone, a spójność przeszkód, takich jak skrzynki i obudowy, nie może być zakładana. Ponadto możliwość błędnych obserwacji lub przesunięć w obsłudze materiałów wymaga systemów, które pozwolą robotowi radzić sobie z takimi błędami bez interwencji człowieka. Prezentujemy nowy pipeline do dokładnej lokalizacji obiektów z wykorzystaniem narzędzi przemysłowych do percepcji wizualnej i dopasowywania powierzchni, który służy do budowy wirtualnej reprezentacji przestrzeni roboczej w środowisku planowania ruchu robota. Ponadto wdrożono strategie obsługi materiałów, korekcji błędów, detekcji i manipulacji w zamkniętych obudowach. Pokazujemy, jak kombinacja tych strategii zwiększa wszechstronność naszej komórki robotycznej w obsłudze różnorodnych materiałów i operacji w rzeczywistych badaniach pilotażowych w fermach owadów. Rozdział 6 zawiera także demonstracje kognitywnej komórki robotycznej realizującej przypadki użycia w hodowli owadów w zakresie obsługi materiałów i zarządzania jakością, wraz z analizą jej wydajności i wynikami badań pilotażowych CoRoSect. Komórka robotyczna osiąga średni wskaźnik skuteczności na poziomie 93.7% we wszystkich zadaniach podczas powtarzanych serii przypadków użycia.

Samenvatting

Cognitieve robotica is een onderzoeksgebied op het kruispunt van robotica en kunstmatige intelligentie (AI). Het heeft tot doel om robotsystemen te voorzien van cognitieve mechanismen, waardoor ze hun omgeving kunnen waarnemen, informatie kunnen verwerken en desgewenst contextgevoelige beslissingen kunnen nemen (Aly et al., 2017; Cangelosi & Asada, 2022; Levesque & Lakemeyer, 2008). Dit onderzoeksgebied adresseert een aantal tekortkomingen van traditionele robotica in de automatisering. Traditionele robots zijn weliswaar effectief in het uitvoeren van voorgeprogrammeerde taken in gestructureerde omgevingen, maar kunnen zich niet aanpassen aan veranderingen, kunnen minder goed omgaan met onzekerheid en kunnen hun kennis niet generaliseren naar andere contexten (Qadeer et al., 2024; Y. Wang, 2010). Industriële automatisering, hoewel zeer efficiënt in een stabiele omgeving, is van nature kwetsbaar: afwijkingen van verwachte input kunnen tot fouten leiden (Cangelosi & Asada, 2022; Galin & Meshcheryakov, 2019; Javaid et al., 2021). Traditionele automatisering blinkt uit in gecontroleerde, repetitieve en zeer voorspelbare domeinen, zoals assemblagelijnproductie. Het heeft echter moeite met contexten die gekenmerkt worden door inconsistentie, variabiliteit, onvolledige informatie of de noodzaak tot interactie met mensen (Dmytriyev et al., 2024; Galin & Meshcheryakov, 2019).

Dit proefschrift presenteert het ontwerp en de implementatie van een veelzijdige cognitieve robotcel, zoals ontwikkeld binnen het Europese Horizon 2020-project 'Cognitive Robotics for automated and digitised Insect Farming' (CoRoSect). CoRoSect heeft tot doel een framework te ontwikkelen voor de inzet van netwerkgebaseerde cognitieve robotsystemen, waarbij insectenkweek een use case vormt die ons in staat stelt om hun sterke en zwakke punten in kaart te brengen. De ongestructureerde omgeving binnen een insectenkwekerij biedt alle mogelijkheden tot waardevolle stresstests voor cognitieve

robotsystemen en legt beperkingen bloot: qua bereikbaarheid en vrijheidsgraden voor flexibele manipulatie in afgesloten ruimtes, voor verfijnde grijptaken met een diversiteit aan objecten en zelfs levende organismen, ten aanzien van kwetsbaarheid voor ruis en occlusie in visuele data die de observatie en plaatsbepaling van objecten beïnvloeden, en de noodzaak van frequente besluitvorming. Het kunnen hanteren van levende insecten in een insectenkwekerij vereist dat robots goed kunnen omgaan met snel veranderende omstandigheden, die unieke problemen creëren afhankelijk van de ontwikkelingsstadia van verschillende insectensoorten. Bijvoorbeeld occlusie door gravende larven, snelle groeicycli die een aangepaste benadering voor elke fase vereisen, of de noodzaak van voortdurende kwaliteitsinspectie. Het doel van dit proefschrift is om inzicht te krijgen in de veelzijdigheid die wordt geboden door cognitieve robotsystemen, en daarmee de beperkingen van een collaboratieve, gearticuleerde robotarm aan te pakken, om zo het toepassingsgebied en de mogelijkheden ervan in een niet sterk-gecontroleerde omgeving te vergroten. Meer concreet zijn de bijdragen die in dit proefschrift worden gepresenteerd gericht op het aanpakken van uitdagingen voor de automatisering van ongestructureerde, mensgerichte werkruimtes, waarin robots materiaal hanteren, kwaliteitsbeheer uitvoeren en fijne handelingen verrichten. De belangrijkste resultaten en bijdragen, belicht in elk hoofdstuk, zijn: het ontwerp en de besturingssoftware van een uitbreiding van de kinematische keten voor een groter werkbereik en grotere handelingsvrijheid in beperkte ruimtes (Hoofdstuk 3), een zacht-en-rigide hybride eind-effector voor veelzijdige materiaalhantering (Hoofdstuk 4), het structurele ontwerp van de robotcel en de implementatie van de besturingssoftware (Hoofdstuk 5), en de implementatie van cognitieve capaciteiten in perceptie, objectlokalisatie en foutcorrectiestrategieën, samen met experimenten en succesvolle demonstraties van use cases in materiaalhantering en kwaliteitsbeheer (Hoofdstuk 6). De robot is geïmplementeerd als prototype, getest en gevalideerd op basis van eindgebruikersvereisten binnen CoRoSect. De veelzijdigheid van de cognitieve robot wordt aangetoond door een verscheidenheid aan unieke use cases

van drie verschillende insectensoorten, namelijk Tenebrio Molitor (meelwormen), Hermetia Illucens (zwarte soldatenvliegen) en Acheta Domesticus (huiskrekels). De resultaten en technologieën worden besproken in de context van het CoRoSect-framework, dat een robotiseringsoplossing voorstelt die in staat is gebleken processen te hanteren van drie van de meest gekweekte insectensoorten in de EU. Deze hoofdstukken zijn gestructureerd rondom de ontwikkeling van de belangrijkste componenten van een cognitieve robotcel.

Acknowledgments

It is with great pleasure and humility that I take this opportunity to acknowledge all those who have supported me in the completion of this work. Writing this dissertation has been a long and demanding process, and I could not have reached this point without the guidance, encouragement, and kindness of my supervisors, friends, and family. Their contributions, whether academic, professional, or personal, have left an enduring mark on my work.

Formally, I would like to express my gratitude to my promoters, Dr. Rico Möckel, Prof.dr. Gerhard Weiss, and Prof.dr.ir Ralf Peeters, whose expertise, patience, and commitment to excellence have guided me throughout this research journey. They not only provided academic supervision but also offered encouragement at moments of uncertainty, which gave me the confidence and support to persevere. I would like to thank Rico for the many years of guidance and collaboration on various projects, which I can trace back to my time as a student. Thank you for the time you invested, your understanding and kindness when it was needed, and your intellectual input, constructive criticism, and thoughtful suggestions that have challenged me to become rigorous and grounded in my work and research. The opportunity to work and travel with you during the CoRoSect project was a memorable and unique opportunity that I am proud to have been a part of. I would like to further thank Gerhard for his support and encouragement in writing my thesis and for the valuable scientific feedback. Finally, I would like to thank Ralf for his guidance and kindness during my work, his willingness to make time for conversation and opening opportunities for my personal development. I also wish to thank those involved along the way, as supervisors and committee members, who contributed valuable insights and perspectives that broadened my understanding and helped guide my early work.

As part of making this research and the CoRoSect project a reality,

I want to thank the staff of the DACS Robotics Lab, namely Lucas, Dean, Jan, Cavid, George, and Guillaume, who provided technical, logistical, and administrative assistance at crucial points of toiling on the robot cell. Their efforts, whether in assembling the CoRoSect robot (and disassembling... and then reassembling many times again), facilitating laboratory experiments, and their technical expertise, played a vital role in developing the robot cell that is the topic of my thesis. None of this would have been possible without the time collectively spent. I need to thank my colleagues Lucas and Dean, who were instrumental in the development of the CoRoSect robot cell and managed technical challenges, making it seem easy. I am equally grateful to Jan and Cavid, who both played a crucial role in implementing technologies and software for the CoRoSect project and helped in creating the groundwork upon which this research could be accomplished. Thanks to you, I will fondly remember the many hours spent abroad at pilot studies and in the lab, making the project a reality. Furthermore, I would like to thank those who contributed in some way to the research done during the development of the robot, namely Guillaume, Margarita, and Simone, but also others in the broader network of individuals who contributed indirectly to the completion of this dissertation.

I would like to express my gratitude to the members of the Department of Advanced Computing Sciences. The academic environment within this community has been a constant source of motivation and inspiration. The discussions, seminars, and interactions I experienced here contributed significantly to the intellectual growth that allowed me to arrive at this dissertation. I am particularly grateful to my office colleagues, Monica, Lucas, and Amir, whose willingness to share their time and experience created an atmosphere of both productivity and camaraderie when I had just started.

I am also grateful for the opportunity to have been a part of the CoRoSect project and the financial and institutional support, without which the research would not have been possible. Through CoRoSect, I had the privilege to meet and work with many industrial and

scientific partners towards a common goal. The time spent at the consortium meetings and pilot studies taught me much and allowed me to gain valuable insight into the practical considerations in industries and professional enterprises. I am especially thankful for the hospitality of the insect farming partners, namely the staff at Nasekomo, Entomotech, the Italian Cricket Farm, and Invertapro, who took great care of us during the long hours spent in difficult conditions, trying to make the CoRoSect pilot studies a success. In addition, I would like to thank colleagues at the Centre for Research & Technology, Hellas (CERTH), for collaborating closely on research during the development of our robot cell.

On a more personal level, I could not have done this without you, Elva, henceforth referred to as 'HoneyBun'. I cannot express in words what the last few years with you have meant to me, HoneyBun (but I hope I can express it by taking you out to dates and dinners). You have been a constant source of comfort, unconditional love, support, and joy. At our first date, when you walked into that sushi restaurant, I had no idea what a profound effect you would have on my life, but I can no longer imagine it without you. Thank you for all the lazy Sunday mornings (I want coffee too), the wolkies throughout the entire city to get ijsje, all the eepy nights, the amazing baked goods, and your delicious chimken curry. HoneyBun, I love that I could count on you for words of support, for listening, and for the adventures we have shared along the way. I love you so much.

I also wish to express profound gratitude to my family. First and foremost, to my parents, thank you for your unconditional love, patience, and belief in me throughout this long process, and especially for listening. You have been my greatest source of stability and encouragement. Your sacrifices, understanding, constant reassurance, and occasional professional advice have made it possible for me to devote myself fully to this endeavour. I appreciate your support, your care, and every small bit of help you gave in facing the challenges and obstacles along the way. *Dziękuję również mojej rodzinie w Polsce,*

której zainteresowanie moją pracą i wsparcie dla niej przypominały mi, że mogę w wielu miejscach szukać wsparcia.

My heartfelt thanks also go to my friends, Carla, Esther, Henry, Jan, Maí, Max, Melissa, Philippe, and Robin, who have walked alongside me during this journey, and many other journeys throughout the years. They have provided not only companionship but also perspective, reminding me of the importance of laughter, rest, and balance in the midst of academic challenges. Their willingness to listen, to encourage, and to distract me with outings, board games, dinners, and moments of joy made the journey far more bearable and meaningful. I hope that we will spend yet more time together, in whichever way, shape or form that might be. This paragraph would not be complete without acknowledging you all for taking part in the fantastical and convoluted stories I have been telling during our Sci-Fi Dungeons and Dragons campaigns, and for being as enthusiastic as you are about this alternate universe we have shaped together. The many adventures we have had throughout the solar system and in outer space, saving the Earth Alliance from ancient alien threats and its own corrupt leadership, will always feel like real memories instead of imagination. Of course, I am looking forward to the countless adventures yet to come!

In closing, I recognise that this dissertation is the product not only of my own efforts but also of the collective support of a wide community. It is to all of you, my promoters, colleagues, family, friends, and institutions, that I extend my deepest thanks.

Kamil Bujnarowski
Maastricht
April 16, 2026

Published Work

Bujnarowski, K., Krüger, J., Karca, C., Dahl, L., & Möckel, R. (2025). Extension of industrial and collaborative robots for increased work space and operation in confined spaces. *Annual Conference Towards Autonomous Robotic Systems*, 475–488

Under Review

Versatile Robotic Assistant for Insect Farming

Hybrid End Effector with Soft Fingers and Modular Elements for Versatile Material Handling

Robotic Visual Inspection for Quality Management in Insect Farming

Curriculum Vitae

Kamil Bujnarowski

k.bujnarowski@maastrichtuniversity.nl
kamilb@casema.nl
LinkedIn



Experience

2021 → 2024 **Horizon 2020 Project: CoRoSect** corosect.eu
Cognitive Robotic System for Digitalized and Networked (Automated) Insect Farms. Core role in the development and control of a collaborative robot cell for insect farming, led by the robotics and AI researchers of Maastricht University.

- *Task Leader* in WP6: Robotic Actions Planning and Control.
- WP7: Cognitive Robots and Smart Mechatronics.

The CoRoSect project successfully conducted large-scale pilots in insect farms across four European countries.

2019 → 2020 **Research Internship, Maastricht University**
Neural Network-Based Prediction of Heart Surface Potentials from Latent Representations of ECG Recordings.

2018 → Now **Teaching Activities, Maastricht University** Autonomous Robotic Systems, Computer Science, Data Analysis, Linear Algebra, Machine Learning, Mathematical Modelling, Mathematical Simulation, Numerical Mathematics, Probability and Statistics, Robotics and Embedded Systems, Software Engineering.

2016 → 2018 **Honours Program Research Path**

- *Serious Games for Elderly and Children, 2017-2018.* Received the Maastricht Research Proposal Competition Award.
- *Autonomous Drone for Search and Rescue, 2016-2017.*

Education

2021 → Now **PhD Candidate, Department of Advanced Computing Sciences, Maastricht University**: Cognitive Robotics and Artificial Intelligence.

2018 → 2020 **Master Artificial Intelligence, Maastricht University** - *Cum Laude*
Thesis title: *Inference and Prediction of Human Intentions from Visual Context Information.*

Education (continued)

2015 → 2018 **Bachelor Data Science and Knowledge Engineering, Maastricht University**
Thesis title: *Auditory Analysis for Serious Games.*

2014 → 2015 **Bachelor Aerospace Engineering, Delft University of Technology**

2007 → 2014 **Rotterdam International Secondary School**

Research Publications

Bujnarowski, K., Krüger, J., Karca, C., Dahl, L., & Möckel, R. (2025). Extension of industrial and collaborative robots for increased work space and operation in confined spaces. *Annual Conference Towards Autonomous Robotic Systems*, 475–488

Bujnarowski, K., Bonizzi, P., Cluitmans, M., Peeters, R., & Karel, J. (2020). Ct-scan free neural network-based reconstruction of heart surface potentials from ecg recordings. *2020 Computing in Cardiology*, 1–4

Bizcaino, D., Bujnarowski, K., Matyschik, M., Mauranen, H., Zhao, R., Bonizzi, P., & Karel, J. (2019). *Neural network-based matrix completion for minimal configuration of body surface potential mapping.* IEEE

Various Deliverable Reports: Horizon 2020 Project CoRoSect

Skills

Languages Native Speaker English, Native Speaker Polish, Strong competency in Dutch

Coding Python, Java, MATLAB, R, LaTeX, C++

Software ROS, MoveIt!, Sunrise Workbench, Halcon, Git, OpenCV, TensorFlow, Keras, Arduino

Soft Skills Highly Adaptable, Team Player, Working Under Pressure, Critical Thinking, Communication Skills, Presenting Skills

Miscellaneous Experience

2022 → 2024 **PhD Representative**
PhD Council, Faculty of Science and Engineering, Maastricht University

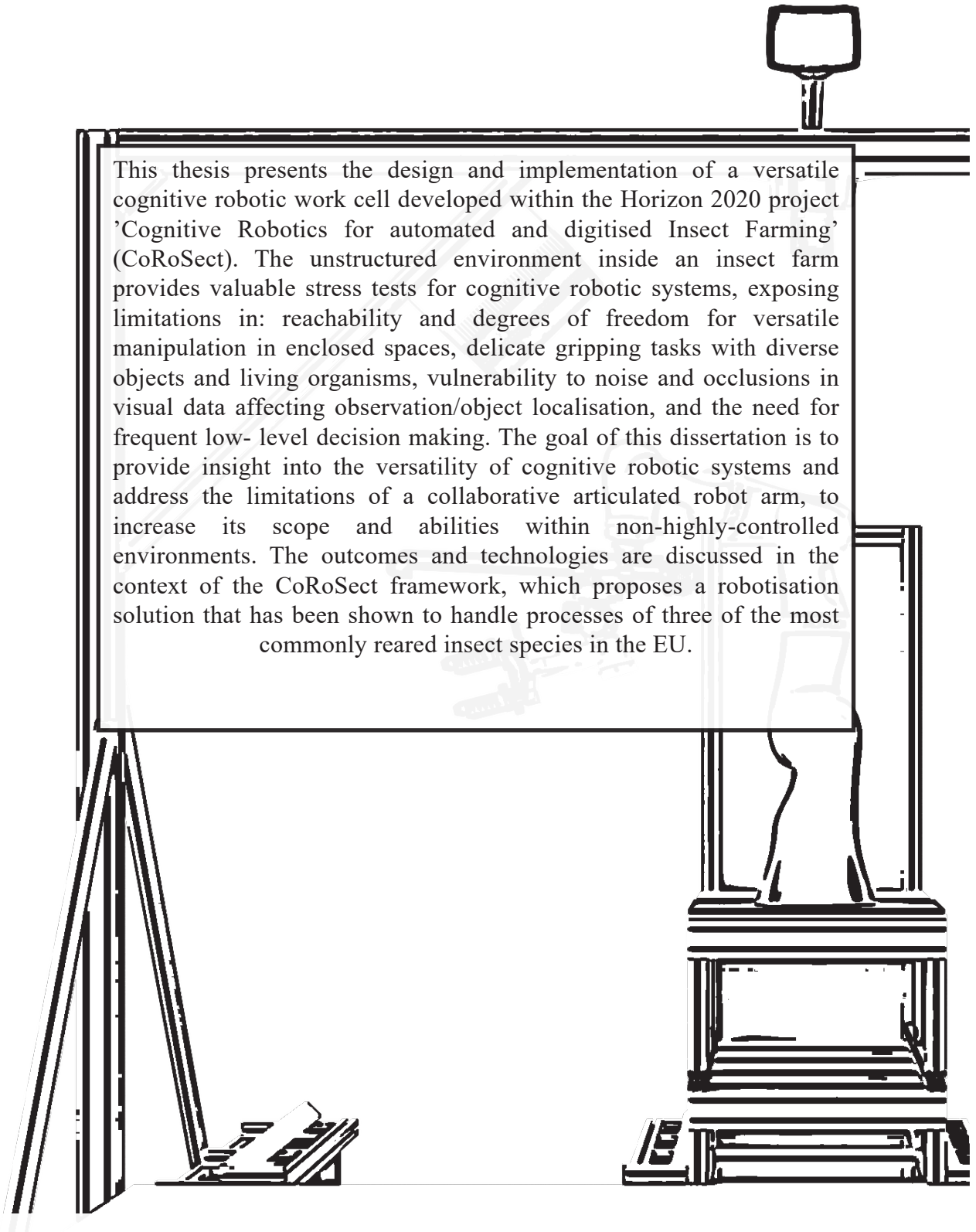
2019 → 2020 **Programme Committee**
Student Representative of the Master's Artificial Intelligence to the Department of Advanced Computing Sciences Program Committee

2018 → 2019 **Student Ambassador**
Promoting the Department of Advanced Computing Sciences through presentations and events organised for pre-university students. Organising and attending information sessions and open days.

About the Author

Kamil Konrad Bujnarowski was born on the 21^{st} of November 1995 in Jelenia Góra, Poland. At the age of five, his family moved to the Netherlands, where he attended international primary and secondary education to obtain an International Baccalaureate (IB) in 2014. He completed both his Bachelor's and Master's degrees at the Department of Advanced Computing Sciences (DACS) at Maastricht University, obtaining a Master's degree in Artificial Intelligence in 2020. During his studies, he was involved in research projects on autonomous drones and educational games at the DACS Robotics Lab, followed by a research internship on deep learning for electrocardiography, and he finished his Master's thesis on the inference and prediction of human intentions in the context of human-robot collaboration.

At the start of 2021, Kamil began as a PhD Candidate at the Robotics Lab of the DACS, under the supervision of Dr. Rico Möckel, Prof. Dr. Gerhard Weiss, and Prof. Dr. Ralf Peeters, working on the Horizon 2020 project 'Cognitive Robotics for automated and digitised Insect Farming' (CoRoSect). His role in this project was leading the software development in robotic action planning and control of a cognitive robot for fine manipulation in the context of insect farming, and he contributed to work packages on smart mechatronics, AI-enabled vision, and human-robot collaboration.



This thesis presents the design and implementation of a versatile cognitive robotic work cell developed within the Horizon 2020 project 'Cognitive Robotics for automated and digitised Insect Farming' (CoRoSect). The unstructured environment inside an insect farm provides valuable stress tests for cognitive robotic systems, exposing limitations in: reachability and degrees of freedom for versatile manipulation in enclosed spaces, delicate gripping tasks with diverse objects and living organisms, vulnerability to noise and occlusions in visual data affecting observation/object localisation, and the need for frequent low- level decision making. The goal of this dissertation is to provide insight into the versatility of cognitive robotic systems and address the limitations of a collaborative articulated robot arm, to increase its scope and abilities within non-highly-controlled environments. The outcomes and technologies are discussed in the context of the CoRoSect framework, which proposes a robotisation solution that has been shown to handle processes of three of the most commonly reared insect species in the EU.

CoRoSect

This project has received funding from the European Union's Horizon 2020 research and innovation programme under grant agreement No. 101016953.